Table of Contents

List of Figures

List of Tables

6.0 CONTAINMENT REQUIREMENTS

6.0.1 Introduction

Because of the amount and complexity of the material presented in Chapter 6.0, an introductory summary is provided below. Detailed discussions of the topics covered in this summary are found in the remainder of the chapter, which is organized as follows.

- Section 6.1 – The overall system performance assessment (PA) methodology used to evaluate compliance with the containment requirements.
- Section 6.2 – A comprehensive list of features, events, and processes (FEPs) that might affect disposal system performance, the screening methodology applied to that list, and the results of the screening process.
- Section 6.3 – Development of the scenarios considered in the system-level consequence analysis.
- Section 6.4 – The conceptual and computational models used to perform the system-level consequence analysis PA, the overall flow of information in the PA, the scenario probabilities, and the construction of a performance measure for comparison with the standard.
- Section 6.5 – The results of the PA.

Additional information supporting this chapter is provided in appendices. See Table 1-1 for a list of these appendices.

The U.S. Department of Energy (DOE) continues to use the same PA methodology for the recertification of WIPP. In general, changes that have been made since the U.S. Environmental Protection Agency (EPA) certified WIPP do not impact PA methodology.

6.0.2 Overview of Chapter 6.0

The EPA determined that the WIPP is in compliance with the Containment Requirements of Title 40 Code of Federal Regulations (CFR) § 191.13 in 1998 (EPA 1998a). The DOE has conducted a new PA for the WIPP. The WIPP Land Withdrawal Act (LWA), Public Law 02-579 as amended by Pubic Law No. 104-201, requires DOE to provide the EPA with documentation of continued compliance with the disposal standards within five years of first waste receipt and every five years thereafter. During review of the initial certification application, EPA required many changes to PA parameters, which have been included in the PA for this recertification application (EPA 1998b). The DOE has also made additional changes to the PA to better represent repository features, such as panel closures, and to account for new information. Table 6-1 summarizes the changes to the PA since the Compliance Certification Application (CCA); additional information is provided in Appendix PA (Attachment MASS, Section 2).

Table 6-1. WIPP Project Changes and Cross References

WIPP Project Change	Cross Reference
Incorporation of 1997 Performance Assessment Verification Test (PAVT) Parameters	
Credit for Passive Institutional Controls	6.4.12.1
K_d (Dissolved-Actinide Matrix Distribution Coefficient)	6.0.2.3.7, 6.4.6.2.2
Probability of Encountering a Brine Reservoir	6.0.2.3.8, 6.4.8, 6.4.12.6
Brine Reservoir Rock Compressibility	6.4.8
Brine Reservoir Porosity	6.4.8
Drill String Angular Velocity	Appendix PA, Attachment MASS (Section16) and Attachment PAR
Waste Permeability	6.4.3.2
Waste Unit Factor	Appendix TRU WASTE
Long-term Borehole Permeability	6.4.7.2
Borehole Plug Permeability	6.4.7.2
Waste Shear Strength and Erodability	Appendix PA, Attachment MASS (Section 16)
DRZ	6.4.5.3, 6.4.10.1
Actinide Solubility	6.4.3.5
Inundated Steel Corrosion Rate	6.4.3.3
Operational Changes	
Option D Panel Closure	6.4.3, 6.4.4
Inventory Update	6.4.3.1, 6.4.3.3
Culebra Water Levels	6.4.6.2, and Appendix PA, Attachment MASS
Spallings Model	6.0.2.3.2; Appendix PA (Section 4.6) and Attachment MASS (Section 16.0)
Drilling Rate	6.0.2.3, 6.2.5.2; Appendix DATA (Section 2 and Attachment A)
Organic Ligands	6.0.2.3.4, 6.4.3.4; Appendix PA, Attachments SOTERM and SCR
FEPs Reassessment	6.2.6; Appendix PA, Attachment SCR
Borehole Plugs Configuration Probability	6.4.7.2
Mining Disposal Horizon to Clay G	Appendix PA, Attachment MASS (Section 20)

From this assessment, the DOE has demonstrated that the WIPP continues to comply with the Containment Requirements of 40 CFR § 191.13. The Containment Requirements are stringent and state that the DOE must demonstrate a reasonable expectation that the probabilities of cumulative radionuclide releases from the disposal system during the 10,000 years following closure will fall below specified limits. The PA analyses supporting this determination must be quantitative and consider uncertainties caused by all significant processes and events that may affect the disposal system, including future inadvertent human intrusion into the repository. A

quantitative PA is conducted using a series of linked computer models in which uncertainties are addressed by a Monte Carlo procedure for sampling selected input parameters.

As required by regulation, results of the PA are displayed as complementary cumulative distribution functions (CCDFs) that display the probability that cumulative radionuclide releases from the disposal system will exceed the values calculated for scenarios considered in the analysis. These CCDFs are calculated using reasonable and, in some cases conservative conceptual models based on the scientific understanding of the disposal system's behavior. Parameters used in these models are derived from experimental data, field observations, and relevant technical literature. Changes to the CCA's parameters and models that have been necessary since the original certification have been incorporated into the PA. Information on the waste already disposed and new estimates of current and projected waste inventories are also incorporated. The overall mean CCDF continues to lie entirely below the specified limits, and the WIPP therefore continues to be in compliance with the containment requirements of 40 CFR Part 191, Subpart B (see Section 6.5.2, Figure 6-1). Sensitivity analysis of results shows that the location of the mean CCDF is dominated by radionuclide releases that could occur on the surface during an inadvertent penetration of the repository by a future drilling operation. Releases of radionuclides to the accessible environment resulting from transport in groundwater through the shaft seal systems and the subsurface geology are resulting negligible, with or without human intrusion, and make no contribution to the location of the mean CCDF. No releases whatsoever are predicted to occur at the ground surface in the absence of human intrusion. The natural and engineered barrier systems of the WIPP provide robust and effective containment of transuranic (TRU) waste even if the repository is penetrated by multiple boreholes.

A list of changes and a citation to where they are discussed is shown in Table 6-1.

6.0.2.1 Conceptual Basis for the Performance Assessment

The foundations of PA are a thorough understanding of the disposal system and the possible future interactions of the repository, waste, and surrounding geology. The recertification application is organized so that site characterization, facility design, and waste characterization are described separately in Chapters 2.0, 3.0, and 4.0, respectively. The DOE's confidence in the results of the recertification PA is based in part on the strength of the original research done during site characterization, experimental results used to develop and confirm parameters and models, the robustness of the facility design, and the knowledge of the updated inventory. Quality assurance (QA) activities, described in Chapter 5.0, demonstrate that the information gathered during these activities is qualified to meet the QA criteria in 40 CFR 194.

Chapters 2.0, 3.0, and 4.0 provide basic descriptions of the disposal system main components. The interactions of the repository and waste with the geologic system, and the response of the disposal system to possible future inadvertent human intrusion, are described in Section 6.4.

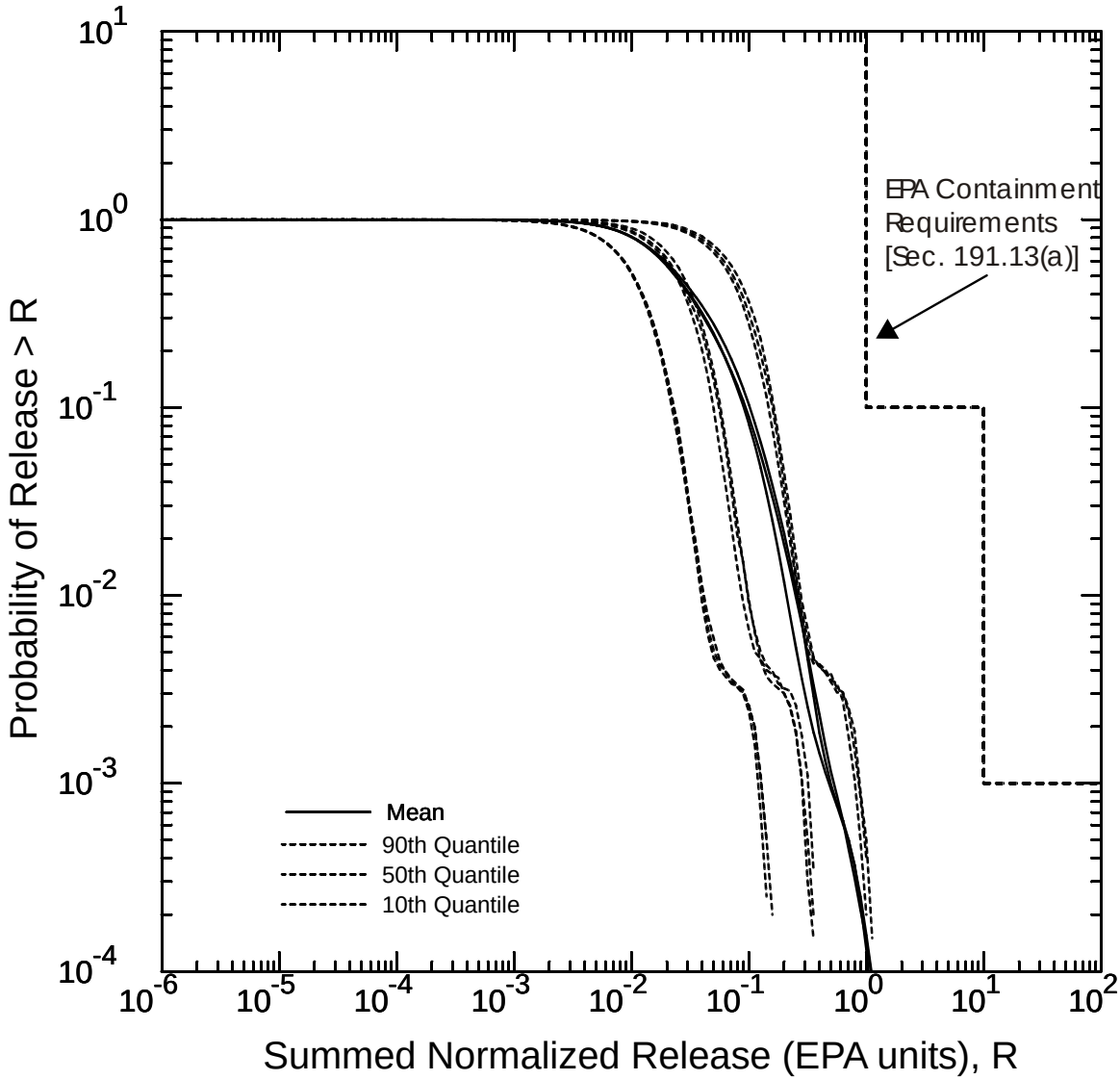

Note: Mean, median, and 10th and 90th percentile CCDFs are shown together with the overall mean. These CCDFs are based on the distributions of CCDFs shown in Figure 6-34, 6-35, and 6-36.

Figure 6-1. Summary CCDFs for Replicates 1, 2, and 3

6.0.2.2 Undisturbed Performance

An evaluation of undisturbed performance, which is defined to exclude human intrusion and unlikely disruptive natural events, is required by regulation (see Sections 191.15 and § 191.24). Evaluation of past and present natural geologic processes in the region indicate that none has the potential to breach the repository within 10,000 years. Disposal system behavior is dominated by the coupled processes of rock deformation surrounding the excavation, fluid flow, and waste degradation. Each of these processes can be described independently, but the extent to which each process occurs is affected by the others.

Deformation of the rock immediately around the repository begins as soon as excavation creates a disturbance in the stress field. Stress relief results in some degree of brittle fracturing and the

formation of a disturbed rock zone (DRZ), which surrounds excavations in all deep mines, including the repository. For the WIPP, the DRZ is characterized by an increase in permeability and a decrease in pore pressure, and may ultimately extend a few meters from the excavated region. Salt will also deform by creep processes, which are a result of deviatoric stress, causing the materials to move inward to fill voids. Salt creep will continue until deviatoric stress is dissipated and the system is once again at stress equilibrium.

The ability of salt to creep, thereby healing fractures and filling porosity, is one of its fundamental advantages as a medium for geologic disposal of radioactive waste and one reason it was recommended by the National Academy of Sciences (NAS). Salt creep provides the mechanism for crushed salt compaction in the shaft seal system, yielding properties approaching those of intact salt within 200 years. Salt creep will also cause the DRZ surrounding the shaft to heal rapidly around the concrete components of the seal system. In the absence of elevated gas pressure in the repository, salt creep would also substantially compact the waste and heal the DRZ around the disposal region. The coupling of salt creep with fluid flow and waste degradation processes results in fluid pressure within the waste disposal region maintaining significant porosity within the disposal region throughout the performance period.

Characterization of the Salado Formation (hereafter referred to as the Salado) indicates that fluid flow does not occur on time scales of interest in the absence of an artificially imposed hydraulic gradient. This lack of fluid flow is the second fundamental reason for the choice of salt as a medium for geologic disposal of radioactive waste. Lack of fluid flow is a result of the extremely low permeability of the evaporite rocks that make up the Salado. Excavation of the repository has disturbed the natural hydraulic gradient and rock properties and has resulted in fluid flow. Small quantities of interstitial brine present in the Salado move toward regions of low hydraulic potential and brine seeps are observed in the underground. The slow flow of brine from halite into more permeable anhydrite marker beds and then through the DRZ into the repository is expected to continue as long as the hydraulic potential within the repository is below that of the far field. The repository environment will also involve gas, and fluid flow that must be modeled as a two-phase process. Initially, the gaseous phase will consist primarily of air trapped at the time of closure, although other gases may form from waste degradation. In the PA, the gaseous phase pressure will rise due to creep closure, gas generation, and brine inflow, creating the potential for flow from the excavated region.

Consideration of waste degradation processes indicates that the gaseous phase in fluid flow and the repository's pressure history will be far more important than if the initial air were the only gas present. Waste degradation can generate significant additional gas by two processes:

1. the generation of hydrogen (H_2) gas by anoxic corrosion of steels, other iron-base (Fe-based) alloys, and aluminum (Al) and Al-based alloys, and

2. the generation of carbon dioxide (CO_2) and methane (CH_4) by anaerobic microbial consumption of waste containing cellulosic, plastic, or rubber materials.

Coupling these gas-generation reactions to fluid flow and salt creep processes is complex. Gas generation will increase fluid pressure in the repository, thereby decreasing the hydraulic gradient and deviatoric stress between the far field and the excavated region and inhibiting the

processes of brine inflow and salt creep. Anoxic corrosion will also consume brine as it breaks down water to oxidize steels and other Fe-based alloys and release H_2. Thus, corrosion has the potential to be a self-limiting process, in that as it consumes all water in contact with steels and other Fe-based alloys, it will cease. Microbial reactions also require water, either in brine or the gaseous phase. It is assumed that microbial reactions will result in neither the consumption nor production of water.

The total volume of gas generated by corrosion and microbial consumption may be sufficient to result in repository pressures that approach lithostatic. Sustained pressures above lithostatic are not physically reasonable within the disposal system, and fracturing of the more brittle anhydrite layers is expected to occur if sufficient gas is present. The conceptual model implemented in the PA causes permeability and porosity of the anhydrite marker beds to increase rapidly as pore pressure approaches and exceeds lithostatic. This conceptual model for pressure-dependent fracturing approximates the hydraulic effect of pressure-induced fracturing and allows gas and brine to move more freely within the marker beds at higher pressures.

Overall, the behavior of the undisturbed disposal system will result in extremely effective isolation of the radioactive waste. Concrete, clay, and asphalt components of the shaft seal system will provide an immediate and effective barrier to fluid flow through the shafts, isolating the repository until salt creep has consolidated the compacted crushed salt components and permanently sealed the shafts. Around the shafts, the DRZ in halite layers will heal rapidly because the presence of the solid material within the shafts will provide rigid resistance to creep. The DRZ around the shaft, therefore, will not provide a continuous pathway for fluid flow. Similarly, the Option D panel closure will provide rigid resistance to creep and rapidly eliminate the DRZ locally by a compressive state of stress. The DRZ is not expected to heal completely around the disposal region, or the operations and experimental regions, and pathways for fluid flow may exist indefinitely to the overlying and underlying anhydrite layers (e.g., Marker Bed (MB)139 and anhydrites a and b). Some quantity of brine will be present in the repository under most conditions and may contain actinides (which dominate the radionuclide inventory and are therefore the elements of primary regulatory interest) mobilized as both dissolved and colloidal species. Gas generation by corrosion and microbial degradation is expected to occur and will result in elevated pressures within the repository. These pressures will not significantly exceed lithostatic, because fracturing within the more brittle anhydrite layers will occur and provide a pathway for gas to leave the repository. Fracturing due to high gas pressures may enhance gas and brine migration from the repository, but gas transport will not contribute to the release of actinides from the disposal system. Brine flowing out of the waste disposal region through anhydrite layers may transport actinides as dissolved and colloidal species, but the quantity of actinides that may reach the accessible environment boundary during undisturbed performance through the interbeds is insignificant and has no effect on the compliance determination. No migration of radionuclides whatsoever is expected to occur vertically through the Salado or through the shaft seal system.

6.0.2.3 Disturbed Performance

Performance assessment is required by regulation to consider scenarios that include intrusions into the repository by inadvertent and intermittent drilling for resources. In the CCA, the probability of these intrusions was based on a future drilling rate of 46.8 boreholes per square

kilometer per 10,000 years. This rate was based on the past record of drilling events in the Delaware Basin, consistent with regulatory criteria. Since the CCA, additional drilling in the Delaware Basin has raised the drilling rate to 52.5 boreholes per square kilometer per 10,000 years (see Appendix DATA, Section DATA-2.0 and Attachment A). Active institutional controls are assumed to be completely effective in preventing intrusion during the first 100 years after closure. Passive institutional controls were originally assumed in the CCA to effectively reduce the drilling rate by two orders of magnitude for the 600 years following the 100 years of active control. However, in certifying the WIPP, EPA denied the application of credit for the effectiveness of passive controls for 600 years. Although the Compliance Recertification Application 2004 PA (2004 PA) does not include a reduced drilling intrusion rate to account for passive institutional controls, future PA may do so. Future drilling practices are assumed to be the same as current practice, also consistent with regulatory criteria. These practices include the type and rate of drilling, emplacement of casing in boreholes, and the procedures implemented when boreholes are plugged and abandoned.

PA results indicate that human intrusion provides the only potential mechanism for significant releases of radionuclides from the disposal system. These releases could occur by five mechanisms:

(1) cuttings, which include material intersected by the rotary drilling bit;

(2) cavings, which include material eroded from the borehole wall during drilling;

(3) spallings, which include solid material carried into the borehole during rapid depressurization of the waste disposal region;

(4) direct brine releases, which include contaminated brine that may flow to the surface during drilling; and

(5) long-term brine releases, which include the contaminated brine that may flow through a borehole after it is abandoned.

The first four mechanisms operate immediately following the intrusion event and are collectively referred to as direct releases. The accessible environment boundary for these releases is the ground surface. The fifth mechanism, actinide transport by long-term groundwater flow, begins when concrete plugs are assumed to degrade in an abandoned borehole and may continue throughout the regulatory period. The accessible environment boundary for these releases may be the ground surface or the lateral subsurface limit of the controlled area.

Repository conditions prior to intrusion will be the same as those for undisturbed performance and all processes active in undisturbed performance will continue to occur following intrusion. Because intrusion provides a pathway for radionuclides to reach the ground surface and to enter the geological units above the Salado, additional processes will occur that are less important in undisturbed performance. These processes include the mobilization of radionuclides as dissolved and colloidal species in repository brine and groundwater flow, and actinide transport in the overlying units. Flow and transport in the Culebra Member of the Rustler Formation (hereafter referred to as the Rustler) are of particular interest because modeling indicates this is the unit to which most flow from a borehole may occur.

6.0.2.3.1 Cuttings and Cavings

In a rotary drilling operation, the volume of material brought to the surface as cuttings is calculated as the cylinder defined by the thickness of the unit and the diameter of the drill bit. The quantity of radionuclides released as cuttings is therefore a function only of the intersected waste activity and the diameter of the intruding drill bit. Like all parameters that describe future drilling activities, the diameter of a drill bit that may intersect waste is speculative. The DOE uses a constant value of 0.311 m (12.25 in.), consistent with bits currently used at the WIPP depth in the Delaware Basin. The intersected waste activity may vary depending on the type of waste intersected, and the DOE considers random penetrations into remote-handled (RH)-TRU waste and each of the 693 different waste streams identified for contact-handled (CH)-TRU waste (569 waste streams were used in the CCA).

The volume of particulate material eroded from the borehole wall by the drilling fluids and brought to the surface as cavings may be affected by the drill bit diameter, the effective shear resistance of the intruded material, the speed of the drill bit, the viscosity of the drilling fluid and the rate at which it is circulated in the borehole, and other properties related to the drilling process. The most important of these parameters, after drill bit diameter, is the effective shear resistance of the intruded material. In the absence of data describing the reasonable and realistic future properties of degraded waste and magnesium oxide (MgO), the DOE used conservative parameter values based on the properties of fine-grained sediment. Other properties are assigned fixed values consistent with current practice. The quantity of radionuclides released as cavings depends on the volume of eroded material and its activity, which is treated in the same manner as the activity of the cuttings.

6.0.2.3.2 Spallings

Unlike releases from cuttings and cavings, which occur with every modeled borehole intrusion, spalling releases will occur only if pressure in the waste-disposal region exceeds the hydrostatic pressure in the borehole. At lower pressures, below about 8 megapascals, fluid in the waste-disposal region will not flow toward the borehole. At higher pressures, gas flow toward the borehole may be sufficiently rapid to cause additional solid material to enter the borehole. If spalling occurs, the volume of spalled material will be affected by the physical properties of the waste, such as its tensile strength and particle diameter. The DOE has based the parameter values used in the PA on reasonable and conservative assumptions. Since the original certification, a revised conceptual model for the spallings phenomena has been developed (see Appendix PA, Section 4.6 and Attachment MASS, Section 16). Model development, execution, and sensitivity studies necessitated implementing parameter values pertaining to waste characteristics, drilling practices and physics of the process. The parameter range for particle size was derived by expert elicitation (EPA 1997, II-G-24).

The quantity of radionuclides released as spalled material depends on the volume of spalled waste and its activity. Because spalling may occur at a greater distance from the borehole than cuttings and cavings, spalled waste is assumed to have the volume-averaged activity of CH-TRU waste rather than the sampled activities of individual waste streams. RH-TRU waste is isolated from the spallings process and does not contribute to the volume or activity of spalled material.

6.0.2.3.3 Direct Brine Flow

Radionuclides may be released to the accessible environment if repository brine enters the borehole during drilling and flows to the ground surface. The quantity of radionuclides released by direct brine flow depends on the volume of brine reaching the ground surface and the concentration of radionuclides contained in the brine. As with spallings, direct releases of brine will not occur if repository pressure is below the hydrostatic pressure in the borehole. At higher repository pressures, mobile brine present in the repository will flow toward the borehole. If the volume of brine flowing from the repository into the borehole is small, it will not affect the drilling operation, and flow may continue until the driller reaches the base of the evaporite section and installs casing in the borehole. This time is estimated to be 72 hours, consistent with current practice. Larger brine flows or large gas flows could cause the driller to lose control of the borehole, and fluid flow, in this case, could continue until repository pressure drops or the hole is contained. The maximum length of time that such flow could continue before the driller controlled the borehole is estimated to be 11 days, consistent with observed drilling events in the Delaware Basin (Appendix PA, Section PA-4.7.8 and Attachment MASS, Section 16.0).

6.0.2.3.4 Mobilization of Actinides in Repository Brine

Actinides may be mobilized in repository brine in two principal ways:

(1) as dissolved species, and

(2) as colloidal species.

The solubilities of actinides depend on their oxidation states, with the more reduced forms (for example, the +III and +IV oxidation states) being less soluble than the oxidized forms (+V and +VI). Conditions within the repository will be strongly reducing because of the large quantity of metallic Fe in the steel containers and the waste, and – in the case of plutonium (Pu) – only the lower-solubility oxidation states (Pu(III) and Pu(IV)) will persist. Microbial activity, if it occurs, will also create reducing conditions. Solubilities also vary with pH. The DOE is therefore emplacing MgO in the waste-disposal region to ensure conditions that favor minimum actinide solubilities. MgO consumes CO_2 and buffers pH, lowering actinide solubilities in WIPP brines. Solubilities in the PA are based on the chemistry of brines that might be present in the waste-disposal region, reactions of these brines with the MgO engineered barrier, and strongly reducing conditions produced by anoxic corrosion of steels and other Fe-based alloys.

The waste contains organic ligands that could increase actinide solubilities by forming complexes with dissolved actinide species. However, these organic ligands also form complexes with other dissolved metals, such as magnesium (Mg), calcium (Ca), Fe, vanadium (V), chromium (Cr), manganese (Mn), and nickel (Ni), that will be present in repository brines due to corrosion of steels and other Fe-based alloys. The CRA-2004 PA speciation and solubility calculations (Attachment SOTERM) confirmed that actinide solubilities are not significantly affected by organic ligands.

Colloidal transport of actinides has been examined and four types have been determined to represent the possible behavior at the WIPP. These include microbial colloids, humic substances, actinide intrinsic colloids, and mineral fragments. Concentrations of actinides

mobilized as these colloidal forms are included in the estimates of total actinide concentrations used in PA.

6.0.2.3.5 Long-Term Brine Flow up an Intrusion Borehole

Long-term releases to the ground surface or groundwater in the Rustler or overlying units may occur after the borehole has been plugged and abandoned. In keeping with regulatory criteria, borehole plugs are assumed to have properties consistent with current practice in the basin. Thus, boreholes are assumed to have concrete plugs emplaced at various locations. Initially, concrete plugs effectively limit fluid flow in the borehole. However, under most circumstances, these plugs cannot be expected to remain fully effective indefinitely. For the purposes of PA, discontinuous borehole plugs above the repository are assumed to degrade 200 years after emplacement. From then on, the borehole is assumed to fill with a silty sand-like material containing degraded concrete, corrosion products from degraded casing, and material that sloughs into the hole from the walls. Of six possible plugged borehole configurations in the Delaware Basin, three are considered either likely or found to adequately represent other possible configurations; one configuration (a two-plug configuration) is explicitly modeled.

If sufficient brine is available in the repository, and if pressure in the repository is higher than in the overlying units, brine may flow up the borehole following degradation of the plugs. In principle, this brine could flow into any permeable unit or to the ground surface if repository pressure were high enough. For modeling purposes, brine is allowed to flow only into the higher permeability units and to the surface. Lower permeability anhydrite and mudstone layers in the Rustler are treated as if they were impermeable, to simplify the analysis while maximizing the amount of flow occurring into units where it could potentially contribute to releases from the disposal system. Model results indicate that essentially all flow occurs into the Culebra, which has been recognized since the early stages of site characterization as the most transmissive unit above the repository and the most likely pathway for subsurface transport.

6.0.2.3.6 Groundwater Flow in the Culebra

Site characterization activities in the units above the Salado have focused on the Culebra. These activities have shown that the direction of groundwater flow in the Culebra varies somewhat regionally, but in the area that lies over the site, flow is southward. Regional variation in groundwater flow direction in the Culebra is influenced by the transmissivity observed and also by the shape of and distribution of rock types in the groundwater basin where the WIPP is located. Site characterization activities have demonstrated that there is no evidence of karst groundwater systems in the controlled area, although groundwater flow in the Culebra is affected by the presence of fractures, fracture fillings, and vuggy pore features. Other laboratory and field activities have focused on the behavior of dissolved and colloidal actinides in the Culebra. These characterization and modeling activities conducted in the units above the Salado confirm that the Culebra is the most transmissive unit above the Salado. The Culebra is the unit into which actinides are likely to be introduced from long-term flow up an abandoned borehole.

Basin-scale regional modeling of three-dimensional groundwater flow in the units above the Salado demonstrates that it is appropriate, for the purposes of estimating radionuclide transport, to conceptualize the Culebra as a two-dimensional confined aquifer. Uncertainty in the flow

field is incorporated in the analysis by using 100 different geostatistically-based transmissivity fields, each of which is consistent with available head and transmissivity data.

Groundwater flow in the Culebra is modeled as a steady-state process, but two mechanisms considered in the PA could affect flow in the future. Potash mining in the McNutt Potash Zone (hereafter referred to as the McNutt) of the Salado, which occurs now in the Delaware Basin outside the controlled area and may continue in the future, could affect flow in the Culebra if subsidence over mined areas causes fracturing or other changes in rock properties. Climatic changes during the next 10,000 years may also affect groundwater flow by altering recharge to the Culebra.

Consistent with regulatory criteria, mining outside the controlled area is assumed to occur in the near future, and mining within the controlled area is assumed to occur with a probability of 1 in 100 per century (adjusted for the effectiveness of active institutional controls during the first 100 years following closure). Consistent with regulatory guidance, the effects of mine subsidence are incorporated in the PA by increasing the transmissivity of the Culebra over the areas identified as mineable by a factor sampled from a uniform distribution between 1 and 1000. Transmissivity fields used in the PA are therefore adjusted and steady-state flow fields calculated accordingly; once for mining that occurs only outside the controlled area, and once for mining that occurs both inside and outside the controlled area. Mining outside the controlled area is considered in both undisturbed and disturbed performance.

The extent to which the climate will change during the next 10,000 years and how such a change will affect groundwater flow in the Culebra are uncertain. Regional three-dimensional modeling of groundwater flow in the units above the Salado indicates that flow velocities in the Culebra may increase by a factor of 1 to 2.25 for reasonably possible future climates. This uncertainty is incorporated in the PA by scaling the calculated steady-state specific discharge within the Culebra by a sampled parameter within this range.

6.0.2.3.7 Actinide Transport in the Culebra

Field tests have shown that the Culebra is best characterized as a double-porosity medium for estimating contaminant transport in groundwater. Groundwater flow and advective transport of dissolved or colloidal species and particles occurs primarily in a small fraction of the rock's total porosity and corresponding to the porosity of open and interconnected fractures and vugs. Diffusion and slower advective flow occur in the remainder of the porosity, which is associated with the low-permeability dolomite matrix. Transported species, including actinides, if present, will diffuse into this porosity.

Diffusion from the advective porosity into the dolomite matrix will retard actinide transport by two mechanisms. Physical retardation occurs simply because actinides that diffuse into the matrix are no longer transported with the flowing groundwater. Transport is interrupted until they diffuse back into the advective porosity. In situ tracer tests have been conducted to demonstrate this phenomenon. Chemical retardation also occurs within the matrix as actinides are sorbed onto dolomite grains. The relationship between sorbed and liquid concentrations is assumed to be linear and reversible. The distribution coefficients (K_ds) that characterize the extent to which actinides will sorb on dolomite were based on experimental data. Based on their

review of the CCA, the EPA required the DOE to use the same ranges but to change the distribution from uniform to log uniform. The DOE continues to use EPA's distributions in CRA-2004 PA. The DOE also corrected a minor error in the calculation of K_ds (see Appendix PA, Attachment PAR).

Modeling indicates that physical and chemical retardation, as supported by field tests and laboratory experiments, will be extremely effective in reducing the transport of dissolved actinides in the Culebra. Experimental work has demonstrated that transport of colloidal actinides is not a significant mechanism in the Culebra. As a result, actinide transport through the Culebra to the subsurface boundary of the controlled area is not a significant pathway for releases from the WIPP. As discussed in Section 6.5.3, the location of the mean CCDF that demonstrates compliance with the containment requirements of 40 CFR § 191.13 is, determined entirely by direct releases at the ground surface during drilling (cuttings, cavings, and spallings).

6.0.2.3.8 Intrusion Scenarios

Human intrusion scenarios evaluated in the PA include both single intrusion events and combinations of multiple boreholes. Two different types of boreholes are considered:

(1) those that penetrate a pressurized brine reservoir in the underlying Castile Formation (hereafter referred to as the Castile), and

(2) those that do not.

The presence of a brine reservoir under the repository is speculative, but cannot be ruled out on the basis of current information. A pressurized brine reservoir was encountered at the WIPP-12 borehole within the controlled area to the northwest of the disposal region and other pressurized brine reservoirs that are associated with regions of deformation in the Castile have been encountered elsewhere in the Delaware Basin. Based on a geostatistical analysis of the distribution of brine encounters in the region, the DOE has estimated that there was a 0.08 probability that a random borehole that penetrates waste in the WIPP will also penetrate an underlying brine reservoir. Upon their review of the CCA, the EPA determined that the DOE should treat this probability as uncertain, ranging from 0.01 to 0.60 in the PAVT. This recertification application uses the EPA's PAVT range (see Appendix PA, Section PA-3.5). The EPA also required the DOE to modify the assumptions concerning Castile properties to increase the brine reservoir volumes (EPA 1998 VII.B.4.d). The EPA determined that changing the rock compressibility of the Castile and the Castile porosity effectively modified the sampled brine reservoir volume to include the possibility of larger brine reservoir volumes like those encountered by the WIPP-12 borehole.

The primary consequence of penetrating a pressurized reservoir is to provide an additional source of brine beyond that which might flow into the repository from the Salado. Direct releases at the ground surface resulting from the first repository intrusion would be unaffected by additional Castile brine even if it flowed to the surface, because brine moving straight up a borehole will not mix significantly with waste. However, the presence of Castile brine could increase radionuclide releases significantly in two ways. First, the volume of contaminated brine that could flow to the surface may be greater for a second or subsequent intrusion into a

repository that has already been connected by a previous borehole to a Castile reservoir. Second, the volume of contaminated brine that may flow up an abandoned borehole after plugs have degraded may be greater for combinations of two or more boreholes that intrude the same panel if one of the boreholes penetrates a pressurized reservoir. Both processes are modeled in the PA.

6.0.2.4 Compliance Demonstration Method

The DOE's approach to demonstrating continued compliance is the PA methodology described in Section 6.1. The PA process comprehensively considers the FEPs relevant to disposal system performance. Those FEPs shown by screening analyses to potentially affect performance are included in quantitative calculations using a system of linked computer models to describe the interaction of the repository with the natural system, both with and without human intrusion. Uncertainty is incorporated in the analysis by a Monte Carlo approach in which multiple simulations (or realizations) are completed using sampled values for 64 imprecisely known or naturally variable input parameters. Distribution functions are constructed that characterize the state of knowledge for these parameters, and each realization of the modeling system uses a different set of sampled input values. A sample size of 100 results in 100 different values of each parameter. Therefore, there are 100 different sets (vectors) of input parameter values. Quality assurance (QA) activities, described in Chapter 5.0, demonstrate that the parameters, software, and analysis used in the PA were the result of a rigorous process conducted under controlled conditions.

Scenario probabilities composed of specific combinations of FEPs are estimated based on regulatory criteria (applied to the probability of future human action) and the understanding of the natural and engineered systems. Cumulative radionuclide releases from the disposal system are calculated for each scenario considered and scenario probabilities are summed for each modeling system realization to construct distributions of CCDFs. Input parameter sampling was performed in three separate replicates, resulting in three independent distributions of CCDFs and allowing the construction of three independent mean CCDFs, each based on 100 individual CCDFs.

6.0.2.5 Results of the Performance Assessment

Section 6.5 addresses the Containment Requirements of 40 CFR Part 191 and the associated criteria of 40 CFR § 194.34. Section 6.5 presents distributions of CCDFs for each replication of the analysis, mean CCDFs, and an overall mean CCDF with the 95 percent confidence interval estimated from the three independent mean distributions.

Families of CCDFs and mean CCDFs for each of the three replicates are also shown in Section 6.5. All 300 individual CCDFs lie below and to the left of the limits specified in 40 CFR § 191.13(a). The overall mean CCDF determined from the three replicates lies entirely below and to the left of the limits specified in 40 CFR § 191.13(a). Thus, the WIPP continues to comply with the containment requirements of 40 CFR Part 191. Comparing the results of the three replicates indicates that the sample size of 100 in each replicate is sufficient to generate a stable distribution of outcomes. Within the region of regulatory interest (that is, at probabilities greater than $10^{-3}/10^{4}$ yr), the mean CCDFs from each replicate are essentially indistinguishable from the overall mean.

As discussed in Section 6.5, examining the normalized releases from cuttings and cavings, spallings, and direct brine release provides insight into the relative importance of each release mode's contribution to the mean CCDF's location and the compliance determination. Releases from cuttings and cavings dominate the mean CCDF. Spallings make a small contribution. Direct brine releases are less important and have very little effect on the location of the mean. Subsurface releases resulting from groundwater transport are less than 10^{-6} EPA units and make no contribution to the mean CCDF's location.

Uncertainties characterized in the natural system and the interaction of waste with the disposal system environment have little effect on the location of the mean CCDF, providing additional confidence in the compliance determination. The natural and engineered barrier systems of the WIPP provide robust and effective containment of TRU waste even if the repository is penetrated by multiple borehole intrusions.

6.1 Performance Assessment Methodology

The EPA, in 40 CFR Part 191, specifies the generally applicable environmental standards for protecting public health and the environment from the disposal of TRU and high-level radioactive wastes. In this section, the DOE addresses compliance with the Containment Requirements of 40 CFR § 191.13 and the associated portions of 40 CFR Part 194 for TRU waste.

Section 191.13 states:

> (a) Disposal systems for spent nuclear fuel or high-level or transuranic radioactive wastes shall be designed to provide a reasonable expectation, based on performance assessments, that the cumulative releases of radionuclides to the accessible environment for 10,000 years after disposal from all significant processes and events that may affect the disposal system shall:
>
> (1) Have a likelihood of less than one chance in 10 of exceeding the quantities calculated according to Table 1 (Appendix A); and
>
> (2) Have a likelihood of less than one chance in 1,000 of exceeding ten times the quantities calculated according to Table 1 (Appendix A).
>
> (b) Performance assessments need not provide complete assurance that the requirements of § 191.13(a) will be met. Because of the long time period involved and the nature of the events and processes of interest, there will inevitably be substantial uncertainties in projecting disposal system performance. Proof of the future performance of a disposal system is not to be had in the ordinary sense of the word in situations that deal with much shorter time frames. Instead, what is required is a reasonable expectation, on the basis of the record before the implementing agency, that compliance with § 191.13(a) will be achieved.

The term accessible environment is defined as: "(1) The atmosphere; (2) land surfaces; (3) surface waters; (4) oceans; and (5) all of the lithosphere that is beyond the controlled area" (40 CFR § 191.12). Further, controlled area means: "(1) A surface location, to be identified by passive institutional controls, that encompasses no more than 100 square kilometers and extends horizontally no more than five kilometers in any direction from the outer boundary of the

original location of the radioactive wastes in a disposal system; and (2) the subsurface underlying such a surface location" (40 CFR § 191.12). The controlled area established by the LWA is shown in Figure 3-1. The release limits listed in Appendix A of 40 CFR Part 191 are reproduced as Table 6-2.

For a release to the accessible environment that involves a mix of radionuclides, the limits in Table 6-2 are used to determine a normalized release (nR) of radionuclides for comparison with the release limits

$$nR = \sum_i \left(Q_i / L_i\right)\left(1 \times 10^6\ Ci/C\right), \tag{6.1}$$

where:

- Q_i = cumulative release in curies (Ci) of radionuclide i into the accessible environment during the 10,000-year period following repository closure.
- L_i = release limit in curies for radionuclide i given in
- C = amount of TRU waste curies to be emplaced in the repository (as described in Section 4.1, TRU wastes contain alpha-emitting transuranic radionuclides with half-lives greater than 20 years).

As indicated in Note 1(e) to Table 1 in Appendix A of 40 CFR Part 191, the "other unit of waste" for TRU waste shall be "an amount of transuranic wastes containing 1 million curies of alpha-emitting transuranic radionuclides with half-lives greater than 20 years."

PAs are the basis for addressing the containment requirements. 40 CFR § 191.12 defines performance as follows:

> "Performance assessment" means an analysis that: (1) identifies the processes and events that might affect the disposal system; (2) examines the effects of these processes and events on the performance of the disposal system; and (3) estimates the cumulative releases of radionuclides, considering the associated uncertainties, caused by all significant processes and events.

The DOE's methodology for PA uses information about the disposal system and the waste to evaluate performance in a regulatory context over the 10,000-year regulatory time period.

The general theory for conducting a PA is presented in this section together with details specific to the PA conducted for the WIPP. Figure 6-2 illustrates the general, high-level steps used by the DOE for this final PA of the WIPP. In this figure, the sections of this chapter are indicated that discuss these steps in detail, and several important features of the WIPP PA are shown.

Table 6-2. Release Limits for the Containment Requirements (EPA 1985, Appendix A, Table 1)

Radionuclide	Release Limit L_i per 1,000 MTHM [1] or Other Unit of Waste (curies)
^{241}Am or ^{243}Am	100
^{14}C	100
^{135}Cs or ^{137}Cs	1,000
^{129}I	100
^{237}Np	100
^{238}Pu, ^{239}Pu, ^{240}Pu, or ^{242}Pu	100
^{226}Ra	100
^{90}Sr	1,000
^{99}Te	10,000
^{230}Th or ^{232}Th	10
^{126}Sn	1,000
^{233}U, ^{234}U, ^{235}U, ^{236}U, or ^{238}U	100
Any other alpha-emitting radionuclide with a half-life greater than 20 years	100
Any other radionuclide with a half-life greater than 20 years that does not emit alpha particles	1,000

[1] Metric tons of heavy metal exposed to a burnup between 25,000 megawatt-days per metric ton of heavy metal (MWd/MTHM) and 40,000 MWd/MTHM.

Section 6.1 presents the basis for the methodology shown in Figure 6-2. Section 6.1.1 presents the conceptualization of risk, Section 6.1.2 discusses the characterization of uncertainty in risk, Section 6.1.3 discusses regulatory criteria for the quantification of risk, Section 6.1.4 discusses calculation of risk, and Section 6.1.5 discusses techniques for probabilistic analysis.

6.1.1 Conceptualization of Risk

The WIPP PA is fundamentally concerned with evaluating risk, for which comparative measures are defined by regulatory standards. The DOE uses a conceptualization for risk similar to that developed for risk assessments of nuclear power plants. This description provides a structure on which both the representation and calculation of risk can be based.

Kaplan and Garrick (1981, 11-12) have represented risk as a set of ordered triples. The DOE uses this representation and defines risk to be a set R of the form

$$R = \left[\left(S_i, pS, \mathbf{cS}_i \right), i = 1, \ldots, nS \right], \tag{6.2}$$

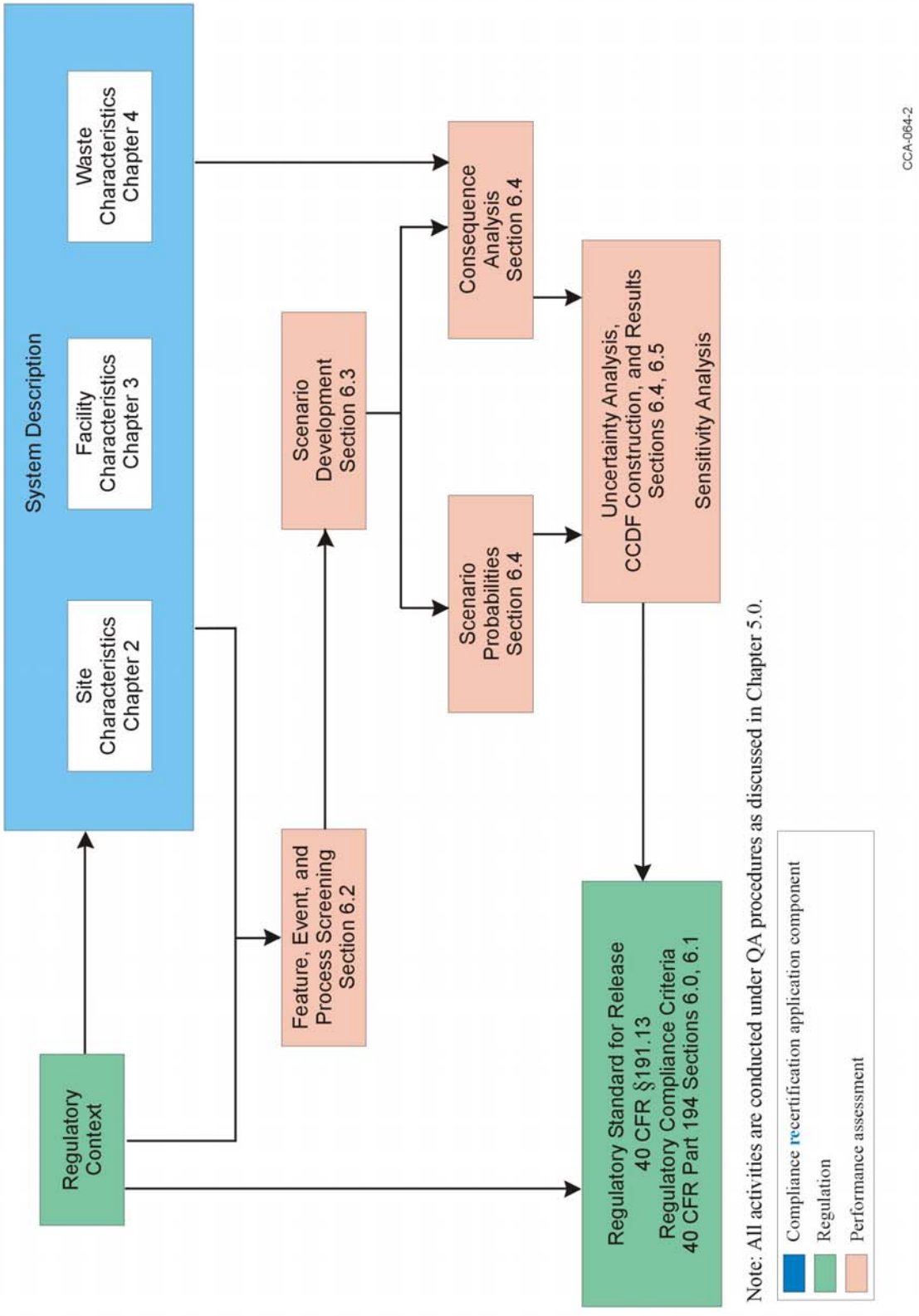

Figure 6-2. Methodology for PA of the WIPP

where

S_i	=	a set of similar occurrences
pS_i	=	probability that an occurrence in set S_i will take place
cS_i	=	a vector of consequences associated with S_i
nS	=	number of sets selected for consideration

and the sets S_i have no occurrences in common (that is, the S_i are disjoint sets). This representation formally decomposes risk into what can happen (the S_i), how likely things are to happen (the pS_i), and the consequences of what can happen (the cS_i). In the WIPP PA, the S_i are scenarios, the pS_i are scenario probabilities, and the vector cS_i contains consequences associated with scenario S_i. Scenario development for the WIPP is discussed in Sections 6.1.2, 6.2, and 6.3. Scenario probabilities and consequence determination are discussed in Section 6.4.

As discussed in the following sections, risk in the set R can be displayed using CCDFs, as required by the EPA. As stated in 40 CFR § 194.34(a),

> The results of performance assessments shall be assembled into "complementary, cumulative distribution functions" (CCDFs) that represent the probability of exceeding various levels of cumulative release caused by all significant processes and events.

In the context of Equation (6.2), CCDFs provide information about the consequences cS_i and the probabilities pS_i associated with the scenarios S_i. The probability that cS exceeds a specific consequence value x is determined by the CCDF F defined by

$$F(x) = \sum_{j=i}^{nS} pS_j, \tag{6.3}$$

where the particular consequence result cS under consideration is ordered so that $cS_i \le cS_{i+1}$ for $i = 1, \ldots, nS-1$, and i is the smallest integer such that $cS_i > x$. The function F represents the probabilities that consequence values plotted on the abscissa will be exceeded. An example estimation of F is shown in Figure 6-3. The steps in the CCDF shown in Figure 6-3 result from the evaluation of F with a discrete number of possible occurrences (that is, futures) represented in the sets S_i. Unless the underlying processes are inherently disjoint, using more sets S_i will tend to reduce the size of these steps and, in the limit, result in a smooth curve. To avoid a broken appearance, the DOE plots estimated CCDFs with vertical lines added at the discontinuities.

6.1.2 Characterization of Uncertainty in Risk

Uncertainty in the analysis can be either stochastic or subjective. Stochastic uncertainty derives from lack of knowledge about the future. Subjective uncertainty derives from lack of knowledge about quantities, properties, or attributes believed to have single or certain values. Stochastic uncertainty can be further subdivided into completeness, aggregation, and stochastic variation. Completeness refers to the extent that a PA includes all possible occurrences that could affect performance for the system under consideration. In terms of the risk representation in Equation (6.2), completeness deals with whether all significant occurrences are included in the union of the sets S_i. The DOE addresses completeness in its development of scenarios, discussed here and

in Sections 6.2 and 6.3. Aggregation refers to the division of the possible occurrences into the sets S_i. Resolution is lost if the S_i are defined too coarsely (for example, if nS is too small). Computational efficiency is affected if nS is too large. Aggregation gives rise to the steps in a single CCDF, as shown in Figure 6-3. The DOE addresses aggregation uncertainty in Sections 6.1.4 and 6.4.13. Stochastic variation is represented by the probabilities pS_i, which are functions of the many factors that affect the occurrence of the individual sets S_i. The DOE addresses stochastic variation in Sections 6.1.4 and 6.4.12.

Stochastic uncertainty is taken into account in PA by evaluating the probability of future events (for example, by assuming that the occurrence of certain future events will be random in space and time), and by considering imprecisely known system properties directly associated with the future events. These imprecisely known system properties can be expressed as variables represented by the vector

$$x_{st} = [x_{st,1}, x_{st,2}, \ldots, x_{st,nV(st)}] , \quad (6.4a)$$

where each $x_{st,j}$ [j = 1, 2, …, nV(st)] is an imprecisely known property required in the analysis, nV is the total number of such properties associated with stochastic uncertainty, and the subscript st denotes stochastic uncertainty.

Subjective uncertainty results from incomplete data or measurement uncertainty. These uncertainties are addressed in Section 6.4. Subjective quantities, properties, or attributes may be associated with stochastic uncertainties (events that might occur in the future).

Subjective uncertainty can be characterized in PA by considering system properties that are imprecisely known. These imprecisely known system properties can be expressed as variables represented by vectors

$$x_{su} = [x_{su,1}, x_{su,2}, \ldots, x_{su,nV(su)}] , \quad (6.4b)$$

where each $x_{su,j}$ [j = 1, 2, …, nV(su)] is an imprecisely known property required in the analysis, nV is the total number of such properties associated with subjective uncertainty, and the subscript su denotes subjective uncertainty.

If the analysis has been developed so that each x_j is a quantity for which the overall analysis requires a single value, the representation for risk in Equation 6.2 can be restated as a function of x_{st} and x_{su}:

$$R(x_{su}) = [S_i(x_{su}), pS_i(x_{su}), cS_i(x_{st,i}, x_{su}), i = 1, \ldots, nS(x_{st}, x_{su})] , \quad (6.5)$$

where $x_{st,i}$ is included in S_i. Probability distributions are then assigned to the individual variables $x_{su,j}$ and $x_{st,j}$, as defined in Equation 6.4. These probability distributions are of the form

$$D_{st,1}, D_{st,2}, \ldots, D_{st,nV(st)} , \quad (6.6a)$$

$$D_{su,1}, D_{su,2}, \ldots, D_{su,nV(su)} , \quad (6.6b)$$

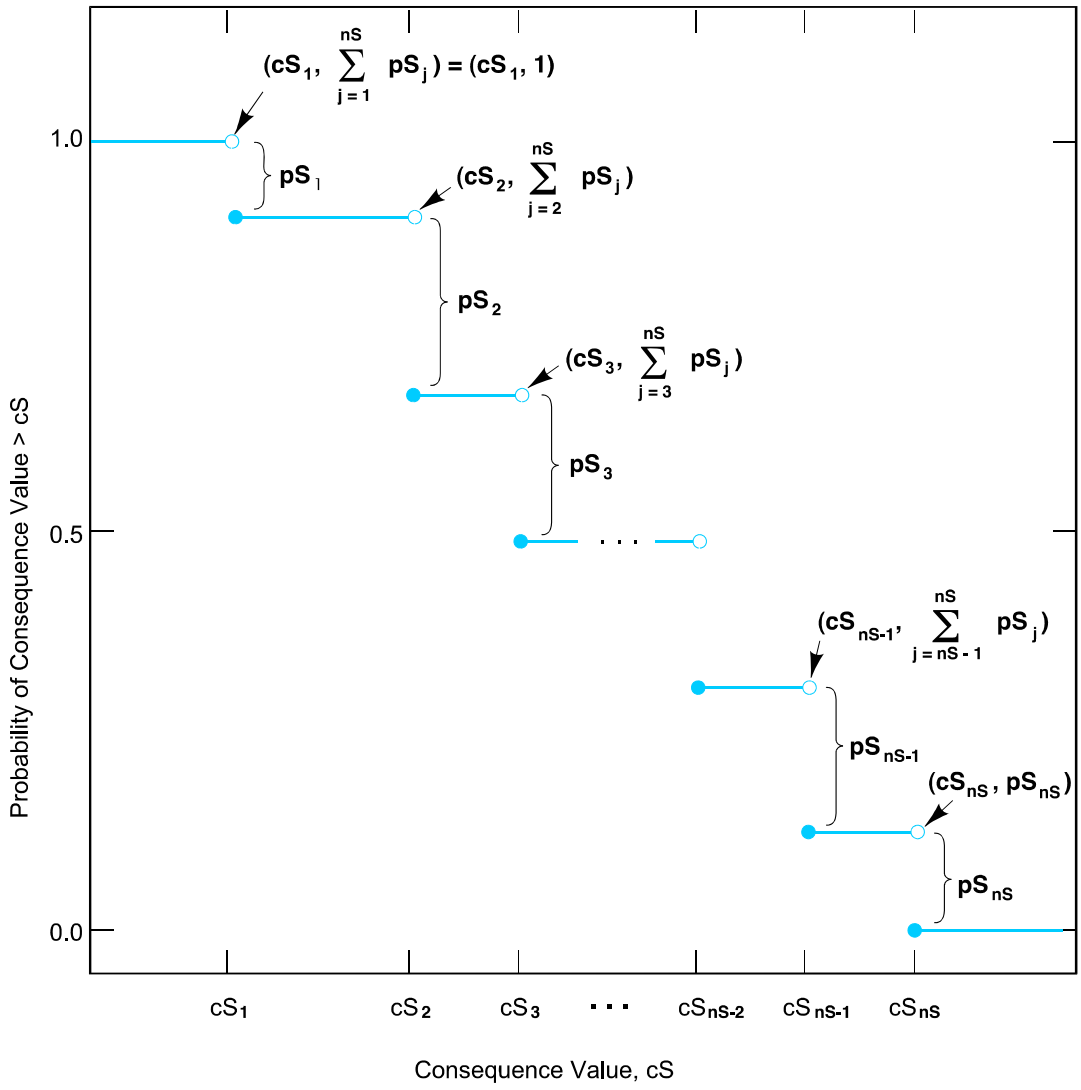

Note: The open and solid circles at the discontinuities indicate the points included on (solid circles) and excluded from (open circles) the CCDF.

CCA-006-2

Figure 6-3. Estimated CCDF For Consequence Results

where the D_js are the distributions developed for the variables x_j, $j = 1, 2,...nV$, and the subscripts *st* and *su* denote distributions associated with x_{st} or x_{su}. The definition of these distributions may also be accompanied by the specification of correlations and various restrictions that further define the possible relations among the x_j. These distributions (along with specified correlations or restrictions) probabilistically specify what the appropriate input to use in the PA calculations might be, given that the analysis is structured so that only one value can be used for each variable, x_j, under consideration for a particular calculation.

Monte Carlo techniques can be used to determine the uncertainty in $R(x_{su})$ associated with both x_{st} and x_{su}. The theory of this technique is similar for characterizing both stochastic and

subjective uncertainty. This technique as applied to determining the risk $R(x_{su})$ associated with x_{su} is developed in the following paragraphs.

Once the distributions in Equation 6.6b have been developed, a sample

$$x_k = (x_{k1}, x_{k2}, \ldots, x_{k,nV}), k = 1, \ldots, nK \quad (6.7)$$

is generated according to the specified distributions and restrictions where nK is the size of the sample. PA calculations are then performed for each sample element x_k, which yields a sequence of risk results of the form

$$R(x_k) = \{[S_i(x_k), pS_i(x_k), cS_i(x_k)], i = 1, \ldots, nS(x_k)\} . \quad (6.8)$$

Each set $R(x_k)$ is the result of one complete set of calculations performed with a set of inputs (that is, x_k) obtained from the distributions assigned in Equation 6.6b. Further, associated with each risk result $R(x_k)$ in Equation 6.8 is a weight[1] that can be used in making probabilistic statements about the distribution of R(x).

A single CCDF can be produced for each set $R(x_k)$ of results shown in Equation 6.8, yielding a family of CCDFs of the form shown in Figure 6-4. The distribution of CCDFs in Figure 6-4 can be summarized with the mean and percentile curves shown in Figure 6-5. These curves result from connecting the mean and percentile values corresponding to individual consequence values on the abscissa of Figure 6-4. The percentile curves probabilistically represent the estimated exceedance probability given a fixed consequence value. For example, the probability is 0.8 that the exceedance probability for a particular normalized release is located between the 10 and 90 percentile curves.

To summarize, considering a family of CCDFs allows a distinction between stochastic uncertainty that controls the shape of a single CCDF and subjective uncertainty that results in a distribution of CCDFs. The stepwise shape of a single CCDF reflects aggregation of future events into similar groups. A family of CCDFs arises from imperfect knowledge of quantifiable properties, or, in other words, subjective uncertainty. The distribution arising from subjective uncertainty involves an infinite number of CCDFs; a family of CCDFs is a sample of finite size.

6.1.3 Regulatory Criteria for the Quantification of Risk

The representation for risk in Equation 6.2 provides a conceptual basis for calculating the CCDF of normalized releases specified in 40 CFR § 194.34(a). Further, this representation provides a structure that can be used for both the incorporation of uncertainties and the representation of the effects of uncertainties, as stated in 40 CFR § 194.34.

[1] In random or Latin hypercube sampling (LHS), this weight is the reciprocal of the sample size (that is, $1/nK$) and can be used in estimating means, cumulative distribution functions, and other statistical properties. This weight is often referred to as the probability for each observation (that is, sample x_k). However, this usage is not technically correct. If continuous distributions are involved, the actual probability of each observation is zero.

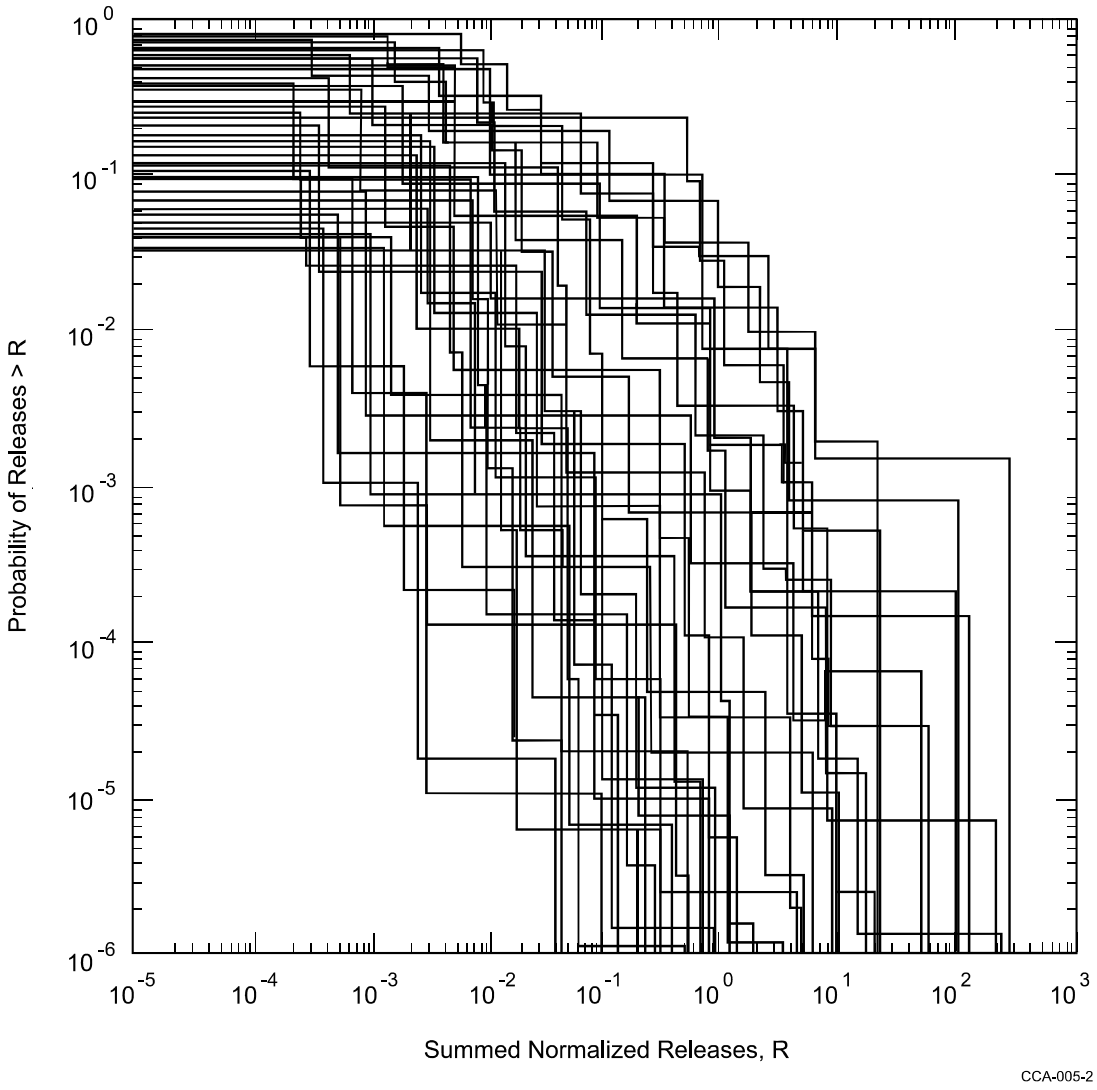

Figure 6-4. Example Distribution of a Family of CCDFs Obtained by Sampling Imprecisely Known Variables

In 40 CFR § 194.34(b), the EPA states that "probability distributions for uncertain disposal system parameter values used in performance assessments shall be developed and documented in any compliance application." The treatment of uncertain parameter values in the performance assessment is discussed in Sections 6.1.4, 6.1.5, and 6.4. Further discussion of distributions assigned to uncertain parameter values is provided in Appendix PA, Attachment PAR.

In 40 CFR § 194.34(c), the EPA states that documentation of the computational techniques used to generate random samples shall be provided. The sampling techniques used are discussed in Section 6.1.5.2. Sampled values are reproduced in tabular form in Appendix PA, Attachment PAR.

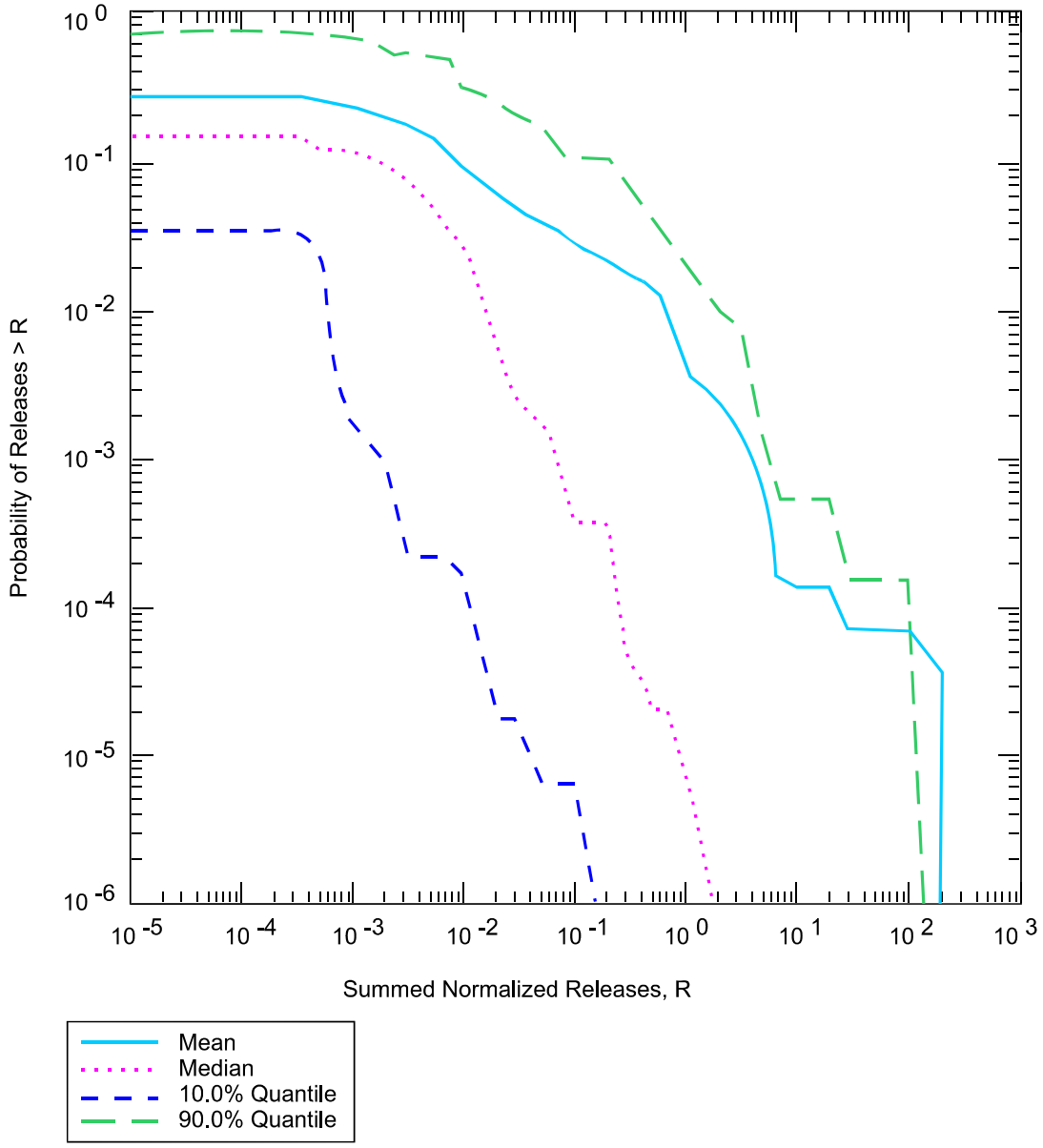

Note: The curves in this figure were obtained by calculating the mean and the indicated percentiles for each consequence value on the abscissa in Figure 6-3. The 90th-percentile curve crosses the mean curve because of highly skewed distributions for exceedance probability. This skew also results in the mean curve being above the median curve.

CCA-007-2

Figure 6-5. Example Summary Curves Derived from an Estimated Distribution of CCDFs

In 40 CFR § 194.34(d), the EPA states that "the number of CCDFs generated shall be large enough such that, at cumulative releases of 1 and 10, the maximum CCDF generated exceeds the 99th percentile of the population of CCDFs with at least a 0.95 probability." The CCDFs resulting from this PA are provided in Section 6.5, with a demonstration that the total number of CCDFs is sufficiently large.

In 40 CFR § 194.34(e), the EPA states that "any compliance application shall display the full range of CCDFs generated." The full range of CCDFs generated is displayed in Section 6.5.

In 40 CFR § 194.34(f), the EPA states that "any compliance application shall provide information which demonstrates that there is at least a 95 percent level of confidence that the mean of the population of CCDFs meets the containment requirements . . . ." Section 6.5 contains a display of the mean CCDF and evidence demonstrating level of confidence.

6.1.4 Calculation of Risk

The methodology presented in Sections 6.1.1and 6.1.2 is based on the work of Kaplan and Garrick (1981) and is one way to estimate the effects of uncertain but characterizable futures. In the Kaplan and Garrick (1981) procedure, the possible futures are defined as literal entities (S_i), and each is associated with a probability of occurrence (pS_i) and a consequence of occurrence (cS_i).

Calculating the probabilities and consequences of future occurrences begins by determining the sets S_i, which are the scenarios to be analyzed. Scenarios are determined through a formal process similar to that proposed by Cranwell et al. (1990, 5-10) and the process used in preliminary PAs for the WIPP. This process has four steps.

1. The FEPs potentially relevant to the WIPP are identified and classified.

2. Certain FEPs are eliminated according to well-defined screening criteria as unimportant or irrelevant to the performance of the WIPP.

3. Scenarios are formed from the remaining FEPs in the context of regulatory performance criteria.

4. Scenarios are specified for consequence analysis.

Through steps 1 and 2 of the scenario development process, the DOE identifies "all significant processes and events that may affect the disposal system" as required by 40 CFR § 191.13(a) and as further addressed in 40 CFR § 194.32. These steps are described in Section 6.2. The grouping of retained FEPs to form scenarios, and the specification of scenarios for consequence analysis, is presented in Section 6.3.

These four steps were used to develop the PA and compliance assessment used in the CCA. This CRA uses the same PA method and basis as that used in the CCA. The steps outlined here were revisited to determine that the basis for the original PA has not been impacted by events, additional information, or regulatory changes that have occurred since the original demonstration of compliance with EPA's disposal standard (as discussed in the following paragraphs).

As discussed in Section 6.2, the DOE eveloped a comprehensive initial list of FEPs for PA. This list assured that the identification of significant processes and events is complete, potential interactions between FEPs are not overlooked, and responses to possible questions are available and well documented. For the CRA-2004, DOE has revisited the initial FEPs list to determine if the screening decisions should be changed as a result of information collected since the EPA certification decision. Specifically, 120 FEPs required updates to their FEP descriptions and/or

screening arguments, and seven of the original baseline FEP screening decisions required a change from their original screening decision. Four of the original baseline FEPs have been deleted or combined with other closely related FEPs. Finally, two new FEPs have been added to the baseline. These two FEPs were previously addressed in an existing FEP; they have been separated for clarity. Table SCR-1 summarizes the changes in the FEP baseline since the CCA. The evaluation of the CCA FEPs list is discussed in Appendix PA, Attachment SCR.

Once scenarios are defined, a calculational methodology for evaluating their consequences must be developed. The calculational methodology must address stochastic uncertainty related to aggregation and stochastic variation, and subjective uncertainty, because of (for example) measurement difficulties or incomplete data. The DOE uses a system of linked computer models to calculate scenario consequences cS_i. As discussed in Section 6.4, these computer models are based on conceptual models that describe the processes relevant to disposal system performance for the defined scenarios. These conceptual models are, in turn, based on site-specific experimental and observational data and the general scientific understanding of natural and engineered systems.

For practical purposes, the DOE separates the calculation of risk because of stochastic uncertainty (represented in an individual CCDF) from risk because of subjective uncertainty (represented by the family of CCDFs). This can be represented mathematically as a double integral of a function with the function representing the probability of exceedance associated with any particular consequence. The inner integral evaluates stochastic uncertainty, or the probability of exceedance associated with any particular consequence. The outer integral evaluates subjective uncertainty and leads to a distribution of exceedance probabilities for any given consequence value. An analytical method for its solution is not available because of the complexity of this double integral for the WIPP. Instead, the DOE approximates the solution of this double integral with a linked system of computer codes. In this computational framework, thePA analysis can be thought of as a double sum, presented here in a stylized form for clarity as

$$\sum_{su}\sum_{st} F(x). \tag{6.9}$$

Here, F(x) is a procedure for estimating the normalized release to the accessible environment associated with each scenario that could occur at the WIPP site. The inner sum denoted with the subscript st is a probabilistic characterization of the uncertainty associated with parameters used to characterize stochastic uncertainty (the x_{st} and D_{st} in Equations 6.4a and 6.6a, respectively). It is the evaluation of F(x) through the inner sum that develops an individual CCDF, as shown in Figure 6-3. The outer sum denoted with the subscript su is a probabilistic characterization of the uncertainty associated with parameters used to characterize subjective uncertainty (the x_{su} and D_{su} in Equations 6.4b and 6.6b, respectively). It is the combined evaluation in the outer sum of the inner sum with F(x) that develops the family of CCDFs, as shown in Figure 6-4.

A separate probabilistic analysis is required to evaluate each sum. Associated with each analysis are parameter distributions representing uncertainty (the D_{st} and D_{su} of Equations 6.6a and 6.6b). For example, uncertainty in the number and time of intrusion boreholes may be associated with the inner sum. The outer sum includes a probabilistic characterization of site properties, such as the permeability of specific rock types.

For the methodology adopted by the DOE to evaluate stochastic uncertainty in the inner sum, consequence calculations are required for model configurations with a set of fixed values for subjective parameters x_{su} taken from their distributions D_{su}, as well as for defined sequences and times of events associated with scenarios. These calculations are referred to in Section 6.4.11 and later sections as deterministic calculations (or deterministic futures). To evaluate stochastic uncertainty and construct a CCDF, the consequences of futures generated probabilistically by random sampling (probabilistic futures) are evaluated in the context of these deterministic futures. This process is discussed in detail in Sections 6.4.12 and 6.4.13.

In certain cases, it may not be obvious whether a particular uncertainty should be classified as subjective or stochastic. For example, whether currently observed geologic properties persist through time could be thought of as either subjective or stochastic uncertainty. For the WIPP, the DOE treats uncertainty associated with significant future human actions as stochastic (for example, drilling for natural resources), and uncertainty in disposal system properties subject to ongoing physical processes as subjective (for example, climate change or gas generation). In particular, DOE's formal separation of evaluating stochastic uncertainty from subjective uncertainty into different probabilistic analyses allows clear understanding of how a particular uncertainty is incorporated.

Once the scenarios are determined and their consequences calculated using the appropriate conceptual and computational models, scenario probabilities must be determined for a CCDF to be constructed. This process is described in Section 6.4.12. CCDF construction is also described in Section 6.4.13.

6.1.5 Techniques for Probabilistic Analysis

Once scenarios are defined, conceptual models are defined, and the computational modeling system developed, DOE uses probabilistic techniques to evaluate the double sum presented above. Monte Carlo analysis is the technique used for probabilistic analysis of the WIPP. Monte Carlo analyses can involve five steps:

1. selecting the variables to be examined and the ranges and distributions for their possible values,
2. generating the samples to be analyzed,
3. propagating the samples through the analysis,
4. performing the uncertainty analysis, and
5. conducting a sensitivity analysis.

These steps are described briefly in the following sections.

Within the general framework of Monte Carlo analysis, PA uses two methods, random sampling and Latin Hypercube Sampling (LHS), to generate the samples propagated through the model system. Random sampling is used to generate samples for stochastic uncertainty, and LHS is used to characterize subjective uncertainty. Each of these methods uses the five steps

summarized in the preceding paragraph, but differs in steps (2) through (5) to account for both subjective and stochastic uncertainty.

6.1.5.1 Selection of Variables and Their Ranges and Distributions

Monte Carlo analyses use a probabilistic procedure for the selection of model input. Therefore, the first step in a Monte Carlo analysis is to select uncertain variables and assign ranges and distributions that characterize them. These variables are typically input parameters to computer models, and the impact of the assigned ranges and distributions can be great; for a given set of conceptual and mathematical models, PA results are largely controlled by the choice of input. Results of uncertainty and sensitivity analyses, in particular, strongly reflect the characterization of uncertainty in the input data.

Information used in the CCA about the ranges and distributions of possible values were drawn from a variety of sources, including field data, laboratory data, and literature. Where sufficient data were not available, the documented solicitation of experts was used. A review process led from the available data to the construction of the distribution functions that characterize uncertainty in input parameters in PA (Appendix PA, Attachment PAR, PAR.2). This addressed the scaling of data collected at experimental scales of observation to the parameter ranges applied to scales of interest in the disposal system. The nature of the available data and the type of analysis unavoidably involved some judgment from investigators and analysts involved. A discussion of parameter ranges developed by this process for the CRA-2004 PA is provided in Appendix PA, Attachment PAR (Section 3). The QA procedures associated with this review process are identified in Section 5.4.2 and Appendix PA, Attachment PAR (Section 2).

The outcome of the review process is a cumulative distribution function (CDF) *D(x)* of the form shown in Figure 6-6 for each independent variable of interest. For a particular variable x_j, the function *D* is defined such that

$$\text{prob}(x < x_j \leq x+\Delta x) = D(x+\Delta x) - D(x) . \qquad (6.10)$$

That is, $D(x+\Delta x) - D(x)$ is equal to the probability that the appropriate value for x_j in the particular analysis under consideration falls between x and $x+\Delta x$.

6.1.5.2 Generation of the Sample

Various techniques are available for generating samples from the assigned distribution functions for the variables, including random sampling, stratified sampling, and LHS. The DOE's PA for WIPP uses random sampling and LHS.

Randomly sampling the occurrence of possible future events is used to generate the possible futures (probabilistic futures) that comprise a CCDF. This sampling is used to select values of uncertain parameters associated with future human activities, or in other words, to incorporate stochastic uncertainty into the WIPP PA. This sampling is used for parameters evaluated in the inner sum of the double sum and included in the parameter set x_{st} with associated distributions D_{st}, as shown in Equations 6.4a and 6.6a respectively. Generating futures comprising a CCDF by random sampling, rather than importance or stratified sampling, as used in previous preliminary PAs, largely eliminates errors from aggregation.

LHS, in which the full range of each variable is subdivided into intervals of equal probability and samples are drawn from each interval, is used to select values of uncertain parameters associated with the physical system being simulated. In other words, LHS incorporates subjective uncertainty into the WIPP PA. This sampling is used for parameters that are evaluated in the outer sum of the double sum and are included in the parameter set x_{su} with associated distributions D_{su}, as shown in Equations 6.4b and 6.6b, respectively. The restricted pairing technique of Iman and Conover (1982, 314-319) is used to prevent spurious correlations within the sample.

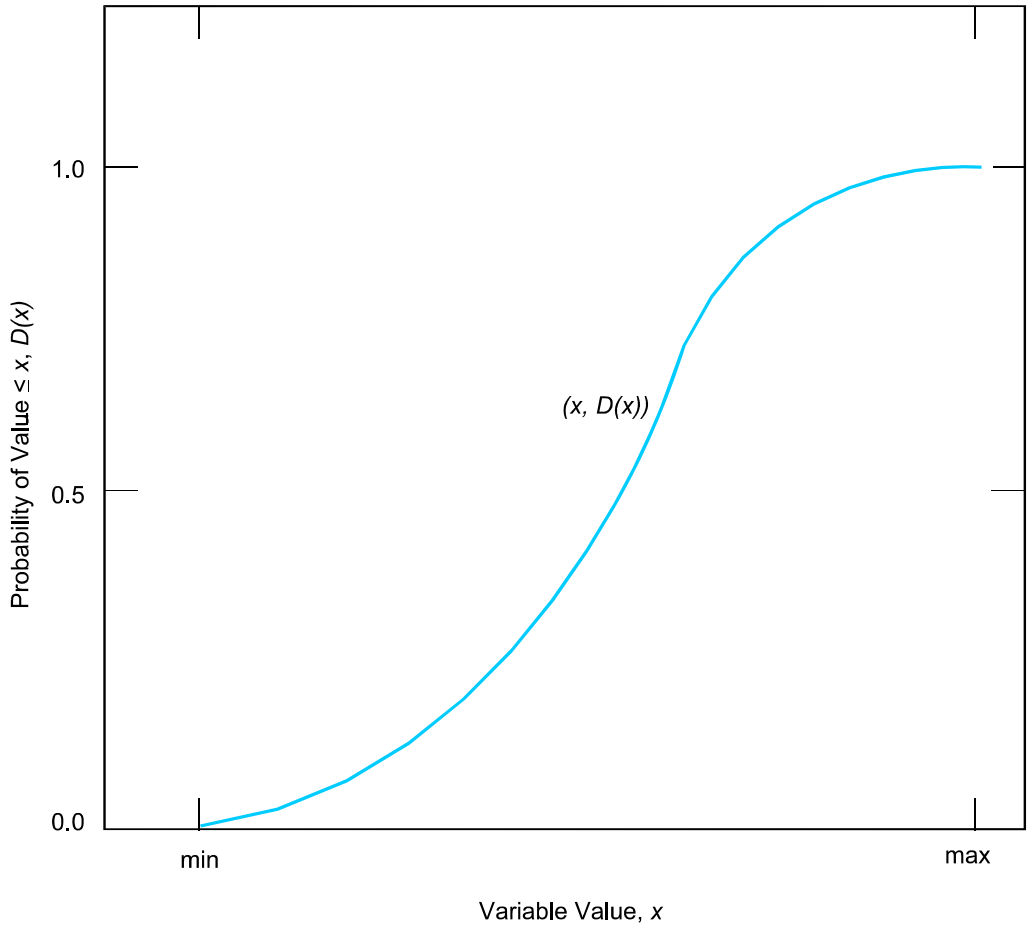

Note: For each value *x* on the abscissa, the corresponding value *D(x)* on the ordinate is the probability that the appropriate value to use in the analysis is less than or equal to *x*.

CCA-008-2

Figure 6-6. Distribution Function for an Imprecisely Known Variable

6.1.5.3 Propagation of the Sample through the Analysis

The next step is the propagation of the sample through the analysis. Each element of the sample is supplied to the model system as input, and the corresponding model system predictions are saved for later use in uncertainty and sensitivity studies. The Software Configuration Management System (SCMS) was developed to facilitate the complex calculations performed by the model system and to store the input and output files from each program.

6.1.5.4 Uncertainty Analysis

Uncertainty analyses evaluate uncertainty in performance estimates that results from uncertainty about imprecisely known input parameters. Once a sample has been generated and propagated through the modeling system, uncertainty in the outcome can be interpreted directly from the display of the results. For the WIPP PA, stochastic uncertainty is represented by the shape of the individual CCDFs displayed in Section 6.5. Subjective uncertainty is represented by the family of CCDFs displayed in Section 6.6.

6.1.5.5 Sensitivity Analysis

Sensitivity analyses determine the contribution of individual input variables to the uncertainty in model predictions. This is the final step in a probabilistic study. Sensitivity analyses can identify parameters for which reductions in uncertainty (that is, narrowing the range of values from which the sample used in the Monte Carlo analysis is drawn) have the greatest potential to increase confidence in the estimate of the disposal system's performance. However, because results of these analyses are inherently conditional on the models, data distributions, and techniques used to generate them, the analyses cannot provide insight on the correctness of the conceptual models and data distributions used. Qualitative judgment about the modeling system must be used with sensitivity analyses to set priorities for PA data acquisition and model development. Sensitivity analyses conducted as part of the WIPP PA are described in Appendix PA.

6.2 Identification and Screening of Features, Events, and Processes

The EPA has provided criteria concerning the scope of PAs in 40 CFR § 194.32. In particular, criteria relating to the identification of potential processes and events that may affect the performance disposal system are provided in Section 194.32(e), which states that

> Any compliance application(s) shall include information which:
>
> (1) Identifies all potential processes, events or sequences and combinations of processes and events that may occur during the regulatory time frame and may affect the disposal system;
>
> (2) Identifies the processes, events or sequences and combinations of processes and events included in performance assessments; and
>
> (3) Documents why any processes, events or sequences and combinations of processes and events identified pursuant to paragraph (e)(1) of this section were not included in performance assessment results provided in any compliance application.

This section, CCA Appendix SCR, and Appendix PA, Attachment SCR fulfill these criteria by documenting DOE's identification, screening, and screening results of all potential processes and events consistent with the criteria specified in 40 CFR § 194.32(e).

As discussed in Section 6.1.4, the first two steps in scenario development involve the identification and screening of FEPs potentially relevant to the performance of the disposal system. This section discusses the development of a comprehensive initial set of FEPs used in the CCA, the methodology and criteria used for screening, the method used to reassess the CCA

FEPs for the CRA-2004, and a summary of the FEPs retained for scenario development. Detailed discussion of the basis for eliminating or retaining particular FEPs is provided in Appendix PA, Attachment SCR. The scenarios formed from retained FEPs are discussed in Section 6.3, and the scenarios specified for consequence analysis are addressed in Section 6.4.12.

The original FEPs generation and screening were documented in the CCA and the resulting FEPs list became the FEPs compliance baseline. The baseline contained 237 FEPs and was documented in Appendix SCR of the CCA. The EPA compliance review of FEPs was documented in EPA's Technical Support Document 194.32: Scope of PA (EPA 1998, V-B-21). The EPA numbered each FEP with a different scheme than the DOE used for the CCA. The DOE has since adopted EPA's numbering scheme.

6.2.1 Identification of Features, Events, and Processes

The first step of the scenario development procedure is identifying and classifying FEPs potentially relevant to the disposal system performance. Catalogs of FEPs have been developed in several national radioactive waste disposal programs, as well as internationally. In constructing a comprehensive list of FEPs for the WIPP, the DOE drew on these other radioactive waste disposal programs.

As a starting point, the DOE assembled a list of potentially relevant FEPs from the compilation developed by Stenhouse et al. (1993) for the Swedish Nuclear Power Inspectorate *Statens Kärnkraftinspektion* (SKI). The SKI list was based on a series of FEP lists developed for other disposal programs and is considered the best documented and most comprehensive starting point for the WIPP. For the SKI study, an initial, raw FEP list was compiled from nine different FEP identification studies (Table 6-3). No additional lists of potentially relevant FEPs have been identified since the initial certification.

The compilers of the SKI list eliminated a number of FEPs as irrelevant to the particular disposal concept under consideration in Sweden; these FEPs were reinstated for the WIPP effort, and several FEPs on the SKI list were subdivided to facilitate WIPP screening. Finally, to ensure comprehensiveness, other FEPs specific to the WIPP were added based on a review of key project documents and a broad examination of the preliminary WIPP list by both project participants and stakeholders. The initial, unedited list is contained in CCA Appendix SCR, Attachment 1. The initial, unedited FEP list was restructured and revised to derive the comprehensive WIPP FEP list in the CCA. The number of FEPs was reduced to 237 to avoid the ambiguities caused by using a generic list. Restructuring the list did not remove any substantive issues from the discussion. As discussed in more detail in CCA Appendix SCR, Attachment 1, the following steps were used to create the WIPP FEP list in the CCA.

- References to subsystems were eliminated because the SKI subsystem classification was not appropriate for the WIPP disposal concept. For example, in contrast to the Swedish disposal concept, canister integrity does not have a role in postoperational performance of the WIPP, and the terms near-field, far-field, and biosphere are not unequivocally defined for the WIPP site.

- Duplicate FEPs were eliminated. Duplicate FEPs arose in the SKI list because individual FEPs could act in different subsystems. FEPs have a single entry in this application list whether they are applicable to several parts of the disposal system, or to a single part only. For example, the FEP *Gas Effects: Disruption* appears in the seals, backfill, waste, canister, and near-field subsystems in the initial FEP list. These FEPs are represented by the single FEP *Disruption Due to Gas Effects* for this application.

Table 6-3. FEP Identification Studies Used in the SKI Study

Study	Country	Number of FEPS Identified
Atomic Energy of Canada Limited (AECL) study of disposal of spent fuel in crystalline rock (Goodwin et al. 1994)	Canada	275
SKI & Swedish Nuclear Fuel and Waste Management Company (SKB) study of disposal of spent fuel in crystalline rock (Andersson 1989)	Sweden	157
National Cooperative for the Storage of Radioactive Waste (NAGRA) Project Gewähr study (NAGRA 1985)	Switzerland	44
UK Department of the Environment Dry Run 3 study of deep disposal of low- and intermediate-level waste (L/ILW) (Thorne 1992)	United Kingdom	305
UK Department of Environment assessment of L/ILW disposal in volcanic rock at Sellafield (Miller and Chapman 1992)	United Kingdom	79
UK Nuclear Industry Radioactive Waste Executive (NIREX) study of the deep disposal of L/ILW (Hodgkinson and Sumerling 1989)	United Kingdom	131
Sandia National Laboratories (SNL) study of deep disposal of spent fuel (Cranwell et al. 1990)	United States	29
NEA Working Group on Systematic Approaches to Scenario Development (OECD 1992)	International	122
International Atomic Energy Agency (IAEA) Safety Series (IAEA 1981)	International	56

- FEPs that are not relevant to the WIPP design or inventory were eliminated. Examples include FEPs related to high-level waste, copper canisters, and bentonite backfill.

- FEPs relating to engineering design changes were eliminated because they are not relevant to a compliance application based on the DOE's design for the WIPP. Examples of such FEPs are Design Modifications: Canister and Design Modification: Geometry.

- FEPs relating to constructional, operational, and decommissioning errors were eliminated. The DOE has administrative and quality control procedures to ensure that the facility will be constructed, operated, and decommissioned properly.

- Detailed FEPs relating to processes in the surface environment were aggregated into a small number of generalized FEPs. For example, the SKI list includes the biosphere FEPs *Inhalation of Salt Particles, Smoking, Showers and Humidifiers*, *Inhalation and*

Biotic Material, Household Dust and Fumes, Deposition (wet and dry), Inhalation and Soils and Sediments, Inhalation and Gases and Vapors (indoor and outdoor), and *Suspension in Air*, which are represented by the FEP *Inhalation* in this application.

- FEPs relating to the containment of hazardous metals, volatile organic compounds (VOCs), and other chemicals that are not regulated by 40 CFR Part 191 were not included.

- A few FEPs were renamed to be consistent with terms used to describe specific WIPP processes (for example, *Wicking*, *Brine Inflow*).

6.2.2 Criteria to Screen Features, Events, and Processes and Categorization of Retained Features, Events, and Processes

FEP screening identifies those FEPs that should be accounted for in PA calculations, and those that need not be considered further. The DOE's process of removing FEPs from consideration in PA calculations involved the structured application of explicit screening criteria. The criteria used to screen out FEPs are explicit regulatory exclusions (SO-R), probability (SO-P), or consequence (SO-C). As discussed in Section 6.2.2.1, all three criteria are derived from regulatory requirements. FEPs not screened as SO-R, SO-P, or SO-C have been retained for inclusion in PA calculations and are classified as undisturbed performance (UP) or disturbed performance (DP) FEPs. These screening criteria and FEP classifiers are discussed in this section, and FEP screening is discussed in Sections 6.2.3, 6.2.4, and 6.2.5.

6.2.2.1 Eliminating Features, Events, and Processes Based on Regulation, Probability, or Consequence

Regulation. Specific FEP screening criteria are established by 40 CFR Part 191 and 40 CFR § 194.25, § 194.32 and § 194.54. These criteria relating to the applicability of particular FEPs represent screening decisions made by the EPA. That is, in the process of developing and demonstrating the feasibility of the 40 CFR Part 191 standard and the 40 CFR Part 194 criteria, EPA considered the relevance, consequence, and/or probability of occurrence of particular FEPs and, in so doing, eliminated some FEPs from consideration. For example, 40 CFR § 194.25 outlines consideration of future states. Future human activities are assumed to be as they are today; therefore other regulations that pertain to human activities can be used to screen FEPs (i.e., State and Federal oil well plugging requirements can be used to screen borehole related FEPs). Section 6.2.5 describes the regulatory screening criteria that pertain to limitations on the type of human-initiated events and processes that need be analyzed.

Probability of occurrence of a FEP leading to significant release of radionuclides. Low-probability events can be excluded based on the criterion provided in 40 CFR § 194.32(d), which states that "PAs need not consider processes and events that have less than one chance in 10,000 of occurring over 10,000 years." In practice, for most FEPs screened out on the basis of low probability of occurrence, it has not been possible to estimate a meaningful, quantitative probability. In the absence of quantitative probability estimates, a qualitative argument has been provided.

Potential consequences associated with the occurrence of the FEPs. The DOE identified two applications of this criterion:

1. FEPs can be eliminated from PA calculations on the basis of insignificant consequence. Consequence can refer to effects on the repository or site or to radiological consequence. In particular, 40 CFR § 194.34(a) states that "The results of PAs shall be assembled into "complementary, cumulative distribution functions" (CCDFs) that represent the probability of exceeding various levels of cumulative release caused by all significant processes and events" (emphasis added). The DOE has omitted events and processes from PA calculations where there is a reasonable expectation that the remaining probability distribution of cumulative releases would not be significantly changed by such omissions.

2. FEPs that are potentially beneficial to subsystem performance may be eliminated from PA calculations, if necessary, to simplify the analysis. This argument may be used when there is uncertainty as to exactly how the FEP should be incorporated into assessment calculations or when incorporation would incur unreasonable difficulties.

In some cases, the effects of a particular event or process, although not necessarily insignificant, can be shown to lie within the range of uncertainty of another FEP already accounted for in the PA calculations. In such cases, the event or process may be considered implicitly included in PA calculations, within the range of uncertainty associated with the included FEP.

The distinctions between the screened out-regulation (SO-R), screened out-probability (SO-P), and screened out-consequence (SO-C) classifications are summarized in Figure 6-7. Although some FEPs could be eliminated from PA calculations based on more than one criterion, the most practical screening criterion was used for classification. In particular, a regulatory screening classification was used in preference to a probability or consequence screening classification, as illustrated in Figure 6-7. FEPs that were not screened out based on any one of the three criteria are included in the PA.

6.2.2.2 Undisturbed Performance Features, Events, and Processes

FEPs classified as UP are accounted for in calculations of undisturbed performance of the disposal system. Undisturbed performance is defined in 40 CFR § 191.12 as "the predicted behavior of a disposal system, including consideration of the uncertainties in predicted behavior, if the disposal system is not disrupted by human intrusion or the occurrence of unlikely natural events." The UP FEPs are accounted for in the PA calculations to evaluate compliance with the Containment Requirements in 40 CFR § 191.13.

6.2.2.3 Disturbed Performance Features, Events, and Processes

FEPs classified as DP are accounted for only in assessment calculations for DP. The DP FEPs that remain following the screening process relate to the potential disruptive effects of future drilling and mining events in the controlled area. Consideration of both DP and UP FEPs is required to evaluate compliance with 40 CFR § 191.13.

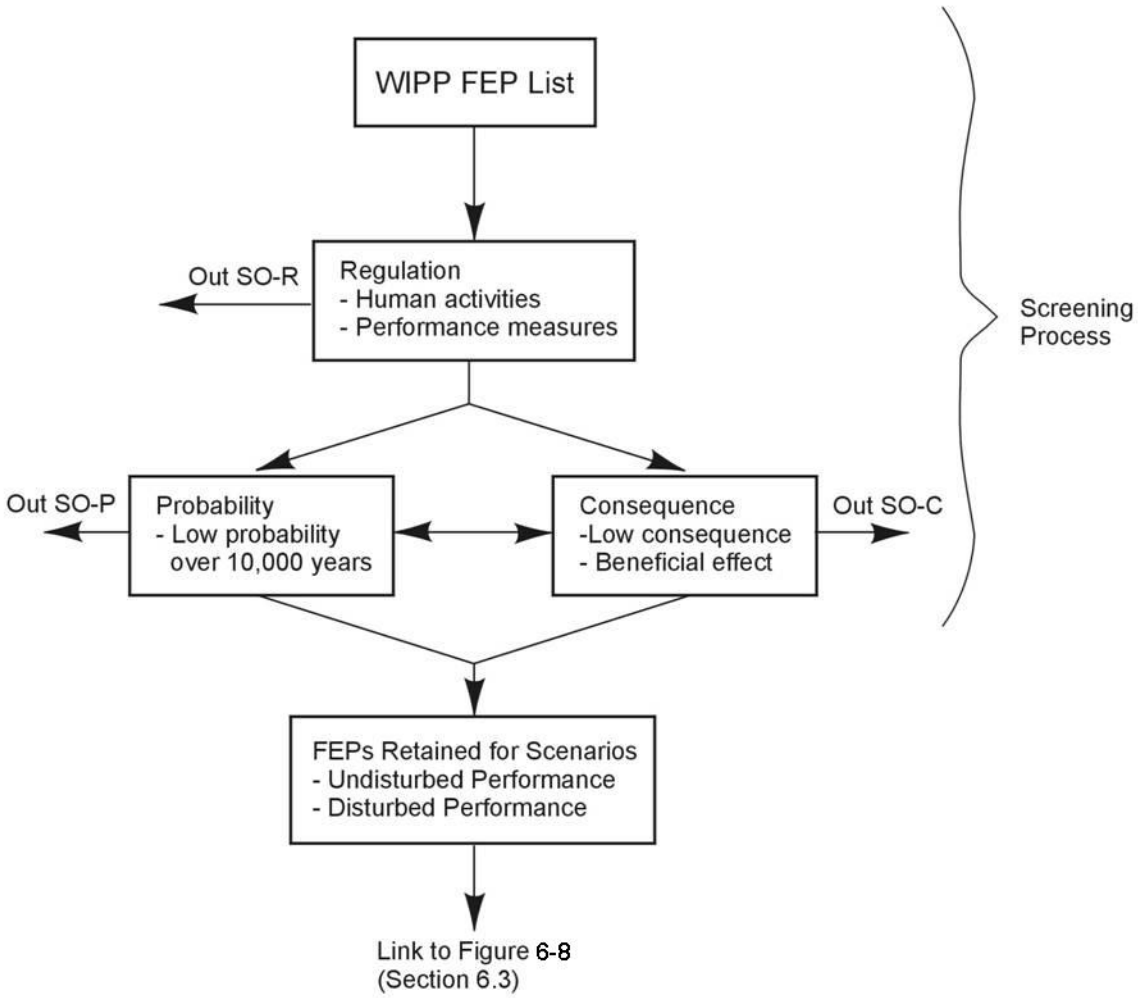

Figure 6-7. Screening Process Based on Screening Classifications

In the following sections, FEPs are discussed under the categories Natural FEPs, Waste- and Repository-Induced FEPs, and Human-Initiated Events and Processes (EPs).

This also allows an evaluation of compliance with the individual dose criterion in 40 CFR § 191.15 and the groundwater protection requirements in 40 CFR § 191.24 (see Chapter 8.0).

6.2.3 Natural Features, Events, and Processes

This subsection briefly discusses natural FEPs with the potential to affect long-term performance of the WIPP disposal system. These FEPs and their screening classifications are listed in Table 6-4; the DOE's detailed screening arguments for natural FEPs are contained in Appendix PA, Attachment SCR. Screening natural FEPs fulfills, in conjunction with the PA calculations, the criterion of the Future States Assumptions in 40 CFR § 194.25(b) that DOE shall "document in any compliance application, to the extent practicable, effects of potential future hydrogeologic, geologic and climatic conditions on the disposal system over the regulatory time frame."

Consistent with Section 194.32(d), the DOE has screened out several natural FEPs from PA calculations based on a low probability of occurrence at or near the WIPP site. In particular, natural events for which there is no evidence indicating that they have occurred within the Delaware Basin were screened on this basis. In this analysis, the probabilities of these events occurring are assumed to be zero. Quantitative, nonzero probabilities for such events, based on numbers of occurrences, cannot be ascribed without considering regions much larger than the Delaware Basin (see for example, FEP N 40, Impact of a Large Meteorite in Appendix PA, Attachment SCR), thus neglecting established geological understanding of the events and processes that occur within particular geographical provinces. No disruptive natural FEPs are likely to occur during the regulatory time frame that could create new pathways or significantly alter existing pathways.

In considering the overall geological setting of the Delaware Basin, the DOE eliminated many FEPs from PA calculations based on low consequence. Events and processes that have had little effect on the characteristics of the region in the past are expected to be of low consequence for the regulatory time period.

6.2.4 Waste- and Repository-Induced Features, Events, and Processes

The waste- and repository-induced FEPs are those that relate specifically to the waste material, waste containers, shaft seals, MgO, panel closures, repository structures, and investigation boreholes. All FEPs related to radionuclide chemistry and radionuclide migration are included in this category. FEPs related to radionuclide transport from future borehole intersections of the WIPP excavation are defined as waste- and repository-induced FEPs. Waste- and repository-induced FEPs and their screening classification are listed in Table 6-5. The DOE's detailed screening discussions for these FEPs are contained in Appendix PA (Attachment SCR).

The DOE has screened out many FEPs in this category on the basis of low consequence to the performance of the disposal system. For example, the DOE has shown that the heat generated by radioactive decay of emplaced RH- and CH-TRU waste will not increase temperature sufficiently to induce significant thermal convection, thermal stresses and strains, or thermally induced chemical perturbations within the disposal system (see Appendix PA, Attachment SCR, FEP W13 and FEP W72). Also, hydration of the emplaced concrete seals and chemical conditioner will be exothermic, but DOE has shown that the heat generated will not significantly affect the disposal system performance (see Appendix PA, Attachment SCR, FEP W72).

Other waste- and repository-induced FEPs were eliminated from PA calculations based on beneficial effect to the performance of the disposal system, if necessary to simplify the analysis.

Waste- and repository-induced FEPs eliminated on the basis of low probability of occurrence over 10,000 years are generally those for which no mechanisms were identified that

Table 6-4. Natural FEPs and Their Screening Classifications

FEPs	Screening Classification	Comments	FEP Number
GEOLOGICAL FEPS			
Stratigraphy			
Stratigraphy	UP		N1
Brine reservoirs	DP		N2
Tectonics			
Changes in regional stress	SO-C		N3
Regional tectonics	SO-C		N4
Regional uplift and subsidence	SO-C		N5
Structural FEPs			
Deformation			
Salt deformation	SO-P	UP near repository.	N6
Diapirism	SO-P		N7
Fracture development			
Formation of fractures	SO-P	UP near repository.	N8
Changes in fracture properties	SO-C	UP near repository.	N9
Fault movement			
Formation of new faults	SO-P		N10
Fault movement	SO-P		N11
Seismic activity			
Seismic activity	UP		N12
Crustal processes			
Igneous activity			
Volcanic activity	SO-P		N13
Magmatic activity	SO-C		N14
Metamorphism			
Metamorphic activity	SO-P		N15
Geochemical FEPs			
Dissolution			
Shallow dissolution	UP		N16
Deep dissolution	SO-P		N18
Breccia pipes	SO-P		N20
Collapse breccias	SO-P		N21
Mineralization			
Fracture infills	SO-C		N22
SUBSURFACE HYDROLOGICAL FEPS			
Groundwater characteristics			
Saturated groundwater flow	UP		N23
Unsaturated groundwater flow	UP	SO-C in Culebra.	N24
Fracture flow	UP		N25

Table 6-4. Natural FEPs and Their Screening Classifications — Continued

FEPs	Screening Classification	Comments	FEP Number
Density effects on groundwater flow	SO-C		N26
Effects of preferential pathways	UP	UP in Salado and Culebra.	N27
Changes in groundwater flow			
Thermal effects on groundwater flow	SO-C		N28
Saline intrusion	SO-P		N29
Freshwater intrusion	SO-P		N30
Hydrological response to earthquakes	SO-C		N31
Natural gas intrusion	SO-P		N32
SUBSURFACE GEOCHEMICAL FEPS			
Groundwater geochemistry			
Groundwater geochemistry	UP		N33
Changes in groundwater chemistry			
Saline intrusion	SO-C		N34
Freshwater intrusion	SO-C		N35
Changes in groundwater Eh	SO-C		N36
Changes in groundwater pH	SO-C		N37
Effects of dissolution	SO-C		N38
GEOMORPHOLOGICAL FEPS			
Physiography			
Physiography	UP		N39
Meteorite impact			
Impact of a large meteorite	SO-P		N40
Denudation			
Weathering			
Mechanical weathering	SO-C		N41
Chemical weathering	SO-C		N42
Erosion			
Aeolian erosion	SO-C		N43
Fluvial erosion	SO-C		N44
Mass wasting	SO-C		N45
Sedimentation			
Aeolian deposition	SO-C		N46
Fluvial deposition	SO-C		N47
Lacustrine deposition	SO-C		N48
Mass wasting	SO-C		N49
Soil development			
Soil development	SO-C		N50
SURFACE HYDROLOGICAL FEPS			
Fluvial			

Table 6-4. Natural FEPs and Their Screening Classifications — Continued

FEPs	Screening Classification	Comments	FEP Number
Stream and river flow	SO-C		N51
Lacustrine			
Surface water bodies	SO-C		N52
Groundwater recharge and discharge			
Groundwater discharge	UP		N53
Groundwater recharge	UP		N54
Infiltration	UP	UP for climate change effects.	N55
Changes in surface hydrology			
Changes in groundwater recharge and discharge	UP		N56
Lake formation	SO-C		N57
River flooding	SO-C		N58
CLIMATIC FEPs			
Climate			
Precipitation (for example, rainfall)	UP		N59
Temperature	UP		N60
Climate change			
Meteorological			
Climate change	UP		N61
Glaciation			
Glaciation	SO-P		N623
Permafrost	SO-P		N63
MARINE FEPs			
Seas			
Seas and oceans	SO-C		N64
Estuaries	SO-C		N65
Marine sedimentology			
Coastal erosion	SO-C		N66
Marine sediment transport and deposition	SO-C		N67
Sea level changes			
Sea level changes	SO-C		N68
ECOLOGICAL FEPs			
Flora & fauna			
Plants	SO-C		N69
Animals	SO-C		N70
Microbes	SO-C	UP for colloidal effects and gas generation	N71
Changes in flora & fauna			

Table 6-4. Natural FEPs and Their Screening Classifications — Continued

FEPs	Screening Classification	Comments	FEP Number
Natural ecological development	SO-C		N72

Legend:

UP FEPs accounted for in the assessment calculations for undisturbed performance for 40 CFR § 191.13 (as well as 40 CFR § 191.15 and Subpart C of 40 CFR Part 191).

DP FEPs accounted for (in addition to all UP FEPs) in the assessment calculations for disturbed performance for 40 CFR § 191.13.

SO-R FEPs eliminated from PA calculations on the basis of regulations provided in 40 CFR Part 191 and criteria provided in 40 CFR § 194.25, .32 and .54

SO-C FEPs eliminated from PA (and compliance assessment) calculations based on consequence.

SO-P FEPs eliminated from PA (and compliance assessment) calculations based on low probability of occurrence.

Table 6-5. Waste- and Repository-Induced FEPs and Their Screening Classifications

FEPs	Screening Classification	Comments	FEP Number
WASTE AND REPOSITORY CHARACTERISTICS			
Repository characteristics			
Disposal geometry	UP		W1
Waste characteristics			
Waste inventory	UP		W2
Heterogeneity of waste forms	DP		W3
Container characteristics			
Container form	SO-C		W4
Container material inventory	UP		W5
Seal characteristics			
Seal geometry	UP		W6
Seal physical properties	UP		W7
Seal chemical composition	SO-C	Beneficial SO-C	W8
Backfill characteristics			
Backfill physical properties	SO-C		W9
Backfill chemical composition	UP		W10
Postclosure monitoring			
Postclosure monitoring	SO-C		W11
RADIOLOGICAL FEPs			
Radioactive decay			
Radionuclide decay and ingrowth	UP		W12
Heat from radioactive decay			
Heat from radioactive decay	SO-C		W13
Nuclear criticality			
Nuclear criticality: heat	SO-P		W14
Radiological effects on material properties			
Radiological effects on waste	SO-C		W15
Radiological effects on containers	SO-C		W16
Radiological effects on seals	SO-C		W17
GEOLOGICAL AND MECHANICAL FEPs			
Excavation-induced fracturing			
Disturbed rock zone	UP		W18
Excavation-induced changes in stress	UP		W19
Rock creep			
Salt creep	UP		W20
Changes in the stress field	UP		W21
Roof falls			

Table 6-5. Waste- and Repository-Induced FEPs and Their Screening Classifications — Continued

FEPs	Screening Classification	Comments	FEP Number
Roof falls	UP		W22
Subsidence			
Subsidence	SO-C		W23
Large scale rock fracturing	SO-P		W24
Effects of fluid pressure changes			
Disruption due to gas effects	UP		W25
Pressurization	UP		W26
Effects of explosions			
Gas explosions	UP		W27
Nuclear explosions	SO-P		W28
Thermal effects			
Thermal effects on material properties	SO-C		W29
Thermally induced stress changes	SO-C		W30
Differing thermal expansion of repository components	SO-C		W31
Mechanical effects on material properties			
Consolidation of waste	UP		W32
Movement of containers	SO-C		W33
Container integrity	SO-C	Beneficial SO-C	W34
Mechanical effects of backfill	SO-C		W35
Consolidation of seals	UP		W36
Mechanical degradation of seals	UP		W37
Underground boreholes	UP		W39
SUBSURFACE HYDROLOGICAL AND FLUID DYNAMICAL FEPs			
Repository-induced flow			
Brine inflow	UP		W40
Wicking	UP		W41
Effects of gas generation			
Fluid flow due to gas production	UP		W42
Thermal effects			
Convection	SO-C		W43
GEOCHEMICAL AND CHEMICAL FEPs			
Gas generation			
Microbial gas generation			
Degradation of organic material	UP		W44
Effects of temperature on microbial gas generation	UP		W45
Effects of pressure on microbial gas generation	SO-C		W46

Table 6-5. Waste- and Repository-Induced FEPs and Their Screening Classifications — Continued

FEPs	Screening Classification	Comments	FEP Number
Effects of radiation on microbial gas generation	SO-C		W47
Effects of biofilms on microbial gas generation	UP		W48
Corrosion			
Gases from metal corrosion	UP		W49
Galvanic coupling	SO-C		W50
Chemical effects of corrosion	UP		
Radiolytic gas generation			
Radiolysis of brine	SO-C		W52
Radiolysis of cellulose	SO-C		W53
Helium gas production	SO-C		W54
Radioactive gases	SO-C		W55
Chemical speciation			
Speciation	UP	UP in disposal rooms and Culebra. SO-C elsewhere, and beneficial SO-C in cementitious seals.	W56
Kinetics of speciation	SO-C		W57
Precipitation and dissolution			
Dissolution of waste	UP		W58
Precipitation	SO-C	Beneficial SO-C	W59
Kinetics of precipitation and dissolution	SO-C	Kinetics of waste dissolution is a beneficial SO-C	W60
Sorption			
Actinide sorption	UP	UP in the Culebra and Dewey Lake. Beneficial SO-C elsewhere	W61
Kinetics of sorption	UP		W62
Changes in sorptive surfaces	UP		W63
Oxidation-reduction chemistry			
Effect of metal corrosion	UP		W64
Oxidation-reduction fronts	SO-P		W65
Oxidation-reduction kinetics	UP		W66
Localized reducing zones	SO-C		W67
Organic complexation			
Organic complexation	UP		W67
Organic ligands	UP		W69
Humic and fulvic acids	UP		W70
Kinetics of organic complexation	SO-C		W71

Table 6-5. Waste- and Repository-Induced FEPs and Their Screening Classifications — Continued

FEPs	Screening Classification	Comments	FEP Number
Exothermic reactions			
Exothermic reactions	SO-C		W72
Concrete hydration	SO-C		W73
Chemical effects on material properties			
Chemical degradation of seals	UP		W74
Chemical degradation of backfill	SO-C		W75
Microbial growth on concrete	UP		W76
CONTAMINANT TRANSPORT MODE FEPs			
Solute transport			
Solute transport	UP		W77
Colloid transport			
Colloid transport	UP		W78
Colloid formation and stability	UP		W79
Colloid filtration	UP		W80
Colloid sorption	UP		W81
Particulate transport			
Suspensions of particles	DP	SO-C for undisturbed conditions	W82
Rinse	SO-C		W83
Cuttings	DP	Repository intrusion only	W84
Cavings	DP	Repository intrusion only	W85
Spallings	DP	Repository intrusion only	W86
Microbial transport			
Microbial transport	UP		W87
Biofilms	SO-C	Beneficial SO-C	W88
Gas transport			
Transport of radioactive gases	SO-C		W89
CONTAMINANT TRANSPORT PROCESSES			
Advection			
Advection	UP		W90
Diffusion			
Diffusion	UP		W91
Matrix diffusion	UP		W92
Thermochemical transport phenomena			
Soret effect	SO-C		W93
Electrochemical transport phenomena			
Electrochemical effects	SO-C		W94
Galvanic coupling	SO-P		W95

Table 6-5. Waste- and Repository-Induced FEPs and Their Screening Classifications — Continued

FEPs	Screening Classification	Comments	FEP Number
Electrophoresis	SO-C		W96
Physicochemical transport phenomena			
Chemical gradients	SO-C		W97
Osmotic processes	SO-C	Beneficial SO-C	W98
Alpha recoil	SO-C		W99
Enhanced diffusion	SO-C		W100
ECOLOGICAL FEPs			
Plant, animal, and soil uptake			
Plant uptake	SO-R	SO-C for 40 CFR § 191.15	W101
Animal uptake	SO-R		W102
Accumulation in soils	SO-C	Beneficial SO-C	W103
Human uptake			
Ingestion	SO-R	SO-C for 40 CFR § 191.15	W104
Inhalation	SO-R	SO-C for 40 CFR § 191.15	W105
Irradiation	SO-R	SO-C for 40 CFR § 191.15	W106
Dermal sorption	SO-R	SO-C for 40 CFR § 191.15	W107
Injection	SO-R	SO-C for 40 CFR § 191.15	W108

Legend:

UP FEPs accounted for in the assessment calculations for undisturbed performance for 40 CFR § 191.13 (as well as 40 CFR § 191.15 and Subpart C of 40 CFR Part 191).

DP FEPs accounted for (in addition to all UP FEPs) in the assessment calculations for disturbed performance for 40 CFR § 191.13.

SO-R FEPs eliminated from PA calculations on the basis of regulations provided in 40 CFR Part 191 and criteria provided in 40 CFR § 194. 25, .32 and .54.

SO-C FEPs eliminated from PA (and compliance assessment) calculations based on consequence.

SO-P FEPs eliminated from PA (and compliance assessment) calculations based on low probability of occurrence.

could result in their occurrence within the disposal system. Such FEPs include explosions resulting from nuclear criticality, and the development of large-scale reduction-oxidation fronts.

6.2.5 Human-Initiated Events and Processes

Assessments of compliance with the Containment Requirements in 40 CFR § 191.13 require consideration of "all significant processes and events," including human-initiated EPs. These EPs and their screening classifications are listed in Table 6-6. The DOE's detailed screening arguments for human-initiated EPs are presented in Appendix PA, Attachment SCR.

The scope of PA is clarified with respect to human-initiated events and processes in 40 CFR § 194.32. Section 194.32(a) states that

> Performance assessments shall consider natural processes and events, mining, deep drilling, and shallow drilling that may affect the disposal system during the regulatory time frame.

Thus, PA must conside human-initiated EPs relating to mining and drilling activities that might take place during the regulatory time frame. In particular, PAs must consider the potential effects of such activities that might take place within the controlled area at a time when institutional controls cannot be assumed to completely eliminate the possibility of human intrusion.

Further criteria concerning the scope of PAs are provided at 40 CFR § 194.32(c):

> Performance assessments shall include an analysis of the effects on the disposal system of any activities that occur in the vicinity of the disposal system prior to disposal and are expected to occur in the vicinity of the disposal system soon after disposal. Such activities shall include, but shall not be limited to, existing boreholes and the development of any existing leases that can be reasonably expected to be developed in the near future, including boreholes and leases that may be used for fluid injection activities.

Table 6-6. Human-Initiated EPs and Their Screening Classifications

EPs	Screening Classification		Comments	FEP Number
	Historical/ Ongoing/ Near Future	Future		
GEOLOGICAL EPs				
Drilling			DP for boreholes that penetrate the waste and boreholes that penetrate Castile brine underlying the waste disposal region. SO-C for other future drilling.	
Oil and gas exploration	SO-C	DP		H1
Potash exploration	SO-C	DP		H2
Water resources exploration	SO-C	SO-C		H3
Oil and gas exploitation	SO-C	DP		H4
Groundwater exploitation	SO-C	SO-C		H5
Archeological investigations	SO-R	SO-R		H6
Geothermal	SO-R	SO-R		H7
Other resources	SO-C	DP		H8
Enhanced oil and gas recovery	SO-C	DP		H9
Liquid waste disposal	SO-R	SO-R		H10
Hydrocarbon storage	SO-R	SO-R		H11
Deliberate drilling intrusion	SO-R	SO-R		H12
Excavation activities				
Conventional underground potash mining	UP	DP	UP for mining outside the controlled area. DP for mining inside the controlled area.	H13
Solution mining for potash	SO-R	SO-R	New to FEP Baseline	H58
Solution mining for other resources	SO-R	SO-R	New to FEP Baseline	H59
Other resources	SO-C	SO-R		H14
Tunneling	SO-R	SO-R		H15
Construction of underground facilities (for example storage, disposal, accommodation)	SO-R	SO-R		H16
Archeological excavations	SO-C	SO-R		H17
Deliberate mining intrusion	SO-R	SO-R		H18
Subsurface explosions				
Resource recovery				

Table 6-6. Human-Initiated EPs and Their Screening Classifications — Continued

EPs	Screening Classification		Comments	FEP Number
	Historical/ Ongoing/ Near Future	Future		
Explosions for resource recovery	SO-C	SO-R		H19
Underground nuclear device testing				
Underground nuclear device testing	SO-C	SO-R		H20
SUBSURFACE HYDROLOGICAL AND GEOCHEMICAL EPs				
Borehole fluid flow				
Drilling-induced flow				
Drilling fluid flow	SO-C	DP	DP for boreholes that penetrate the waste. SO-C for other future drilling.	H21
Drilling fluid loss	SO-C	DP	DP for boreholes that penetrate the waste, SO-C for other future drilling	H22
Blowouts	SO-C	DP	DP for boreholes that penetrate the waste and boreholes that penetrate Castile brine underlying the waste disposal region. SO-C for other future drilling.	H23
Drilling-induced geochemical changes	UP	DP	SO-C for units other than the Culebra.	H24
Fluid extraction				
Oil and gas extraction	SO-C	SO-R		H25
Groundwater extraction	SO-C	SO-R		H26
Fluid injection				
Liquid waste disposal	SO-C	SO-C		H27
Enhanced oil and gas production	SO-C	SO-C		H28
Hydrocarbon storage	SO-C	SO-C		H29
Fluid-injection induced geochemical changes	UP	SO-R	SO-C for units other than the Culebra	H30
Flow through abandoned boreholes			Classification distinguishes the time when drilling occurs.	

Table 6-6. Human-Initiated EPs and Their Screening Classifications — Continued

EPs	Screening Classification		Comments	FEP Number
	Historical/ Ongoing/ Near Future	Future		
Natural borehole fluid flow	SO-C	DP	DP for boreholes that penetrate Castile brine underlying the waste disposal region. SO-C for other future boreholes.	H31
Waste-induced borehole flow	SO-R	DP	DP for boreholes that penetrate the waste. SO-C for other future boreholes.	H32
Borehole-induced solution and subsidence	SO-C	SO-C		H34
Borehole-induced mineralization	SO-C	SO-C		H35
Borehole-induced geochemical changes	UP	DP	SO-C for units other than the Culebra	H36
Excavation-induced flow			Classification distinguishes the time when excavation occurs.	
Changes in groundwater flow due to mining	UP	DP	UP for mining outside the controlled area. DP for mining inside the controlled area.	H37
Changes in geochemistry due to mining	SO-C	SO-R		H38
Explosion-induced flow				
Changes in groundwater flow due to explosions	SO-C	SO-R		H39
GEOMORPHOLOGICAL EPs				
Land use and disturbances				
Land use changes	SO-R	SO-R		H40
Surface disruptions	UP	SO-R		H41
SURFACE HYDROLOGICAL EPs				
Water control and use				
Damming of streams or rivers	SO-C	SO-R		H42
Reservoirs	SO-C	SO-R		H43
Irrigation	SO-C	SO-R		H44
Lake usage	SO-R	SO-R		H45
Altered soil or surface water chemistry by human activities	SO-C	SO-R		H46

Table 6-6. Human-Initiated EPs and Their Screening Classifications — Continued

EPs	Screening Classification		Comments	FEP Number
	Historical/ Ongoing/ Near Future	Future		
CLIMATIC EPs				
Anthropogenic climate change				
Greenhouse gas effects	SO-R	SO-R		H47
Acid rain	SO-R	SO-R		H48
Damage to the ozone layer	SO-R	SO-R		H49
MARINE EPs				
Marine activities				
Coastal water use	SO-R	SO-R		H50
Seawater use	SO-R	SO-R		H51
Estuarine water use	SO-R	SO-R		H52
ECOLOGICAL EPs				
Agricultural activities				
Arable farming	SO-C	SO-R		H53
Ranching	SO-C	SO-R		H54
Fish farming	SO-R	SO-R		H55
Social and technological developments				
Demographic change and urban development	SO-R	SO-R		H56
Loss of records	NA	DP		H57

Legend:
UP FEPs accounted for in the assessment calculations for undisturbed performance for 40 CFR § 191.13 (as well as 40 CFR § 191.15 and Subpart C of 40 CFR Part 191).
DP FEPs accounted for (in addition to all UP FEPs) in the assessment calculations for disturbed performance for 40 CFR § 191.13.
SO-R FEPs eliminated from performance assessment calculations on the basis of regulations provided in 40 CFR Part 191 and criteria provided in 40 CFR § 194. 25, .32 and .54.
SO-C FEPs eliminated from PA (and compliance assessment) calculations based on consequence.
SO-P FEPs eliminated from PA (and compliance assessment) calculations based on low probability of occurrence.
NA FEPs not applicable to the particular category.

PAs must consider all human-initiated EPs relating to activities that have taken place or are reasonably expected to take place outside the controlled area in the near future.

In order to implement the criteria in Section 194.32 relating to the scope of PA, the DOE has divided human activities into three categories: (1) human activities that are currently taking place and those that took place prior to the time of the compliance application, (2) human activities that might be initiated in the near future after submission of the compliance application, and (3) human activities that might be initiated after repository closure. The first two categories

of EPs are considered under undisturbed performance; EPs in the third category lead to disturbed performance conditions.

(1) Historical and current human activities include resource extraction activities that have taken place and are currently taking place outside the controlled area. These activities are of potential significance insofar as they could affect the geological, hydrological, or geochemical characteristics of the disposal system or groundwater flow pathways outside the disposal system. Current human activities taking place within the controlled area are essentially those associated with development of the WIPP repository. Historical activities include existing boreholes.

(2) Near-future human activities include resource extraction activities that may occur outside the controlled area based on existing plans and leases. Thus, the near future includes the expected lives of existing mines and oil and gas fields, and the expected lives of new mines and oil and gas fields that the DOE expects will be developed based on existing plans and leases. These activities are of potential significance insofar as they could affect the geological, hydrological, or geochemical characteristics of the disposal system or groundwater flow pathways outside the disposal system. The only human activities expected to occur within the controlled area in the near future are those associated with WIPP repository development. The DOE assumes that any activity in the near future, based on existing plans and leases, will be initiated prior to repository closure. Activities initiated prior to repository closure are assumed to continue until their completion.

(3) Future human activities include activities that might be initiated within or outside the controlled area after repository closure. This includes drilling and mining for resources within the disposal system when institutional controls cannot be assumed to completely eliminate the possibility of such activities. Future human activities could influence the transport of contaminants within and outside the disposal system by directly removing waste from the disposal system or altering the geological, hydrological, or geochemical characteristics of the disposal system.

To satisfy the criteria in 40 CFR § 194.32, PAs must consider the potential effects of historical, current, near-future, and future human activities on the disposal system performance. The criterion in 40 CFR § 194.25(a) concerned with predicting the future states of society requires that PAs and compliance assessments "shall assume that the characteristics of the future remain what they are at the time the compliance application is prepared." This criterion has been applied to eliminate the following human-initiated EPs from PA calculations:

- drilling associated with geothermal energy production (H7), liquid waste disposal (H10), hydrocarbon storage (H11), and archeological investigations (H6);
- excavation activities associated with tunneling (H15) and construction of underground facilities (H16) (for example, storage, disposal, and accommodation);
- changes in land use (H40);
- anthropogenic climate change (H47, H48 and H49);

- changes in agricultural practices (H53, H54 and H55);
- demographic change, urban developments, and technological developments (H56); and
- solution mining (H58 and H59).

As discussed in Chapter 8.0, compliance assessments (to determine compliance with 40 CFR § 191.15 and Subpart C of 40 CFR Part 191) need to consider the UP of the disposal system.

6.2.5.1 Historical, Current, and Near-Future Human Activities

Historical, current, and near-future human activities could affect WIPP site characteristics after the submission of this application, and could influence the disposal system performance. The hydrogeological impacts of historical, current, and near-future potash mining outside the controlled area are accounted for in calculations of the undisturbed performance of the disposal system. Near-future potash mining is assumed to continue for the expected economic life of each mine. The potential consequences to the disposal system performance from other human-initiated EPs expected to occur in the Delaware Basin in the near future are discussed in Appendix PA, Attachment SCR, which describes how these EPs are eliminated based on low consequence.

6.2.5.2 Future Human Activities

PA (but not compliance assessments, as discussed in Chapter 8.0) must consider the effects of future human activities on the disposal system performance. The EPA has provided criteria relating to future human activities in 40 CFR § 194.32(a), which limits the scope of consideration of future human actions in PAs to mining and drilling.

6.2.5.2.1 Criteria Concerning Future Mining

The EPA provides additional criteria concerning the type of future mining that should be considered by the DOE in 40 CFR § 194.32(b):

> Assessments of mining effects may be limited to changes in the hydraulic conductivity of the hydrogeologic units of the disposal system from excavation mining for natural resources. Mining shall be assumed to occur with a one in 100 probability in each century of the regulatory time frame. Performance assessments shall assume that mineral deposits of those resources, similar in quality and type to those resources currently extracted from the Delaware Basin, will be completely removed from the controlled area during the century in which such mining is randomly calculated to occur. Complete removal of such mineral resources shall be assumed to occur only once during the regulatory time frame.

Thus, considering future mining may be limited to mining within the controlled area at locations of resources that are similar in quality and type to those currently extracted from the Delaware Basin. Potash is the only resource identified within the controlled area in quality similar to that currently mined from underground deposits elsewhere in the Delaware Basin. Within the controlled area, the McNutt of the Salado provides the only potash of appropriate quality. The hydrogeological impacts of future potash mining within the controlled area are accounted for in DP calculations of the disposal system. Consistent with 40 CFR § 194.32(b), all economically

recoverable resources in the vicinity of the disposal system (outside the controlled area) are assumed to be extracted in the near future.

6.2.5.2.2 Criteria Concerning Future Drilling

With respect to future drilling, in the preamble to 40 CFR Part 194, the EPA "reasoned that while the resources drilled for today may not be the same as those drilled for in the future, the present rates at which these boreholes are drilled can nonetheless provide an estimate of the future rate at which boreholes will be drilled." Criteria concerning the consideration of future deep and shallow drilling[2] in PAs are provided in 40 CFR § 194.33. These criteria require that, to calculate future drilling rates, the DOE should examine the historical rate of drilling for resources in the Delaware Basin. Historical drilling for purposes other than resource exploration and recovery (such as WIPP site investigation) need not be considered in determining future drilling rates.

In particular, when calculating the frequency of future deep drilling, 40 CFR § 194.33(b)(3)(i) states that the DOE should

> Identify deep drilling that has occurred for each resource in the Delaware Basin over the past 100 years prior to the time at which a compliance application is prepared.

Oil and gas are the only known resources below 655 m (2,150 ft) that have been exploited over the past 100 years in the Delaware Basin. However, some potash and sulfur exploration boreholes have been drilled in the Delaware Basin to depths in excess of 2,150 feet (655 meters) below the surface relative to where the drilling occurred. Thus, consistent with 40 CFR § 194.33(b)(3)(i), the DOE used the historical record of deep drilling associated with oil, gas, potash and sulfur exploration, and oil and gas exploitation in the Delaware Basin to determine the rate of deep drilling within the controlled area and throughout the basin in the future, as discussed in Appendix DATA, Section 2 and Attachment A. Deep drilling may occur within the controlled area after the end of active institutional control (100 years after disposal).

In calculating the frequency of future shallow drilling, 40 CFR § 194.33(b)(4)(i) states that the DOE should

> Identify shallow drilling that has occurred for each resource in the Delaware Basin over the past 100 years prior to the time at which a compliance application is prepared.

An additional criterion with respect to calculating future shallow drilling rates is provided in 40 CFR § 194.33(b)(4)(iii):

> In considering the historical rate of all shallow drilling, the Department may, if justified, consider only the historical rate of shallow drilling for resources of similar type and quality to those in the controlled area.

[2] The EPA has defined two types of drilling in 40 CFR § 194.2: deep drilling, defined as "drilling events in the Delaware Basin that reach or exceed a depth of 2,150 ft below the surface relative to where such drilling occurred"; and shallow drilling, defined as "drilling events in the Delaware Basin that do not reach a depth of 2,150 ft below the surface relative to where such drilling occurred."

As an example, EPA states in the preamble to 40 CFR Part 194 that "if only non-potable water can be found within the controlled area, then the rate of drilling for water may be set equal to the historical rate of drilling for non-potable water in the Delaware Basin over the past 100 years." Thus, the DOE may limit the rate of future shallow drilling based on a determination of the potential resources in the controlled area. Shallow drilling associated with water, potash, sulfur, oil, and gas extraction has taken place in the Delaware Basin over the past 100 years. However, of these resources, only water and potash are present at shallow depths (less than 655 m [2,150 ft] below the surface) within the controlled area. Thus, consistent with 40 CFR § 194.33(b)(4), the DOE used the historical record of shallow drilling associated with water and potash extraction in the Delaware Basin in calculations to determine the rate of shallow drilling within the controlled area, as discussed in Appendix DATA, Section 2 and Attachment A.

The EPA also provides a criterion in 40 CFR § 194.33(d) concerning the use of future boreholes subsequent to drilling:

> With respect to future drilling events, performance assessments need not analyze the effects of techniques used for resource recovery subsequent to the drilling of the borehole.

Thus, PAs need not consider the effects of techniques used for resource extraction and recovery that would occur after the drilling of a future borehole.

The EPA provides an additional criterion to limit the severity of human intrusion scenarios that must be considered in PAs. In 40 CFR § 194.33(b)(1), EPA states that

> Inadvertent and intermittent intrusion by drilling for resources (other than those resources provided by the waste in the disposal system or engineered barriers designed to isolate such waste) is the most severe human intrusion scenario.

Thus, human intrusion scenarios involving deliberate intrusion need not be considered in PAs.

6.2.5.2.3 Screening of Future Human-Initiated EPs

Future human-initiated EPs accounted for in PA calculations for the WIPP are those associated with mining and deep drilling within the controlled area at a time when institutional controls cannot be assumed to completely eliminate the possibility of such activities. All other future human-initiated EPs, if not eliminated from PA calculations based on regulation, have been eliminated based on low consequence or low probability. For example, the effects of future shallow drilling within the controlled area were eliminated from PA calculations on the basis of low consequence to the performance of the disposal system. These screening decisions are listed in Table 6-6 and are discussed in Appendix PA, Attachment SCR.

6.2.6 Reassessment of Features, Events, and Processes for the Compliance Recertification

As part of the recertification effort, the DOE assessed the impacts of new information on the original FEPs baseline to determine if changes to the original decisions are necessary. The FEPs baseline could be affected by new information from literature, experiments, observations from monitoring programs, or changes implemented by the DOE (moving the WIPP horizon to Clay G, for example). The processes and results of the FEPs baseline reassessment are documented in Appendix PA, Attachment SCR.

The FEP assessment resulted in the addition of two new FEPs to better represent solution mining (H57 and H58) and the deletion of four FEPs (by combining the deleted FEPs into other related FEPs). Seven screening decisions were also changed as a result of new information. However, only three FEPs previously screened out were screened into the CRA-2004 PA. The impact of organic ligands (W68 and W69) was screened into the CRA-2004 PA as a result of new information. This FEP screening decision change is the only impact to the PA system. The inclusion of ligands is discussed in Section 6.4.3.4. The FEP Surface Disruptions (H41) was also screened in. This FEP was already implicitly included in PA through past site characterization and current monitoring data (Appendix PA, Attachment SCR). The changes to the FEPs baseline are summarized in Table 6-7.

6.3 Scenario Development and Selection

This section addresses scenarios formed from FEPs that were retained for PA calculations, and introduces the specification of scenarios for consequence analysis. Probabilities associated with scenarios are discussed in Section 6.4.12.

Logic diagrams are used to illustrate the formation of scenarios for consequence analysis from combinations of FEPs that remain after FEP screening (Cranwell et al. 1990) (Figure 6-8). Each scenario shown in Figure 6-8 is defined by a combination of occurrence and

Table 6-7. FEPs Reassessment Summary Results

EPA FEP I.D.	FEP Name	Summary of Change
FEPs Combined with other FEPs		
N17	Lateral Dissolution	Combined with N16, "Shallow Dissolution." N17 removed from baseline.
N19	Solution Chimneys	Combined with N20, "Breccia Pipes." N19 removed from Baseline.
H33	Flow Through Undetected Boreholes	Combined with H31, "Natural Borehole Fluid Flow." H33 removed from baseline.
W38	Investigation Boreholes	Addressed in H31, "Natural Borehole Fluid Flow," and H33, "Flow Through Undetected Boreholes." W38 removed from baseline.
FEPs With Changed Screening Decisions		
W50	Galvanic Coupling	SO-P to SO-C
W68	Organic Complexation	SO-C to UP
W69	Organic Ligands	SO-C to UP
H27	Liquid Waste Disposal	SO-R to SO-C
H28	Enhanced Oil and Gas Production	SO-R to SO-C
H29	Hydrocarbon Storage	SO-R to SO-C
H41	Surface Disruptions	SO-C to UP (HCN)
New FEPs for CRA-2004		
H58	Solution Mining for Potash	Separated from H13, "Potash Mining."
H59	Solution Mining for Other Resources	Separated from H13, "Potash Mining."

nonoccurrence of all potentially disruptive EPs. Disruptive EPs are defined as those that create new pathways, or significantly alter existing pathways for fluid flow and, potentially, radionuclide transport within the disposal system. Each of these scenarios also contains a set of features and nondisruptive EPs that remain after FEP screening. As shown in Figure 6-8, undisturbed performance (UP) and disturbed performance (DP) scenarios are considered in consequence modeling for the WIPP PA. The (UP) scenario, as discussed in Chapter 8.0, is used for compliance assessments. Important aspects of (UP) and (DP) are summarized in this section.

6.3.1 Undisturbed Performance

Undisturbed performance is defined in 40 CFR § 191.12 to mean "the predicted behavior of a disposal system, including consideration of the uncertainties in predicted behavior, if the disposal system is not disrupted by human intrusion or the occurrence of unlikely natural events." Considering only (UP) is required for compliance assessments with respect to the Individual and Groundwater Protection Requirements (40 CFR § 191.15 see Chapter 8.0). Undisturbed performance is also considered with (DP) for PAs with respect to the Containment Requirements (40 CFR § 191.13).

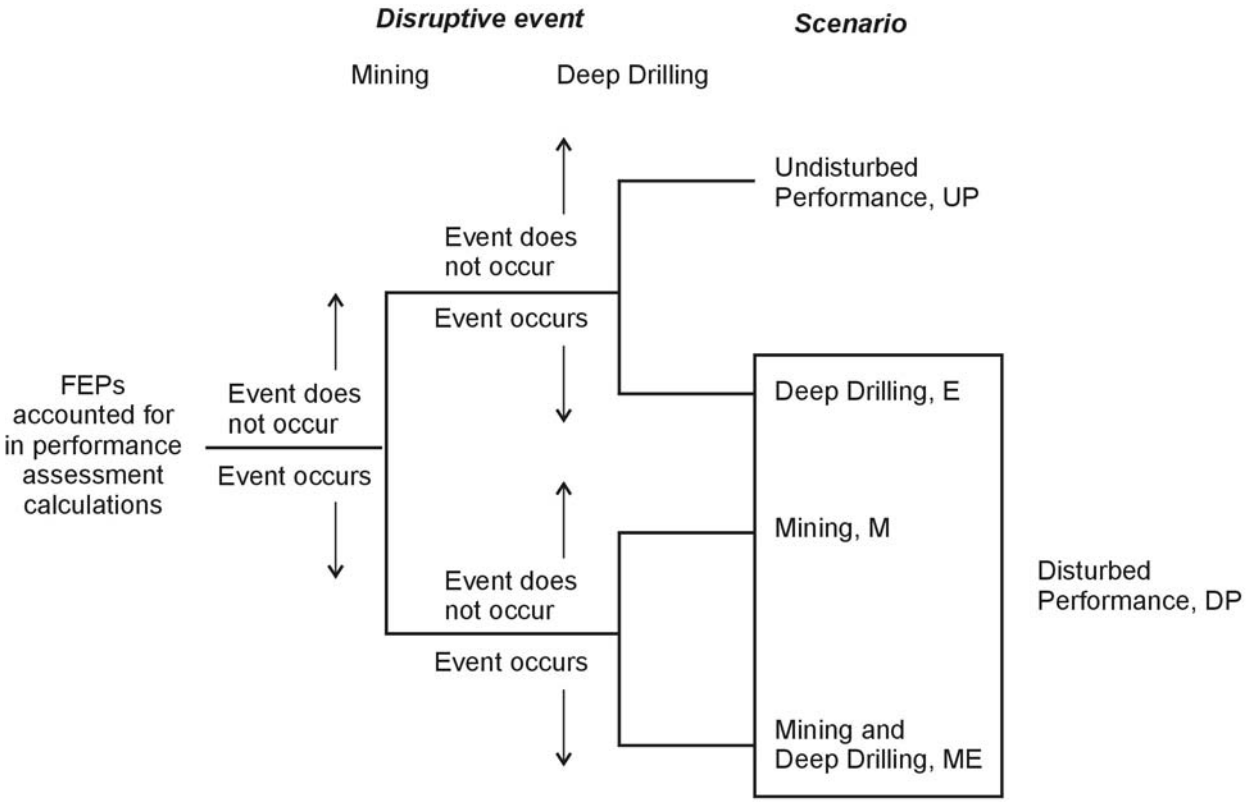

Figure 6-8. Logic Diagram for Scenario Analysis

No potentially disruptive natural EPs are likely to occur during the regulatory time frame (Section 6.2.3 and Appendix PA, Attachment SCR). Therefore, all naturally occurring EPs retained for scenario construction are nondisruptive and are considered as part of (UP). The only natural features and waste- and repository-induced FEPs retained after screening that are not

included in the (UP) scenario but are included in (DP) are those directly associated with the potential effects of future deep drilling within the controlled area. These drilling-related FEPs are discussed in Section 6.3.2. Potash mining outside the controlled area does not constitute a disruption of the disposal system by human intrusion and is included in the (UP) scenario. In total, 70 (UP) FEPs were identified (Section 6.2.3). These FEPs have been assigned a screening designator (UP) in tables in Section 6.2.3 and are listed separately in Table 6-8. Table 6-8 also contains references to text in Section 6.4 that describes the conceptual models, which account for the UP FEPs.

Among the most significant FEPs that will affect the (UP) within the disposal system are excavation-induced fracturing, gas generation, salt creep, and MgO in the disposal rooms.

- The repository excavation and consequent changes in the rock stress field surrounding the excavated opening will create a DRZ immediately adjacent to excavated openings. The DRZ will exhibit mechanical and hydrological properties different than those of the intact rock.

- Organic material in the waste may degrade because of microbial activity, and brine will corrode metals in the waste and waste containers, with concomitant generation of gases. Gas generation may result in pressures sufficient to both maintain or develop fractures and change the fluid flow pattern around the waste disposal region.

- At the repository depth, salt creep will tend to heal fractures and reduce the permeability of the DRZ and the crushed salt component of the long-term shaft seals to near that of the host rock salt.

- The MgO engineered barrier emplaced in the disposal rooms will react with CO_2 and maintain mildly alkaline conditions. Corrosion of metals in the waste and waste containers will maintain reducing conditions. These effects will decrease radionuclide solubility.

Radionuclides can become mobile as a result of waste dissolution and colloid generation following brine flow into the disposal rooms. Colloids may be generated from the waste (humics, mineral fragments, and actinide intrinsic colloids) or from other sources (humics, mineral fragments, and microbes).

Conceptually, there are several pathways for radionuclide transport within the undisturbed disposal system that may result in releases to the accessible environment (Figure 6-9). Contaminated brine may migrate away from the waste-disposal panels if pressure within the panels is elevated by gas generated from corrosion or microbial consumption. Radionuclide transport may occur laterally, through the anhydrite interbeds toward the subsurface boundary of the accessible environment in the Salado, or through access drifts or anhydrite interbeds to the base of the shafts. In the latter case, if the pressure gradient between the panels and overlying strata is sufficient, contaminated brine may migrate up the shafts. As a result, radionuclides may be transported directly to the ground surface, or laterally away from the shafts, through permeable strata such as the Culebra, toward the subsurface boundary of the accessible environment. These conceptual pathways are shown in Figure 6-9.

The modeling system described in Section 6.4 includes potential radionuclide transport along other pathways, such as migration through Salado halite. However, the natural properties of the undisturbed system make radionuclide transport to the accessible environment via these other pathways unlikely.

6.3.2 Disturbed Performance

Assessments for compliance with 40 CFR § 191.13 need to consider the potential effects of future disruptive natural and human-initiated EPs on the performance of the disposal system. As discussed in Section 6.2.3, no potentially disruptive, natural EPs are considered sufficiently likely to require inclusion in analyses of either (UP) or (DP). The only future human-initiated EPs retained after FEP screening are those associated with mining and deep drilling (but not the subsequent use of a borehole) within the controlled area when institutional controls cannot be assumed to eliminate the possibility of such activities (Sections 6.2.5.2 and 6.4.12.1). In total, 21 (DP) FEPs associated with future mining and deep drilling have been identified. These FEPs were assigned a screening designator "DP" in tables in Section 6.2 and are listed separately in Table 6-9. Table 6-9 also contains references to text in Section 6.4 that describes the conceptual models which account for the DP FEPs.

For evaluating the consequences of (DP), the DOE has defined the mining scenario, M, the deep drilling scenario, E, and a mining and drilling scenario, ME. These scenarios are described in the following sections.

6.3.2.1 The Disturbed Performance Mining Scenario

The (DP) mining scenario, M, involves future mining within the controlled area.

Consistent with the criteria stated by the EPA in 40 CFR § 194.32 (b) for PA calculations, the effects of potential future mining within the controlled area are limited to changes in hydraulic conductivity of the Culebra that result from subsidence (as described in Section 6.4.6.2.3.

Radionuclide transport may be affected in the M scenario if a head gradient between the waste-disposal panels and the Culebra causes brine contaminated with radionuclides to move from the waste-disposal panels to the base of the shafts and up to the Culebra. The changes in the Culebra transmissivity field may affect the rate and direction of radionuclide transport within the Culebra. Features of the M scenario are illustrated in Figure 6-10.

The three disturbed performance FEPs labeled "M" in Table 6-9 relate to the occurrence and effects of future mining. The modeling system used for the M scenario is similar to that developed for the UP scenario, but with a modified Culebra transmissivity field in the controlled area to account for the mining effects.

6.3.2.2 The Disturbed Performance Deep Drilling Scenario

The DP deep drilling scenario, E, involves at least one deep drilling event that intersects the waste disposal region. The EPA provides criteria for analyzing the consequences of future drilling events in PAs in 40 CFR § 194.33(c):

Performance assessments shall document that in analyzing the consequences of drilling events, the Department assumed that:

(1) Future drilling practices and technology will remain consistent with practices in the Delaware Basin at the time a compliance application is prepared. Such future drilling practices shall include, but shall not be limited to: the types and amounts of drilling fluids; borehole depths, diameters, and seals; and the fraction of such boreholes that are sealed by humans; and

Table 6-8. Undisturbed Performance FEPs

UP FEPs	Section
NATURAL FEPs	
Geological	
Stratigraphy	
Stratigraphy	6.4.2
Structural effects	
Seismic activity	
Seismic activity	6.4.5.3
Geochemical	
Dissolution	
Shallow dissolution	6.4.6.2
Subsurface hydrological	
Groundwater characteristics	
Saturated groundwater flow	6.4.5 6.4.6
Unsaturated groundwater flow	6.4.6
Fracture flow	6.4.6.2
Effects of preferential pathways	6.4.6.2
Subsurface geochemical	
Groundwater geochemistry	
Groundwater geochemistry	6.4.3.4 6.4.6.2
Geomorphological	
Physiography	
Physiography	6.4.2
Surface hydrological	
Groundwater recharge and discharge	
Groundwater discharge	6.4.10.2
Groundwater recharge	6.4.10.2
Infiltration	6.4.10.2
Changes in surface hydrology	
Changes in groundwater recharge and discharge	6.4.9
Climatic	
Climate	
Precipitation (for example, rainfall)	6.4.9
Temperature	6.4.9
Climate change	
Meteorological	
Climate change	6.4.9

Table 6-8. Undisturbed Performance FEPs — Continued

UP FEPs	Section
WASTE- AND REPOSITORY-INDUCED FEPs	
Waste and repository characteristics	
Repository characteristics	
Disposal geometry	6.4.2.1
Waste characteristics	
Waste inventory	6.4.3.3
Container characteristics	
Container material inventory	6.4.3.3
Seal characteristics	
Seal geometry	6.4.3
Seal physical properties	6.4.4
Backfill characteristics	
Backfill chemical composition	6.4.3.4
Radiological	
Radioactive decay	
Radionuclide decay and ingrowth	6.4.5.4.2 6.4.12.4
Geological and Mechanical	
Excavation-induced fracturing	
DRZ	6.4.5.3
Excavation-induced changes in stress	6.4.3.1
Rock creep	
Salt creep	6.4.3.1
Changes in the stress field	6.4.3.1
Roof falls	
Roof falls	6.4.5.3
Effects of fluid pressure changes	
Disruption due to gas effects	6.4.5.2
Pressurization	6.4.5.2
Effects of explosions	
Gas explosions	6.4.5.3
Mechanical effects on material properties	
Consolidation of waste	6.4.3.1
Consolidation of seals	6.4.4
Mechanical degradation of seals	6.4.4
Underground boreholes	6.4.5.3
Subsurface hydrological and fluid dynamics	
Repository-induced flow	

Table 6-8. Undisturbed Performance FEPs — Continued

UP FEPs	Section
Brine inflow	6.4.3.2
Wicking	6.4.3.2
Effects of gas generation	
Fluid flow due to gas production	6.4.3.2
Geochemical and chemical	
Gas generation	
Microbial gas generation	
Consumption of organic materials	6.4.3.3
Effects of temperature on microbial gas generation	6.4.3.3
Effects of biofilms on microbial gas generation	6.4.3.3
Corrosion	
Gases from metal corrosion	6.4.3.3
Chemical effects of corrosion	6.4.3.3
Chemical speciation	
Speciation	6.4.3.4 6.4.3.5
Precipitation and dissolution	
Dissolution of waste	6.4.3.5
Sorption	
Actinide sorption	6.4.3.6 6.4.6.2.1
Kinetics of sorption	6.4.6.2.1
Changes in sorptive surfaces	6.4.6.2.1
Reduction-oxidation chemistry	
Effect of metal corrosion	6.4.3.5
Reduction-oxidation kinetics	6.4.3.5
Organic complexation	
Organic complexation	6.4.3.4
Organic ligands	6.4.3.4
Humic and fulvic acids	6.4.3.6 6.4.6.2.2
Chemical effects on material properties	
Chemical degradation of seals	6.4.4
Microbial growth on concrete	6.4.4
Contaminant transport mode	
Solute transport	

Table 6-8. Undisturbed Performance FEPs — Continued

UP FEPs	Section
Solute transport	6.4.5.4 6.4.6.2.1
Colloid transport	
Colloid transport	6.4.6.2.2
Colloid formation and stability	6.4.3.6
Colloid filtration	6.4.6.2.2
Colloid sorption	6.4.6.2.2
Microbial transport	
Microbial transport	6.4.6.2.2
Contaminant transport processes	
Advection	
Advection	6.4.5.4 6.4.6.2
Diffusion	
Diffusion	6.4.5.4 6.4.6.2
Matrix diffusion	6.4.6.2
HUMAN-INITIATED EPs	
Geomorphological	
Surface disruptions	6.4
Geological	
Excavation activities	
Potash mining outside controlled area	6.4.6.2.3 6.4.12.8 6.4.13.8
Subsurface hydrological and geochemical	
Borehole fluid flow	
Drilling-induced flow	
Drilling induced geochemical changes	6.4.6.2
Fluid injection	
Fluid injection-induced geochemical changes	6.4.6.2
Flow through abandoned boreholes	
Borehole-induced geochemical changes	6.4.6.2
Excavation-induced flow	
Changes in groundwater flow due to mining	6.4.6.2.3 6.4.12.8 6.4.13.8

1

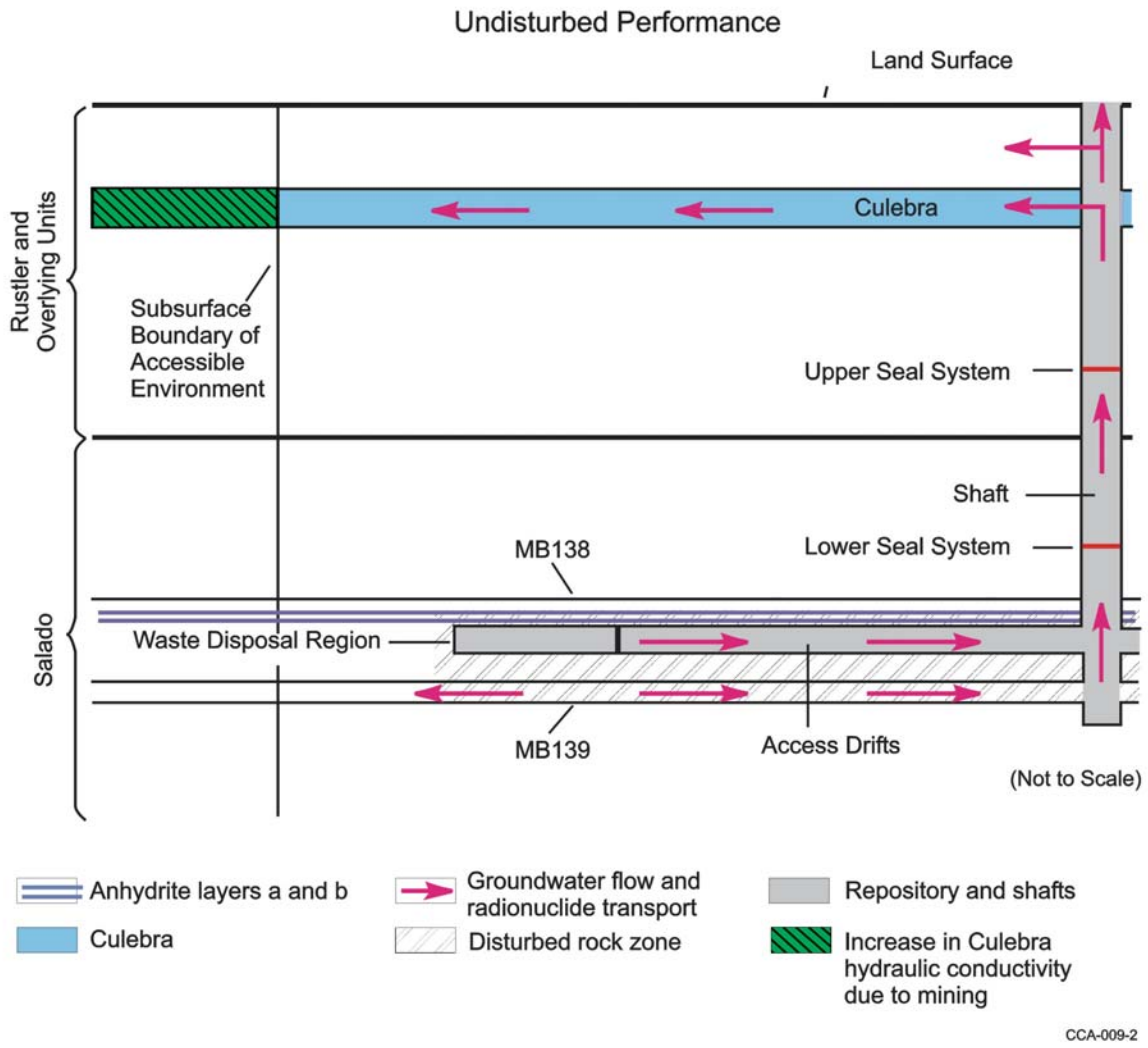

Figure 6-9. Conceptual Release Pathways for the Undisturbed Performance Scenario

(2) Natural processes will degrade or otherwise affect the capability of boreholes to transmit fluids over the regulatory time frame.

Consistent with these criteria, there are several pathways for radionuclides to reach the accessible environment in the E scenario. Before any deep drilling intersects the waste, potential release pathways are identical to those in the UP scenario.

If a borehole intersects the waste in the disposal rooms, releases to the accessible environment may occur as material entrained in the circulating drilling fluid is brought to the surface, as discussed in Section 6.4.7.1. Particulate waste brought to the surface may include cuttings, cavings, and spallings. Cuttings are the materials cut by the drill bit as it passes through waste. Cavings are the materials eroded by the drilling fluid in the annulus around the drill bit. Spallings are the materials forced into the circulating drilling fluid if there is

Table 6-9. Disturbed Performance FEPs

(FEPs)	Scenario	Section
ALL UP FEPs		
NATURAL FEPs		
Geological		
Stratigraphy		
Brine reservoirs	E1	6.4.8 6.4.12.6
WASTE- AND REPOSITORY-INDUCED FEPs		
Waste and repository characteristics		
Waste characteristics		
Heterogeneity of waste forms	E1, E2	6.4.12.4
Contaminant transport mode		
Particulate transport		
Suspensions of particles	E1, E2	6.4.7.1
Cuttings	E1, E2	6.4.7.1
Cavings	E1, E2	6.4.7.1
Spallings	E1, E2	6.4.7.1 6.4.13.7
HUMAN-INITIATED EPs		
Geological		
Drilling		
Oil and gas exploration	E1, E2	6.4.7 6.4.12.2
Potash exploration	E1, E2	6.4.7 6.4.12.2
Oil and gas exploitation	E1, E2	6.4.7 6.4.12.2
Other resources	E1, E2	6.4.7 6.4.12.2
Enhanced oil and gas recovery	E1, E2	6.4.7 6.4.12.2
Excavation activities		
Potash mining	M	6.4.6.2.3 6.4.12.8 6.4.13.8
Subsurface hydrological and geochemical		
Borehole fluid flow		
Drilling-induced flow		
Drilling fluid flow	E1, E2	6.4.7.1
Drilling fluid loss	E2	6.4.7.1.1
Blowouts	E1, E2	6.4.7.1.1

Table 6-9. Disturbed Performance FEPs — Continued

(FEPs)	Scenario	Section
Drilling-induced geochemical changes	E1, E2	6.4.6.2
Flow through abandoned boreholes		
Natural borehole fluid flow	E1, E2	6.4.7.2 6.4.12.7 6.4.13
Waste-induced borehole flow	E1, E2	6.4.7.2 6.4.12.7 6.4.13
Borehole-induced geochemical changes	E1, E2	6.4.6.2
Excavation-induced flow		
Changes to groundwater flow due to mining	M	6.4.6.2.3 6.4.12.8 6.4.13.8
Ecological		
Social and technological developments		
Loss of records	M, E1, E2	6.4.7 6.4.12.1

Legend:
M Mining within the controlled area.
E1 Deep drilling that intersects the waste disposal region and a brine reservoir in the Castile.
E2 Deep drilling that intersects a waste disposal panel.

sufficient pressure in the waste disposal panels. During drilling, contaminated brine may flow up the borehole and reach the surface, depending on fluid pressure within the waste disposal panels.

When abandoned, the borehole is assumed to be plugged in a manner consistent with current practice in the Delaware Basin (see Section 6.4.7.2; and Appendix DEL, Sections DEL.5 and DEL.6; Appendix DATA, Section 2, and CCA Appendix PA, Attachment MASS, Section.16.3). An abandoned intrusion borehole with degraded casing and/or plugs may provide a pathway for fluid flow and contaminant transport from the intersected waste panel to the ground surface if the fluid pressure within the panel is sufficiently greater than hydrostatic. Additionally, if brine flows through the borehole to overlying units, such as the Culebra, it may carry dissolved and colloidal actinides that can be transported laterally to the accessible environment by natural groundwater flow in the overlying units.

Alternatively, the units intersected by an intrusion borehole may provide sources for brine flow to a waste panel during or after drilling. For example, in the northern Delaware Basin, the Castile, which underlies the Salado, contains isolated volumes of brine at fluid pressures greater than hydrostatic (as discussed in Section 2.2.1.2.2). The WIPP-12 penetration of one of these reservoirs provided data on one brine reservoir within the controlled area. The location and properties of brine reservoirs cannot be reliably predicted; thus, the possibility of a deep borehole penetrating both a waste panel and a brine reservoir is accounted for in consequence analysis of the WIPP, as discussed in Section 6.4.8. Such a borehole could provide a connection for brine

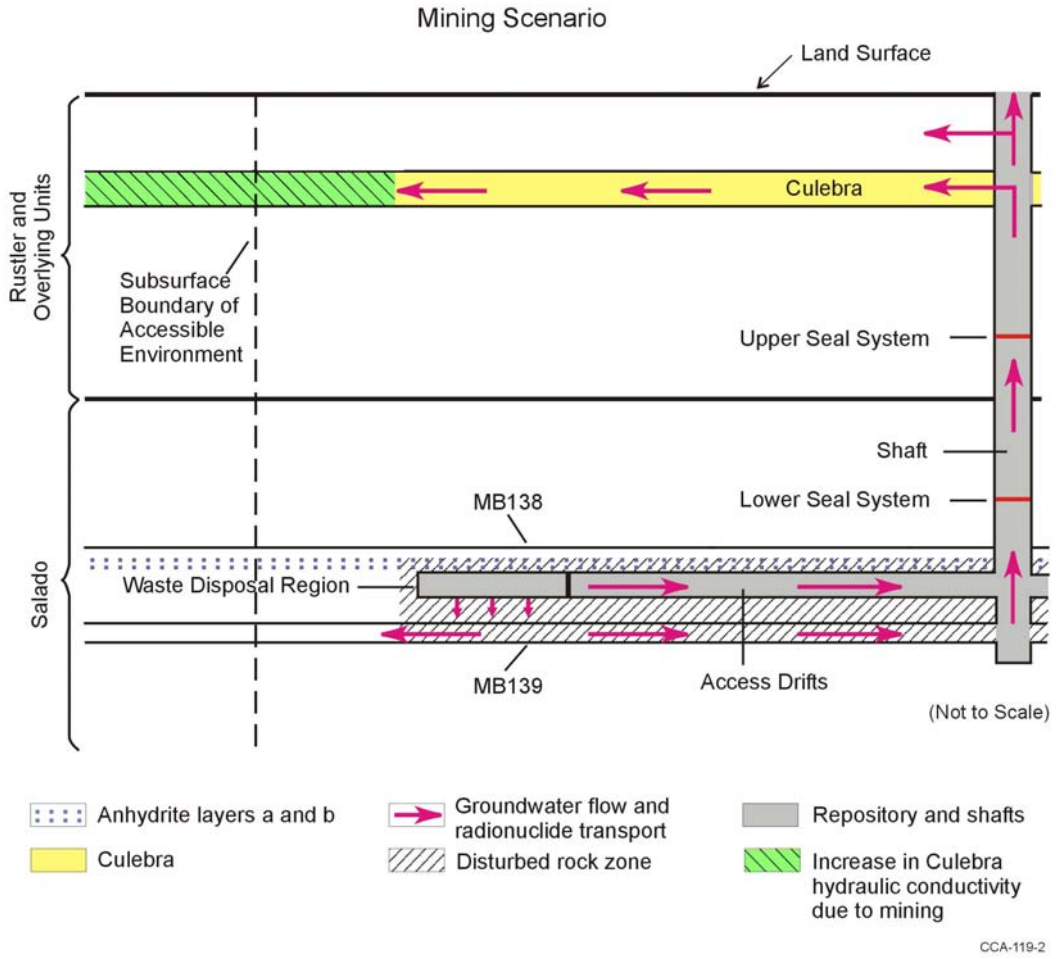

Figure 6-10. Conceptual Release Pathways for the Disturbed Performance Mining Scenario

flow from the Castile to the waste panel, thus increasing fluid pressure and brine volume in the waste panel.

A borehole that is drilled through a disposal room pillar, but does not intersect waste, could also penetrate the brine reservoir underlying the waste disposal region. Such an event would, to some extent, depressurize the brine reservoir, and thus would affect the consequences of any subsequent reservoir intersections. The PA does not take credit for possible brine reservoir depressurization.

The DOE has distinguished two types of deep drilling events by whether or not the borehole intersects a Castile brine reservoir. A borehole that intersects a waste disposal panel and penetrates a Castile brine reservoir is designated an E1 event. The 18 DP FEPs labeled "E1" in Table 6-9 relate to the occurrence and effects of an E1 drilling event. A borehole that intersects a waste panel but does not penetrate a Castile brine reservoir is designated an E2 event. The 18 DP FEPs labeled "E2" in Table 6-9 relate to the occurrence and effects of an "E2" drilling event.

In order to evaluate the consequences of future deep drilling, the DOE has divided the E scenario into three drilling subscenarios; E1, E2, and E1E2, distinguished by the number of E1 and E2 drilling events that are probabilistically assumed to occur in the regulatory time frame. These subscenarios are described in order of increasing complexity in the following sections.

6.3.2.2.1 The E2 Scenario

The E2 scenario is the simplest scenario for inadvertent human intrusion into a waste disposal panel. In this scenario, a panel is penetrated by a drill bit; cuttings, cavings, spallings, and brine flow releases may occur; and brine flow may occur in the borehole after it is plugged and abandoned. Sources for brine that may contribute to long-term flow up the abandoned borehole are the Salado or, under certain conditions, the units above the Salado. An E2 scenario may involve more than one E2 drilling event. Features of the E2 scenario are illustrated in Figure 6-11. A modeling system has been developed to evaluate the consequences of an E2 scenario during which single or multiple E2 events occur.

6.3.2.2.2 The E1 Scenario

Any scenario with one inadvertent penetration of a waste panel that also penetrates a Castile brine reservoir is called E1. Features of this scenario are illustrated in Figure 6-12.

Sources of brine in the E1 scenario are the brine reservoir, the Salado and, under certain conditions, the units above the Salado. However, the brine reservoir is conceptually the dominant source of brine in this scenario. The model configuration developed for the E1 scenario evaluates the consequences of futures that have only one E1 event.

6.3.2.2.3 The E1E2 Scenario

The E1E2 scenario is defined as all futures with multiple penetrations of a waste panel of which at least one intrusion is an E1. One case of this scenario, with a single E1 event and a single E2 event penetrating the same panel, is illustrated in Figure 6-13. However, the E1E2 scenario can include many possible combinations of intrusion times, locations, and types of event (E1 or E2). The sources of brine in this scenario are those listed for the E1 scenario, and multiple E1 sources may be present. The E1E2 scenario has a potential flow path not present in the E1 or E2 scenarios: flow from an E1 borehole through the waste to another borehole. This flow path has the potential to (1) bring large quantities of brine in direct contact with waste and (2) provide a less restrictive path for this brine to flow to the units above the Salado (via multiple boreholes) compared to either the individual E1 or E2 scenarios. It is both the presence of brine reservoirs and the potential for flow through the waste to other boreholes that make this scenario different in terms of potential consequences from combinations of E2 boreholes. The extent to which flow occurs between boreholes, as estimated by modeling, determines whether combinations of E1 and E2 boreholes at specific locations in the repository should be treated as E1E2 scenarios or as independent E1 and E2 scenarios in the consequence analysis.

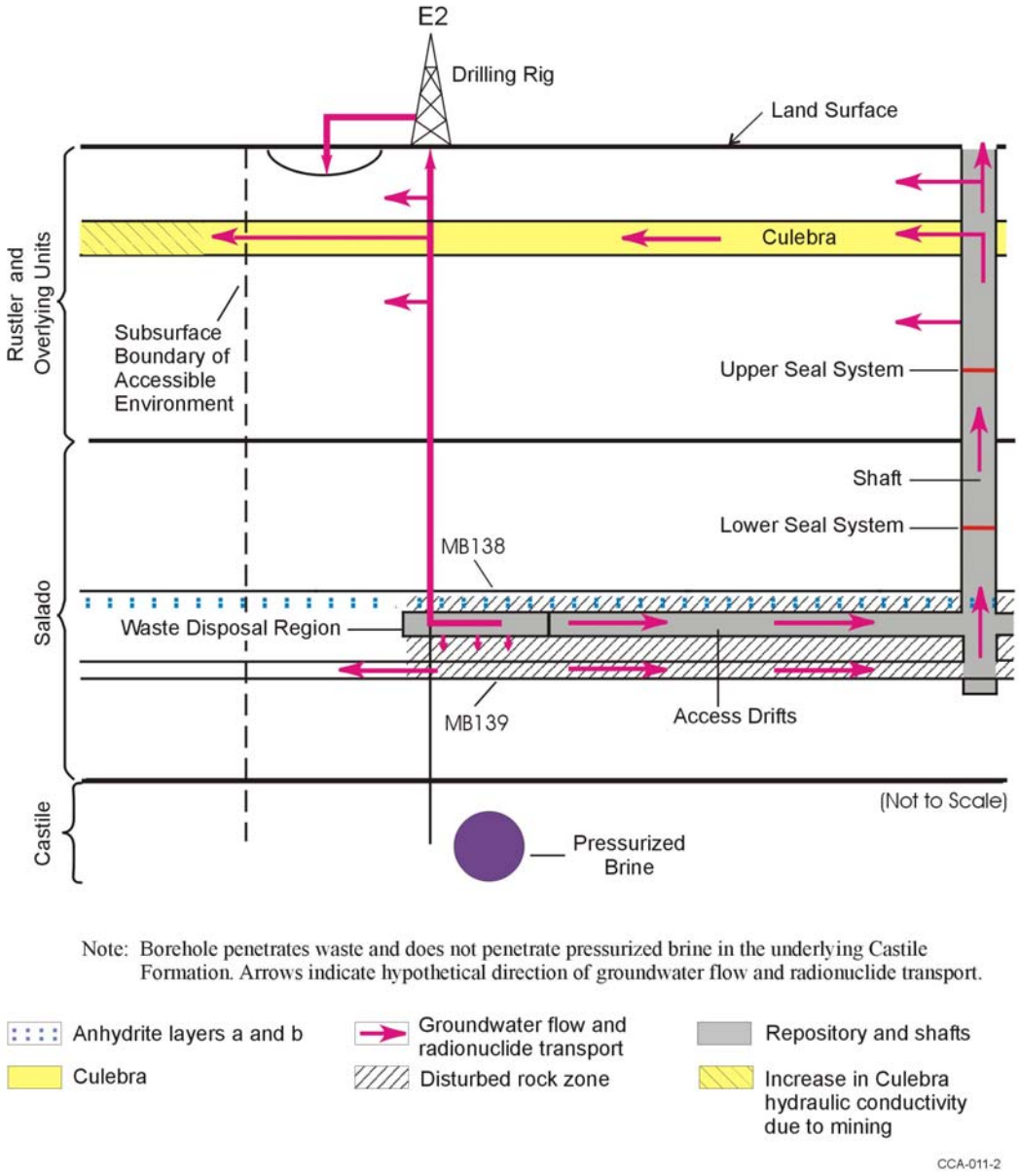

Figure 6-11. Conceptual Release Pathways for the Disturbed Performance Deep Drilling E2 Scenario

The possible combinations of drilling events make the modeling configuration for the E1E2 scenario differ in significant ways from that used to evaluate E1 and E2 scenarios. This configuration is described in Section 6.4.13.5.

6.3.2.3 The Disturbed Performance Mining and Deep Drilling Scenario

Mining in the WIPP site (the M scenario) and deep drilling (the E scenario) may both occur in the future. The DOE calls a future in which both of these events occur the ME scenario. The

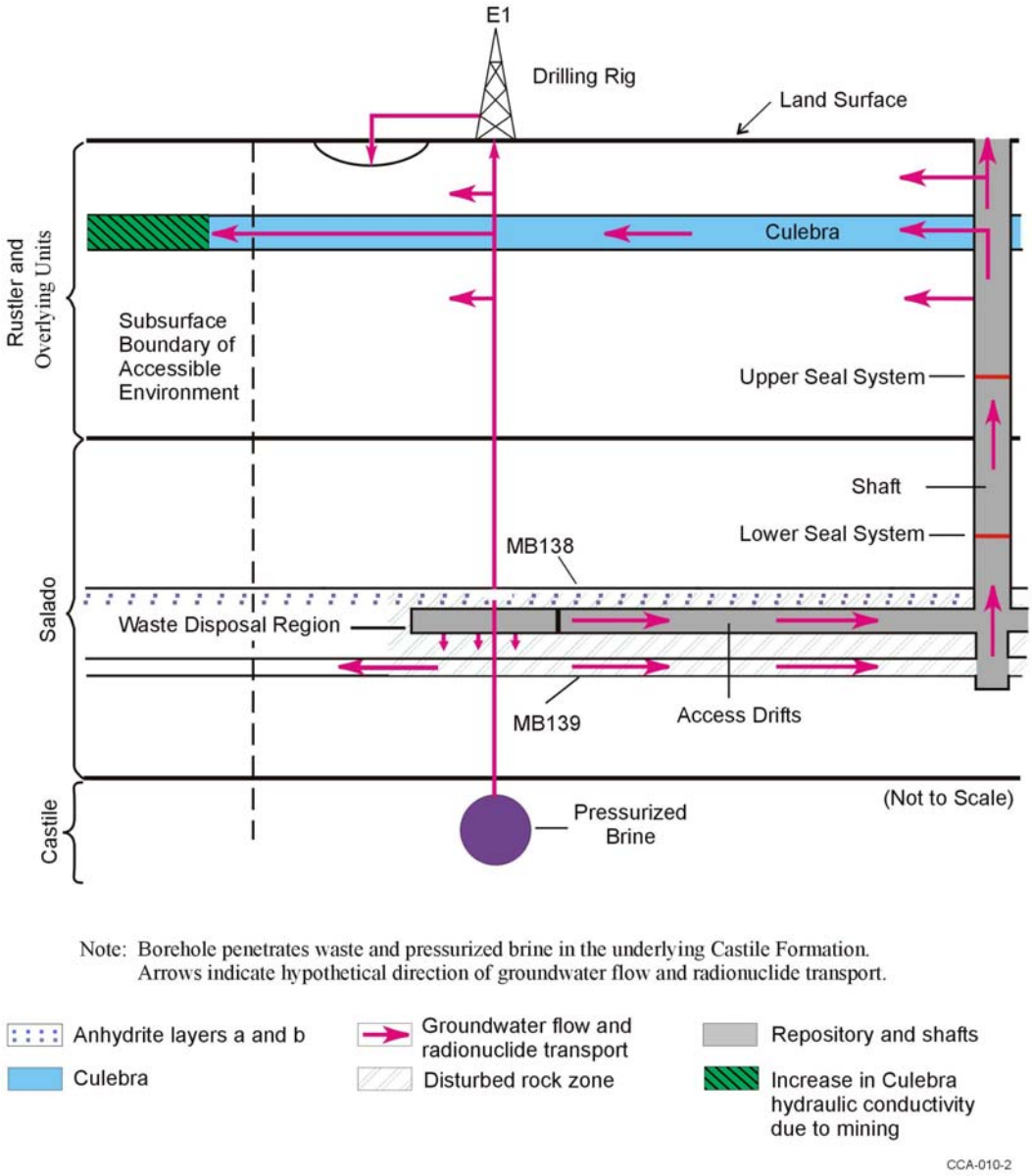

Figure 6-12. Conceptual Release Pathways for the Disturbed Performance Deep Drilling Scenario E1

occurrence of both mining and deep drilling do not create processes beyond those already described separately for the M and E scenarios. For example, the occurrence of mining does not influence any of the interactions between deep boreholes and the repository or brine reservoirs. Nor does the occurrence of drilling impact the effects of mining on Culebra hydrogeology. The difference between the M and E scenarios considered separately and the ME scenario is that the combination of borehole transport to the Culebra (E) and a transmissivity field impacted by mining (M) may result in more rapid transport of actinides to the accessible environment. For example, because the M scenario does not include drilling the only pathway for actinides to reach the Culebra is up the sealed shafts. For clarity in describing

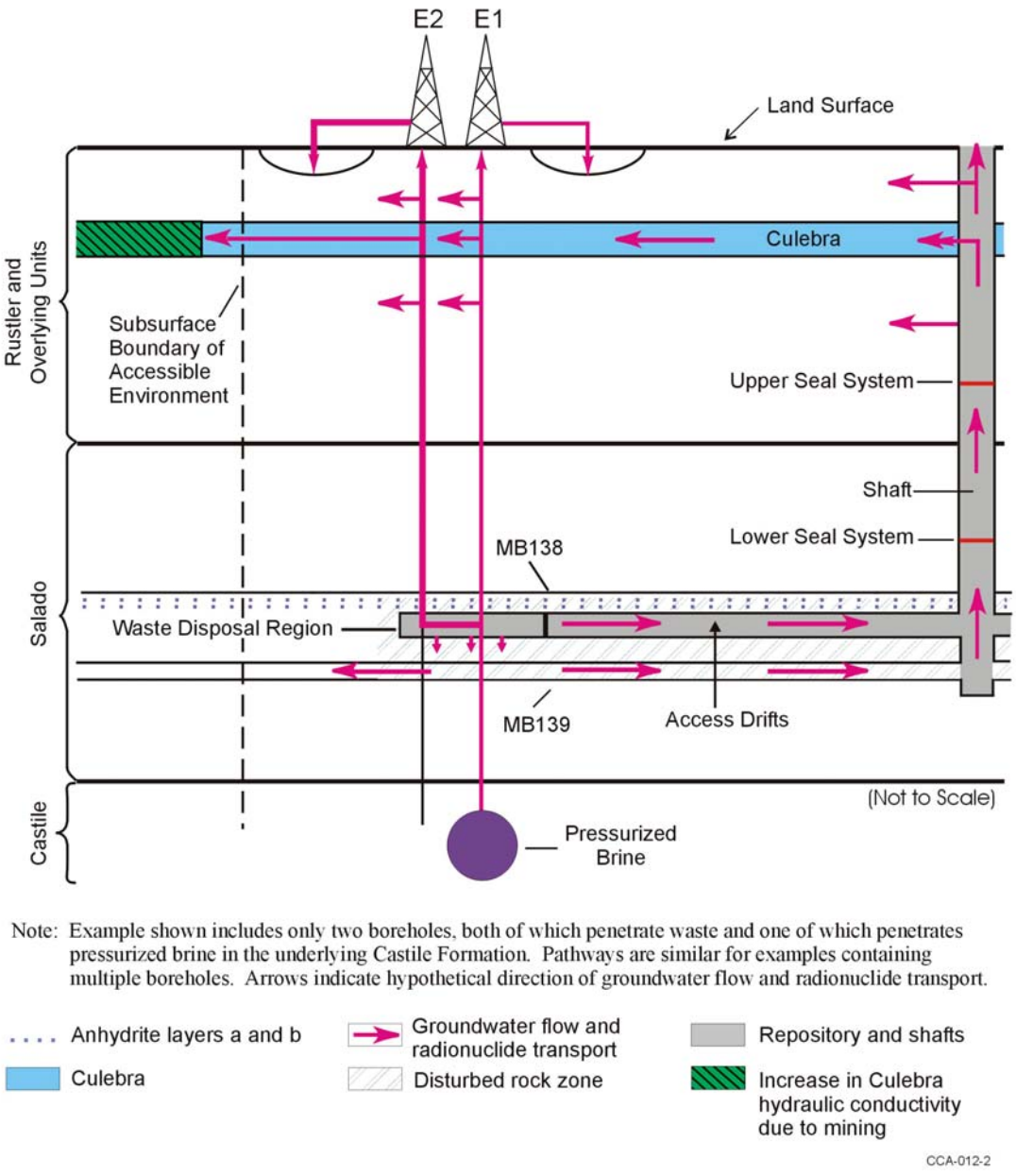

Figure 6-13. Conceptual Release Pathways for the Disturbed Performance Deep Drilling Scenario E1E2

computational results, the ME scenario has been subdivided according to the types of deep drilling subscenarios into the ME1 scenario (M and E1), the ME2 scenario (M and E2), and the ME1E2 scenario (M and E1E2).

The system used to model flow and transport in the Culebra for the ME scenario is similar to that used for the E scenario. However, in the ME scenario, the Culebra transmissivity field is modified to account for mining within the controlled area.

6.3.3 Scenarios Retained for Consequence Analysis

The scenarios described in Sections 6.3.1 and 6.3.2 have been retained for consequence analysis to determine compliance with the Containment Requirements in 40 CFR § 191.13. The modeling systems used to evaluate the consequences of these UP and DP scenarios are discussed in Section 6.4. For consequence analysis, the scenarios and subscenarios are further subdivided into scenarios, S_i. The S_i scenarios are distinguished by, for example, the time of occurrence of disruptive events. The S_i scenarios are generated, and their probabilities determined, by probabilistic sampling of selected processes and events (see Sections 6.1.5.2 and 6.4.12).

6.4 Calculation of Scenario Consequences

Scenario consequence, cS_i, is the third element of the ordered triples shown in Equation (6.2) in Section 6.1.1. Estimating cS_i requires quantitative modeling. PA uses a linked system of individual computer codes. This section discusses the conceptual and computational models and some parameter values used to estimate the consequence of the scenarios described in Section 6.3. Additional discussion of conceptual models and modeling assumptions is provided in Appendix PA, Section PA-2. Additional descriptions of sampled parameter values are included in Appendix PA, Section 5.0 and Attachment PAR.

6.4.1 Types of Models

A single modeling system was used to represent the disposal system and calculate the CCDFs presented in Section 6.5. The modeling system, however, can be conveniently described in terms of various submodels, with each describing a part of the overall system. This section provides, for each submodel defined, an integrated, summary description of the conceptual model, mathematical model, numerical model, computational model, experimental data, and model parameters used. These terms are described below.

The models used in the WIPP PA, as in other complex analyses, exist at four different levels:

(1) **Conceptual models** are a set of qualitative assumptions that describe a system or subsystem for a given purpose. At a minimum, these assumptions concern the geometry and dimensionality of the system, initial and boundary conditions, time dependence, and the nature of the relevant physical and chemical processes. The assumptions should be consistent with one another and with existing information within the context of the given purpose.

(2) **Mathematical models** represent the processes at the site. The conceptual models provide the context within which these mathematical models must operate and define the processes they must characterize. The mathematical models are predictive in the sense that, once provided with the known or assumed properties of the system and possible perturbations to the system, they predict the response of the system. The processes represented by these mathematical models include fluid flow, mechanical deformation, radionuclide transport in groundwater, and removal of waste through intruding boreholes.

(3) **Numerical models** are developed to approximate mathematical model solutions because most mathematical models do not have closed-form solutions.

(4) The complexity of the system requires computer codes to solve the numerical models. The implementation of the numerical model in the computer code with specific initial and boundary conditions and parameter values is generally referred to as the **computational model**.

Data are descriptors of the physical system being considered, normally obtained by experiment or observation. Parameters are values necessary in mathematical, numerical, or computational models. The distinction between data and parameters can be subtle. Parameters are distinct from data, however, for three reasons. First, data may be evaluated, statistically or otherwise, to generate model parameters to account for uncertainty in data. Second, some parameters have no relation to the physical system, such as the parameters in a numerical model to determine when an iterative solution scheme has converged. Third, many model parameters are applied at a different scale than one directly observed or measured in the physical system. The distinction between data and parameter values is described further in Appendix PA, Attachment PAR, where distribution derivations for specific parameters are given. The interpretation and the scaling of experimental and field data are discussed in Appendix PA, Attachment PAR for individual and sampled parameters, as appropriate.

6.4.2 Model Geometries

Although the specific geometries used in PA models are developed after the conceptual and mathematical models are defined, they are introduced here because they provide a useful framework for presenting the full discussion of the modeling system. PA represents the three-dimensional geometry of the disposal system (repository, shafts, and controlled area) using two primary two-dimensional simplifications. In the first geometry, processes that act on the entire disposal system occur within the repository and are simulated in the BRAGFLO (BRine And Gas FLOw) computer code using a geometry that approximates a north-south vertical cross section through the disposal system and some surrounding rock. This geometry simulates processes in the disposal system, such as two-phase flow and movement of actinides, as well as processes acting only within the repository, such as creep closure of disposal rooms and gas generation. In the second geometry, groundwater flow and actinide transport in the Culebra, which provides a potential pathway for lateral transport of actinides to the accessible environment, are simulated in the MODFLOW-2000 and SECOTP2D computer codes using a two-dimensional horizontal geometry that treats the Culebra as a single layer. These two geometries are discussed in the following sections. PA codes and the flow of numerical information through the PA are described in Section 6.4.11 and referenced appendices.

6.4.2.1 Disposal System Geometry

A single disposal system geometry is used in the BRAGFLO computational model (see Appendix PA, Section PA-4.2) with four different maps of material properties: one for undisturbed conditions; one for the E1 intrusion event; one for the E2 intrusion event; and one for the E1E2 intrusion event (see Section 6.4.13.5). The geometry and material maps used in BRAGFLO are similar; each models fluid flow calculations that represent the three-dimensional physical system in a two-dimensional plane cutting vertically through the repository and surrounding strata. Side views of the vertical cross section and two of the material maps are presented in Figures 6-14 and 6-15. In these figures, the boundaries of grid blocks discretized in

the model are shown with dashed lines; each grid block is associated with material properties representing an important feature of the disposal system. These associations between grid blocks and material properties are shown by color and number in the figures. The two figures differ in that the material property map used for E1 intrusion events (Figure 6-15) includes a material region representing the borehole (Column 26) that is not present in the undisturbed case (Figure 6-14). The borehole region vertically transects other material regions and connects the single panel (Rows 10, 11, and 12) with the Castile brine reservoir (Rows 1 and 2), marker beds, overlying units, and the surface. The E2 intrusion event material regions are similar to those of E1, except that the modeled borehole region does not extend below the repository and therefore does not contact a brine reservoir.

Figures 6-14 and 6-15 show the relationship among material regions in the model and how connections are made within the finite-difference scheme. However, by illustrating equidimensional grid blocks, the volumetric relationship between grid blocks is greatly distorted. To show the volumetric relationship among nodal blocks and between the repository and host formations, a scaled side view of the vertical cross section used in BRAGFLO is shown in Figure 6-16. An undistorted 1:1 vertical:horizontal scale side view is in the upper left corner of Figure 6-16; at this scale, important model features are not resolvable. Therefore, two other views are provided in which the vertical scale has been exaggerated to show model features. Notice that the modeling system extends 14 miles (22.4 km) from the edge of the excavated repository in each direction, north and south. The borehole is not centered; rather it is located 24.17 km from the north boundary and 22.46 km from the south boundary. Figure 6-16 colors are consistent with colors for material regions in Figures 6-14 and 6-15.

Effects of flow in the third (out-of-plane) dimension are approximated with a two-dimensional element configuration that simulates convergent or divergent flow to the north and south centered on the repository in intact rocks laterally away from the repository. In this text, the term width corresponds to the x (lateral) dimension of nodes, thickness refers to the y (vertical) dimension, and depth refers to the z (out-of-plane) dimension. The effects of the grid assumptions on fluid flow processes in the Salado are discussed in Appendix PA, Attachment MASS, Section 4.1.

Based on observations in the existing excavations, the DOE approximates the regionally variable dip in the Salado by incorporating a 1-degree dip to the south in the BRAGFLO computational mesh. This dip is not indicated in Figures 6-14, 6-15, and 6-16.

The BRAGFLO definition of hydrostratigraphic units follows formation and member divisions. Inside the Salado, however, further subdivision of hydrostratigraphy has been made based on the observed permeability differences between anhydrite-rich interbeds and halite-rich intervals.

This further subdivision has been made only at elevations near the repository horizon, because only in this region are such distinctions important. The models and assumptions representing the various regions of material properties shown in Figures 6-14 and 6-15 are discussed in Section 6.4.3 and Appendix PA, Section 4.2. The thickness of hydrostatigraphic units used in BRAGFLO are tabulated in Appendix PA, Attachment PAR, Table PAR-49.

6.4.2.2 Culebra Geometry

Although the BRAGFLO model contains a discretization of the Culebra and calculates flow there, the DOE uses a more detailed representation to estimate potential radionuclide releases to the accessible environment resulting from lateral subsurface transport through the Culebra. The conceptual model for flow and transport in this geometry is discussed in Section 6.4.6.2. The boundary and initial conditions applied to this geometry are discussed in Section 6.4.10.2. MODFLOW-2000 and SECOTP2D are used to simulate groundwater flow and radionuclide transport in the Culebra. The SECOFL2D code was used in the CCA to simulate groundwater flow and has been replaced with MODFLOW-2000. The groundwater flow and transport conceptual models have not changed; the implementation of the groundwater model has been updated. The manner in which this geometry is linked to the BRAGFLO geometry described in the preceding section is discussed in Sections 6.4.6.2, 6.4.11, and Appendix PA, Section 4.9. The grids used to model the Culebra are discussed in Section 6.4.6.2 and Appendix PA, Section 4.8 (see also Appendix PA, Attachments MASS and TFIELD).

6.4.3 The Repository

The repository, as shown in Figure 3-2, is represented by areas marked Waste Panel and rest of repository (RoR) north and south in Figures 6-14 and 6-15. These regions include a waste disposal panel, panel closures (DRF_PCS, CONC_PCS, Anhydrite AB, and DRZ_PCS), two areas that represent the other panels and access drifts in the rest of the waste disposal region (RoR north and south), the operations region (Ops), and the experimental region at the north end of the repository (Exp). The shaft (which is further subdivided into two primary regions marked Upper Shaft and Lower Shaft) intersects the repository between the operations region and the experimental region. The shaft is discussed in Section 6.4.4. For human-intrusion events, the borehole intersects the waste disposal region in the Panel. In two-dimensional fluid flow codes, a grid block's length, volume, and cross-sectional area of faces connected to other grid blocks are important model features. For each region of the repository depicted, the BRAGFLO model geometry preserves the excavated volume. Lateral dimensions have been determined to preserve volume and retain important cross-sectional areas and distances between defined regions, as discussed below. These simplifications are conservative with respect to fluid contact with waste, which is a critical factor in determining the quantity of actinides mobilized in the aqueous phase. The simplifications are conservative because (1) all pillars have been removed from the modeled panel, resulting in homogeneous waste regions through which fluid can flow directly; and (2) the panels in the rest of the repository areas do not have pillars, resulting in a large homogeneous region that is assigned an average permeability within the range of those experimentally determined (see Section 6.4.3.2 and Appendix PA, Attachment MASS Section 3.1).

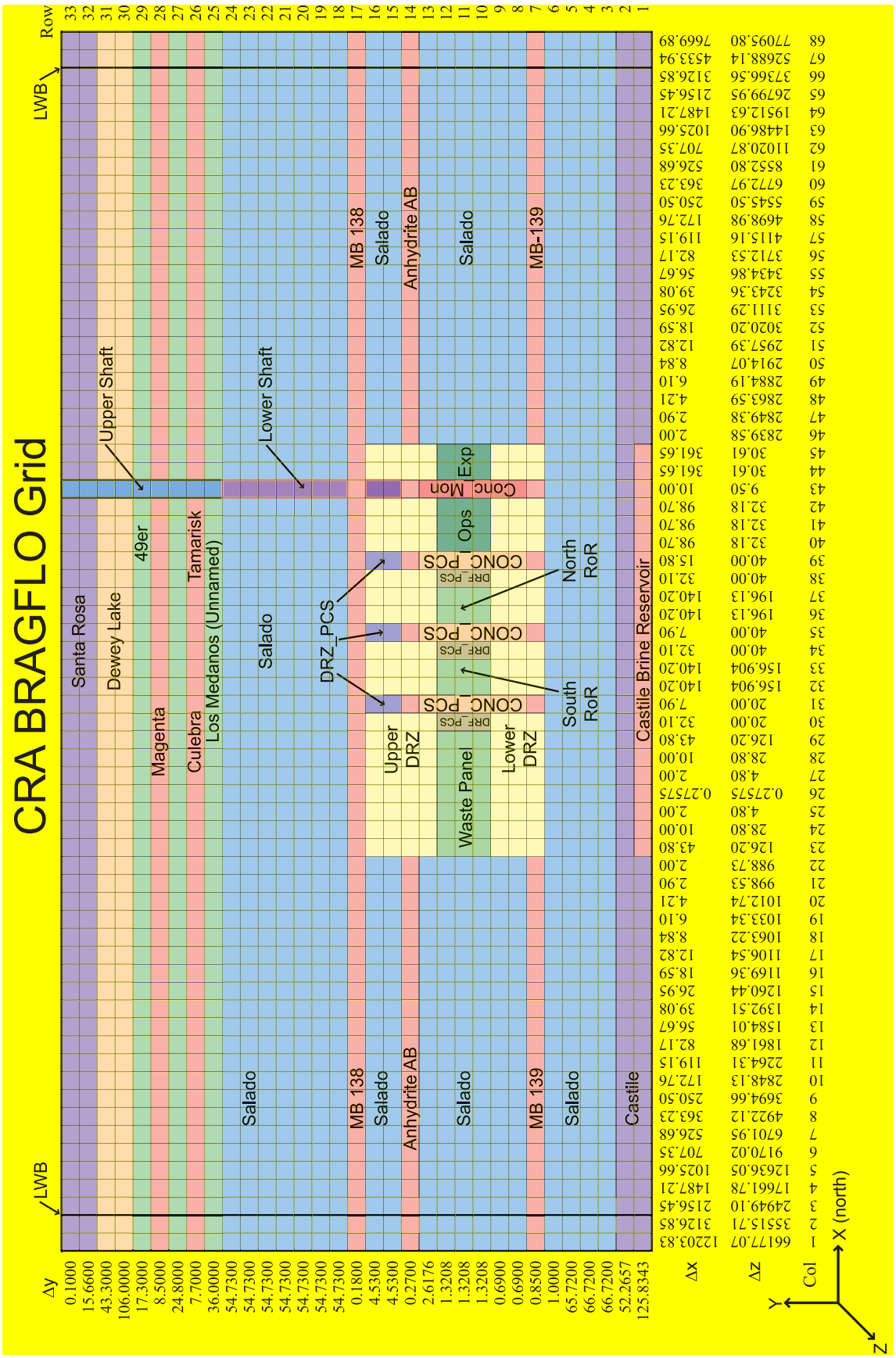

Figure 6-14. A Side View of the BRAGFLO Elements and Material Regions Used for Simulation of Undisturbed Performance

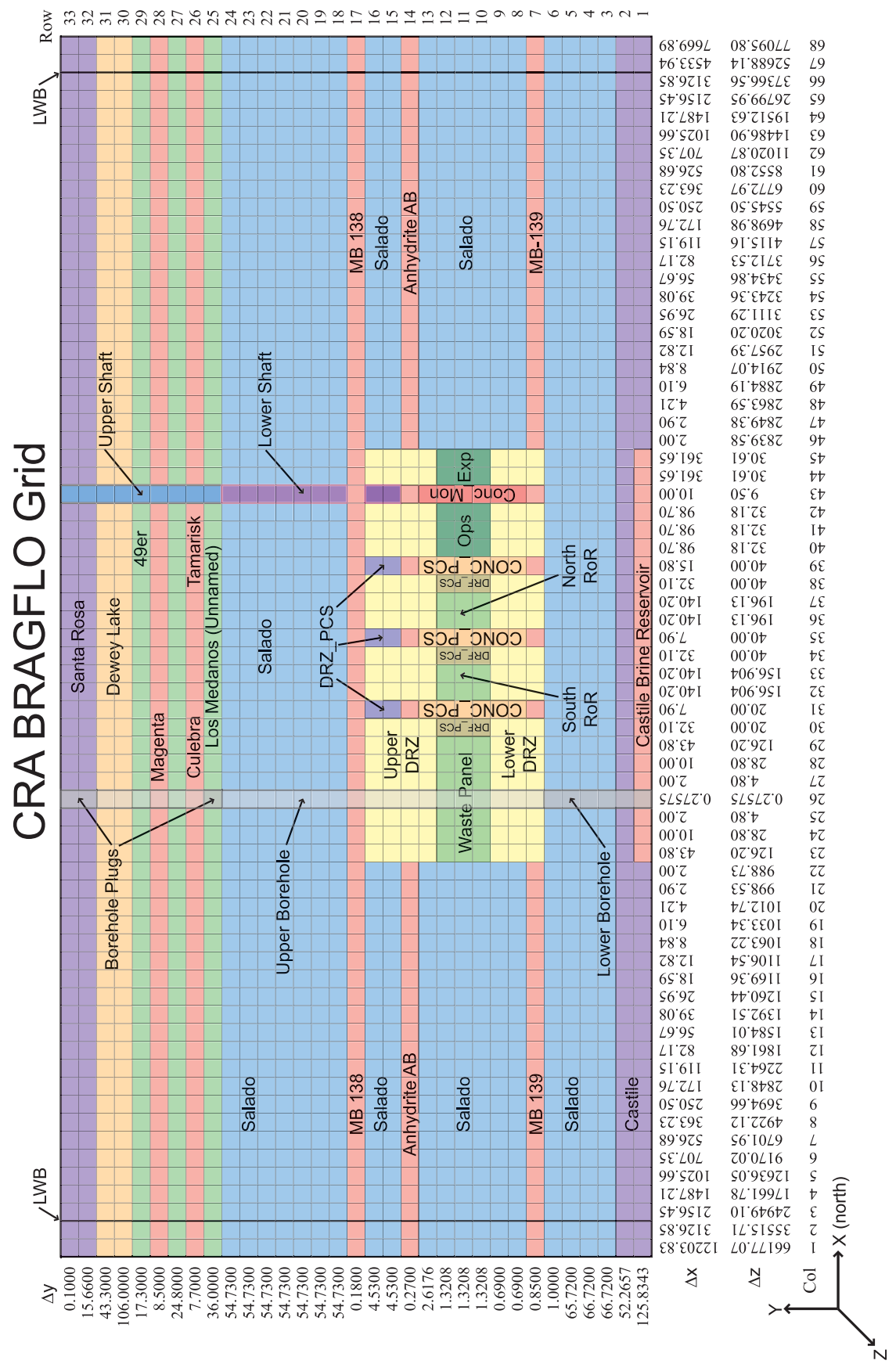

Figure 6-15. A Side View of the BRAGFLO Elements and Material Regions Used to Simulate the E1 Event

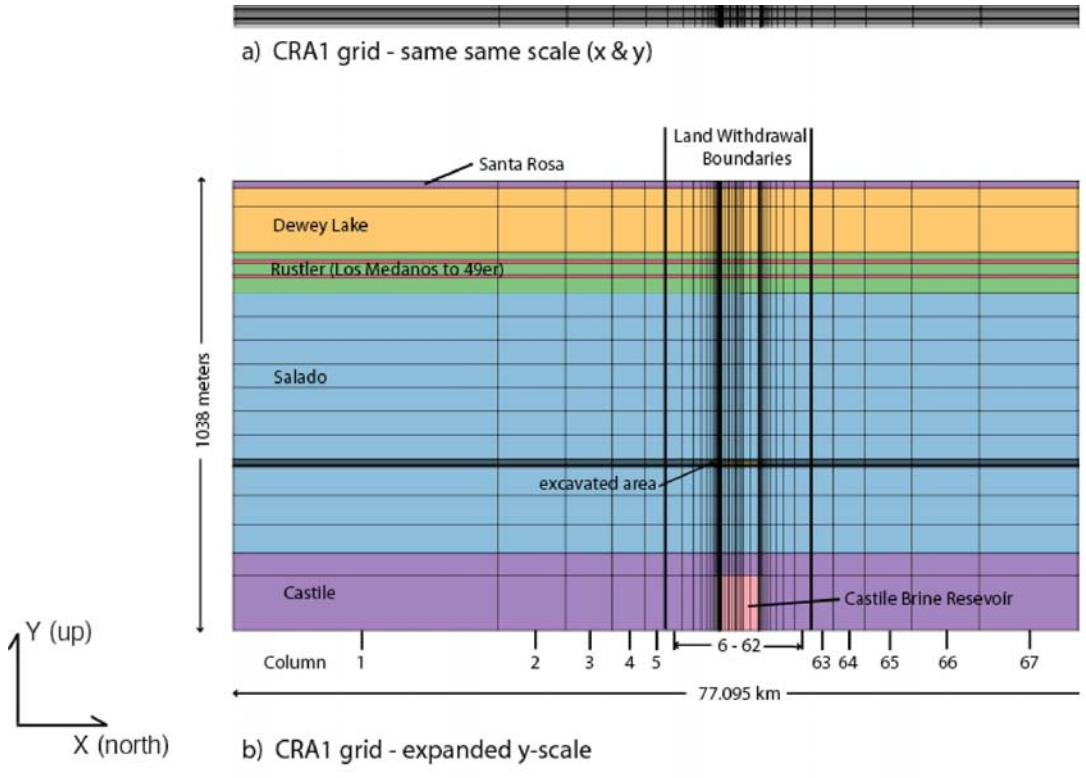

Figure 6-16. A Side View of the BRAGFLO CRA-2004 Geometry Drawn to Scale

The single panel that is represented individually (Panel) is discretized to simulate radial flow to and from the borehole that intersects it. In the CCA grid, the distance from the borehole to the shaft was 1260 m (4133.8 ft), the true distance from the shaft to the south end of the waste disposal region. In the current grid, the distance is 1097 m (3599 ft). The distance was reduced during the re-gridding process that accounted for the Option D panel closures and refinements to represent two RoRs (see Appendix PA, Attachment MASS, Section 4.2.4). In BRAGFLO, the single panel region is the southernmost portion of the repository. It occupies this position because separate modeling activities indicate that slightly larger releases may result from a panel in this position than from alternative placements (see Vaughn et al. 1995).

Panel closures were originally represented generically, since there were four options for the panel closure design. A condition of the original WIPP certification requires the DOE to use the Option D panel closure design constructed with Salado Mass Concrete (SMC). The closure representation for this analysis is modified in the models to better represent the Option D panel closures (see Appendix PA, Section 4.2.8, Attachment MASS, and Chapter 9.0). The panel closure between the panel and the rest of the repository has a cross-sectional area equal to the cross-sectional area of the drifts between panels. The length and total volume of modeled panel closures is consistent with the Option D design. The panel closure between the rest of the repository and the operations regions has a cross-sectional area equal to the cross-sectional area of the drifts between the north end of the waste disposal region and the operations regions. Because there are two closures between the waste disposal region and the shafts in the operations

regions, the modeled panel closures between the rest of the repository and the operations regions have a length and volume consistent with two panel closures.

A number of submodels have been defined within the repository region and are described in this section. The submodels that have been defined for repository processes are Creep Closure (6.4.3.1), Repository Fluid Flow (6.4.3.2), Gas Generation (6.4.3.3), Chemical Conditions in the Repository (6.4.3.4), Dissolved Actinide Source Term (6.4.3.5), and Source Term for Colloidal Actinides (6.4.3.6).

6.4.3.1 Creep Closure

Salt creep occurs naturally in the Salado halite in response to deviatoric stress. Inward creep of rock and the repository response is generally referred to as creep closure. Creep closure of excavated regions begins immediately because of excavation-induced deviatoric stress. If the rooms were empty, closure would proceed to the point where the void volume created by the excavation would be eliminated as the surrounding formation returns to a uniform stress state. In the waste disposal region, waste consolidation continues until loading in the surrounding rock is uniform, at which point salt creep and waste consolidation ceases. The amount of waste consolidation that occurs and the time it takes to consolidate are governed by properties of the waste (waste strength, modulus, etc.), properties of the surrounding rock, the dimensions and location of the room, and the quantities of fluids present.

Fluids that could affect closure are brine that may enter the repository from the Salado or an intrusion borehole, air present in the repository when it is sealed, and gas produced by reactions occurring during waste degradation. Closure and consolidation can be slowed by fluid pressure in the repository. This can be quantified according to the principle of effective stress:

$$\sigma_T = \sigma_e + p \,, \tag{6.11}$$

where σ_T is the stress caused by the weight of the overburden (an essentially constant value), p is the pressure of the repository pore fluid, and σ_e is the stress applied to the waste matrix. In this formulation, the waste is considered a skeleton structure containing pore fluids. As the pore pressure increases, an increasing amount of overburden stress is supported by pore fluid pressure, p, and less overburden stress is supported by the strength of the waste matrix. Waste consolidation will cease when the sum of the stresses felt by the waste matrix and fluid pressure reaches lithostatic pressure. If gas and brine quantities in the repository stabilize, creep closure will act to establish a constant pressure and pore volume.

In summary, creep closure of waste disposal areas will cause their volume to decrease as the Salado deforms to consolidate and encapsulate the waste, changing waste porosity and permeability. Resistance to creep closure will be caused by waste strength and fluid pressure.

Three major material-response models are required for closure analyses. The first model describes how the halite creeps as a function of time and stress. The second model describes the state of waste consolidation as a function of applied stress. A third constitutive model is used to model inelastic behavior of anhydrite marker beds (see Appendix PA, Attachment MASS, Section 13.0).

Halite deformation is predicted using a multimechanism deformation steady-state creep model with work hardening and recovery transient response. For the conditions of the WIPP, creep mechanisms are governed by the temperature and shear stress at a given location in the surroundings at any time. Although WIPP conditions are expected to be nearly isothermal at the ambient natural underground temperature, several mechanisms can be active at the same time because of the large range of stress states that occur around underground rooms and shafts. The focus of the model's mechanistic part is definition of steady-state creep strain, with transient creep strain described through a multiplier on the steady-state rate, thus accommodating both transient changes in stress loading and unloading.

The volumetric plasticity model is the mathematical model for room closure and waste consolidation. The model is discussed further and the experimental data used in this model are summarized and interpreted in Butcher and Mendenhall (1992), Butcher et al. (1991, 65-76) and Luker et al. (1991).

The volumetric plasticity model, multimechanism deformation model, and the inelastic constitutive model for anhydrite were numerically implemented in the SANTOS computer code to calculate the closure of disposal rooms for PA (Appendix PA, Attachment PORSURF).

As a boundary condition, SANTOS requires fluid pressure estimates and hence the quantity of gas present in a disposal room. These estimates are obtained using the average stoichiometry model of gas generation (Section 6.4.3.3) with different rates of gas generation that reflect different assumptions about the quantity of brine available in a waste disposal room. The different rates of gas generation used in SANTOS bound the possible conditions for gas content in the repository. With the volumetric plasticity model and the fluid pressure boundary condition, SANTOS calculates the pore volume of the disposal room through time.

In PA, SANTOS calculates the time-dependent effects on volume as a result of creep closure. These effects are linked to the fluid-flow code BRAGFLO by a porosity surface, which is a look-up table relating porosity (void volume) to (1) time after sealing and (2) gas pressure. At the beginning of a time step, BRAGFLO evaluates the pressure of a cell in the waste disposal regions; the pressure is sensitive to brine and gas flow and the previous pore volume of the cell. The code then consults the porosity surface to find the appropriate void volume of the cell for a given time and pressure. The void volume in the cell is iteratively adjusted during a time step for consistency with gas generation, fluid movement, and repository pressure. Additional details about the porosity surface method are included in Appendix PA, Attachment PORSURF. The porosity surface method of incorporating the creep closure's dynamic effect in PA has been compared to more complex techniques that are computationally impractical in a PA (Freeze et al. 1995). In these comparisons, the porosity surface method was found to reasonably represent behavior observed in more complex models.

The operations area and experimental area (Columns 40 to 45 in Figures 6-14 and 6-15) are modeled as unfilled after closure in this PA. The operations and experimental areas are expected to close in less than 200 years and do not require a porosity surface, in contrast to the region containing waste (Vaughn et al. 1995). These areas are assumed to be "pre-closed" and are assigned a constant low porosity (18 percent) over the entire regulatory time frame.

Additional modeling confirmed that new waste types (compacted waste forms) and waste containers (pipe overpacks) do not impact the adequacy of the original porosity surface modeled in the CCA PA. The porosity surface used in the CCA is used in this analysis.

6.4.3.2 Repository Fluid Flow

Fluid flow modeling within the repository is concerned with (1) fluid flow and distribution in the waste, (2) fluid flow to and from the Salado and shafts, and (3) fluid flow between the repository and intrusion boreholes. These are important in assessing gas generation rates (Section 6.4.3.3), repository pressure, and the mobility of radionuclides in the disposal system. Additional discussion of this topic is provided in Appendix PA, Section PA-4.2.

Disposal region fluid flow is affected by the geometrical association of pillars, rooms, drifts, panel closures, possible borehole locations, time-dependent properties of waste areas resulting from creep closure, flow interactions with other parts of the disposal system, and reactions that generate gas. As described in Section 6.4.3.1, creep closure changes disposal region porosity. Depending on material properties and conditions, brine may flow into the disposal region through the DRZ, or, during disturbed conditions, through a borehole. Brine contained in the Salado may flow to the waste disposal region because of pressure gradients created by the excavation. Brine flow into the repository may be reduced as repository pressure increases, and brine may be expelled from the repository if pressure in the repository exceeds brine pressure in the immediately surrounding rock or borehole. Gas may be generated as waste decomposes, causing a pressure increase. Gas may flow away from the waste area to the anhydrite marker beds by hydrofracturing processes in the DRZ and anhydrite interbeds. Gas flow into intact, halite-rich rock is not expected because of the expected high threshold pressure of halite (see Section 6.4.5.1).

Fluid flow in the disposal system is conceptualized using principles of multiphase flow, except for Culebra flow and transport modeling. In multiphase flow, a residual brine saturation (S_{br}), is defined, which is the minimum saturation at which the brine phase has a nonzero relative permeability; below this saturation, brine is immobile. In accordance with two-phase flow theory, the residual gas saturation (S_{gr}) in the disposal system corresponds to the gas saturation necessary to create an incipient gas-phase relative permeability; below this saturation, waste-generated gas is immobile. The multiphase flow techniques adopted by the DOE are described in Appendix PA, Section 4.2 and Attachment MASS, Section 3.0.

The intrinsic permeability of waste at a given time can influence repository system performance by affecting the flow rate of gas or brine through the waste. Tests reported by Luker et al. (1991, 693-702) on simulated waste have shown material permeabilities of 10^{-12} to 10^{-16} m^2 on waste compacted under a lithostatic load. PA assigns waste permeability as a constant at 2.4×10^{-13} m^2 (Table 6-10). This permeability value was adopted from the value used in the PA verification test (EPA 1998, TSD V-B-14).

Because two-phase relationships have not been measured for waste, PA determines a range of possible two-phase conditions for the repository by applying the LHS technique to parameters within the Brooks-Corey two-phase equations. These and other parameters in the disposal room and repository flow model are shown in Tables 6-10 and 6-11. Details about the two-phase

equations and parameters used in PA are included in Appendix PA, Section 4.2; Attachment MASS, Section 3.0; and Attachment PAR (Parameters 6 and 7).

Material properties in the waste are assumed to be homogeneous and are distributed in the BRAGFLO model to cells whose volumes are much larger than an individual waste container.

Two processes that may occur on scales smaller than the cell volumes in BRAGFLO are wicking (the retention of brine in a capillary fringe) and puddling (the capture of brine in isolated pockets of waste caused by waste heterogeneity). Wicking is accounted for in the gas generation model (Section 6.4.3.3). Vaughn et al. (1995) found that puddling can be neglected.

The experimental and operations regions (Columns 44 and 45 and 40 through 42, respectively, in Figures 6-14 and 6-15) are represented in PA with a porosity of 18 percent and a permeability of 10^{-11} m^2 as a conservative upper bound. For postoperational performance, the panel closures (Columns 31, 35, and 39 in Figures 6-14 and 6-15) are represented with a porosity of 5 percent and a median permeability of 1.78×10^{-19} m^2, as discussed in Appendix PA, Section 4.2, Attachment PAR, Parameter 10, and Attachment MASS, Section 19.0.

6.4.3.3 Gas Generation

Gas will be produced in the repository by a variety of chemical reactions, primarily those occurring among brine, metals, microbes, cellulosic, plastic, and rubber materials, and release of the dissolved gases produced by these reactions to the gaseous phase. The dominant processes are anoxic corrosion of steels and other Fe-based alloys in the waste containers, and the waste and microbial consumption of cellulosic, plastic, and rubber materials. Anoxic corrosion of steels and other Fe-based alloys and Al, and Al-base alloys by water in the brine will occur, producing H_2. Microbial consumption of cellulosic, plastic, and rubber materials could produce a variety of gases; however, for the current waste inventory, CO_2 and CH_4 are expected to dominate (as predicted at the time of the CCA). Radiolysis was demonstrated by laboratory experiment and model calculations to be insignificant (see Appendix PA, Attachment SCR, FEP W15 and W53).

Table 6-10. Repository[1] and Panel Closures Parameter Values

Parameter (units)	Maximum	Minimum	Median or Constant
Permeability, k (square meters) – Waste Region	–	–	2.4×10^{-13}
Permeability, k (square meters) – Operations and Experimental Regions	–	–	10^{-11}
Permeability (square meters) – Panel Closures	1×10^{-17}	2.00×10^{-21}	1.78×10^{-19}
Initial Effective Porosity (percent) – Waste Region	–	–	84.8
Effective Porosity (percent) – Operations and Experimental Regions	–	–	18.0
Effective Porosity (percent) – Panel Closures	–	–	5
Threshold Pressure, P_t (pascals) – Repository [1]	–	–	0
Threshold Pressure, P_t (pascals) – Panel Closures [2]	–	–	1.72×10^{6}
Residual Brine Saturation, S_{br} (unitless) – Repository	0.552	0	0.276
Residual Brine Saturation, S_{br} (unitless) – Operations and Experimental Regions	–	–	0
Residual Brine Saturation, S_{br} (unitless) – Panel Closures	0.60	0	0.20
Residual Gas Saturation, S_{gr} (unitless) – Repository	0.15	0	0.075
Residual Gas Saturation, S_{gr} (unitless) – Operations and Experimental Regions	–	–	0
Residual Gas Saturation, S_{gr} (unitless) – Panel Closures	0.40	0	0.20
Pore Distribution Parameter, λ (unitless) – Repository	5.78	1.44	2.89
Pore Distribution Parameter, λ (unitless) – Operations and Experimental Regions	–	–	0.7
Pore Distribution Parameter, λ (unitless) – Panel Closures	8.10	0.11	0.94
Maximum Capillary Pressure (pascals) – Repository and Panel Closures	–	–	10^{8}
Pore Compressibility (1/pascals) – Repository [3]	–	–	0
Pore Compressibility (1/pascals) – Panel Closures	–	–	6×10^{-11}

[1] Unless specifically listed, Repository refers to operations, experimental, and waste regions.

[2] Threshold pressure (P_t) determined from the relationship: $P_t = PCT\_A \cdot k^{PCT\_EXP}$ where PCT_A and PCT_EXP are constants and k is the permeability.

[3] Accounted for in porosity surface.

Gas generation will affect repository pressure, which is important in other submodels of the disposal system, such as those calculating creep closure (Section 6.4.3.1), interbed fracturing (Section 6.4.5.2), two-phase flow (Section 6.4.3.2), and the radionuclide releases associated with spallings during an inadvertent drilling intrusion (Section 6.4.7). Thus, gas generation must be estimated in PA.

Table 6-11. BRAGFLO Fluid Properties

Parameter (units)	Value
Reference Temperature (kelvin)[1]	300.15
Liquid Density (kilograms per cubic meter) [1,2] at	
Atmospheric Pressure	1,220.0
8 megapascals	1,223.0
15 megapascals	1,225.7
Liquid Viscosity (pascals * seconds) [2]	2.1×10^{-3}
Liquid Compressibility (1/pascals) [2]	3.1×10^{-10}
Gas Density (kilograms per cubic meter) [1,2] at:	
Atmospheric Pressure	0.0818
8 megapascals	6.17
15 megapascals	11.1
Gas Viscosity (pascals * seconds) [2]	8.93×10^{-6}

[1] These values applied to fluids in all material regions in BRAGFLO.

[2] See Appendix PA (Section 4.2) for equations of state.

PA uses the average-stoichiometry model to estimate gas generation occurring in the waste-disposal region. This model was developed for WIPP PA based on gas-generation experiments performed for the WIPP (see CCA Appendix MASS, Section MASS.8 and MASS Attachment 8-2). The average-stoichiometry model accounts for gas formed by anoxic corrosion of steels and other Fe-based alloys, and microbial consumption of cellulosic, plastic, and rubber materials. For calculating repository pressure and gas flow, the density and viscosity of the generated gas are assumed to be those of H_2. In the average-stoichiometry model, gas is assumed to be generated at a rate dependent on the availability of brine in the computational cell. Gas can be generated by anoxic corrosion in all realizations, and is assumed to be generated by microbial activity in half of the realizations. The average-stoichiometry model is based on experimental data on the rates of gas generation from anoxic corrosion of steels and microbial consumption of papers under inundated and humid conditions. These data were used to develop ranges of possible gas-generation rates, as shown in Table 6-12. In BRAGFLO, a gas-generation rate is determined from the rates listed in Table 6-12 by a linear-interpolation method that combines humid and inundated rates based on the effective liquid saturation (Appendix PA, Section PA-4.2.5).

The effective liquid saturation in a computational cell of BRAGFLO for the purpose of gas generation is the computed liquid saturation in that cell plus an adjustment for uncertainty in the capillary rise (wicking) characteristics of the waste. Refer to Attachment PA, Sections PA-4.2.5 and PA-4.2.6, Attachment PAR (Parameter 8) for details on the treatment of wicking in the gas-generation model.

Anoxic corrosion is represented by a generic equation given in Appendix PA (Section PA-4.2.4). This equation accounts only for corrosion of steels and other Fe-based alloys in the repository by the reaction expected to dominate.

Table 6-12. Average-Stoichiometry Gas Generation Model Parameter Values

Parameter (units)	Maximum	Minimum	Median or Constant
Inundated Corrosion Rate for Steel without CO_2 Present (meters per second)	3.17×10^{-14}	0	1.59
Humid Corrosion Rate for Steel	–	–	0
Probability of Microbial Consumption of Plastic and Rubber Materials in the Waste in the Event of Significant Microbial Gas Generation (see Figure PAR-1) where 0 represents corrosion and no significant microbial gas generation. 1 represents cellulosic degradation only, and 2 represents cellulosic, plastic, and rubber consumption	2	0	2
Rate for Microbial Activity Under Humid Conditions (mole per kilogram ∗ second)	1.27×10^{-9}	0	6.34×10^{-10}
Rate for Microbial Activity under Brine-Inundated Conditions (mole per kilogram ∗ second)	9.51×10^{-9}	3.17×10^{-10}	4.92×10^{-9}
Factor β for Microbial Reaction Rates (unitless)	1.0	0	0.5
Anoxic Corrosion Stoichiometric Factor X (unitless)	–	–	1.0
Average Density of Cellulosic Materials in CH-TRU Waste (kilograms per cubic meter)	–	–	58
Average Density of Cellulosic Materials in RH-TRU Waste (kilograms per cubic meter)	–	–	4.5
Average Density of Steels and Other Fe-Based Alloys in CH-TRU Waste (kilograms per cubic meter)	–	–	110.0
Average Density of Steels and Other Fe-Based Alloys in RH-TRU Waste (kilograms per cubic meter)	–	–	110.0
Average Density of Plastic Materials in CH-TRU Waste (kilograms per cubic meter)	–	–	42.0
Average Density of Plastic Materials in RH-TRU Waste (kilograms per cubic meter)	–	–	4.9
Average Density of Rubber Materials in CH-TRU Waste (kilograms per cubic meter)	–	–	14.0
Average Density of Rubber Materials in RH-TRU Waste (kilograms per cubic meter)	–	–	3.1
Bulk Density of Steel Containers, CH-TRU Waste (kilograms per cubic meter)	–	–	170.0
Bulk Density of Steel Containers, RH-TRU Waste (kilograms per cubic meter)	–	–	480.0
Bulk Density of Plastic Liners, CH-TRU Waste (kilograms per cubic meter)	–	–	16.0
Bulk Density of Plastic Liners, RH-TRU Waste (kilograms per cubic meter)	–	–	1.4
Total Volume of CH-TRU Waste (cubic meters)	–	–	1.69×10^{5}
Total Volume of RH-TRU Waste (cubic meters)	–	–	7.08×10^{3}
Wicking Saturation (unitless)	1.0	0	0.5

Because the total quantity of Al and Al-base alloys is small compared to the quantity of steels and other Fe-based alloys, corrosion of Al is omitted for simplicity. The steels and other Fe-based alloys are depleted separately in each computational cell (that is, a cell-by-cell basis), and gas generation can continue in cells, depending on parameter values, until all the steels and other Fe-based alloys are consumed. Brine in cells is consumed as gas generation proceeds. If a cell has a brine saturation equal to zero, it cannot produce gas by anoxic corrosion.

It is assumed there is no passivation of steels or other Fe-based alloys by CO_2 and H_2S produced by microbial activity because microbial gas generation is too slow and also because CO_2 will be removed from the gaseous phase by reacting with MgO. Details of the equations and parameter values are given in Appendix PA, Attachment PAR (Parameters 1 through 5) and Appendix BARRIERS.

Microbial activity occurs in only half the realizations because of uncertainties associated with this process (Appendix PA, Attachment MASS, Section 8.0). Like anoxic corrosion, microbial gas production is represented by a generic equation, given with other details in Appendix PA (Section 4.2.5). The inventory of cellulosic, plastic, and rubber materials is depleted on a cell-by-cell basis. Depending on parameter values, gas generation by microbial activity can continue until all cellulosic materials in the cell are degraded. Reaction with the MgO engineered barrier consumes CO_2 (see Section 6.4.3.4 and Appendix PA, Attachment SOTERM). Thus, the net quantity of gas developed by microbial consumption of cellulosic, plastic, and rubber materials is correlated with constituents of the waste disposal region. It is assumed that microbial activity neither produces nor consumes water, but its rate is dependent on the amount of liquid present in a computational cell.

Microbes may also consume plastic and rubber materials in the repository. The DOE assumes that in half of the simulations where microbial consumption of cellulosic materials occurs, microbes also consume plastic and rubber materials in the waste-disposal region. As with cellulosic materials, these plastic and rubber materials are depleted on a cell-by-cell basis. Parameter values for the average-stoichiometry model are summarized in Table 6-12 and detailed in Appendix PA, Attachment PAR (Parameters 1 through 5).

6.4.3.4 Chemical Conditions in the Repository

The chemical conditions in the repository determine actinide solubilities, parameters demonstrated in past analyses as important to disposal-system performance. In scenarios with the potential to cause releases to the accessible environment, the DOE has determined that chemical conditions can be modeled in PA as homogeneous throughout the waste-disposal area and constant (with the exception of brine content) throughout the 10,000-year regulatory period. This use of constant, homogeneous conditions is based on the assumption of equilibria (for most processes) among brine (the composition of which is determined by the scenario being considered), minerals that are abundant in the Salado, the MgO engineered barrier, and the actinides in the waste. Some exceptions to this assumption are present in performance-assessment models and are discussed where appropriate. In addition to the following discussion, information supporting this position is presented in Appendix PA, Attachments SOTERM and BARRIERS.

Brine and waste within the WIPP repository are modeled as a homogeneous mixture of dissolved and solid-state species. Thermodynamic equilibrium is assumed for dissolved actinide concentrations, but oxidation-reduction reactions between the actinides and other waste components are not assumed to reach equilibrium. Although materials in the waste will actually dissolve at different rates, the assumption of instantaneous solubility equilibria and, along with assumed disequilibrium oxidation-reduction conditions, yields the largest reasonable concentration of dissolved and colloidal actinides in the repository. No chemical microenvironments that influence the overall chemical environment are expected to persist, nor is supersaturation expected during the 10,000-year regulatory period. The average temperature of the WIPP is expected to increase by less than 10°C from its ambient value of 28°C as a result of radioactive decay and exothermic reactions, such as MgO hydration and carbonization, and the effect of this small increase is assumed negligible (see Appendix PA, Attachment SCR, FEPs W72 and W73).

Brine composition in the repository can vary depending on the sequence of future human events. Calculating brine mixing from different sources is not feasible in PA. The DOE has made the reasonable simplification that in the undisturbed performance and E2 scenarios, which do not include penetration of a Castile brine reservoir, all brine in the repository will have the composition of Salado brine (see Appendix PA, Attachment SOTERM). In these scenarios, there is no process that could introduce Castile brine into the repository. For the E1 and E1E2 scenarios, which include penetration of a brine reservoir in the Castile, brine in the repository is assumed to have the composition of Castile brine at all times. Even though some Salado brine may enter the repository in these scenarios, it is reasonable to assume that Castile brine dominates because the quantity of brine that can flow from a reservoir through a borehole and into the repository is substantial compared to the quantity of brine entering from the Salado.

The chemical environment in the repository after closure is expected to be strongly reducing (that is, lowered oxidation states are expected for elements that can occur in more than one oxidation state). Any gaseous or dissolved oxygen present in the repository will be consumed quickly either by aerobic microbial activity or by oxic corrosion after repository closure. Moreover, the repository will contain large amounts of metallic Fe, and anoxic corrosion has been shown to produce considerable quantities of H_2, Fe(II) oxides and hydroxides, and dissolved Fe(II) species under expected repository conditions (see Appendix MASS, MASS Attachment 8-3 of the CCA). Despite the overall reducing conditions, however, a condition of oxidation-reduction disequilibrium is assumed in that oxidation-reduction reactions between dissolved actinides in possible oxidation states are not assumed to occur.

MgO in polypropylene "supersacks" is emplaced on top of the three-layer waste stacks to create conditions that reduce actinide solubilities in the repository (see Section 3.3.3; Appendix BARRIERS; and Appendix PA, Attachment SOTERM, Section SOTERM-2.0). If brine flows into the repository, MgO will react with water in brine and in the gaseous phase to produce brucite ($Mg[OH]_2$). MgO will react with essentially all of the CO_2 that could be produced by complete microbial consumption of the cellulosic, plastic, and rubber materials in the waste, and will initially create hydromagnesite with the composition $Mg_5(CO_3)_4(OH)_2{\cdot}4H_2O$ and will eventually form magnesite with the composition $MgCO_3$ (Appendix BARRIERS; Appendix PA, Attachment SOTERM, Section 2). The most important MgO hydration and carbonation reactions that will occur in the WIPP are:

$$MgO + H_2O(aq \text{ or } g) \rightarrow Mg(OH)_2 \quad (6.12)$$

$$5Mg(OH)_2 + 4CO_2(aq \text{ or } g) \rightarrow Mg_5(CO_3)_4(OH)_2 \cdot 4H_2O. \quad (6.13)$$

$$Mg_5(CO_3)_4(OH)_2 \cdot 4H_2O + CO_2(aq \text{ and/or } g) \rightarrow 5MgCO_3 + 5H_2O \quad (6.14)$$

In these equations, "aq or g" indicates that the H_2O or CO_2 that reacts with MgO or brucite could be present in the aqueous phase (brine) or the gaseous phase. In the CCA, it was assumed that magnesite would be the dominant Mg carbonate in the repository during the 10,000-year regulatory period, and that the brucite-magnesite carbonation reaction (Reaction 6.14) will buffer f_{CO_2} in WIPP whether or not significant microbial CO_2 production occurs. For the PAVT, the EPA specified that the brucite-hydromagnesite carbonation reaction (6.13) will buffer f_{CO_2} in the WIPP whether or not significant microbial CO_2 production occurs (BARIERS-2.4.1). For the CRA-2004 PA, the brucite-hydromagnesite carbonation reaction (6.13) will buffer (control) the fugacity (essentially the partial pressure) of CO_2 at a relatively low value of about $10^{-5.50}$ atm if significant microbial activity occurs. If microbial activity occurs, the predicted value of f_{CO_2} will be identical for both Salado and Castile brine. The brucite-hydromagnesite buffer will control f_{CO_2} effectively because: (1) the DOE is emplacing more than enough MgO to ensure the consumption of essentially all CO_2 that could be produced in the repository, and (2) the reactivity of the MgO being emplaced in the WIPP is such that its carbonation rate exceeds the CO_2 production rate. The brucite dissolution reaction

$$Mg(OH)_2 \rightleftharpoons Mg^{2+} + 2OH^- \quad (6.15)$$

will buffer the pH at about 9 in both Salado and Castile brine if microbial activity occurs (see Appendix PA, Attachment SOTERM, Section 2). For the CRA-2004 PA vectors with microbial activity, the composition of Salado or Castile brine at equilibrium with major Salado minerals such as halite and anhydrite, the f_{CO_2} established by Reaction 13, and the pH established by Reaction 6.15, have been used to calculate actinide solubilities.

The CRA-2004 PA does not assume the same reaction will control f_{CO_2} for vectors without significant microbial CO_2 production. In the absence of microbial activity, the carbonation reaction

$$Mg(OH)_2 + Ca^{2+} + CO_2(aq \text{ and/or } g) \rightleftharpoons CaCO_3 + Mg^{2+} + H_2O(aq \text{ or } g) \quad (6.16)$$

will buffer f_{CO_2} at $10^{-5.48}$ atm in Salado brine and at $10^{-6.15}$ atm in Castile brine (see BARRIERS-2.4.2.3). Reaction 6.15 will buffer the pH at about 9 in both Salado and Castile brine (see Appendix PA, Attachment SOTERM, Section 2). For the 2004 PA vectors without microbial activity, the composition of Salado or Castile brine at equilibrium with major Salado minerals, the f_{CO_2} established by Reaction 6.16, and the pH established by Reaction 6.15, have been used to calculate actinide solubilities.

There is a relatively small amount of portlandite $Ca(OH)_2$ associated with the Portland cement used to dewater process sludges. The quantity of portlandite is too small, however, to overcome the buffer capacity of the reactions described above.

The DOE will emplace significantly more MgO than is needed to maintain the chemical conditions discussed above. The excess MgO emplaced relative to the amount that is needed has been termed a safety factor. The MgO safety factor is defined as:

$$\text{MgO safety factor} = (MgO_{emplaced}) \div (MgO_{required}), \quad (6.17)$$

where $MgO_{emplaced}$ is the quantity of MgO to be emplaced in the repository and $MgO_{required}$ is the quantity of MgO required to consume the maximum amount of CO_2 produced by microbial consumption of all of the emplaced cellulosic, plastic, and rubber materials. This analysis uses: (1) current in the emplaced TRU waste and emplaced materials, and (2) the quantity of MgO emplaced. The EPA has specified a 1.67 safety factor be maintinaed in the repository. Therefore, there will be more than enough MgO to ensure that the conditions described above will be established in the repository (see Appendix BARRIERS, Sections BARRIERS-2.0 and BARRIERS-2.6).

NOTE TO TECH EDITOR: A new equation was added and all subsequent equation numbers and reference to them will need to be revised.

The waste contains organic ligands that could dissolved complexes with actinides and thus increase their solubilities. There are four organic ligands of potential concern in the waste: acetate, citrate, ethylenediaminetetraacetic acid (EDTA), and oxalate. These organic ligands could increase the solubilities of the actinides in the waste because: (1) they are soluble in aqueous solutions such as WIPP brines, and (2) they are known to form complexes with the actinides (see Appendix PA, Attachment SOTERM, Section SOTERM-5.0) Therefore, the effects of acetate, citrate, EDTA, and oxalate have been included in the Fracture-Matrix Transport (FMT) calculations of actinide solubilities for the CRA-2004 PA. These organic ligands will also form complexes with dissolved, cationic species of several metals present in the repository. These metals will thus compete with the actinides for the binding sites on these organic ligands. The effects of two of these metals, Mg^{2+} and Ca^{2+}, have been included in the solubility calculations for the CRA-2004 PA. Including complexation of actinides and of Mg^{2+} and Ca^{2+} by acetate, citrate, EDTA, and oxalate in the solubility calculations for the CRA-2004 PA has confirmed the conclusion in the CCA that organics will not increase the solubilities of the actinides significantly (see CCA Appendix SOTERM, Section SOTERM.5.0).

6.4.3.5 Dissolved Actinide Source Term

The actinide source term used in the CRA-2004 PA calculations represents the aqueous concentrations of thorium (Th), uranium (U), Pu, and americium (Am) in the repository. The source term is the sum of the dissolved species (solubility) and the mobile suspended (colloidal) species of each of these actinides (see Section 6.4.3.6). The source term represents the mobile concentrations of Th, U, Pu, and Am that could be released from the repository in brine.

The actinide source term is limited to those radionuclides that could significantly affect the long-term performance of the WIPP. These radionuclides are all isotopes of Th, U, Pu, and Am. Their potential effects on the long-term performance of the repository can be ordered as Pu ≈ Am >> U > Th (Helton 1998). Other actinides, especially neptunium (Np), were included in the

laboratory and modeling studies used to develop the actinide source term because it was not known which actinides could significantly affect the long-term performance of the repository.

Although commonly referred to as "actinide," these radioelements are almost always present in the waste as solid actinide oxides or solid actinide salts and, if they dissolve in WIPP brines, will form complex species (usually referred to as "complexes") with nonradioactive, inorganic, dissolved species such as carbonate ion (CO_3^{2-}), chloride ion (Cl^-) or hydroxide ion (OH^-), or with nonradioactive, organic, dissolved species such as acetate, citrate, EDTA, or oxalate (see Section 6.4.3.4).

The postclosure chemical environment in the repository will be strongly reducing (see Section 6.4.3.4; Appendix PA, Attachment SOTERM, Section SOTERM-2.0). Previous studies of actinide chemistry imply that, under these conditions, Th will exist as Th(IV) (Appendix PA, Attachment SOTERM, Section 4.1); U will exist as U(IV) or U(VI) (Section 4.2); Np will speciate as Np(IV) or Np(V) (Section 4.3); Pu will exist as Pu(III) and Pu(IV) (Section 4.4); and Am will speciate as Am(III) (Section 4.5). Several actinide oxidation states will be unstable under the strongly reducing conditions expected in the repository. These include Np(VI), Pu(V), Pu(VI), and Am(V). Pu(V) and Pu(VI) could occur in isolated microenvironments in the repository, however, the DOE concludes that would not persist in significant quantities because diffusive transport through any brine present and (especially in the event of human intrusion) advective transport of brine would expose any oxidized Pu to reducing materials like metallic Fe from waste containers and Fe-based materials in the waste, Fe(II)-bearing solids produced by anoxic corrosion of metallic Fe, dissolved Fe(II) species, and metallic Al in the waste (Appendix SOTERM, Sections SOTERM-2 and SOTERM-4; Marcinowski 2001). Microbial activity, if it occurs, would also help create reducing conditions.

The DOE incorporated the uncertainties regarding the oxidation states of U and Pu in PA by assigning a probability of 0.5 that they will exist in the U(IV) and Pu(III) oxidation states, and a probability of 0.5 that these elements will speciate in the U(VI) and the Pu(IV) oxidation states (see also Appendix PA, Section SOTERM-5.2). The oxidation state for both elements is selected by a single variable in the LHS. Therefore, in approximately half of the PA realizations, the oxidation states of the transported actinides are Th(IV), U(IV), Pu(III), and Am(III); and, in the other half of the realizations, the oxidation states are Th(IV), U(VI), Pu(IV), and Am(III).

Laboratory studies with neodymium(III) (Nd(III)), Am(III), and Cm(III) were used to develop a solubility model for the +III actinides, and this model was used to predict the solubilities of Pu(III) and Am(III). Similarly, Th(IV) was used to develop a solubility model for the +IV actinides, which was used for Th(IV), U(IV), Np(IV), and Pu(IV). Literature data for Np(V) were used to develop a solubility model for the +V actinides, which was used only for Np(V). The +V model was not used for other actinides because Pu(V) would not persist in significant quantities in the WIPP. Using the oxidation-state analogy to extend the +III and +IV solubility models to Pu(III) and to U(IV), Np(IV), and Pu(IV), respectively, is valid for these reasons: First, the chemical behavior, especially the speciation and solubilities, of Nd(III), Pu(III), Am(III), and Cm(III) is very similar. Second, the chemical behavior of Th(IV), U(IV), Np(IV), and Pu(IV) is similar, although the solubility of Th(IV) is higher those of U(IV), Np(IV), and especially Pu(IV). Third, Nd, Am, and Cm speciate only in the +III oxidation state, and Th speciates only in the +IV oxidation state under typical laboratory conditions, thus making

experiments with these actinides much easier to carry out and interpret than those with actinides that occur in more than one oxidation state, such as Pu.

The FMT calculations of actinide solubilities for the CRA-2004 PA featured the establishment of equilibrium of Salado brine (GWB) or Castile brine (ERDA-6) with halite and anhydrite, minerals present in large quantities in the Salado at the repository horizon. (These brines are described in Appendix PA, Attachment SOTERM, Section SOTERM-2.2.1). The effects of the MgO included the equilibrium of Salado brine or Castile brine with brucite and hydromagnesite ($Mg_5(CO_3)_4(OH)_2 \cdot 4H_2O$) in the performance-assessment vectors with microbial activity, and with brucite and calcite in the vectors without microbial activity (see Appendix BARRIERS, Section 2; and Appendix PA, Attachment SOTERM). For the 1997 PAVT, it was assumed that Salado brine (Brine A) or Castile brine (ERDA-6) would be in equilibrium with brucite and hydromagnesite ($Mg_5(CO_3)_4(OH)_2 \cdot 4H_2O$) in all of the performance-assessment vectors (both with and without microbial activity) (EPA 1998a, 1998b). For the CCA, equilibria among Salado brine (Brine A) and Castile brine (ERDA-6) and brucite and magnesite were assumed (CCA Appendix BACK).

The FMT calculations for the CRA-2004 PA also included the effects of acetate, citrate, EDTA, and oxalate on the speciation and solubilities of the +III, +IV, and +V actinides (see Appendix PA, Attachment SOTERM). The FMT calculations for the CCA PA and the 1997 PAVT did not include organic ligands.

Table 6-13 provides the solubilities calculated for the +III, +IV, and +V actinides and estimated for the +VI oxidation state for the CRA-2004 PA, and compares them to the solubilities calculated or estimated for the CCA PA and the 1997 PAVT. An uncertainty range of +1.4 orders of magnitude and -2.0 orders of magnitude was applied to the FMT predictions for the CRA-2004 PA (see Appendix PA, Attachment SOTERM, Section SOTERM-3.6). This is the same uncertainty range used for the CCA PA and the 1997 PAVT. LHS was used to sample solubilities from these ranges.

A thermodynamic speciation and solubility model was not developed for U(VI); instead, literature data estimated the solubilities of U(VI) in the repository (Appendix PA, Attachment SOTERM, Section SOTERM-3.0; based on Hobart and Moore [1996]). These estimates have not been used for other actinides in the repository because Np and Pu will not persist in significant quantities in the +VI oxidation state.

The actinide inventory is depleted on a cell-by-cell basis by the computer code NUTS (NUclide Transport Systems) for the undisturbed, E1, and E2 scenarios. The treatment of the E1E2 scenario is described in Section 6.4.13.5. In a computational cell, the processes affecting dissolved actinide concentrations are dissolution of solid actinide compounds, advection of dissolved actinides by brine flow from neighboring cells, and interaction with colloidal particles (see Section 6.4.3.6). NUTS dissolves each actinide until the maximum concentrationdetermined by the actinide-source-term algorithms is obtained or an inventory limit is reached. In the

Table 6-13. Actinide Solubilities (M) Calculated (+III, +IV, and +V) or Estimated (+VI) for the CRA-2004 PA, the 1997 PAVT, and the CCA

Actinide Oxidation State and Brine	CRA-2004 Solubilities, Microbial Vectors[1]	CRA-2004 Solubilities, Nonmicrobial Vectors[1]	1997 PAVT Solubilities[2]	CCA Solubilities[3]
+III, Salado brine	3.07×10^{-7}	3.07×10^{-7}	1.2×10^{-7}	5.82×10^{-7}
+III, Castile brine	1.69×10^{-7}	1.77×10^{-7}	1.3×10^{-8}	1.3×10^{-8}
+IV, Salado brine	1.19×10^{-8}	1.24×10^{-8}	1.3×10^{-8}	4.4×10^{-6}
+IV, Castile brine	2.47×10^{-8}	5.84×10^{-9}	4.1×10^{-8}	6.0×10^{-9}
+V, Salado brine	1.02×10^{-6}	9.72×10^{-7}	2.4×10^{-7}	2.3×10^{-6}
+V, Castile brine	5.08×10^{-6}	2.13×10^{-5}	4.8×10^{-7}	2.2×10^{-6}
+VI, Salado brine[4]	8.7×10^{-6}	8.7×10^{-6}	8.7×10^{-6}	8.7×10^{-6}
+VI, Castile brine[4]	8.8×10^{-6}	8.8×10^{-6}	8.8×10^{-6}	8.8×10^{-6}

[1] Brush and Xiong (2003a) and Downes (2003a,b).

[2] Trovato (1997, Attachment 2), U.S. EPA (1998a, Table 5), U.S. EPA (1998b, Subsection 4.10.4, Tables 4.10-1, 4.10-3 and 4.10-4; and Subsection 12.4, Table 12.4-1), and U.S. EPA (1998c, Subsections 5.26–5.32 and Section 6.0, Table 6.4).

[3] CCA Appendix SOTERM, Table SOTERM-2; based on Novak et al. (1996, Table 1, columns entitled "@Mg"), except that Novak et al. (1996) used molal instead of molar units.

[4] Hobart and Moore (1996).

repository, the transfer of actinides between solid phases and solution is tracked to preserve mass balance of the actinide inventory. Outside the repository, the model does notprecipitate actinides into the solid phase, thereby giving a conservative measure of mobile actinide concentrations (see Appendix PA, Attachment SCR, FEP W59).

See Appendix PA, Attachment SOTERM, Section SOTERM-7.0, for a detailed description of the implementation of the actinide source term in PA.

6.4.3.6 Source Term for Colloidal Actinides

Colloidal actinides are discussed in greater detail in Appendix PA, Attachment SOTERM Section 6. Colloidal particles form in the repository through a variety of processes, including waste degradation, microbial activity, rock decomposition, and chemical condensation. These particles may also be carried into the repository by liquids moving from the Salado or through boreholes. Because of the presence of soils, nutrients, and cellulosic substrates for microbial action in WIPP waste (see Appendix TRU WASTE), humic substances and microbes will be present in disposal room brines, or may form in situ. Actinide-intrinsic colloids may form in the disposal rooms from condensation of dissolved actinides. Mineral fragments, as well as humic substances and microbes, may provide surfaces on which dissolved actinides could sorb.

Four types of colloidal particles are believed to cover the range of possible behavior of all colloid types (see Appendix PA, Attachment SOTERM). The four particle types considered in PA are microbes, humic and fulvic acids (humic substances), actinide-intrinsic (intrinsic), and mineral

fragments. The concentration of actinides carried by each colloidal particle type depends on many of the same chemical conditions that govern the concentration of dissolved actinides.

Actinide concentrations associated with humic substances and microbes are linked to dissolved actinide concentrations through proportionality constants based on experimental results. For humic substances, actinide complexation constants from WIPP-specific experiments or published literature are coupled with experimentally determined site-binding densities and solubilities of different types of humic substances in WIPP brines. For microbes, actinide uptake was experimentally determined through experiments with WIPP-relevant bacteria cultures. Actinide concentrations associated with mineral fragment-type colloidal particles are based on results from experiments designed to determine mobile concentrations in brines, coupled with site-binding densities of mineral substrates. For the plutonium(IV) polymer, actinide concentrations are determined through solubility experiments conducted from over- and undersaturated ranges of pmH values. Intrinsic colloids of other actinides were determined to be negligible and are eliminated from PA calculations. For more discussion on this topic, refer to Appendix PA, Attachment SOTERM.

Actinides associated with microbes and humics are related to the concentration of dissolved actinides in the repository through proportionality constants determined from interpretation of WIPP-relevant experiments and the literature (Appendix PA, Attachment SOTERM). The proportionality-constant relationship is not based on thermodynamic equilibrium but is simply an empirical relationship. The concentration of actinides associated with the plutonium(IV) polymer is a constant value determined from experimental results at the pmH conditions dictated by the presence of the MgO engineered barrier. Likewise, the concentration of actinides associated with mineral colloids is also a constant value, not linked to the concentration of dissolved actinides. Actinides associated with humics and microbes represent most of the colloidal actinide source term. Consequently, the colloidal actinide source term is closely related to the dissolved actinide source term. As discussed in Section 6.4.6.2, however, the source terms are considered separately for transport in the Culebra.

For PA, the concentration of each actinide element on each colloidal particle type during a realization is a fixed value. The concentration parameters are summarized in Table 6-14. Actual values of actinide concentrations on colloidal particles are constrained by inventory limits.

The concentrations of colloidal actinides indicated in this section are assumed to be actinides mobilized on colloidal particles. The indicated concentrations will be entrained in moving brine. For conservatism, it is assumed that no actinides sorb onto colloidal particles that are not mobile in the repository. Thus, all actinides in the repository will be present in the solid phase, dissolved in the aqueous phase, or colloidal actinides suspended in the aqueous phase.

When actinide inventory in a model cell is sufficient, the concentration of colloidal actinides will be at the values indicated in Table 6-14. The total concentration of an actinide in solution and suspension is limited by the amount of solids available from the inventory. This condition is called “inventory-limited.”

Colloid concentrations are calculated by the source-term procedure described in Appendix PA, Section SOTERM-4.3.2. Processes affecting the transport of colloids in the Culebra are addressed in Section 6.4.6.2.2.

6.4.4 Shafts and Shaft Seals

The four shafts connecting the repository to the surface are represented in PA with a single shaft, represented by two primary regions above the repository, and a concrete monolith (Figures 6-14 and 6-15). This single shaft has a cross section and volume equal to the total cross section and volume of the four real shafts it represents and is separated from the waste disposal regions by the true north-south distance from the waste to the nearest shaft (the Waste Shaft). Upon closure of the repository, the shafts will be sealed as described in Section 3.3.1. The seal system was originally represented in the CCA PA by 11 discrete modeled regions in the shaft. The representation was simplified by modeling the behavior of these 11 regions with two primary regions (Upper Shaft and Lower Shaft in Figures 6-14 and 6-15) that have properties simulating the behavior of the original 11 regions (see Appendix PA, Section PA-4.2.7). An analysis of the CCA results concluded that no significant flow of gas or brine would occur within the shaft seal system over the 10,000-year regulatory period. The new shaft model underwent peer review as required by 40 CFR § 194.27 and was incorporated in BRAGFLO (see Appendix PA, Section PA-4.2.7; Section 9.3.1.3.4; and Appendix PEER). The current

Table 6-14. Colloid Concentration Factors

	Concentration on Mineral Fragments [1]	Concentration as Intrinsic Colloid [1]	Proportion Sorbed on Microbes [2 5]	Maximum Sorbed on Microbes [3]	Proportion Sorbed on Humics [2]		Maximum Sorbed on Humics [1]
					Salado	Castile	
Th(IV)	2.6×10^{-8}	0.0	3.1	0.0019	6.3	6.3	1.1×10^{-5}
U(IV)	2.6×10^{-8}	0.0	0.0021	0.0021	6.3	6.3	1.1×10^{-5}
U(VI)	2.6×10^{-8}	0.0	0.0021	0.0023	0.12	0.51	1.1×10^{-5}
Np(IV)	2.6×10^{-8}	0.0	12.0	0.0027	6.3	6.3	1.1×10^{-5}
Np(V)	2.6×10^{-8}	0.0	12.0	0.0027	9.1×10^{-4}	7.4×10^{-3}	1.1×10^{-5}
Pu(III)	2.6×10^{-8}	0.0	0.3	6.8×10^{-5}	0.19	1.37d	1.1×10^{-5}
Pu(IV)	2.6×10^{-8}	1.0×10^{-9}	0.3	6.8×10^{-5}	6.3	6.3	1.1×10^{-5}
Am(III)	2.6×10^{-8}	0.0	3.6	NA	0.19	1.37d	1.1×10^{-5}

[1] In units of moles colloidal actinide per liter

[2] In units of moles colloidal actinide per mole dissolved actinide

[3] In units of moles total mobile actinide per liter

[4] A cumulative distribution from 0.065 to 1.60 with a mean value of 1.1 was used.

[5] Microbial colloids are not included in futures without microbial gas generation.

NOTE: The colloidal source term is added to the dissolved source term to arrive at a total source term. Mineral fragments were provided with distributions, but the maximum was used as described in Appendix PA, Attachment SOTERM. Humic proportionality constants for III, IV, and V were provided with distributions, but only the Castile Am(III) and Pu(III) were sampled.

model divides the shaft into an upper region with all elements above the Salado and a lower region with all Salado elements. These regions are assigned material property distributions that

represent the combined properties of all the individual materials in series. Seal material parameter values used in the PA are provided in Table 6-15.

Conceptually, the shafts are assumed to be surrounded by a DRZ in the Salado. Within the bedded halite, the DRZ begins to form immediately after excavation and develops progressively from unloading as the formation creeps toward the excavated area. From a sealing perspective, the most important characteristic of the DRZ is the higher permeability that results from dilatant deformation and increased pore volume.

The properties of the DRZ are known to vary with the type of adjacent material, time, and depth. When the shaft seals are emplaced, back pressures will progressively develop as the surrounding salt creeps inward. The back pressure applied by the seal material will progressively reduce the magnitude of the stress differential, which is the source for the DRZ microfracturing mechanism. The back pressure also results in a higher mean stress, which induces DRZ healing. The shaft DRZ permeability will, over time, approach that of the intact halite. Also, since the creep rate of the salt surrounding the shafts depends on depth, the back pressures supplied by the seal materials will result in DRZ healing at rates that increase with depth. The relative stiffness of the seal material is a factor, as well.

The DRZ surrounding the shaft is not explicitly represented in the BRAGFLO mesh (Figures 6-14 and 6-15). Rather, the mesh was simplified to represent only the cross-sectional area of the four WIPP shafts, and the permeability values of the seal components at different times have been adjusted (in the parameter database) to account for the shaft DRZ. This adjustment, which yields effective permeabilities, can be done because in Darcy flow, the flux through a porous medium is a linear function of the product of the permeability and the cross-sectional area across which flow occurs. Thus, the flux that would occur through a shaft and its surrounding DRZ can be modeled equivalently using the shaft cross-sectional area with a higher seal component permeability. Equations for the derivation of the effective permeabilities are given in Appendix PA, Attachment PAR (Parameters 64 and 65).

6.4.5 The Salado

The Salado is the principal natural barrier to fluid flow between the waste disposal panels and the accessible environment. Fluid flow in the Salado under natural (undisturbed) conditions is discussed in Section 2.2.1.3. Repository excavation has altered natural pressure gradients in the Salado, creating the potential for fluid flow into the excavation. Fluid flow, gas generation, and volume changes from creep closure alter the pressure gradients through time. Salt creep, as well as possible fracturing from high repository pressure, alters the permeability and other flow properties of the rock near the repository. Depending on pressure gradients and altered material properties, gas and brine flow may be enhanced in affected portions of the Salado.

For PA, the DOE conceptualizes the Salado as a porous medium composed of several rock types arranged in layers, through which flow occurs according to Darcy's law. Two rock types, impure halite and anhydrite, are used to represent the intact Salado. Once sampled, model parameters for all layers are uniform and constant, with two exceptions: porosity and permeability. The assumption of constant properties is based on observed compositional and

structural regularity in layers exposed by the repository and on inferred small For several meters above and below the repository, a DRZ has higher permeability than intact rock and offers little

Table 6-15. Shaft Materials Parameter Values

Parameter (units)	Maximum	Minimum	Median or Constant
UPPER SHAFT MATERIAL			
Residual Brine Saturation, S_{br} (unitless)	0.6	0	0.2
Residual Gas Saturation, S_{gr} (unitless)	0.4	0	0.2
Maximum Capillary Pressure (pascals) [1]	–	–	10^8
Permeability (square meters)	3.16×10^{-17}	3.16×10^{-21}	5.01×10^{-19}
Porosity (percent)	–	–	29.1
LOWER SHAFT MATERIAL (0 to 200 years)			
Initial Brine Saturation, (unitless)	–	–	5.34×10^{-1}
Permeability (square meters) [2]	3.16×10^{-17}	1.0×10^{-20}	6.31×10^{-19}
Maximum Capillary Pressure (pascals)[1]	–	–	10^8
Effective Porosity (percent)	–	–	11.3
LOWER SHAFT MATERIAL (200 to 10,000 years)			
Initial Brine Saturation, (unitless)			5.34×10^{-1}
Permeability (square meters)[2]	1×10^{-18}	3.16×10^{-23}	7.94×10^{-21}
Maximum Capillary Pressure (pascals)[a]	–	–	10^8
Effective Porosity (percent)	–	–	11.3

[1] Capillary pressure for all shaft materials is set to 0.

[2] These values represent the permeabilities of the seal material incorporating the surrounding DRZ

resistance to flow between anhydrite interbeds and the repository. Porosity can vary from its initial value due to pressure-dependent compressibility. As discussed in Section 6.4.5.2, a model has been implemented in interbeds to simulate the effects of fracturing caused by high repository pressure as pore pressure approaches or exceeds lithostatic.
Specific information about the three submodels used to represent impure halite, Salado interbeds, and the DRZ is presented in the following sections.

6.4.5.1 Impure Halite

The PA uses a single porous medium with spatially constant rock and hydrologic properties (labeled "Salado" in Figures 6-14 and 6-15) in PA to represent intact, halite-rich layers in the Salado and minor interbeds contained within layers that are not explicitly represented. A comparison was made between the simplified stratigraphy used in the PA model and a model with a more detailed stratigraphy in the vicinity of the repository. This comparison supports use of stratigraphic representation for PA. This model comparison is described in Christian-Frear and Webb (1996).

Gas may not be able to flow through intact, halite-rich strata of the Salado under realistic conditions for the repository. Gas flow in liquid-saturated rock depends on the gas pressure required to overcome capillary resistance to initial gas penetration and interconnected gas

pathways that allow gas flow (threshold pressure). While the permeability of halite is known to be low, its threshold pressure has never been measured. An empirical relationship between threshold pressure and permeability in non-WIPP rocks (Davies 1991, 17-19) suggests that threshold pressure will be high enough that gas will be unable to flow through the halite-rich strata of the Salado under any conditions foreseeable for the WIPP (see Appendix PA, Attachment MASS, Section MASS-13.1). The DOE values for halite threshold pressure are consistent for generic material of low permeability and prevent gas flow into the impure halite regions (Table 6-16). This is a conservative assumption because gas flow in halite would decrease the pressure in the repository and the driving force available for flow elsewhere. Table 6-16 shows various parameter values used in modeling the Salado impure halite. Additional information on parameter values is contained in Appendix PA, Attachment PAR (Parameters 17 through 19 and Table PAR-2).

Table 6-16. Salado Impure Halite Parameter Values

Parameter (units) [1]	Maximum	Minimum	Median or Constant
Permeability (square meters)	10^{-21}	10^{-24}	3.16×10^{-23}
Effective Porosity (percent)	3.0	0.10	1.0
Threshold Pressure, P_t (pascals) [2]	1.13×10^{8}	1.03×10^{7}	3.41×10^{7}
Residual Brine Saturation, S_{br} (unitless)	0.60	0	0.3
Residual Gas Saturation, S_{gr} (unitless)	0.40	0	0.2
Pore Distribution Parameter, λ (unitless)	1.0	0.20	0.7
Maximum Capillary Pressure (pascals)	–	–	10^{8}
Rock Compressibility (1/pascals)[3]	1.92×10^{-10}	2.94×10^{-12}	9.75×10^{-11}

[1] See Table 6-11 for fluid properties.

[2] Threshold pressure (P_t) determined from the relationship: $P_t = PCT\_A \cdot k^{PCT\_EXP}$ where PCT_A and PCT_EXP are constants and k is the permeability.

[3] Pore compressibility = rock compressibility/effective porosity.

6.4.5.2 Salado Interbeds

Three distinct anhydrite interbeds are modeled in BRAGFLO, representing MB138 (see Figures 6-14 and 6-15), anhydrite layers a and b (Anhydrite AB), and MB139. The three interbeds have the same set of model parameters, and the parameters are initially spatially constant. Porosity and permeability can vary spatially during a simulation, depending on the extent of interbed fracturing. The interbeds differ only in position and thickness.

The three interbeds explicitly represented in the BRAGFLO model are included because they exist in the disturbed region, as modeled around the repository within which fluid is expected to be able to flow with relative ease compared to the surrounding formation. MB139 and anhydrite layers a and b are present within the DRZ that forms around excavations, as shown by Park and Holland (2003) in their analysis of the effects of raising the repository horizon 2.34 meters (7.67 feet). MB138 is included along with a thick DRZ because of uncertainty in the extent and properties of the DRZ and the associated long-term isolation of MB138 from the repository. A more detailed examination of the DRZ was necessary to incorporate the Option D panel closure

into the PA grid. Even though the DRZ would not reach MB 138, PA models the potential for a hydraulic connection between MB 138 and the repository through the DRZ.

In BRAGFLO, brine flows between the Salado and the repository in response to fluid potential gradients that may form over time. Because of the impure halite's low permeability and relatively small surface area, direct brine flow between the impure halite and the repository is relatively small. The interbeds included in the BRAGFLO model of the Salado, however, serve as conduits for brine flow between the impure halite and the repository. Conceptually, brine flows laterally along higher permeability interbeds towards or away from the repository and vertically between the interbeds and the lower permeability halite. Because the interbeds have a very large contact area with adjacent halite-rich rock, even a very small flux from the halite into the interbeds (for brine inflow) or to the halite from the interbeds (for brine outflow) can accumulate significant quantities of brine. In this manner, halite serves as a source or sink for brine in the repository. It is expected that, because of density differences between gas and brine and their stratification within the repository, brine outflow will be predominantly in MB139, and gas outflow will occur in anhydrite a and b or MB138. However, the model does not preclude other flow patterns.

Interbeds contain natural fractures that may be partially healed, but anhydrite lithologies proximal to disposal rooms will be highly distorted as the rooms creep closed. Fractured and distorted anhydrite would not be expected to heal in a manner expected of the DRZ in salt. If high pressure is developed in an interbed, its preexisting fractures may dilate or new fractures may form, altering its porosity and permeability. Pressure-dependent changes in permeability are supported by experiments conducted in the WIPP and in the laboratory (Beauheim et al. 1993). Accordingly, the DOE has implemented in BRAGFLO a porous-media model of interbed dilation and fracturing that causes the porosity and permeability of an interbed's computational cell to increase as its pore pressure rises above a threshold value. Model details are presented in Appendix PA, Section PA-4.2 and Attachment MASS, Section MASS-13.0. To the extent that it occurs, interbed dilation or fracturing is expected to increase the transmissivity of interbed intervals. The threshold pressure of dilated or fractured interbeds is expected to be low because apertures of the fractures increase; thus, fluid is expected to flow outward readily if adequate pressure dilates the interbeds.

The model used to simulate the effects of interbed dilation or fracturing is explained in detail in Appendix PA, Attachment MASS, Section MASS-13.0. In summary, it assigns a fracture initiation pressure above the initial pressure at which local fracturing takes place. Changes in permeability and porosity occur above this pressure. Below this fracture initiation pressure, an interbed has the permeability and compressibility assigned by LHS to represent intact rock. Below the fracture initiation pressure, the initial sampled porosity is modified slightly with pressure caused by compressibility. Above the fracture initiation pressure, the local compressibility of the interbed is assumed to increase linearly with pressure. This greatly increases the rate at which porosity increases with increasing pore pressure. Additionally, permeability increases by a power function of the ratio of altered porosity to initial porosity. For numerical reasons (that is, to prevent unbounded changes in parameter values that would create numerical instabilities in codes), a pressure is specified above which porosity and permeability change no further.

Parameters associated with the interbeds are shown in Table 6-17. Table 6-18 lists parameters used to model interbed dilation and fracture. Additional information about interbed parameters is included in Appendix PA, Attachment PAR, Table 2, and Parameters 20 through 25.

Table 6-17. Parameter Values for Salado Anhydrite Interbeds a and b, and MB138 and MB139

Parameter (units) [1]	Maximum	Minimum	Median or Constant
Permeability (square meters)	7.94×10^{-18}	10^{-21}	1.29×10^{-19}
Effective Porosity (percent)	1.7	0.60	1.1
Threshold Pressure, P_t (pascals) [2]	5.28×10^{6}	2.32×10^{5}	9.74×10^{5}
Residual Brine Saturation, S_{br} (unitless)	0.174	0.00778	0.084
Residual Gas Saturation, S_{gr} (unitless)	0.197	0.014	0.077
Pore Distribution Parameter, λ (unitless)	0.842	0.491	0.644
Maximum Capillary Pressure (pascals)	–	–	10^{8}
Rock Compressibility (1/pascals) [3]	2.75×10^{-10}	1.09×10^{-11}	8.26×10^{-11}

[1] See Table 6-11 for fluid properties.

[2] Threshold pressure (P_t) determined from the relationship: $P_t = PCT\_A \cdot k^{PCT\_EXP}$ where PCT_A and PCT_EXP are constants and k is the permeability.

[3] Pore compressibility = Rock compressibility/effective porosity.

Table 6-18. Fracture Parameter Values for Salado Anhydrite Interbeds a and b, and MB138 and MB139

Parameter (units)	Constant
Fracture initiation pressure at MB139, base of shaft (pascals)	12.7×10^{6}
Increment to give full fracture porosity (percent), MB139 and MB138 [1]	3.9
Increment to give full fracture porosity (percent), Anhydrite a and b [1]	23.9
Full fracture permeability (square meters)	10^{-9}
Increment above fracture initiation pressure to obtain full fracture pressure (pascals) [1]	3.8×10^{6}

[1] A fitting parameter to yield desired dilation over a variation in pressure.

6.4.5.3 DRZ

In the DRZ (see Figures 6-14 and 6-15) near the repository, permeability and porosity are expected to generally increase in both halite and interbeds. These increases are due to a variety of processes. Creep closure and stress-field alterations as the result of the excavation are the dominant causes, similar to the processes discussed for forming the DRZ around the shaft (see Section 6.4.4). The increases in permeability and porosity in interbeds are not likely to be completely reversible with creep closure of the disposal rooms. The increase in DRZ permeability increases the ability of fluid to flow from interbeds to the waste disposal region. The increase in DRZ porosity provides a volume in which some fluid could be retained so that it does not contact waste or slow actinide movement.

In approximating the effects of the DRZ, PA conservatively overestimates brine flow toward the repository (see Appendix PA, Attachment MASS, Section 13). In the model, the permeability of this region is increased relative to intact Salado rock for the duration of a realization. The porosity of the modeled DRZ is increased by a fixed value of 0.0029 (0.29 percent) above the sampled porosity of the intact Salado impure halite. The modeled DRZ extends above and below the repository from the base of MB138 to MB139, thereby retaining the geometry used in the CCA and 1997 PAVT. The PA treatment of the DRZ creates a region that may allow fluid flow between the repository and affected interbeds. Table 6-19 shows parameter values used in the PA representation of the DRZ.

Table 6-19. DRZ Parameter Values

Parameter (units) [1]	Maximum	Minimum	Median or Constant
Permeability (square meters)	3.16×10^{-13}	3.98×10^{-20}	10^{-16}
Effective porosity (percent) [2]	3.3	0.04	1.29
Threshold pressure, P_t (pascals)	–	–	0
Residual brine saturation, S_{br} (unitless)	–	–	0
Residual gas saturation, S_{gr} (unitless)	–	–	0
Pore distribution parameter, λ (unitless)	–	–	0.7
Maximum capillary pressure (pascals)	–	–	10^8
Rock compressibility (1/pascals) [3]	–	–	7.41×10^{-10}

[1] See Table 6-11 for fluid properties.

[2] The DRZ effective porosity value for each realization is equivalent to the sampled value for the Salado halite plus 0.0029 (0.0029 is the difference between the medians for the DRZ and the halite).

[3] Pore compressibility = rock compressibility/effective porosity.

The DOE originally used a constant permeability for the DRZ over the 10,000-year regulatory time frame. However, the EPA required the DOE to treat the DRZ permeability as uncertain during the PAVT (EPA 1998, TSD V-B-14). The range is sampled to determine a fixed value for each realization over the 10,000-year period. Additionally, in the 1997 PAVT, the anhydrite fracture model was applied to the DRZ to capture the effects of halite fracture under high repository pressures. As was done in the 1997 PAVT, the CRA-2004 PA treats the DRZ permeability as an uncertain parameter, and the anhydrite fracture model is also applied to the DRZ. The parameter values are shown in Table 6-19.

6.4.5.4 Actinide Transport in the Salado

The DOE considers actinide transport in the Salado to be a possible mechanism for release to the accessible environment. As in other areas of the disposal system, actinides in the Salado may be transported as dissolved species or as colloidal particles. Actinide transport is affected by a variety of processes that may occur along the flow path.

The DOE uses the NUTS code (see Appendix PA, Section PA-4.3) to model the migration of radionuclides in the repository and surrounding formations. NUTS models radionuclide transport within all regions for which BRAGFLO computes brine and gas flow, and uses as input

for each realization the corresponding BRAGFLO velocity field, pressures, porosities, saturations, and other model parameters including (for example) the geometrical grid, residual saturation, material map, and compressibility.

The PA uses NUTS in two ways. First, the code is used in a computationally fast tracer mode to identify those BRAGFLO realizations for which it is unnecessary to do full transport calculations because contaminated brine never reaches the top of the salt or the accessible environment within the Salado. Such realizations cannot contribute to the total integrated release of radionuclides from the disposal system. If the tracer calculation indicates a possibility of consequential release, a computationally slow calculation of the full transport of each radionuclide is performed (see Appendix PA, Section 6.7.2).

6.4.5.4.1 NUTS Tracer Calculations

All BRAGFLO realizations are evaluated using NUTS in a tracer mode to identify realizations for which there is no possibility of radionuclides reaching the accessible environment. The tracer simulations consider an infinitely soluble, nondecaying, nondispersive, and nonsorbing species as a tracer element. The tracer is given a unit concentration in all waste disposal areas of 1 kilogram per cubic meter. If this tracer does not reach the selected boundaries (the top of the Salado and the land withdrawal boundary within the Salado) in a cumulative mass greater than or equal to 10^{-7} kilograms within 10,000 years, it is assumed there is no consequential release to these boundaries. If a cumulative mass greater than or equal to 10^{-7} kilograms does reach the selected boundaries within 10,000 years, a complete transport analysis is conducted. The value of 10^{-7} kilograms is selected because, regardless of the isotopic composition of the release, it corresponds to a normalized release less than 10^{-6} EPA units, the smallest release displayed in CCDF construction. The largest normalized release would be 9.98×10^{-7} EPA units, which corresponds to 10^{-7} kilograms of ^{241}Am, if the release was entirely ^{241}Am

6.4.5.4.2 NUTS Transport Calculations

For BRAGFLO realizations with greater than 10^{-7} kilograms reaching the boundaries in the tracer calculations, NUTS models the transport of five different species of radionuclides (^{241}Am, ^{239}Pu, ^{238}Pu, ^{234}U, and ^{230}Th). These radionuclides represent a larger number of radionuclides, as discussed in Appendix TRU WASTE. For decay purposes, radionuclides were grouped together based on similarities such as isotopes of the same element and those with similar half-lives, to simplify the calculations, as discussed in CCA Appendix WCA.3.2.3. For transport purposes, solubilities are lumped to represent both dissolved and colloidal forms. These groupings simplify and expedite calculations.

NUTS models radionuclide transport by advection (see Appendix PA, Attachment MASS). NUTS disregards sorptive and other retarding effects throughout the entire flow region. Physically, some degree of retardation must occur at locations within the repository and the geologic media, and the disregard of retardation processes is therefore conservative. NUTS also disregards reaction-rate aspects of dissolution and colloid formation processes, and mobilization is assumed to occur instantaneously. Neither molecular nor mechanical dispersion is modeled in NUTS. These processes are assumed to be insignificant in comparison to advection, as discussed further in Appendix PA, Attachment MASS.

Colloidal actinides are subject to retardation by chemical interaction between colloids and solid surfaces and by clogging of small pore throats (that is, sieving). There will be some interaction of colloids with solid surfaces in the anhydrite interbeds. The low permeability of intact interbeds is reason to expectpore apertures are small and some sieving will occur. However, colloidal particles, if not retarded, are transported slightly more rapidly than the average velocity of the bulk liquid flow. Because the effects on transport of slightly increased average pore velocity and retarding interactions with solid surfaces and sieving are offsetting, the DOE assumes residual effects of these opposing processes will be either small or beneficial and does not incorporate them in modeling of actinide transport in the Salado interbeds.

If brine that has been in the repository moves into interbeds, it is likely that mineral precipitation reactions will occur. Precipitated minerals may contain actinides as trace constituents. The beneficial effects of the possible mineral co-precipitation process are neglected in PA. Furthermore, colloidal-sized precipitates will behave like mineral-fragment colloids, which are destabilized by brines, quickly agglomerating and settling by gravity. The beneficial consequence of colloid precipitation is also disregarded in PA.

Additional processes that may impact transport in Salado interbeds are related to fractures, channeling, and viscous fingering. Interbeds contain natural fractures. Because of the low permeability of unfractured anhydrite, most fluid flow occurring in interbeds will occur in fractures. Even though some properties of naturally fractured interbeds are characterized by in-situ tests (see Section 2.2.1.3), other uncertainty exists in the characteristics of the fracture network that may be created if gas pressure in the repository becomes high. The PA modeling system accounts for the possible effects on porosity and permeability of fracturing through use of a fracturing model (see Section 6.4.5.2). The processes and effects associated with fracture dilation or fracture propagation that are not already captured by the PA fracture model are negligible (see CCA Appendix MASS, Section MASS.13.3 and MASS Attachment 13.2). Of those processes not already incorporated, channeling is considered to have the greatest potential effect.

Channeling is the movement of fluid through the larger aperture portions of a fracture network (that is, areas of local high permeability). It could locally enhance actinide transport. However, it is assumed that the effects of channeled flow in existing or altered fractures will be negligible on the scale of the disposal system. The DOE believes this assumption is reasonable because processes that act to limit the effectiveness of channels or disperse actinides in them are likely to occur. First, if gas is present in the fracture network, it will be present as the nonwetting phase and will occupy the portions of the fracture network with relatively large apertures, where the highest permeabilities will exist locally. The presence of gas thus removes the most rapid transport pathways from the contaminated brine and decreases the impact of channeling. Second, brine penetrating the Salado from the repository is likely to be completely miscible with in-situ brine. Because of miscibility, diffusion or other local mixing processes will probably broaden fingers (reduce concentration gradients) until the propagating fingers are indistinguishable from the advancing front.

Gas will likely penetrate the liquid-saturated interbeds as a fingered front rather than as a uniform front. Fingers form because of the difference in viscosity between the invading fluid (gas) and the resident fluid (liquid brine), and because of channeling effects. This process does

not affect actinide transport, however, because actinides of interest are transported only in the liquid phase, which will not displace gas in the relatively high-permeability regions because of capillary effects.

6.4.6 Units Above the Salado

The geology and hydrology of units above the Salado are discussed in Sections 2.1.3 and 2.2.1.4, respectively. In this section, the assumptions, simplifications, and models used in PA of these units are described. Because it is unlikely that these units will be impacted by UP, modeling these units is performed mainly because regulations require considering the effects of inadvertent human intrusions. See Appendix PA, Attachment MASS, Section 14 for additional discussion on the units above the Salado.

The principal purpose of BRAGFLO calculations for units above the Salado is to determine the quantity of brine entering each unit from an intrusion borehole or the shaft. It is unrealistic to assume that all flow up an intrusion borehole enters the Culebra. Accordingly, BRAGFLO parameters are specified so that brine flow from the intrusion borehole is possible not only into the Culebra but also into the Magenta, Dewey Lake, and overlying units (as well as to the ground surface), depending on whether liquid rises above the Culebra in the intrusion borehole. Some of the assumptions regarding the properties of units above the Salado are made specifically to allow model simplification and are conservative with respect to actinide transport in the Culebra (that is, overestimate releases).

Consistent with accepted stratigraphic conventions for the area, discussed in Section 2.1.3, the units above the Salado are subdivided into seven layers in PA; these are, in order of lowest to highest, the Los Medaños, the Culebra, the Tamarisk, the Magenta, the Forty-niner, the Dewey Lake, and the units above the Dewey Lake. The conceptual model for each of these layers is described sequentially in the following sections.

A fundamental assumption in the PA conceptual model for modeling actinide transport to the accessible environment in units above the Salado is that lateral actinide transport through rock formations is possible within the next 10,000 years only in the Culebra. This assumption is appropriate for several reasons relating to the properties of other rock units and the groundwater basin conceptual model, discussed in following sections.

Section 2.2.1.4 describes the hydrology of the units above the Salado in terms of the groundwater basin conceptual model. Insight into groundwater basin processes indicates that it is possible to significantly simplify the hydrologic models in the units above the Salado to obtain reasonable estimates of actinide transport (see Corbet and Knupp 1996; Appendix PA, Attachment MASS, Section MASS-14). Therefore, the DOE calculates actinide transport in the units above the Salado with a two-dimensional conceptual and mathematical model. The models used for actinide transport in the units above the Salado are a simplified implementation of the groundwater basin conceptual model. The mathematical model is implemented in the computer codes MODFLOW-2000 and SECOTP2D (see Appendix PA, Section PA-4.8).

6.4.6.1 The Los Medaños

The Los Medaños (formerly the unnamed lower member of the Rustler, Row 25 in Figures 6-14 and 6-15) rests above the Salado. Its transmissivity was measured (see Section 2.2.1.4.1.1) and found to be low, which is consistent with expectations based on its anhydrite, gypsum, halite, clay, and siltstone composition (see Section 2.1.3.5.1). In PA, this member is treated as impermeable, which prevents liquid flow and actinides from entering this unit. The DOE assumes that because of the low permeability of the Los Medaños assumption any brine entering it from an intrusion borehole would be contained well within the site boundary for more than 10,000 years. This treatment is conservative because allowing flow from a borehole or shaft into the Los Medaños would, if anything, decrease flow into the Culebra. This would reduce the release of actinides from the Culebra to the accessible environment. In PA, the thickness of Los Medaños is 36 m (118 ft), and its permeability is zero.

6.4.6.2 The Culebra

The Culebra is represented in BRAGFLO as Row 26 in Figures 6-14 and 6-15. The model geometries for Culebra flow calculations and transport calculations are discussed in this section. Boundary and initial conditions for this geometry are discussed in Section 6.4.10.2. Supplementing the discussion in this section are additional details about the Culebra modeling provided in Section 6.4.13 and Appendix PA, Section PA-4.9.

Conceptually, radionuclides might be introduced into the Culebra through brine flow up the sealed shafts. However, the chief source of actinides in the Culebra is modeled as long-term releases from a borehole that intersects the repository. If radionuclides are introduced into the Culebra, they may be transported from the point of introduction by groundwater flowing naturally through the Culebra.

The Culebra is conceptualized as a confined aquifer. For fluid flow, it is conceptualized as a heterogeneous porous medium represented by variations in transmissivity. A heterogeneous velocity field is used for transport calculations, but all other rock properties (e.g., porosity, K_d) are conceptualized as constant (homogeneous) across the model area. The Culebra is conceptualized as having two types of porosity; a portion associated with high-permeability features where transport occurs by advection, and the rest associated with low-permeability features where flow does not occur and retardation occurs by physical processes (diffusion) and chemical processes (sorption). This type of conceptual model is commonly referred to as "double-porosity." In this conceptual model, transport and retardation of colloidal particles are also considered. This section addresses fluid flow in the Culebra. The transport and retardation of dissolved actinides will be discussed principally in Section 6.4.6.2.1. The transport and retardation of colloidal particles will be discussed principally in Section 6.4.6.2.2.

In the Culebra conceptual model used in PA, the spatial distribution of transmissivity in the Culebra is important. Other potentially important processes acting on Culebra flow and transport are climate change (Section 6.4.9 and CCA Appendix MASS, Section MASS.17) and the effects of subsidence caused by potash mining in the McNutt (Section 6.4.6.2.3 and CCA Appendix MASS, Section MASS.15.4).

The MODFLOW-2000 code uses two-dimensional horizontal grids to simulate groundwater flow. A regional grid approximately 14 miles × 19 miles (22 kilometers × 30 kilometers) (Figure 6-17) with spatially varying transmissivity determines the flow fields in the WIPP region from hydraulic head distributions controlled by distant topographic and hydrologic features (that is, boundary conditions). The grid is made up of 68,768 uniform 100 m × 100 m (328.08 ft) cells. Because this grid is used to define the boundary conditions for the flow and transport calculations, it is discussed in detail in Section 6.4.10.2, along with the specification of boundary conditions. Details about the development and calibration of the flow fields are given in Appendix PA, Attachment TFIELD. For transport in the region of interest, a local grid 7.5 km × 5.4 km (4.5 mi × 3.1 mi) with finer discretization is used in SECOTP2D (Figure 6-18). The grid for the transport domain contains 150 columns and 108 rows of 50 m × 50 m (164 ft) cells, resulting in 16,200 grid blocks.

The local SECOTP2D domain boundaries (Figure 6-18) were chosen to capture all flow paths from the modeled release point above the center of the disposal panels to the accessible environment. Because past analyses indicated that transport in the Culebra occurs within a region that lies from southeast of the repository to west of the repository, the transport domain extends slightly beyond the southern and western boundaries of the controlled area. Because it is not needed, a strip in the northern portion of the controlled area has been omitted from the SECOTP2D domain to ease the computational burden.

Flow directions and transmissivities in the Culebra vary significantly from location to location within and past the site boundary. Consequently, the effects of flow in the region around the WIPP site are important in the conceptual model. The boundaries to the flow model are discussed in Section 6.4.10.2; the domain itself is shown in Figure 6-17.

The conceptual model for the Culebra assumes that fluid fluxes and directions in the future will be the same as at repository closure, unless future mining within the site occurs, in which case changes to fluid flow are calculated. A steady-state flow field is used to represent this assumption. Conditions assumed at site closure are the subsidence effects of mining in the near future outside the site boundary, climate change, and heads similar to those measured in late 2000 (see Appendix PA, Attachment MASS, Sections MASS-15.4 and MASS-14.2, and Attachment TFIELD).

The factors controlling fluid flow in the Culebra are the hydraulic gradient, distribution of transmissivity, and porosity. The hydraulic gradient and transmissivities used in PA are coupled because they are calibrated to observed conditions by a process described in Appendix PA, Attachment TFIELD. Flow fields are calculated with the code MODFLOW-2000 assuming homogeneous porosity in the Culebra. This single value is the total porosity for the Culebra, including both advective and diffusive porosity, as discussed below. Using a single porosity for the flow calculation does not introduce inconsistency with transport calculations because (1) steady-state flow fields are used so flux through the system is not dependent on porosity, and (2) the velocity of liquid for transport is calculated based on a double-porosity model implemented in SECOTP2D. Thus, the important factors for flow calculations are the hydraulic gradient and transmissivity variation.

Because BRAGFLO models a vertical section of the disposal system, the spatial distribution of transmissivity cannot be represented in the BRAGFLO grid. The source term of actinides in the Culebra is calculated in part from BRAGFLO flow fields, so parameters for the Culebra are required in BRAGFLO. Specifically, a single value of Culebra permeability representative for the Culebra in the area immediately over the waste-emplacement panels is input to partition fluid flow among the stratigraphic units along the human-intrusion borehole.

BRAGFLO calculates gas flow and brine flow that may occur up a borehole (see Section 6.4.7). The MODFLOW-2000 code models flow of the liquid phase only. The possible effects of gas on Culebra flow are not modeled. This simplification is reasonable because after gas pressure is relieved by flow to the surface during drilling, little gas will remain in the repository. This gas will move up the borehole at low rates and tend to move directly to the top of the liquid-saturated section of the borehole, bypassing the Culebra. Any gas that does enter the Culebra will tend to displace brine from fractures and reduce the potential for actinide transport. Based on previous modeling (Lappin et al. 1989, Appendix E.1.5.1), the effect of the mass of brine being injected into the Culebra on the natural flow is negligible. Parameter values used in BRAGFLO to describe the Culebra are shown in Table 6-20. Parameter values used in MODFLOW-2000 are shown in Table 6-21. See Appendix PA, Attachment PAR, Table 2 for additional Culebra parameter information.

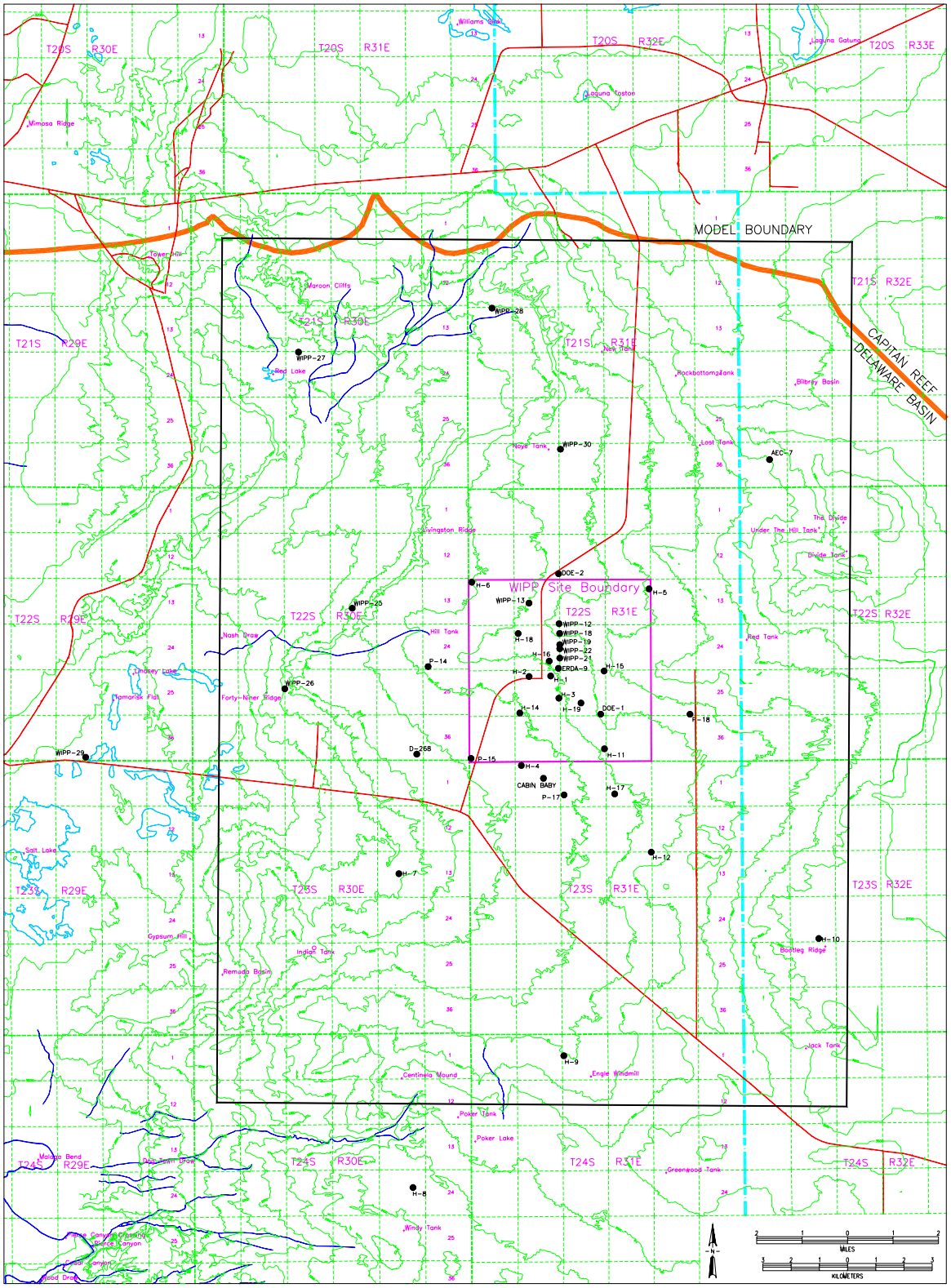

Figure 6-17. The MODFLOW-2000 Domain Used in the Groundwater Model of the Culebra

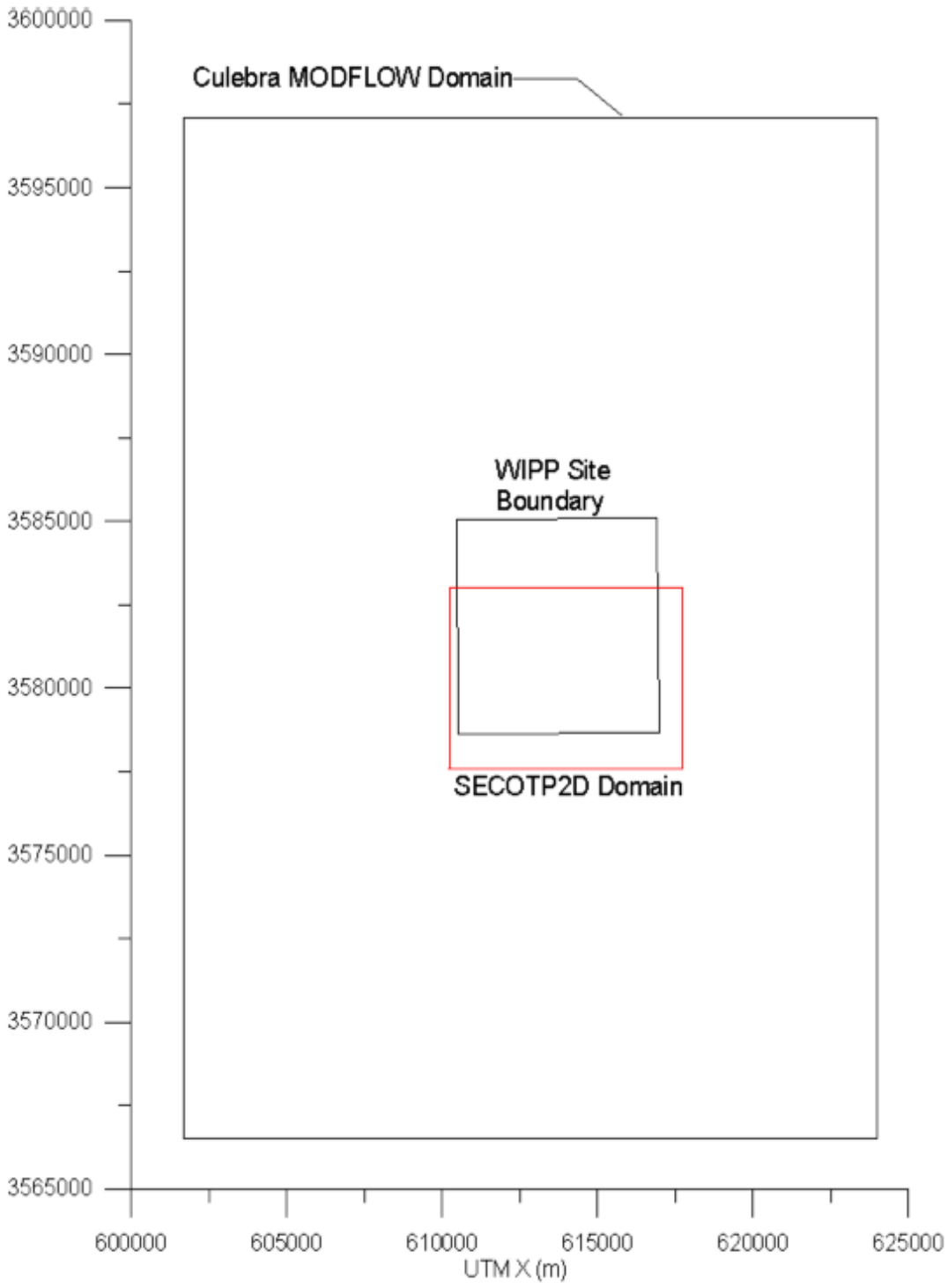

Figure 6-18. Extent of SECOTP2D Domain with Respect to the MODFLOW-2000 Culebra Domain and WIPP Site Boundary

Three different thicknesses of the Culebra were assumed in PA modeling. BRAGFLO uses a thickness of 7.7 m (25.3 ft), representative of the Culebra over the waste disposal panels. For calibrating transmissivity fields (see Appendix PA, Attachment TFIELD) and calculating flow in the Culebra with MODFLOW-2000, a thickness of 7.75 m (25.4 ft) is assumed, consistent with an average thickness over the area modeled. For transport calculations using SECOTP2D, a thickness of 4 m (13 ft) is assumed, consistent with the observed thickness of the Culebra active in transport, which is discussed in Section 6.4.6.2.1. Using different thicknesses does not introduce inconsistencies in the modeling, however, because the transmissivities used in these codes are consistent, and transmissivity governs the total flux of fluid through the Culebra. Furthermore, the fluid flux used in the SECOTP2D model is calculated by MODFLOW-2000, ensuring consistency.

The spatial variation in transmissivity observed in the Culebra is incorporated by assigning different transmissivity values to every computational cell in the model. Because there is uncertainty in the estimated value of Culebra transmissivity where measurements have

Table 6-20. Culebra Parameter Values for the BRAGFLO Model

Parameter (units) [1]	Value
Permeability (square meters)	7.73×10^{-14}
Effective porosity (percent)	15.1
Rock compressibility (1/pascals) [2]	10^{-10}
Threshold pressure, P_t (pascals) [3]	1.5×10^{4}
Residual brine saturation, S_{br} (unitless)	0.084
Residual gas saturation, S_{gr} (unitless)	0.077
Pore distribution parameter, λ (unitless)	0.644
Maximum capillary pressure (pascals)	10^{8}
Thickness (meters)	7.70
Initial Pressure (pascals)	9.14×10^{5}

[1] See Table 6-11 for fluid properties in BRAGFLO.

[2] Pore compressibility = rock compressibility/effective porosity.

[3] Threshold pressure (P_t) determined from relationship: $P_t = PCT\_A \cdot k^{PCT\_EXP}$, where PCT_A and PCT_EXP are constants and k is the permeability.

Table 6-21. MODFLOW-2000 Fluid Properties

Parameter (units)	Value
Liquid density (kilograms per cubic meter)	1,000
Liquid compressibility (1/pascals)	4.4×10^{-10}

not been made, 100 different transmissivity fields were developed. Each transmissivity field statistically represents the natural variation in transmissivity that honors measured data according to certain criteria. Monte Carlo simulations using a large number of equally-likely transmissivity fields are a statistically sound method of characterizing the uncertainty associated with

transmissivity in the Culebra. For details of the generation and use of transmissivity fields and criteria, refer to Appendix PA, Attachment TFIELD.

Regional flow directions and fluxes are calculated with the regional domain, as described earlier and shown in Figure 6-18. To increase resolution of transport processes a finer grid is used. Within MODFLOW-2000, each 100-m × 100-m cell is divided into four 50-m ×-50 m cells with exactly the same transmissivity as the 100-m × 100-m cell. Darcy velocities are calculated in the 50-m × 50-m cells and then mapped directly into the SECOTP2D grid (Figure 6-18), which also consists of 50-m × 50-m cells. Consistency between the flow calculated in the regional domain and flow in the local domain is important, and is assured by interpolation of the boundary conditions and transmissivity field properties of the regional domain onto the local domain. This process of calculating two flow fields with domains of different extent and resolution is for practical reasons only. It is a method of incorporating regional effects in finely discretized local flow fields that has relatively low computational burden, compared to other possible methods. Additional discussion of this process is provided in Section 6.4.10.2.

In summary, flow in the Culebra is calculated with the code MODFLOW-2000, using a conceptual model of a confined aquifer, regional flow effects, uniform porous medium, steady state, and transmissivity variation. In addition, the effects of subsidence caused by potash mining in the McNutt are incorporated during the flow calculation, as discussed in Section 6.4.6.2.3.

6.4.6.2.1 Transport of Dissolved Actinides in the Culebra

Actinides may be introduced into the Culebra by brine flowing up a borehole or up the shaft. Three principal processes have been demonstrated to occur naturally that affect the transport and retardation of dissolved actinides. Dissolved actinides will be carried by advection in the natural flow of Culebra groundwater. Dissolved actinides will diffuse into the matrix. Dissolved actinides will sorb to varying extents onto the different minerals lining pore walls or fractures. It is possible that dissolved actinides may participate as trace constituents in reactions between water and rock and be bound in newly formed minerals, but this phenomenon is not included in the conceptual model. These processes are complicated to characterize because of known stratigraphic variation in the Culebra and expected heterogeneity in solution chemistry along the possible flow paths from the injection point to the accessible environment.

The basic stratigraphy of the Culebra is continuous across the WIPP site (CCA Appendix FAC, Section FAC.4.1.2), and contains layers with significantly different properties (Holt and Powers 1984, 1986, 1990, and CCA Appendix FAC, Section FAC.5.2). Hydraulically, there are two distinct layers in the Culebra. Mercer and Orr (1979) report the result of a tracer and temperature survey that suggests there is no significant flow in the upper 4.3 m (14 ft) of the Culebra. Culebra hydraulic testing at well H-14 indicates generally low permeabilities but a slightly higher permeability in the upper portion (Beauheim 1987). In descriptions from the air intake shaft, Holt and Powers (1990) noted that most of the fluid produced came from the lower portion of the Culebra. Hydraulic tests at the H-19 hydropad indicate that the permeability of the Culebra's upper portion is significantly lower than the permeability of the lower portion (Beauheim 2000). Consistent with hydraulic indicators, tracer tests conducted at H-19 confirmed that the Culebra's upper portion makes no significant contribution to the transport of dissolved

species, although it may retard solute transport by diffusion into it (Meigs et al. 2000). The Culebra at the WIPP site is conceptualized as having very low permeability in the upper approximately 3 m (9.8 ft), and variable permeability in the lower portion, which can be lower than the upper portion in regions where the Culebra as a whole is relatively impermeable. Thus, the bulk of the data indicates that the majority of the flow and transport takes place in the lower portions of the Culebra. Accordingly, for transport calculations, an effective thickness of 4 m (13.1 ft) is assumed (Meigs and McCord 1996).

There is considerable variability in the structure and size of porous features in the Culebra, including fractures (of a variety of dimensions and interconnectedness), vugs, and interparticle and intercrystalline porosity (Holt 1997). The principal flow occurs in features with the high permeability, and slower flow and diffusion are primary processes in lower permeability features. Tracer test interpretations indicate that at some locations, flow occurs predominantly through fractures (advective porosity is low) and at other locations, slower transport indicates that flow occurs in other permeable features, such as vugs connected by microfractures, and possibly interparticle porosity (higher advective porosity). Tracer test interpretations also indicate that matrix diffusion is an important process in high-permeability regions of the Culebra. In other words, at least two scales of porosity are needed to represent the transport processes in the Culebra (that is, a double-porosity model). At some locations of low permeability, fractures may be absent or filled with gypsum. An alternative conceptual model for transport at these locations is uniform single porosity with a high porosity. To simplify calculations, the uniform single-porosity model was not implemented; the double-porosity model implemented results in faster transport.

In SECOTP2D, advective porosity represents the porous features in which flow occurs. Advective porosity values are low, which is representative of flow in fractures. Diffusive porosity represents those porous features in which no flow occurs and diffusion and sorption occur. Diffusive porosities are large relative to advective porosity, representing the vugs, interparticle, and intercrystalline porosity of the bulk rock.

The processes that occur in the advective porosity portion of the Culebra are advection (flow), dispersion (spreading caused by heterogeneity), diffusion within the advective porosity, and diffusion into the diffusive porosity. Important factors in this conceptual model are the velocities of fluid in the advective porosity, free-water diffusion coefficients, and dispersion coefficients. The most important factor is the fluid velocity. Free-water tracer diffusion coefficients are specified for actinides. Dispersive spreading at the scale of disposal-system modeling is dominated by the effects of heterogeneities explicitly incorporated in the transmissivity fields input to MODFLOW-2000. This eliminates the need to account for larger-scale features by specifying a modeling dispersion coefficient larger than those observed at the hydropad-test scale.

Fluid velocity in SECOTP2D is coupled to the results of the fluid flow modeling conducted with MODFLOW-2000 (see the preceding section). Fluid flow directions and volumetric fluxes in SECOTP2D are calculated in MODFLOW-2000. The flow velocities in the transport calculation are determined using the fluxes from the fluid flow calculation, the Culebra thickness specified for the transport calculation, and the advective porosity specified for the transport calculation.

Because a different transmissivity field is used and the values of several important parameters are sampled, each realization uses a different velocity field.

Retardation is conceptualized as a function of physical effects of diffusion into diffusive porosity and sorption. Diffusion is parameterized by the diffusive porosity (which is essentially a reservoir for diffusion), tortuosity, matrix block length, and free-water diffusion coefficient. Tortuosity represents the tortuous structure of the porosity within the matrix; it slows the diffusion process. The matrix block length is a conceptual construct representing the ratio of the surface area between advective and diffusive porosity to the volume of diffusive porosity features; physical retardation increases as the matrix block length decreases. Physical retardation also increases if tortuosity or the free-water diffusion coefficient of diffusive porosity are larger. See Appendix PA, Sections 4.8 and 4.9 and Attachment MASS, Section 15.2 for more details.

Chemical retardation of dissolved actinides is conceptualized to occur by sorption onto dolomite grains exposed in diffusive porosity because of the large amount of dolomite present in the Culebra. Chemical retardation increases if diffusive porosity is smaller, because there is a larger volume of rock for sorption. Although clay minerals are present and would sorb actinides in the Culebra, their effects are not included in the conceptual model or specified parameter values. Effective properties for the rock matrix, which is assumed to be homogeneous, and solution chemistry are assumed and are incorporated directly in the specified parameters for the retardation model (see Appendix PA, Attachment MASS, Section 15.2, and Attachment PAR, Parameters 49 through 57).

The PA uses a linear isotherm model to represent the retardation that occurs as dissolved actinides are sorbed onto dolomite. This model uses a single parameter K_d to express a linear relationship between sorbed concentration and liquid concentration. The K_ds used in PA were determined from experimental data and are conservatively chosen. Thus, the model predictions of sorption are less than or equal to actual sorption expected along the possible flow paths in the Culebra should a release occur (Appendix PA, Attachment MASS, Section MASS-15.2; and CCA Appendix MASS, Attachment 15-1). Other important parameters in the linear isotherm model are the diffusive porosity and the grain density of the Culebra because these determine the mass of dolomite available on which sorption can occur. Consistent with the assumption of homogeneous rock properties in the conceptual model, K_ds and grain densities are selected, applied to the entire transport domain, and held constant for an entire realization. See CCA Appendix SECOTP2D (Section 7, User Interactions, Input and Output Files) and Appendix PA, Attachment PAR (Parameters 49 through 57) for details of parameter definitions and values.

Selecting the parameter values required by the SECOTP2D model for physical retardation and chemical retardation is performed in LHS according to the CDFs described in Appendix PA, Attachment PAR. Important parameter values are summarized in Table 6-22 and Table 6-23.

Table 6-22. Matrix Distribution Coefficients (K_ds) and Molecular Diffusion Coefficients for Dissolved Actinides in the Culebra

Actinide	K_d (cubic meters per kilogram)			Molecular Diffusion Coefficients (square meters per second) [1] Constant
	Maximum	Minimum	Median	
U(IV)	10.0	0.70	2.6	1.53×10^{-10}
U(VI)	0.020	3.0×10^{-5}	7.7×10^{-4}	4.26×10^{-10}
Th(IV)	10.0	0.70	2.6	1.53×10^{-10}
Pu(III)	0.40	0.02	0.09	3.00×10^{-10}
Pu(IV)	10.0	0.70	2.6	1.53×10^{-10}
Am(III)	0.40	0.02	0.09	3.00×10^{-10}

[1] See Attachment MASS

Table 6-23. Culebra Parameters Required for SECOTP2D

Parameter (units)	Maximum	Minimum	Median or Constant
Advective porosity (percent)	1.0	0.01	0.10
Diffusive porosity (percent)	25.0	10.0	16.0
Half matrix block length (meters)	0.50	0.05	0.275
Longitudinal dispersivity, αL (meters)	–	–	0
Transverse dispersivity, αT (meters)	–	–	0
Grain density (cubic kilograms per cubic meter)	–	–	2.82
Effective thickness (meters)	–	–	4.0
Fracture tortuosity (unitless)	–	–	1.0
Diffusive tortuosity (unitless)	–	–	0.11

In summary, the conceptual model for dissolved actinide transport includes the following: transport in advective porosity, physical retardation (diffusion) into diffusive porosity, chemical retardation (sorption) in diffusive porosity, homogeneous rock properties, and a linear isotherm to describe the sorption process. Some of the more important parameters are advective porosity, diffusive porosity, tortuosity, matrix block length, molecular diffusion coefficients, K_d, and the grain density of dolomite in the Culebra.

6.4.6.2.2 Transport of Colloidal Actinides in the Culebra

Colloidal particles are subject to many of the same processes that affect dissolved actinides, but because of their size, several additional processes affect them. There are three process differences. Colloidal particles in general are preferentially carried in the center of pore throats by faster-moving fluid, which could cause slightly increased rates of transport compared to dissolved species. Colloidal particles can be filtered from flowing groundwater when they encounter small-aperture features in the pore network. Finally, colloidal particles may undergo different sorption processes than dissolved species.

The primary distinction in the transport behavior of the different colloidal particles is whether particles diffuse into the matrix from fractures. This is controlled by the difference between the size of colloidal particles and the mean pore-throat diameters in the diffusive porosity of the Culebra. Colloidal particles that are smaller than the pore throats can diffuse into the diffusive porosity. Actinide intrinsic colloids and humic materials are small enough for this to occur. The conceptual model for these particles includes the processes of advection, diffusion, and dispersion in the advective porosity; diffusion into diffusive porosity; and sorption of actinides in diffusive porosity. This model is analogous to that specified for dissolved actinides, although the parameter values are different. The conceptual model assumes that other retardation processes (for example, filtration) will not occur for actinide-intrinsic colloids and humic materials.

In contrast, colloidal particles larger than pore throats will be excluded from the matrix and will remain in advective porosity. Microbes and mineral fragments are conceptualized as larger than the mean pore-throat diameter in Culebra diffusive porosity. The conceptual model for these particles includes the processes of advection and filtration by small-aperture features that occur within advective porosity. See Appendix PA, Attachment MASS, CCA Section MASS.15.3 for additional discussion.

Experiments demonstrated that mineral fragments and microbes are attenuated so effectively by the advective porosity in the Culebra that it was unnecessary to include those colloids in PA calculations. Under the neutral to slightly basic geochemical conditions expected in the Culebra, humic substances did not influence the sorption behavior of dissolved actinides. Therefore, actinides associated with humic substances were treated as dissolved species in the PA calculations. The only actinide-intrinsic colloid found in significant concentrations was Pu(IV)-polymer. At the WIPP, the total amount of Pu(IV)-polymer introduced to the Culebra was insignificant with respect to the EPA normalized release limit, and so was not included in transport calculations. See Appendix PA, Attachment SOTERM (Section SOTERM-6.0) and Appendix PA, Attachment MASS (Section MASS-15.3.1) for details. See Appendix PA, Attachment MASS (Section MASS-15.3.3) for alternative modeling approaches considered.

Indigenous microbes, humics, and mineral fragment colloids in the Culebra may react with dissolved actinides introduced to the Culebra to create new colloidal actinides. Newly formed actinide-bearing microbial and mineral colloids, however, will be attenuated similarly to colloidal actinides introduced from the repository. Therefore, disregarding the impact of newly formed microbial and mineral fragment colloidal actinides is conservative. Experimental results indicate that humics do not interact with dissolved actinides under Culebra geochemical conditions. Consequently, the quantity of newly formed humic actinides will be insignificant.

6.4.6.2.3 Subsidence Due to Potash Mining

Subsidence effects caused by potash mining are included in this PA because of specific criteria in the EPA's 40 CFR Part 194. To incorporate the effects of subsidence caused by mining, PA uses the conceptual model provided by EPA in 40 CFR Part 194 and supporting documents.

The conceptual model for mining is based on information found in 40 CFR § 194.32 (b) and (c) and clarified in the Preamble and Background Information. These subparts of Section 194.32 (b) and (c) state:

> (b) Assessments of mining effects may be limited to changes in the hydraulic conductivity of the hydrogeologic units of the disposal system from excavation mining for natural resources. Mining shall be assumed to occur with a one in 100 probability in each century of the regulatory time frame. Performance assessments shall assume that the mineral deposits of those resources, similar in quality and type to those resources currently extracted from the Delaware Basin, will be completely removed from the controlled area during the century in which such mining is randomly calculated to occur. Complete removal of such minerals resources shall be assumed to occur only once during the regulatory time frame.
>
> (c) Performance assessments shall include an analysis of the effects on the disposal system of any activities that occur in the vicinity of the disposal system prior to disposal and are reasonably expected to occur in the vicinity of the disposal system soon after disposal. Such activities shall include, but shall not be limited to, existing boreholes and the development of any existing leases that can be reasonably expected to be developed in the near future, including boreholes and leases that may be used for fluid injection activities.

Section 194.32 establishes assumptions as to what gets mined, when it gets mined, and the effects of mining on the disposal system—a conceptual model. Within the disposal system, mineral resources similar in quality and type to those currently mined outside the disposal system may be mined at an uncertain time in the future. Outside the disposal system, mineral resources reasonably expected to be mined in the near future should be assumed to be mined. These effects are included in analyses of both disturbed and undisturbed performance. Inside the disposal system, whether and when a mining event occurs after the active institutional control period is determined by a probabilistic model. Outside the disposal system, what is reasonably expected to be mined is assumed to be mined by the end of WIPP disposal operations. With respect to consequence analysis, mining affects only the hydraulic conductivity of the disposal system units.

The DOE has identified areas assumed to be mined in a manner consistent with the conceptual model and other guidance presented by the EPA in 40 CFR Part 194. The only natural resource currently mined near WIPP is potash in the McNutt, and it is the only mineral considered for future mining. Appendix PA, Attachment TFIELD, Section 9 describes the method used to determine the extent of mining in the McNutt both inside and outside the disposal system. This description also presents additional relevant discussion by the EPA on the extent of mining. The extent of mining outside the disposal system used in this PA is shown in Figure 6-19. It is based on the map of existing leases presented in Chapter 2.0 (Figure 2-44), setbacks from existing boreholes, and the presence of ore in the lease (see Appendix PA, Attachment MASS, Section MASS-15). Inside the disposal system, a region that could be mined in the future is specified based exclusively on the quality and type of ore present. This region was presented in Figure 2-45 (see Chapter 2.0).

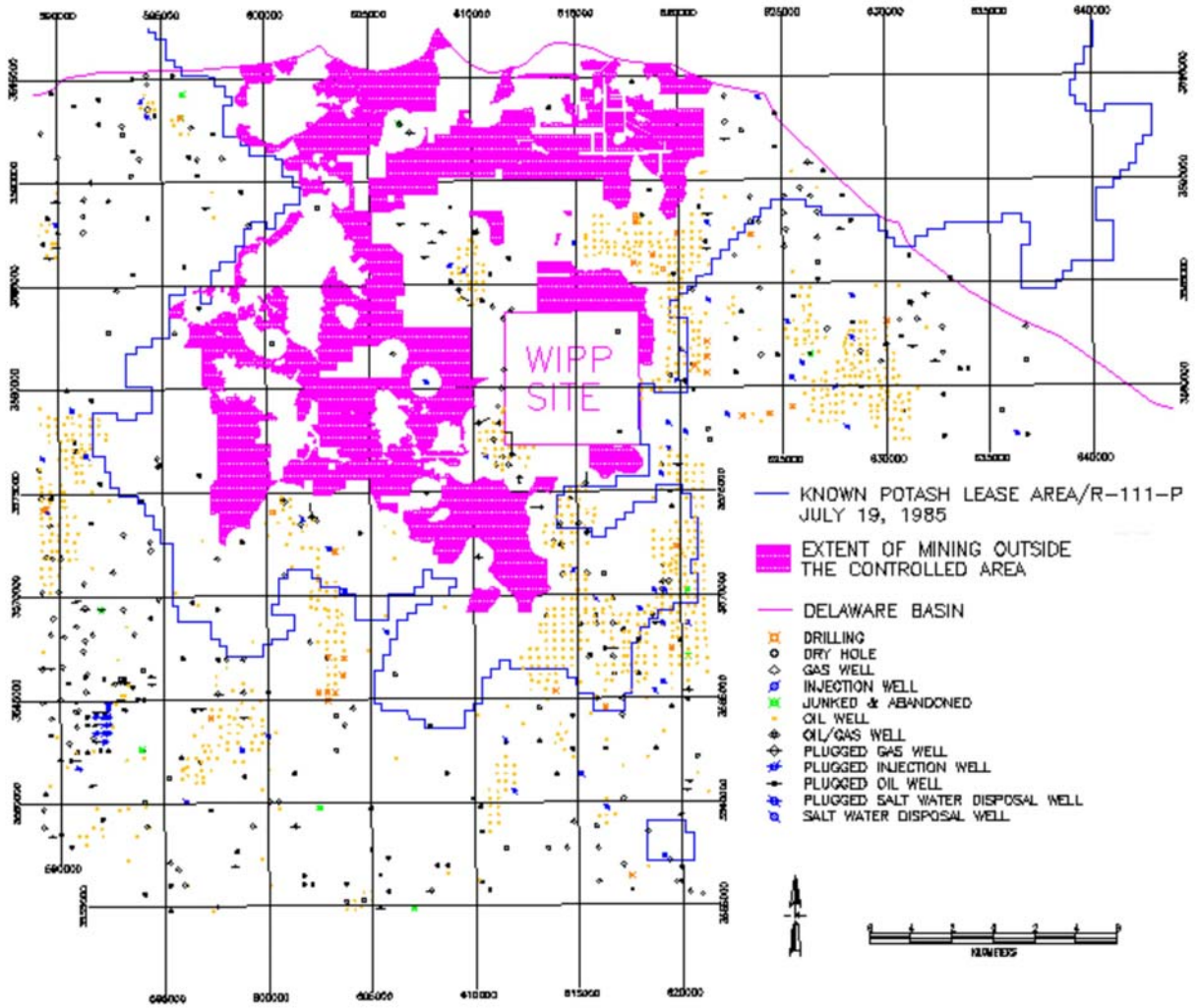

Figure 6-19. Extent of Mining in the McNutt in Undisturbed Performance within MODFLOW-2000 Regional Model Domain

The EPA clarified its conceptual model on the effects of mining on hydraulic conductivity of the disposal system units in the Preamble to 40 CFR Part 194 (EPA 1996a, 61 FR 5229). The EPA states

> Some natural resources in the vicinity of WIPP can be extracted by mining. These natural resources lie within the geologic formations found at shallower depths than the tunnels and shafts of the repository and do not lie vertically above the repository. Were mining of these resources to occur, this could alter the hydrologic properties of overlying formations—including the most transmissive layer in the disposal system, the Culebra dolomite—so as to either increase or decrease groundwater travel times to the accessible environment. For the purposes of modeling these hydrologic properties, this change can be well represented by making corresponding changes in the values for the hydraulic conductivity. The Agency has conducted a review of the data and scientific literature discussing the effects mining can induce in the hydrologic properties of a

> formation. Based on its review of available information, the Agency expects that mining can, in some instances, increase the hydraulic conductivity of overlying formations by as much as a factor of 1,000, although smaller and even negligible changes can also be expected to occur. Thus, the final rule requires DOE to consider the effects of mining in performance assessments. In order to consider the effects of mining in performance assessments, the DOE may use the location-specific values of hydraulic conductivity, established for the different spatial locations within the Culebra dolomite, and treat them as sampled parameters varying between unchanged and increased 1,000-fold relative to the value that would exist in the absence of mining.

This section adds four important clarifying concepts. First, the EPA concluded that there are no minerals vertically above the repository similar in quality and type to those currently extracted elsewhere in the Delaware Basin. Second, the EPA does not draw conclusions about whether mining will increase or decrease groundwater travel times to the accessible environment. Third, it may be assumed that the important effects of change in hydraulic conductivity occur only in the Culebra. Fourth, the spatially variant hydraulic conductivities established in the Culebra by the DOE may be multiplied, where impacted by mining, by a factor from 1 to 1,000. The DOE applied EPA's guidance regarding hydraulic conductivity to the transmissivity at Culebra locations.

In using the EPA's conceptual model for mining, the DOE makes assumptions with respect to two topics in order to formulate the mathematical model. The angle of draw is a parameter necessary to translate the area mined in the McNutt to the area affected in the Culebra. In its Background Information Document for 40 CFR Part 194, the EPA discusses the possible range in the value of angle of draw (EPA 1996b, 9-36). The DOE examined the Background Information for 40 CFR Part 194 (see EPA 1996b, 9-47) and concluded that a 45° angle of draw is the value most consistent with the EPA's discussions and calculations. Second, the Agency does not specify a distribution to the multiplicative factor. As discussed in Appendix PA, Attachment PAR (Parameter 46), the DOE has assigned a uniform distribution to this variable. As discussed in the introduction to Appendix PA, Attachment PAR, a uniform distribution is appropriate when only lower and upper bounds of the range are known.

Applying the angle of draw to the mined areas presented in 6-20 and 6-21 makes the area impacted in the Culebra larger than the area actually mined in the McNutt. The area in the Culebra impacted by mining is shown in Figure 6-20 for outside the controlled area, and in Figure 6-21 for inside and outside the controlled area. These figures are plotted on the regional domain of the MODFLOW-2000 model, which calculated the effects of subsidence caused by mining on flow directions and rates in PA.

The effects of mining outside the disposal system are included in the undisturbed performance scenario, and, therefore, the effects are included in all scenarios. In other words, all calculations of transport in the Culebra include the effects of mining outside the controlled area. This is the undisturbed mining case because mining within the controlled area has not occurred.

These effects are incorporated by multiplying location-specific values in the transmissivity field in the area labeled "Mining Zones " in Figure 6-21 by a factor (mining multiplier) between 1 and 1,000 that is randomly sampled in LHS. The same factor is applied to all affected nodal blocks. In every vector of the LHS, the steady-state flow fields used in the 10,000-year transport simulation incorporate this change to the transmissivity field. These simulations, followed by a

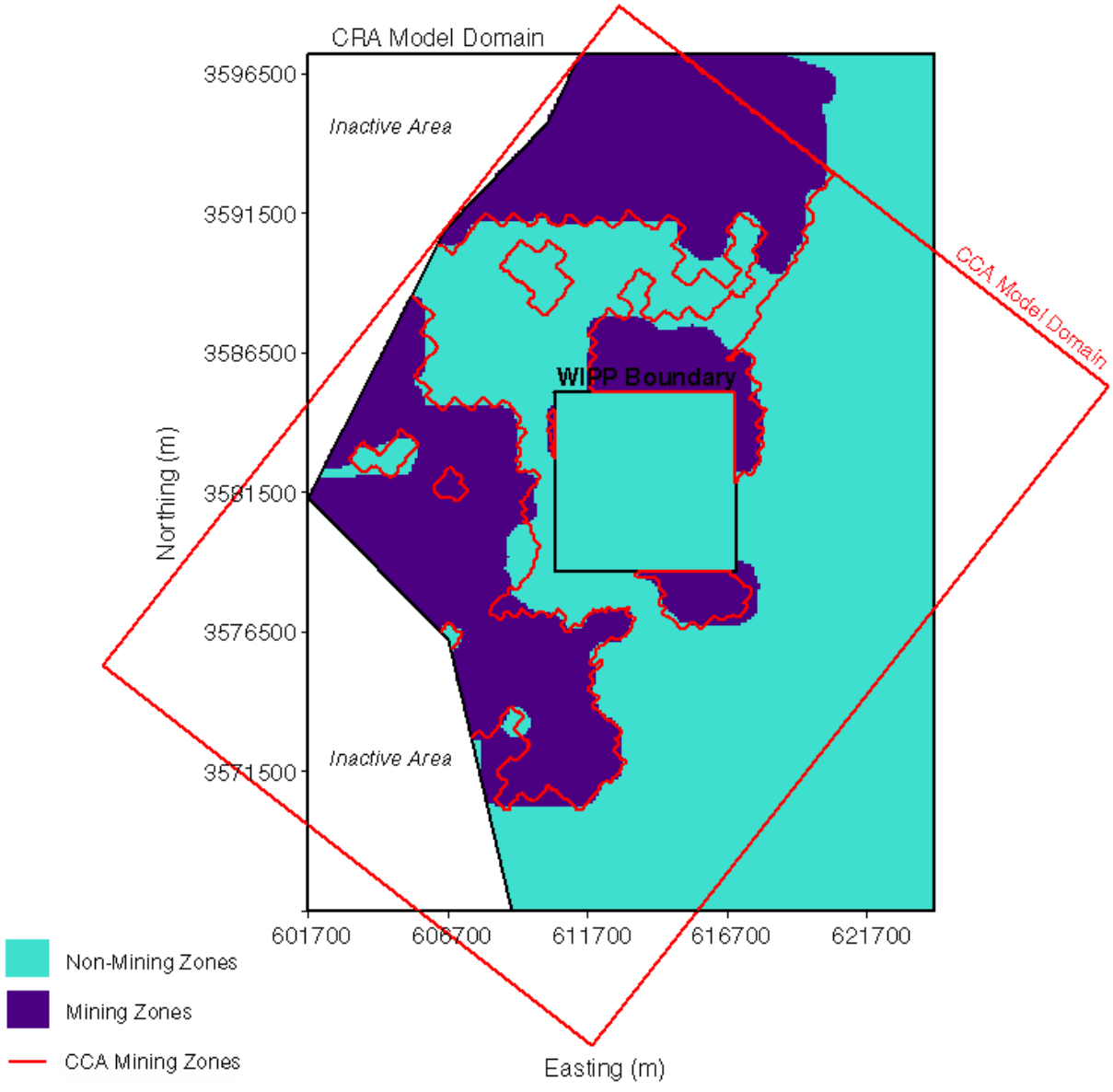

Figure 6-20. Extent of Impacted Area in the Culebra from Mining in the McNutt Potash Zone of the Salado Outside the Controlled Area for Undisturbed Performance

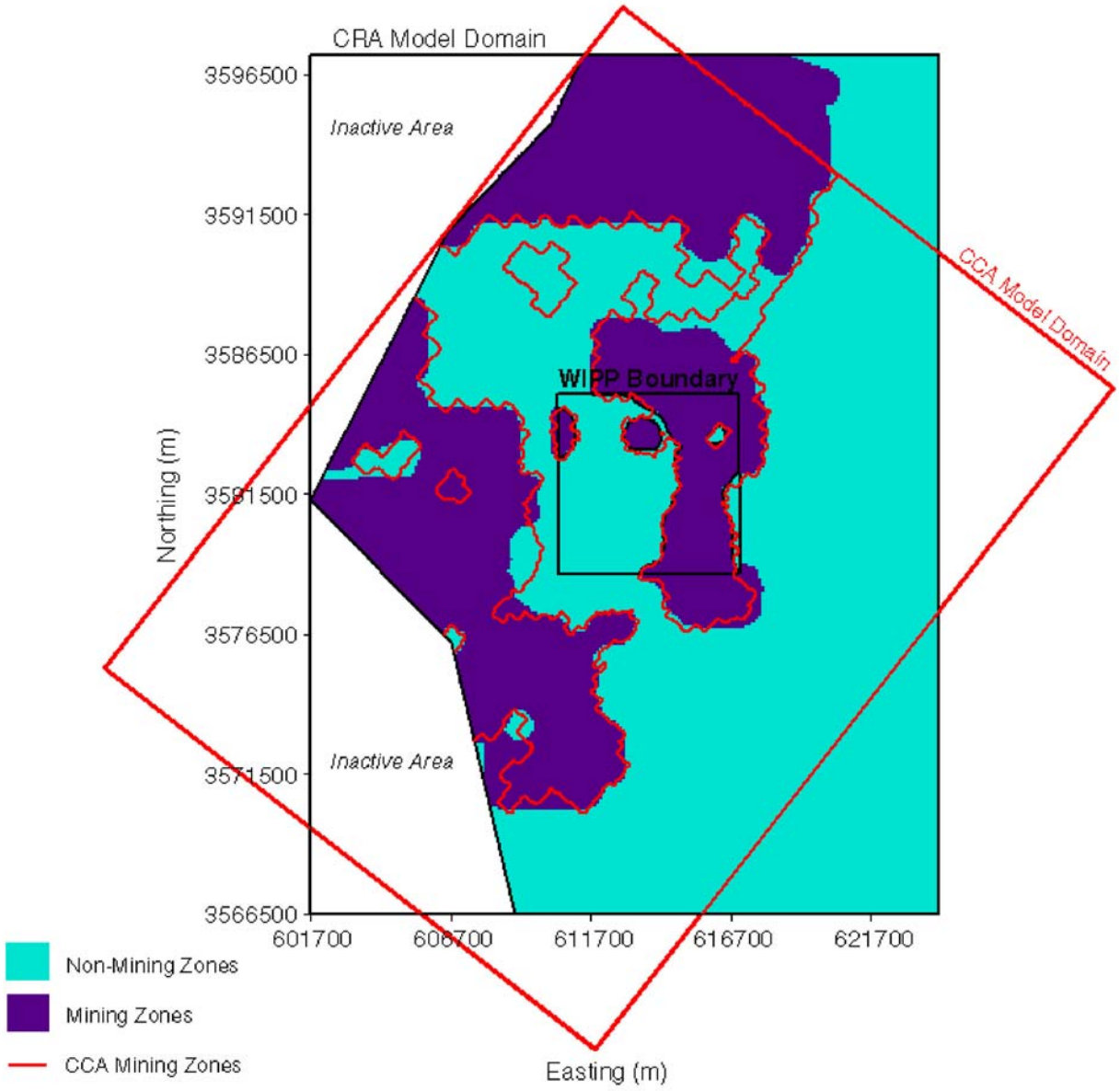

Figure 6-21. Extent of Impacted Area in the Culebra for Disturbed Performance if Mining in the McNutt Potash Zone of the Salado Occurs in the Future Within and Outside of the Controlled Area

transport simulation (as discussed in preceding sections), develop reference conditions for the transport of actinides in the Culebra in the undisturbed mining case.

If mining occurs within the controlled area, an area of the Culebra inside and outside the disposal system is affected. This is the disturbed mining case. To evaluate the impact of disturbed mining, a second simulation of Culebra flow directions and rates is executed. In this second simulation, the affected location-specific values in the transmissivity field within the controlled area are multiplied by the same mining multiplier used for the undisturbed mining case outside the controlled area. These simulations, followed by a transport simulation (as discussed in preceding sections), develop reference conditions (see Section 6.4.11) for transporting actinides following mining inside the controlled area.

The implementation of the EPA's probability model for future mining is presented in Section 6.4.12.8. A discussion of how the reference simulations for the undisturbed and disturbed mining cases are used in CCDF construction is presented in Section 6.4.13.

6.4.6.3 The Tamarisk

The Tamarisk (Row 27 in Figures 6-14 and 6-15) rests between the more transmissive Culebra and Magenta. An in-situ hydraulic test determined that the transmissivity of the Tamarisk is lower than the transmissivity of the Los Medaños (see Section 2.2.1.4.1.3). This low transmissivity is consistent with expectations because of its anhydrite, gypsum, and clay composition (see Section 2.1.3.5.3). In PA, this member is treated as impermeable. This may cause increased flow through the adjacent Culebra and Magenta. This treatment is considered conservative in that allowing flow from the intrusion borehole or shaft into the Tamarisk would, if anything, decrease flow into the Culebra, which would reduce the consequence of radionuclide release to the Rustler. In PA, the thickness of the Tamarisk is assumed to be 24.8 m (81.4 ft) and its permeability is effectively zero (Appendix PA, Attachment PAR).

6.4.6.4 The Magenta

The Magenta is described in Sections 2.1.3.5.4 and 2.2.1.4.1.4 and is shown as Row 28 in Figures 6-14 and 6-15. Transport of actinides through the Magenta to the accessible environment is not modeled. The assumption that no releases will occur from the Magenta is based on the hydraulic test results from wells on the WIPP site (Beauheim 1987, 110-118), which indicate that the Magenta is a porous medium with no hydraulically significant fractures (in contrast to the Culebra), and that its conductivity is lower than that of the Culebra. Early numerical simulations of flow and transport in the Magenta suggested much slower transport than in the Culebra (Barr et al. 1983, 26-27). Therefore, no radionuclides entering the Magenta will reach the accessible environment boundary within the 10,000-year time frame. Accordingly, the BRAGFLO model geometry reasonably approximates the effects of Magenta flow. The Magenta permeability is chosen conservatively as the lowest of measured values near the center of the WIPP site, in order to yield a lower reasonable amount of brine (and radionuclide) storage within the Magenta while continuing to yield an upper bounding flow into the Culebra. The volumes of brine and radionuclides to be stored in the Magenta are tracked and documented, however. Magenta parameter values are summarized in Table 6-24 and are described in more detail in Appendix PA, Attachment PAR.

6.4.6.5 The Forty-niner

In evaluations of radionuclide transport, flow in the Forty-niner is considered insignificant because of its low transmissivity (see Section 2.2.1.4.1.5). As with the Tamarisk and Los Medaños, the Forty-niner is assigned a permeability of effectively zero in PA (Appendix PA, Attachment PAR). This treatment is considered conservative because allowing flow from the intrusion borehole or shaft into the Forty-niner would, if anything, decrease flow into the Culebra, which would reduce the consequence of radionuclide release to the Rustler. Its modeled thickness is 17.3 m (56.8 ft). It is shown as Row 29 in Figures 6-14 and 6-15.

6.4.6.6 Dewey Lake

Release of actinides to the accessible environment from transport in the Dewey Lake is assumed not to occur even if contaminated brine reaches the unit, because the sorptive capacity of this unit appears large. This assumption is based on an analysis (Wallace et al. 1995) that demonstrated that the potential sorption capacity of the Dewey Lake is sufficient to prevent releases for 10,000 years. This analysis consisted of (1) a literature review on the sorptive capacity of redbeds and (2) an estimate of the minimum sorption required to prevent actinide releases that enter the Dewey Lake to the accessible environment in 10,000 years.

Comparison of the sorption values for the Dewey Lake analogues established by literature review with the minimum sorption required to prevent release indicates that the likely sorptive capacity of the Dewey Lake is orders of magnitude greater than required to prevent release. Therefore, the DOE assumes that chemical retardation occurring in the Dewey Lake will prevent release within 10,000 years of any actinides that might enter it. Geological and hydrological information on the Dewey Lake is presented in Sections 2.1.3.6 and 2.2.1.4.2, respectively. Dewey Lake parameter values are summarized in Table 6-25 (see also Appendix PA, Attachment PAR). The Dewey Lake is shown in Figures 6-14 and 6-15.

Table 6-24. Model Parameter Values for the Magenta

Parameter (units)	Minimum	Maximum	Mean or Constant
Permeability (square meters)			6.31×10^{-16}
Effective porosity (percent)	2.7	25.2	13.8
Rock compressibility (1/pascals) [1]	1.16×10^{-10}	4.55×10^{-10}	2.64×10^{-10}
Threshold pressure, P_t (pascals) [2]			5.06×10^{4}
Residual brine saturation, S_{br} (unitless)			0.084
Residual gas saturation, S_{gr} (unitless)			0.077
Pore distribution parameter, λ (unitless)			0.644
Maximum capillary pressure			10^{8}
Thickness (meters)			8.5
Initial pressure (pascals)			9.47×10^{5}

[1] Pore compressibility = rock compressibility/effective porosity.

[2] Threshold Pressure (P_t) determined from the relationship: $PCT\_A \cdot k^{PCT\_EXP}$, where PCT_A and PCT_EXP are constants and k is the permeability.

Table 6-25. Dewey Lake Parameters for the BRAGFLO Model

Parameter (units)	Minimum	Maximum	Mean or Constant
Permeability (square meters)			5.01×10^{-17}
Effective porosity (percent)	3.5	24.8	14.3
Rock compressibility (1/pascals) [1]			10^{-8}
Threshold pressure, P_t (pascals) [2]			0
Residual brine saturation, S_{br} (unitless)			0.084
Residual gas saturation, S_{gr} (unitless)			0.077
Pore distribution parameter, λ (unitless)			0.644
Maximum capillary pressure (pascals)			10^8
Thickness (meters)			149.3
Initial pressure (below water table at 980 m, 43.3 m below top of formation) (pascals)			hydrostatic
Initial pressure, 20% liquid saturation above water table (atmospheres)			1

[1] Pore compressibility = rock compressibility/effective porosity.

[3] Threshold pressure (P_t) determined from the relationship: $PCT\_A \cdot k^{PCT\_EXP}$, where PCT_A and PCT_EXP are constants and k is the permeability.

6.4.6.7 Supra-Dewey Lake Units

The units overlying the Dewey Lake are discussed in Sections 2.1.3.7 through 2.1.3.10 and are shown as Rows 32 and 33 in Figures 6-14 and 6-15. Because these units are thin and predominantly unsaturated at the WIPP site, brine that might enter from the borehole (assuming brine can reach this elevation) is assumed to flow downward to the Dewey Lake, where any actinides will be sorbed. These units are included in BRAGFLO, however, and the possibility of actinide transport into them from a borehole is considered in the PA. Actinide transport within the Supra-Dewey Lake units is not modeled, and it is assumed that there can be no actinide release to the accessible environment through these units. For PA, the units overlying the Dewey Lake are represented as a single hydrostratigraphic unit whose parameters are shown in Table 6-26.

6.4.7 The Intrusion Borehole

In accordance with the requirements of 40 CFR § 194.33(b)(1), DOE models consequences of inadvertent and intermittent intrusion into the repository during drilling for natural resources as the most severe human intrusion scenario that could affect long-term performance of the disposal system. This section discusses the conceptual models used for drilling (particulate release during drilling, direct brine release during drilling, and long-term brine flow) and refers to appropriate discussions of numerical modeling codes.

This section does not address the likelihood that inadvertent human intrusion will occur.

Table 6-26. Supra-Dewey Lake Unit Parameters for the BRAGFLO Model

Parameter (units)	Value
Permeability (square meters)	10^{-10}
Effective porosity (percent)	17.5
Rock compressibility (1/pascals) [1]	5.71×10^{-8}
Threshold pressure, P_t (pascals) [2]	0
Residual brine saturation, S_{br} (unitless)	0.084
Residual gas saturation, S_{gr} (unitless)	0.077
Pore distribution parameter, λ (unitless)	0.644
Maximum capillary pressure (pascals)	10^8
Thickness (meters)	15.76
Initial pressure, 8.36% liquid saturation (atmospheres)	1

[1] Pore compressibility = rock compressibility/effective porosity.

[2] Threshold pressure (P_t) determined from the relationship: $PCT\_A \cdot k^{PCT\_EXP}$, where PCT_A and PCT_EXP are constants and k is the permeability.

The DOE's treatment of the probability of inadvertent human intrusion is discussed in Section 6.4.12.

Human intrusion scenarios require simulating penetration of an intrusion borehole into the waste disposal region. There are two effects associated with drilling: releases from the drilling itself and possible releases from the long-term effects on fluid flow in the disposal system after the borehole casing and plugs have degraded. Both types of releases are estimated for two different types of intrusions: those that intersect pressurized brine in the Castile (E1 events; see Section 6.3.2.2.2), and those that do not (E2 events: see Section 6.3.2.2.1).

6.4.7.1 Releases During Drilling

Consistent with the criterion of 40 CFR § 194.33(c)(1), releases that may occur during and immediately following the drilling event are modeled assuming that future drilling practices will be the same as at present (see CCA Appendix DEL, Sections DEL.5, DEL.6 and Appendix DATA, Section 2.0 and DATA, Attachment A, for a complete description of historical and present drilling practices). Figure 6-22 shows a schematic representation of a standard rotary drilling operation inadvertently penetrating the repository. A drill bit is attached to the bottom of a string of steel pipe, the lowest segments of which are reinforced collars. The drill bit, collars, and pipe are collectively referred to as the drill string. As the drill string rotates, liquid, referred to as drilling mud, is pumped down the interior of the pipe and out through the bit. The drilling fluid cools and lubricates the bit and then returns to the surface outside the pipe in the annulus between the pipe and the borehole wall.

During its return flow, the mud carries the cuttings to the surface where they settle out in a mud pit. The mud is typically a water-based brine that is weighted with additives to maintain a hydrostatic pressure in the borehole equal to or greater than the normally anticipated fluid pressures in the formations being drilled. Salt-saturated brines are generally used in evaporites

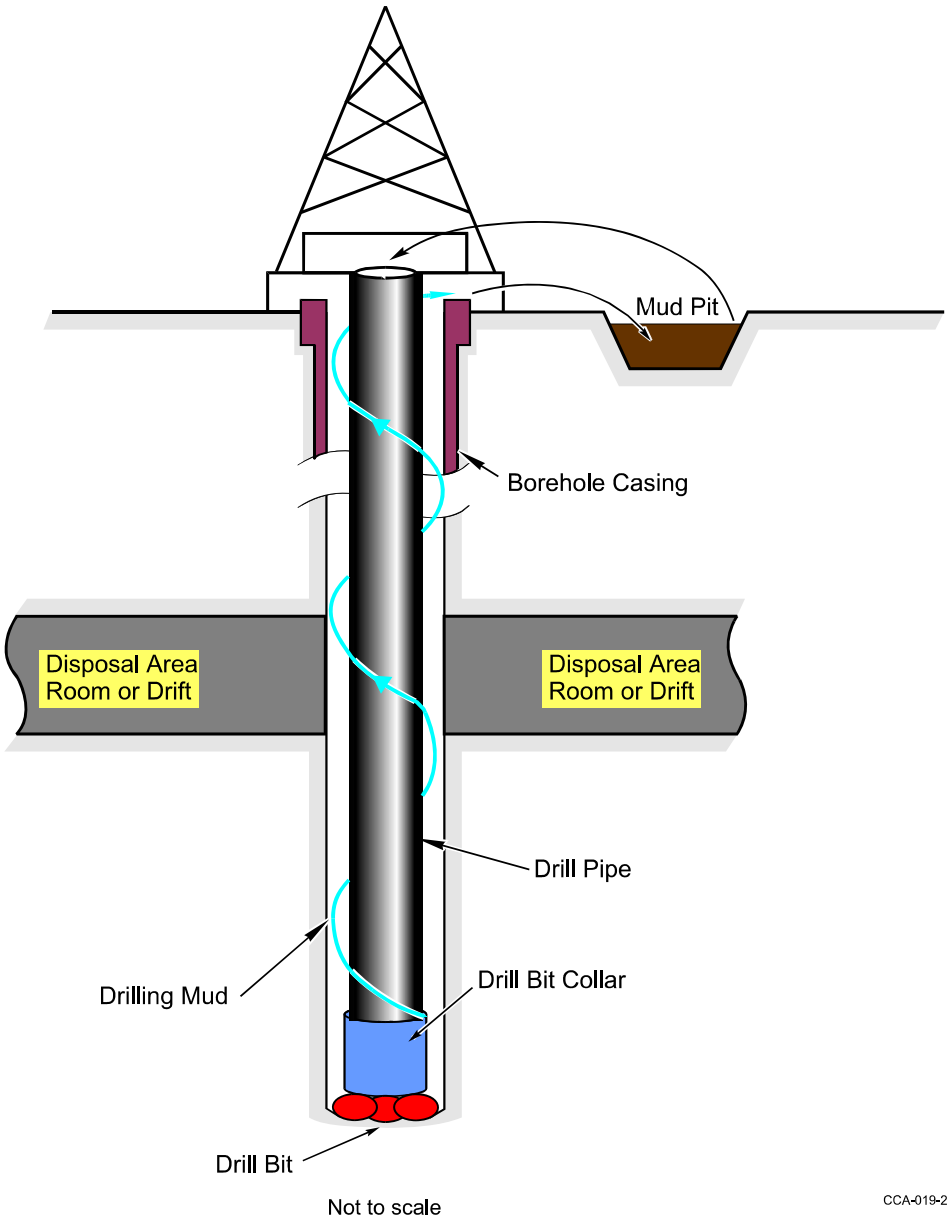

Figure 6-22. Schematic Representation of a Rotary Drilling Operation Penetrating the Repository

to prevent dissolution of the formation. Steel casing is installed in boreholes before entering the salt section to protect the near-surface units from contamination with fluids from deeper units and, after drilling through the salt section, to prevent hole closure on the drill string and subsequent in-hole hardware.

If a rotary drill bit penetrates the waste, radionuclides may be brought to the surface by four means. First, some quantity of cuttings that contain material intersected by the drill bit will be

brought to the surface. Second, cavings, which contain material eroded from the borehole wall by the circulating drill fluid, may also be brought to the surface by the circulating drilling mud. Third, releases of radionuclides may occur if the repository contains fluids at pressures higher than the pressure exerted by the drilling fluid. Spalling of waste material into the borehole may occur if high-pressure gas flows into the borehole. Brine, as well as gas, may enter the borehole from the repository if the driller is unable to control the pressure within the well or chooses not to control the pressure. The brine may flow to the surface, and if it has been in contact with waste, it may contain dissolved or suspended radionuclides.

Releases of particulate waste material (that is, cuttings, cavings, and spallings) are modeled using the CUTTINGS_S and DRSPALL codes, as described in Section 6.4.11 and Appendix PA, Sections PA-4.5 and PA-4.6 Attachment MASS (Section 16.1) discusses the conceptual basis for the model. As discussed in Section 6.4.12.4, cuttings and cavings are calculated separately for CH-TRU and RH-TRU waste, with distinct waste streams considered. Spallings are calculated as homogeneous waste obtained by averaging over all CH-TRU waste. For all releases during drilling, appropriate corrections are made for radioactive decay. Releases of dissolved or suspended radionuclides contained in brine are modeled using the BRAGFLO and PANEL codes, as described in the next section. Casing is assumed to be intact through the Rustler and overlying units during drilling, and there is assumed to be no communication between the borehole and those units. For all direct releases, actinides that enter the borehole are conservatively assumed to reach the surface.

6.4.7.1.1 Direct Brine Release During Drilling

Direct brine release refers to the possibility that brine containing actinides may flow from the waste panels up a borehole to the surface during drilling (Appendix PA, Section PA-4.7 and Attachment MASS, Section 16.2). It is conceptualized that direct brine release to the surface will not occur every time a borehole penetrates the waste panels but rather that it can occur only when two conditions are met. The first condition is the presence of mobile brine in the waste panels. Because of brine consumption by corrosion and low initial saturation, it is possible for liquid saturations below the residual saturation to exist in the repository, in which case direct brine release cannot occur. The second condition is that the pressure in the waste panels must be greater than the pressure at the base of the drilling mud column. Drillers in the Delaware Basin use a salt-saturated mud with a specific gravity of about 1.23 while drilling through the Salado. This corresponds to a pressure of approximately 8 megapascals at the repository horizon (see Appendix PA, Attachment MASS, Section 16.2 and CCA Appendix MASS, Attachment 16-2). If fluid in the waste panels is below this pressure, no direct brine release during drilling can occur because liquid flow in the repository is away from the borehole.

In the conceptual model, resolution of the details of flow near the borehole is considered important, as the changing physical conditions over the short duration of this flow can significantly impact estimates of the total volume released. It is not assumed that a direct brine release would be noticed by the driller (EPA 1996a, 61 FR 5230). Also important to the conceptual model is how long direct brine release occurs. There are several ways in which the direct brine release could be stopped. A driller might detect higher flow rate to the mud pit and take action to mitigate consequences. Alternatively, direct brine release will stop when the driller cases the hole after reaching the base of the salt section. As discussed in Appendix PA,

Section PA-4.7 and CCA Appendix DEL (Section 7.5), the DOE assumes that for low volumes of fluid flow, the borehole will be controlled and cased within 72 hours after penetrating the repository. In all cases, all fluid flow to the surface during drilling is assumed to cease within 11 days after penetrating the repository.

In the conceptual model for direct brine release, several other assumptions are related to other conceptual models. The processes of direct solids release from cuttings, cavings, spall, and direct brine release are treated separately, although the direct brine release model does account for the effects of solids removal (spall) on fluid flow near the well bore. Direct brine release will affect the pressure and saturation in the repository. However, it is assumed that these effects are negligible over the long term because of their transient and local nature; thus, they are not accounted for in long-term (10,000-year) BRAGFLO disposal system calculations. This assumption simplifies modeling because it allows detailed consideration of direct brine release over a short time period, without having to couple the results of these calculations back into the disposal system simulations.

The area over which fluid flow can occur during direct brine release is assumed to be the rooms and drifts of waste panels, the DRZ, room pillars, and panel closures. Because local-scale, short-duration flow is important, the geometry of the waste panels is considered important and is represented in the model. It is assumed that the flow interactions with the Salado other than the DRZ are unimportant during direct brine release. For this model, pillars are arbitrarily assumed to have the properties of the DRZ rather than intact halite, although in reality their properties are probably like a DRZ at their edge and intact halite in their core. Since the DRZ permeability is greater than the permeability of intact halite, this assumption is conservative. A two-dimensional geometry is used parallel to the repository horizon, with a 1 degree dip from north to south. The geometry of the grid used is shown in Figure 6-23.

The BRAGFLO code is used to calculate direct brine release; the mathematical and computational model is called the BRAGFLO direct brine release model (Appendix PA, Section PA-4.7). The initial and boundary conditions for this model are derived from the corresponding BRAGFLO disposal system simulation through several codes, including CUTTINGS_S. Some of the parameters derived from the BRAGFLO disposal system model are permeabilities, porosities, two-phase flow properties, and the height of the waste region. Initial saturations and pressures in the BRAGFLO direct brine release model are mapped from the BRAGFLO disposal system model. Other parameters used in the BRAGFLO direct brine release models are consistent with those used in the BRAGFLO disposal system model (Appendix PA, Section PA-4.7).

It is possible that a direct brine release could occur from a panel connected by a previously-drilled, abandoned borehole to a brine reservoir in the Castile. If this happened, flow directly between the two boreholes, analogous to the E1E2 scenario for long-term performance, might affect the estimate of the total brine released. The direct brine release for this possibility is calculated by BRAGFLO (direct brine release) by placing a

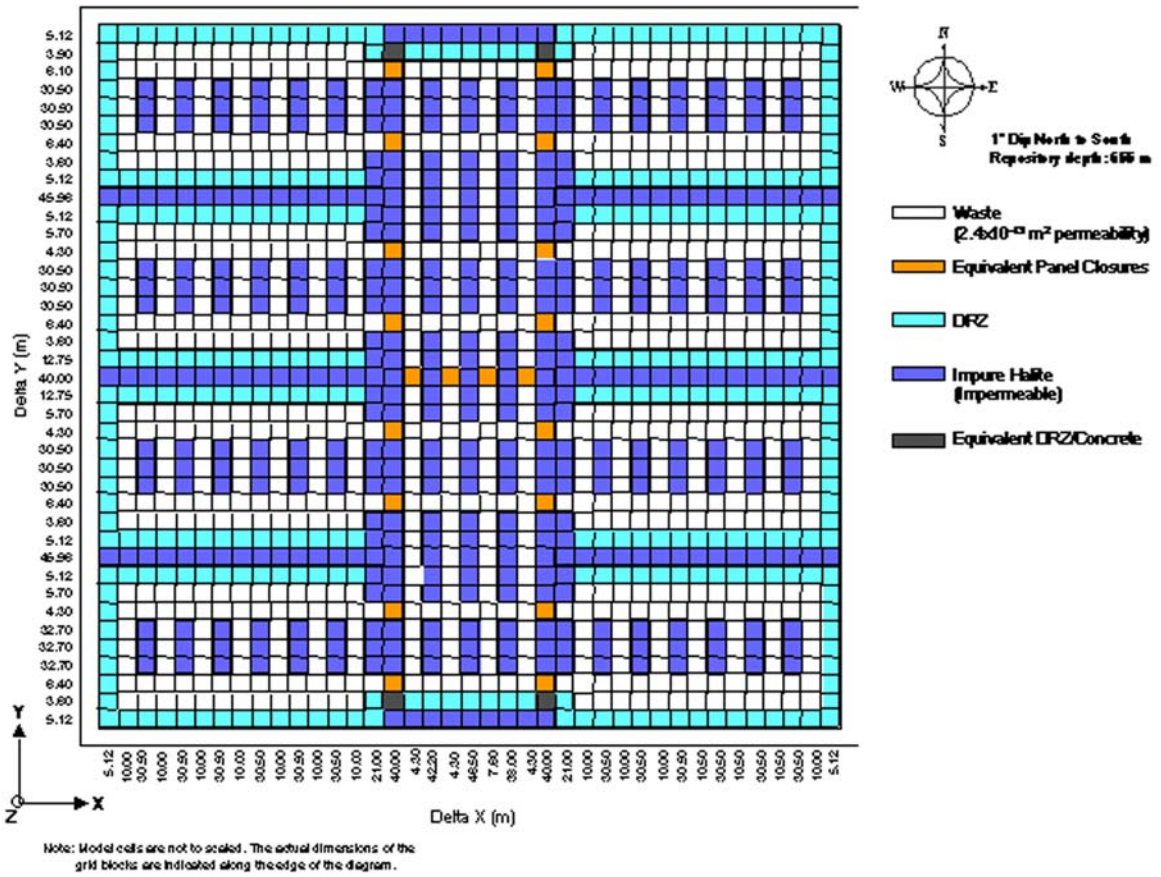

Figure 6-23. Repository-Scale Horizontal BRAGFLO Mesh Used for Direct Brine Release Calculations

constant-pressure, flowing injection well as a boundary condition in the model. The locations of these boreholes are shown in Figure 6-23. It is assumed that a direct brine release from a panel with a previously-drilled, abandoned borehole of the E2 type is unaffected by the presence of the other borehole. Thus, reference direct brine release conditions are calculated for previously unintruded and E2-intruded panels, and for previously-intruded E1 panels. Details about the properties assigned to the flowing-well boundary condition are discussed in Appendix PA, Section PA-4.7. Details about how the consequences of direct brine releases from other possible combinations of boreholes are accounted for in the CCDF are discussed in Section 6.4.13.

A borehole could penetrate the repository anywhere. For simplification, the BRAGFLO direct brine release model assumes that calculating direct brine release from several defined locations provides meaningful reference results for the possible variation in release because of location. The locations of boreholes from which representative results are calculated are indicated in Figure 6-23. In construction of a CCDF (see Section 6.4.13), the direct brine release associated with a borehole whose position is randomly selected is correlated with the reference release most consistent with the geometry near the location of the random borehole.

Accurate representation of the flow into the borehole is important in the BRAGFLO direct brine release model. Accordingly, a number of mathematical methods that are not used to calculate

long-term releases are applied to the conditions in the borehole for calculating direct brine releases. The methods used appear in Appendix PA, Section PA-4.7.

6.4.7.2 Long-Term Releases Following Drilling

Long-term releases to the ground surface or into groundwater in the Rustler or overlying units may occur after the hole has been plugged and abandoned (Appendix PA, Attachment MASS, Section 16.3). As required by regulation, the plugging and abandonment of future boreholes are assumed to be "consistent with practices in the Delaware Basin at the time a compliance application is prepared" [40 CFR § 194.33(c)(1)]. Examining current practices in the Delaware Basin indicates that all boreholes abandoned recently are plugged to meet state and federal regulatory requirements protecting groundwater and natural resources (see Appendix DATA, Section DATA-2.0 and Attachment A; CCA Appendix DEL, Sections DEL.5.5 and DEL.6]; Appendix PA, Attachment MASS, Section MASS-16.3). These plugs will effectively prevent flow in abandoned boreholes for some period of time after emplacement. However, some plugs may fail and radionuclides may be transported in brine flowing up the borehole.

Borehole plug configurations used today in the Delaware Basin vary based on the local stratigraphy encountered in the hole, its total depth, and the types of fluids present. All holes are plugged with some combination of solid concrete plugs isolating different fluid-bearing horizons from each other and from the ground surface. As discussed in detail in Appendix PA, (Attachment MASS (Section 16.3), SNL (2003),) and CCA Appendix DEL (DEL Attachment 7), six different plug configurations are identified that are potentially relevant to future borehole abandonment practice at the WIPP. As discussed in Appendix PA, Attachment MASS (Section 16.3.3) and SNL (2003), these six plug configurations can be approximated for PA by three conceptual plugging patterns. The three plugging configurations addressed in the PA are described in the following section. Probabilities of occurrence for each of these three plugging configurations are discussed in Section 6.4.12.7. Parameters used to describe the borehole and its plugs are summarized in Table 6-27.

6.4.7.2.1 Continuous Concrete Plug through the Salado and Castile

In this configuration, a continuous concrete plug is assumed to exist throughout the Salado and Castile (Appendix PA, Attachment MASS, Section 16.3 and SNL (2003). Such a plug could be installed in keeping with current regulatory requirements of the New Mexico Oil Conservation Division Order R-111-P (State of New Mexico 1988, 10), which is applicable within the potash leasing area that includes the WIPP site. The continuous plug protects potash mining operations from possible hydrocarbon contamination. A continuous concrete plug is also used to approximate flow in boreholes with numerous concrete plugs throughout the salt section.

Examples of such plugging configurations currently used in the Delaware Basin are described in Appendix PA, Attachment MASS, Section 16.3.

Because concrete within a continuous plug will be physically confined and will have very little brine flow through it, degradation will be minimal and limited to the upper and lower ends of the plug (see Appendix PA, Attachment MASS, Section 16.3.3, Appendix C). For the CCA PA the

Table 6-27. Intrusion Borehole Properties for the BRAGFLO and CUTTINGS_S Models

Parameter (units)	Maximum	Minimum	Median or Constant [1]
Permeability of open hole (0 to 200 years) (square meters)	–	–	10^{-9}
Permeability of concrete plugs (0 to 200 years in Rustler and at surface) (square meters) [2]	1×10^{-17}	1×10^{-19}	10^{-18}
Permeability of borehole fill material (>200 years) (square meters) [2]	1×10^{-11}	1×10^{-14}	3.16×10^{-13}
Permeability of lower borehole fill material (>1,200 years) (square meters) [2]	1×10^{-12}	5×10^{-17}	2.24×10^{-14}
Effective porosity (percent)	–	–	0.32
Pore compressibility (1/pascals)	–	–	0
Diameter (meters)	–	–	0.311
Threshold pressure, P_t (pascals)	–	–	0
Pore distribution parameter, λ (unitless)	–	–	0.94
Residual brine saturation, S_{br} (unitless)	–	–	0
Residual gas saturation, S_{gr} (unitless)	–	–	0

[1] Parameters with no maximum and minimum values are treated as constants in the PA.

[2] Borehole permeabilities are for the two-plug case. Continuous three-plug case is treated as undisturbed performance.

permeability of the continuous concrete plug was 5×10^{-17} m^2 for all the plugging configurations. For this application, the DOE adopted EPA's 1997 PAVT range of 10^{-17} to 10^{-19} m^2. Because of the small cross-sectional area and low permeability of the potential pathway, long-term releases through a continuous concrete plug are not calculated explicitly for the PA, and are assumed to be zero.

6.4.7.2.2 The Two-Plug Configuration

In the two-plug configuration, two concrete plugs are assumed to have a significant effect on long-term flow in the borehole (Appendix PA, Attachment MASS, Section16.3 and CCA Appendix MASS Attachment 16-3, Figure 2). The lower plug of interest is assumed to be located somewhere between the hypothetical Castile brine reservoir and underlying formations. A second plug is located within the lower portion of the Rustler, immediately above the Salado. Additional plugs that have little effect on long-term flow are also assumed to be present deeper in the hole and at the land surface.

In E1-type intrusions with two plugs, the brine reservoir and the repository are assumed to be in direct communication through an open cased hole immediately following drilling. The plugs are located in the borehole Column 26 of the BRAGFLO mesh in Figure 6-15 in Rows 32 and 33 (the surface plug) and Row 25 (the Los Medaños). The plugs located below the brine reservoir are not modeled explicitly. Plugs are assigned initial sampled permeabilities of 10^{-17} to 10^{-19} square meters pursuant to EPA's 1997 PAVT parameters. The open segments of borehole between the plugs are assigned an initial permeability of 10^{-9} m^2. Steel casing above the Salado is assumed to begin to degrade within decades after abandonment and is assumed to have failed

completely after 200 years. The concrete plugs above the Salado are also assumed to fail after 200 years, as a result of chemical degradation where they are in contact with brine. The plug below the Castile brine reservoir is in a less aggressive chemical environment, and its properties remain constant in PA.

After the upper plugs and casing have failed, the borehole is assumed to be filled by a silty, sand-like material containing degraded concrete, corrosion products, and material that sloughs into the hole from the walls. Thus, 200 years after the time of intrusion, the entire borehole region in the BRAGFLO model, including the sections previously modeled as concrete plugs, is assigned a permeability corresponding to silty sand. This permeability is sampled from a log-uniform distribution from 10^{-11} square meters to 10^{-14} square meters.

One thousand years after the plug at the base of the Rustler has failed, permeability of the borehole region below the waste-disposal panel in the BRAGFLO model used for E1-type intrusions is decreased from its sampled value by one order of magnitude. For the remainder of the 10,000-year period, the borehole is modeled with its sampled permeability value above the repository and the adjusted value below. Conceptually, the decrease in permeability below the panel corresponds to compaction of the silty, sand-like material by partial creep closure of the borehole's lower portion. As discussed in Appendix PA, Attachment MASS, Section 16, creep closure of boreholes will not be significant above the repository horizon but will be effective at greater depths because of the greater lithostatic stress. Nowhere in the borehole is creep closure assumed to close the hole completely in the regulatory time frame, but closure will be sufficient at depths below the repository to reduce the permeability of the material filling the hole.

6.4.7.2.3 The Three-Plug Configuration

In the three-plug configuration, three concrete plugs are assumed to affect long-term flow in the borehole (Appendix PA, Attachment MASS, Section 16.3). Two of the plugs are identical to those modeled in the two-plug configuration. The third plug is located within the Castile above the brine reservoir and below the waste-disposal panel. This plug is assumed to behave the same as the lower plug in the two-plug configuration: that is, its properties remain unchanged in PA. Otherwise, all portions of the borehole in the three-plug configuration are assumed to have the same material properties as the corresponding regions in the two-plug configuration, with adjustments to borehole-fill permeability occurring 1,000 years after failure of the overlying plug (Appendix PA, Attachment MASS, Section).

Because the three-plug configuration isolates the repository from the brine reservoir for the time period during which the middle plug remains effective, and because the portion of the borehole above the middle plug will already be filled with silty, sand-like material before the middle plug fails, the DOE chose not to model this configuration explicitly in the BRAGFLO calculations. Boreholes in which the three-plug configuration is emplaced are assumed to result in long-term releases comparable to those calculated for E2 intrusions, regardless of whether they penetrate a Castile brine reservoir. Consequences of E1-type intrusions with the three-plug configuration are assumed for the purposes of CCDF construction to be identical to those of E2 intrusions occurring at the same time.

6.4.8 Castile Brine Reservoir

As discussed by Section 2.2.1.2.2, high-pressure Castile brine was encountered in several WIPP area boreholes, including the WIPP-12 borehole within the controlled area and the ERDA-6 borehole northeast of the site. Consequently, the conceptual model for the Castile includes the possibility that brine reservoirs underlie the repository. The E1 and E1E2 scenarios include borehole penetration of both the repository and a brine reservoir in the Castile. The properties of the borehole are discussed in Section 6.4.7.

Unless a borehole penetrates both the repository and a brine reservoir in the Castile, the Castile is conceptually unimportant to PA because of its expected low permeability. Two regions are specified in the Castile horizon in the disposal system geometry: the Castile (Rows 1 and 2 in Figure 6-14) and a reservoir (Row 1, Columns 23 to 45 in Figure 6-15). The Castile region has an extremely low permeability, which prevents it from participating in fluid flow processes.

It is unknown whether a brine reservoir exists below the repository. As a result, the conceptual model for the brine reservoirs is somewhat different from those for known major properties of the natural barrier system, such as stratigraphy. The principal difference is that a reasonable treatment of the uncertainty of the existence of a brine reservoir requires assumptions about the spatial distribution of such reservoir and the probability of intersection (see Appendix MASS, Section MASS.18.1 and CCA MASS Attachment 18-6 for the development of the probability used in the CCA). The EPA required the DOE to use a range of probabilities for a borehole hitting a brine reservoir of 0.01 to 0.60 in the 1997 PAVT (EPA 1998, VII.B.4.d). The DOE added a parameter representing this range of subjective uncertainty for the CRA-2004 PA (Appendix PA, Section PA-3.5).

In addition to the stochastic uncertainty in the location and hence in the probability of intersecting reservoirs, there is also uncertainty in the properties of reservoirs. The manner in which brine reservoirs would behave if penetrated is treated as subjective uncertainty (see Section 6.2.2), and is incorporated in the BRAGFLO calculations of disposal system performance. The conceptual model for the behavior of such brine reservoir is discussed below.

Where they exist, Castile brine reservoirs in the northern Delaware Basin are believed to be fractured systems, with high-angle fractures spaced widely enough that a borehole can penetrate through a volume of rock containing a brine reservoir without intersecting any fractures and therefore not producing brine. They occur in the upper portion of the Castile (Popielak et al. 1983, G-2). Appreciable volumes of brine have been produced from several reservoirs in the Delaware Basin, but there is little direct information on the areal extent of the reservoirs or the existence of the interconnection between them. Data from WIPP-12 and ERDA-6 indicate that fractures have a variety of apertures and permeabilities, and they deplete at different rates. Brine occurrences in the Castile behave as reservoirs—that is, they are bounded systems. The properties specified for brine reservoirs are pressure, permeability, compressibility and porosity. Brine reservoir parameter values used in this PA are shown in Table 6-28.

Brine reservoir pressure in the PA is based on measured pressures in Castile and Salado anhydrites. These values are determined by analyzing brine pressures observed in Salado and Castile anhydrites, corrected for the difference in depth between the observed location and

WIPP-12. The analysis is documented in CCA Appendix MASS (Section 18 and MASS Attachments 18-1 and 18-2) and Appendix PA (Attachment PAR, Parameter 27).

Table 6-28. Parameter Values Used for Brine Reservoirs in the BRAGFLO Calculations

Parameter (units)	Maximum	Minimum	Median or Constant [1]
Permeability (square meters)	1.58×10^{-10}	2.0×10^{-15}	1.58×10^{-12}
Effective porosity (percent)	0.9208	0.1842	0.87
Rock compressibility (1/pascals) [2]	10^{-10}	2.0×10^{-11}	4×10^{-11} (mode)
Initial pressure (pascals)	1.70×10^{7}	1.11×10^{7}	1.27×10^{7}
Threshold pressure, P_t (pascals) [3]	4.59×10^{-6}	2.28×10^{-4}	4.6×10^{-5}
Pore distribution parameter, λ	–	–	0.70
Residual brine saturation, S_{br} (unitless)	–	–	0.20
Residual gas saturation, S_{gr} (unitless)	–	–	0.20

[1] Parameters with no maximum and minimum values are treated as constants in the PA.

[2] Pore compressibility = rock compressibility/effective porosity.

[3] Threshold pressure (P_t) determined from the relationship: $PCT\_A \cdot k^{PCT\_EXP}$, where PCT_A and PCT_EXP are constants and k is the permeability.

The permeability of brine reservoirs is based on analyzing brine reservoirs tested by DOE in drillholes ERDA-6 and WIPP-12 (Popielak et al. 1983, Sections H-3.4.3 and H-3.4.4). Values used in the PA are shown in Table 6-28. The derivation of these values from the referenced study is documented in Appendix PA, Attachment PAR.

The bulk compressibility range is based on a reanalysis of WIPP-12 data that was requested by the EPA in their 1997 PAVT (EPA 1998). Beauheim (1997) provides a detailed description of this analysis and parameter range.

An effective porosity is defined for the reservoir portion of the Castile in the disposal system geometry (Row 1, Columns 23 to 45 in Figure 6-15). In the EPA's 1997 PAVT (EPA 1998), the EPA specified a range of brine volumes for the reservoir based on an EPA reanalysis of the amount of brine in the reservoir encountered by WIPP-12. The analysis concluded that PA should represent a total volume of brine in the brine reservoir that ranges between 3.40×10^{6} and 1.70×10^{7} m^3. Since the brine reservoir is represented by a region of constant volume, the effective porosity is used to provide the total brine volume in the reservoir rather than representing the actual value, and is not representative of the actual host rock's porosity. This treatment results in an effective porosity range between 0.1842 and 0.9208. The effective porosity is correlated to the values for the bulk compressibility (see Appendix PA, Section 4.2.1 for a detailed discussion of this relationship).

The CRA-2004 PA treatment of brine reservoir volume and porosity is consistent with the 1997 PAVT. In contrast, the CCA PA used a discrete distribution of brine volumes in the reservoir (see CCA Appendix MASS, Section MASS.18 and MASS Attachment 18-3).

The threshold pressure, pore distribution parameter, and residual saturations are parameters describing two-phase flow behavior and are required by BRAGFLO. Because saturations in the brine reservoir remain very near 1.0 in all preliminary and current PAs, the values of these parameters were not important to the model results. The parameter values used in the CRA-2004 PA are the same as those in the 1997 PAVT.

6.4.9 Climate Change

The present climate at the WIPP and the geologic record of past climate change in southeastern New Mexico are discussed in Section 2.5 and Appendix CLI of the CCA. Although meaningful quantitative predictions of future climate for the next 10,000 years are not feasible, effects of reasonably possible climate changes on disposal system performance must be considered. For the WIPP, uncertainty about these effects is incorporated in the PA by considering the effects of various possible future climates on groundwater flow and potential radionuclide transport in groundwater. Direct effects of climate change that do not involve groundwater flow do not affect the long-term performance of the WIPP because of its depth below the land surface. Examples of such direct effects are changes in wind patterns, thermal effects related to changes in surface temperature, and near-future impacts on surface facilities. Long-term effects of climate change on the near-surface portions of the shaft seal system (see Section 6.4.4) are not incorporated in the analysis because BRAGFLO modeling indicates that system performance is unaffected by the behavior of the shaft seal system's upper portion. Additional aspects of climate change screened out from the PA, including glaciation at the site and possible future anthropogenic changes, are discussed in Appendix PA, Attachment SCR (FEPs N62 and H47 through H49).

The effects of postulated climate change on groundwater flow were evaluated outside of the PA calculations using a regional three-dimensional groundwater basin model based on the basin hydrology introduced in Section 2.2.1.1. For the regional analysis, climate-related factors that might affect groundwater flow (such as precipitation, temperature, and evapotranspiration) are treated through a single model parameter, potential recharge, which controls the rate at which water is added to the model at the water table. As described in Appendix PA, Attachment MASS, Section MASS-17.0, changes in this parameter allow simulation of regional groundwater flow under a range of different future states in which the climate may be wetter, the water table may be higher, and groundwater velocity in all units may increase. These and other simulations discussed in CCA Appendix MASS (Section MASS.15 and MASS Attachment 15-7) show that the regional, three-dimensional effects of climate change can be reasonably approximated in PA by directly scaling specific discharge in the two-dimensional, steady-state groundwater velocity field of the Culebra. The velocity field is calculated using MODFLOW-2000, as described in Section 6.4.6.2. Radionuclide transport in the Culebra is then calculated by SECOTP2D using the scaled velocity fields.

Scaling the two-dimensional velocity field is done using the Climate Index (Table 6-29), a dimensionless factor by which the specific discharge in each grid block of the SECOTP2D domain is multiplied. As summarized in Appendix PA, Attachment PAR (Parameter 48), the Climate Index is a sampled parameter in the PA with a bimodal distribution ranging from 1.00 to 1.25 and from 1.50 to 2.25. A single value of the Climate Index is chosen in LHS for each sample element and held constant throughout the 10,000-year SECOTP2D simulation. Each

realization of disposal system performance thus represents a different approximation of future climate. Those

Table 6-29. Climate Change Properties for the SECOTP2D Model

Parameter (units)	Maximum	Minimum	Median
Climate index (dimensionless)	2.25	1.00	1.17

realizations in which the sampled value is close to its maximum of 2.25 represent the most extreme changes in groundwater flow that may result from climatic change.

Sampled values close to the minimum of 1.00 represent climatic changes that have little effect on groundwater-flow velocities. Because all sampled values of the Climate Index are greater than 1.00, climate change as implemented in the PA can only increase the rate of groundwater flow.

The distribution assigned to the Climate Index parameter is based on the results of three-dimensional basin modeling that considers future changes in the temporal pattern of potential recharge (see CCA Appendix MASS, Section MASS.17 and MASS Attachment 17-1, Section F). Potential recharge is defined as the maximum rate at which water can be added at the water table. Recharge itself is a model result and ranges from zero to the potential recharge. For those areas where the water table is at the ground surface and modeling indicates that water is discharging to the land surface through a seepage face, the potential recharge does not enter the model and has no effect on groundwater flow. In areas where the water table is below the land surface, potential recharge becomes actual recharge and tends to cause the water table to rise. If potential recharge is zero, the water table in an idealized basin will tend to fall until it is a horizontal plane with an elevation equal to the lowest topographic point in the basin. Sufficiently large values of potential recharge will cause the water table to rise to the land surface everywhere. Smaller, nonzero values result in solutions with water tables at the land surface at topographic lows (discharge areas) and at some distance below the land surface at topographic highs (recharge areas). Changes in potential recharge cause the elevation of the water table to rise or fall. In the three-dimensional modeling of the WIPP region, potential recharge was assumed to be spatially invariant across the regional model domain and assumed to change through time in response to climate changes.

Both steady-state and transient three-dimensional regional analyses were executed with values of potential recharge varied so that the elevation of the water table ranged from approximately its present position to at or near the land surface. The latter condition provides an upper bound for regional groundwater-flow velocities during future wetter climates. For all simulations examining the effects of climate change, recharge is assumed to be greater at some time in the future than it is at present. Present recharge is assumed to be the same as its minimum value during the Holocene. The dominant effects on climate change during the next 10,000 years are assumed to be natural rather than anthropogenic. This assumption is consistent with regulatory guidance provided by the EPA indicating that considering the effects of climate change should be limited to natural processes (EPA 1996a, 61 FR 5227).

Because of uncertainty about recharge rates during future wet periods and the timing of these periods, transient analyses use two fundamentally different patterns for the change in potential recharge. The first pattern used in the analysis corresponds to a continuation of the inferred climate patterns of the Holocene (see Section 2.5.1 and CCA Appendix CLI, Section 3), with wetter peaks occurring 500, 2,000, 4,000, 6,000, 8,000, and 10,000 years in the future. Potential recharge is assumed to increase and decrease linearly during the wet periods 500 years before and after the peaks, and the wet periods are each separated by 1,000 years of a drier climate, like that of the present. Several different values were examined for the maximum potential recharge imposed at the wet peaks; the largest value was chosen to provide a steady-state solution with the water at, or close to, the land surface throughout the model domain. As discussed in Appendix MASS (CCA Section MASS.17 and MASS Attachment 17-1, Section F), a continuation of the Holocene climatic variability is considered likely during the next 10,000 years, and is assigned a relatively high probability of occurrence (0.75). This recharge function and its probability of occurrence are reflected in the lower portion of the bimodal distribution assigned to the Climate Index parameter.

The second recharge pattern assumes that potential recharge will increase from its present value to a specified larger value 500 years in the future, and that potential recharge will then remain constant throughout the rest of the 10,000-year simulation. As with the Holocene pattern, several different values were examined, the largest resulting in a steady-state solution with the water table at, or close to, the land surface throughout the model domain. Conceptually, this pattern corresponds to a future in which the climate either becomes continuously wetter or the frequency of wetter periods becomes large enough that the hydrologic response is indistinguishable from that of a continuously wetter climate. Step-increase recharge functions were used to simulate the effects of major disruptions of the Holocene climate, analogous to those that might occur during the next 10,000 years in a transition from the present warm interglacial climate to the early stages of a future glacial climate. As discussed in CCA Appendix MASS (Section MASS.17), such disruptions to the Holocene climate are considered unlikely, and the step function is assigned a relatively low probability of occurrence (0.25). This recharge pattern and its probability of occurrence are represented by the upper portion of the bimodal distribution assigned to the Climate Index parameter.

As reported in CCA Appendix MASS (Section MASS.17 and MASS Attachment 17-1, Section E), 17 transient and 54 steady-state, regional, three-dimensional, groundwater-flow simulations were run to examine effects of climate change. Simulations considered both potential recharge functions with varying peak recharge rates and different sets of assumptions about regional rock properties. Total specific discharge into and out of the Culebra within a model region was calculated for each simulation approximately corresponding to the controlled area. Values for the Climate Index parameter were determined by comparing the total lateral specific discharge calculated for each simulation. The largest observed increase in flow for those simulations using realistic values of rock properties was a factor of 2.1. Although some simulations produced a slight reduction in flow, Climate Index parameter values less than 1.0 are not considered in the PA. Changes in flow direction in the Culebra were also noted in some three-dimensional simulations, with a shift in flow toward the west corresponding to a regional increase in the elevation of the water table. These potential changes in flow direction are not incorporated in the two-dimensional flow and transport modeling to simplify the computational process. This treatment is conservative with respect to radionuclide transport because the most

rapid transport possible under any climate conditions will be through the most conductive portion of the Culebra south and east of the repository. Any shift of the flow away from this high conductivity zone would result in slower transport through less permeable rock. Restricting the effects of climate change to a uniform linear scaling of specific discharge in the SECOTP2D model is, therefore, a conservative assumption.

6.4.10 Initial and Boundary Conditions for Disposal System Modeling

The solution of many mathematical models used in PA requires specification of a starting point, called initial conditions, and specification of how the region modeled (that is, volume) interacts with the regions not modeled (boundary conditions). Initial values are required for all of the parameters appearing in a computer code. In practice, however, the term "initial conditions" refers to the values assigned to the primary variables used to describe the system, examples of which may be pressure, composition, and saturation. The term "boundary condition" refers to the specification of primary variables that control the interaction of the modeled region with the regions excluded from the model. In many studies, applied boundary conditions are static in time, although computer codes that implement time-dependent boundary conditions are not uncommon. A common practice in modeling groundwater flow is to place modeled system boundaries somewhat distant from the region in which model results are of interest. This helps ensure that uncertainty in the natural boundaries of the system does not unduly influence model results in the region of interest. The DOE adopts this practice in its application of BRAGFLO and MODFLOW-2000 to the WIPP.

The following sections describe the initial and boundary conditions specified for the major codes used in this PA. Initial values of parameters not discussed in the following sections are set equal to the values assigned from the PA database or LHS sampling discussed elsewhere in Section 6.4.

6.4.10.1 Disposal System Flow and Transport Modeling (BRAGFLO and NUTS)

In BRAGFLO, initial conditions to simulate the regulatory period are consistent with the following:

1. there are no gradients for flow in the far-field Salado;

2. Salado far-field pore pressures are elevated above hydrostatic from the surface but below lithostatic; and

3. near the repository, excavation and waste emplacement results in partial drainage of the DRZ, subsequent evaporation of drained brine into mine air, and removal from the modeled system by air exchanged to the surface.

The term "far-field" refers to the region that is not influenced by the DRZ drainage mentioned in (3). For units above the Salado, initial pressures are consistent with observed pore pressures or normal hydrostatic gradients (Appendix PA, Section 4.2.2).

Estimating the effects of drainage of the DRZ that occurs during the operational period, (3) above, is not simple. For each vector sampled in LHS, the DOE estimates this by using

BRAGFLO to simulate a period of time representing disposal operations. This calculation is called the start-up simulation and covers five years from t = ~5 years to t = 0 years, corresponding to the amount of time a typical panel is expected to be open during disposal operations. Most of the initial parameters used during the regulatory period simulation (t = 0 to t = 10,000 years) are also assigned for the start-up simulations, with some exceptions, described below.

The initial pressures in the Salado for the start-up simulation are based on a sampled pressure at the elevation of MB139 at the shaft and adjusted throughout the Salado and the DRZ to account for changes in hydraulic head due to elevation change. This parameter is discussed in Appendix PA, Attachment PAR (Parameter 26). The adjustment assumes hydrostatic equilibrium. The DRZ permeability is set at 10^{-17} square meters for the start-up simulation. Based on observed changes in the DRZ, the DRZ porosity is adjusted upwards 0.0029 (0.29 percent) from the sampled value for intact, impure halite. Initial pressure for the start-up simulation in the excavated regions is set to atmospheric. The shaft exists and is modeled as unfilled with the same physical properties as the excavation.

For the start-up simulation, an initial water-table surface is specified within the Dewey Lake at an elevation of 980 m (3,215 ft) above mean sea level. This elevation is consistent with observations discussed in Chapter 2, Section 2.2.1.4.2.1. Above the water table, pressure is maintained at one atmosphere, 0.101 megapascals; liquid saturations in these computational cells are held constant at residual liquid saturation (Section 6.4.6.6, Table 6-25). Below the water table, initial liquid saturations in all regions except the repository and shaft are 100 percent. Pressures are set consistent with a hydrostatic gradient below the water table within the Dewey Lake, as well as in the Rustler, except for the Magenta and Culebra. Initial pressures in the Culebra and Magenta are set at 0.9141 and 0.9465 megapascals, respectively. These values are based on fluid level and fluid density data collected from well C-2737, which is located directly over the waste panels (Beauheim 2003). Even though the natural properties of units above the Salado vary considerably over the domain modeled by BRAGFLO, the BRAGFLO initial condition of constant pressure and constant properties for each layer is considered reasonable because BRAGFLO calculates the long-term flux of brine from the borehole or shaft to each unit or to the surface. For this purpose, the pressure and properties at the borehole or shaft are important, but details of regional hydraulic head and unit properties are not.

For the start-up simulation, permeabilities of all units above the Salado are set to zero so that flow cannot occur from these units into the shaft. This modeling assumption is adopted as a simple method of accounting for the effective liners in the shafts during disposal operations.

No-flow boundary conditions are assigned in the BRAGFLO model of the disposal system along all of the exterior boundaries of the computational mesh, except at the far field boundaries of the Culebra and Magenta and the top of the model (that is, the ground surface, Appendix PA, Section PA-4.2.10). The ground surface is maintained at atmospheric pressure. The boundaries of the Culebra and Magenta are maintained at pressures of 0.9141 megapascals and 0.9465 megapascals, respectively, corresponding to the initial pressure conditions used in the Culebra and Magenta. The pressure in the Castile brine reservoir is set at its sampled value for the start-up simulation.

During the start-up simulation, fluid flow calculated by BRAGFLO from the Salado and the DRZ into the excavated region simulates the effect of drainage into the repository during the operational period. Following the start-up simulations, initial conditions are specified for the regulatory period simulation. Boundary conditions for the regulatory period simulation are the same as those for the start-up simulation.

The regulatory period simulation begins with conditions consistent with the sealing of the repository by shaft seals. Certain properties assigned for the start-up simulation are changed to make model conditions consistent with the emplacement of waste and completion of sealing. The liquid saturation in the waste-disposal region of the repository is set at 0.015, which is a conservative value (Butcher 1996), and other areas of the excavation are assigned zero liquid saturation (100 percent gas saturation) regardless of the quantity of brine that may have flowed into the excavation during the start-up simulations. This is consistent with the observed ability of circulating mine air to remove any inflowing brine by evaporation. The entire repository is assigned an initial pressure of one atmosphere. Pressures and saturations in model regions representing rock remain as they were at the end of the start-up simulation. Permeabilities of the units above the Salado are reset to the values specified as discussed in Section 6.4.6. The shaft is assigned properties for shaft seal materials discussed in Section 6.4.4 and Appendix PA, Section PA-4.2.6. Waste is emplaced in the waste-disposal regions at a density of 1.17×10^2 kg/m^3 for ferrous metals and 5.55×10^1 kg/m^3 for biodegradable materials. Other waste properties are assigned as discussed in Section 6.4.3.2. Panel closure properties discussed in Section 6.4.3.2 are assigned to the panel closure regions. Permeability in the DRZ is sampled for each realization and remains constant for the regulatory period (see Appendix PA, Attachment PAR). Corrosion and biodegradation reactions that produce gas are modeled to begin at the start of the regulatory period simulation, and their rates depend on the sampled parameter values for the gas generation model (see Section 6.4.3.3) and the availability of brine. Modeling of creep consolidation through the use of the porosity surface also begins at this time (see Section 6.4.3.1).

6.4.10.2 Culebra Flow and Transport Modeling (MODFLOW-2000, SECOTP2D)

Two principal factors were considered when selecting the boundaries for the MODFLOW-2000 model of the Culebra. First, model boundaries should coincide with natural groundwater divides where feasible, or be far enough from the area of most interest (the SECOTP2D transport domain) to have minimal influence in that area. Second, the model domain should encompass all features with the potential to affect Culebra water levels at the WIPP site (e.g., potash tailings ponds).

The modeling domain is approximately 22.3 km (14 mi) east-west by 30.6 km (19 mi) north-south, aligned with the compass directions (see Figure 6-17 in Section 6.4.6.2). This is the same as the domain used by LaVenue et al. (1990), except that the current domain extends 1 km farther to the west. The modeling domain is discretized into 68,768 uniform 100-m × 100-m cells. The northern model boundary is slightly north of the end of Nash Draw, 12 km (7.5 mi) north of the northern WIPP site boundary. The eastern boundary lies in a low-transmissivity region that contributes little flow to the modeling domain. The southern boundary lies 12.2 km (7.6 mi) south of the southern WIPP site boundary, slightly over 1.7 km (1 mi) south of the southernmost well (H-9) and far enough from the WIPP site to have little effect on transport rates

on the site. These boundaries are all assigned constant-head conditions based on head measurements made in model domain wells. The western model boundary passes through the IMC tailings pond due west of the WIPP site in Nash Draw. However, a no-flow boundary (a flow line) is specified in the model from this tailings pond up the axis of Nash Draw to the northeast, reflecting the concept that groundwater flows down the axis of Nash Draw, forming a groundwater divide. Similarly, another no-flow boundary is specified from the tailings pond down the axis of the southeastern arm of Nash Draw to the southern model boundary, coinciding with a flow line in the regional modeling of Corbet and Knupp (1996). Thus, the northwestern and southwestern corners of the modeling domain are specified as inactive cells in MODFLOW-2000, leaving 53,769 active cells.

Initial conditions are not required for the Culebra flow calculations because these are steady state. Initial actinide concentrations in the transport simulations are assumed to be zero.

6.4.10.3 Initial and Boundary Conditions for Other Computational Models

In addition to BRAGFLO, MODFLOW-2000, and SECOTP2D, several other codes are used in PA that require initial and boundary conditions. In general, these codes are strongly coupled to BRAGFLO, analogous to the manner in which SECOTP2D is coupled to MODFLOW-2000. These additional codes are NUTS, PANEL, the BRAGFLO direct brine release model (BRAGFLO), and CUTTINGS_S.

NUTS transports radionuclides through the BRAGFLO domain based on fluid flow characteristics as calculated by BRAGFLO and, therefore, does not need explicit definition of flow boundary conditions. As actinide transport is not of concern until the repository contains waste and is sealed, a start-up simulation is not executed with NUTS. Boundary conditions for advective transport are consistent with the boundary conditions assumed for fluid flow. Molecular transport boundary conditions for NUTS simulations consist of no diffusion or dispersion in the normal direction across far-field boundaries. Initial actinide concentrations are zero in all regions except the waste. Actinide concentrations in the waste region brine are assigned as discussed in Section 6.4.3.5 (Table 6-13).

PANEL estimates the transport of radionuclides from the repository to the Culebra for the E1E2 scenario (Appendix PA, Section PA-4.4). PANEL assumes homogeneous mixing within a panel of the waste disposal region to determine a source term for radionuclides. PANEL is strongly coupled to BRAGFLO, in that the flux of liquid up the borehole and out the separate panel in BRAGFLO is provided as the flux of liquid leaving the mixing volume in PANEL. Liquid leaving the mixing cell in PANEL is assumed to arrive at the Culebra, thereby maximizing the source of actinides to the Culebra.

Models for direct release to the surface are also strongly coupled to BRAGFLO. CUTTINGS_S (cuttings, cavings, and spall) and BRAGFLO (for direct brine release) acquire fluid pressure, fluid saturation, and other necessary quantities from the appropriate BRAGFLO disposal system model simulation. It is assumed in the direct release models that radionuclides, once entrained in drilling fluid, remain in the drillhole until they reach the surface. In other words, there is no interaction between drilling fluid and the formations between the repository and the surface.

Boundary conditions in the direct brine release model are no-flow except for the sources and sinks of brine through borehole nodes and at the surface.

6.4.11 Numerical Codes Used in Performance Assessment

To evaluate scenario consequences for both undisturbed and disturbed performance, DOE uses many computer codes to simulate relevant features of the disposal system. The flow of information and primary roles of the codes used are discussed in this section; the mathematical models implemented by the codes are discussed in Appendix PA. Parameter values and disposal system conditions must be passed between codes several times in an assessment.

The codes are executed under the requirements of the SCMS), which creates and maintains a complete record of the input data and results of each calculation, along with the exact codes used to create those results. For this application, PA codes used in conjunction with LHS or random sampling were executed under the SCMS.

The major computer codes and the flow of information among them are illustrated in Figure 6-24. As discussed in Section 6.1.4 and indicated in Figure 6-24, some of these codes are used to calculate reference conditions for deterministic futures associated with the parameters in x_{su} (Equation 6.4b [Section 6.1.2]) and their associated uncertainty characterized by distributions D_{su} (Equation 6.6b [Section 6.1.2]). The results of these codes are then used constructing the consequences of probabilistic futures. There are three major steps in evaluating scenario consequences for deterministic futures: (1) preparing input from submodels executed independent of LHS (for example, SANTOS, PEST), (2) LHS of the variables x_{su} in the PA parameter database, and (3) executing the sampling-dependent PA codes (those within the deterministic futures box indicated by dashed lines in Figure 6-24).

Some PA codes are used to calculate probabilistic futures; that is, future events that occur randomly in time and space, and uncertainty of associated parameters in x_{st} (Equation 6.4a [Section 6.1.2]) and characterized by distributions in D_{su} (Equation 6.6a [Section 6.1.2]). There are two major steps in evaluating scenario consequences for probabilistic futures: (1) random sampling of the parameter database, and (2) executing the codes.

Figure 6-24 indicates only those codes that perform the bulk of the computational effort related to simulating the significant physical processes occurring within the disposal system. In addition, a variety of additional codes are used in this PA. These additional codes are transfer data between codes, prepare input files, model output processing, and perform similar tasks. These codes are also executed within the SCMS.

Because these additional codes are not expressly used to simulate physical processes, they have been omitted from discussion here and on Figure 6-24 for clarity. A comprehensive description of the coupling of codes used in this PA is provided in Appendix PA.

Figure 6-25 shows an alternative method of visualizing how the various PA codes relate to each other and to the estimation of scenario consequences. This figure shows a vertical cross section of the disposal system, associating the major codes with the particular components of the system each code simulates. As shown in the figure, BRAGFLO, SANTOS, NUTS, and PANEL address the Salado. PEST, MODFLOW-2000, and SECOTP2D address the Culebra.

CUTTINGS_S, BRAGFLO (direct brine release), DRSPALL, and PANEL address the immediate consequences of inadvertent human intrusion through one or more exploratory boreholes. Combined, Figures 6-24 and 6-25 illustrate the flow of information through major PA codes and the relationship between the codes and the physical system being simulated.

The parameter database is the initial element in the PA process. The database includes the parameters used in PA codes that pertain to the technical aspects of disposal system performance. Parameters pertaining only to the execution of the codes (for example, convergence criteria for Newton-Raphson numerical solvers) are generally not included in the database, but are recorded in input files and traceable through the SCMS. Parameters in the database fall into two categories: those that are assigned fixed values, and those that are uncertain and are therefore assigned a range of values according to a CDF.

Vectors (sets) of parameter values are created from the uncertain variables in the database by LHS of each variable for a set of simulations in the PA. In this PA, 64 parameters are sampled using LHS, and 100 vectors are assembled in each replicate (see Section 6.5). The values assigned to each sampled parameter in each of the vectors in this PA are included in Appendix PA, Attachment PAR. Each of the fixed parameter values from the database and a vector of sampled parameter values are combined to form a realization (a set of input parameters). Each realization is then propagated through the PA codes within the dashed lines shown in Figure 6-24.

Assessing each realization requires that the codes shown in Figure 6-24 for deterministic futures be executed under four code sequence configurations, one each for the undisturbed performance scenario (E0), the E1 scenario, the E2 scenario, and the E1E2 scenario.

Each intrusion scenario may occur with or without mining. The techniques used for each scenario are described in Section 6.4.13.

As shown in Figure 6-25, information for some of the major codes comes from the following additional sources: the SANTOS, PEST, DRSPALL, and FMT codes.

The SANTOS code develops the porosity surface, describing porosity as a function of time and pressure; this information is used in the BRAGFLO code (see Appendix PA, Section PA-4.2 and Attachment PORSURF). PEST is coupled with MODFLO-2000 to calculate numerous possible and equally likely Culebra transmissivity fields; these transmissivity fields are used inthe MODFLOW-2000 code (see Appendix PA, Attachment TFIELD). FMT is used to calculate solubility parameters entered into the parameter database. These parameters, as well as sampled solubility distribution parameters, calculated solubilities for the PA. Actinide solubility in the repository is used by the codes NUTS and PANEL. DRSPALL calculates the volume of solid material that could be removed from the repository by spallings for a set if initial pressure conditions and uncertain parameters. The code CUTTINGS_S uses the DRSPALL results to determine the volume removed by spallings for intrusions at different times and locations.

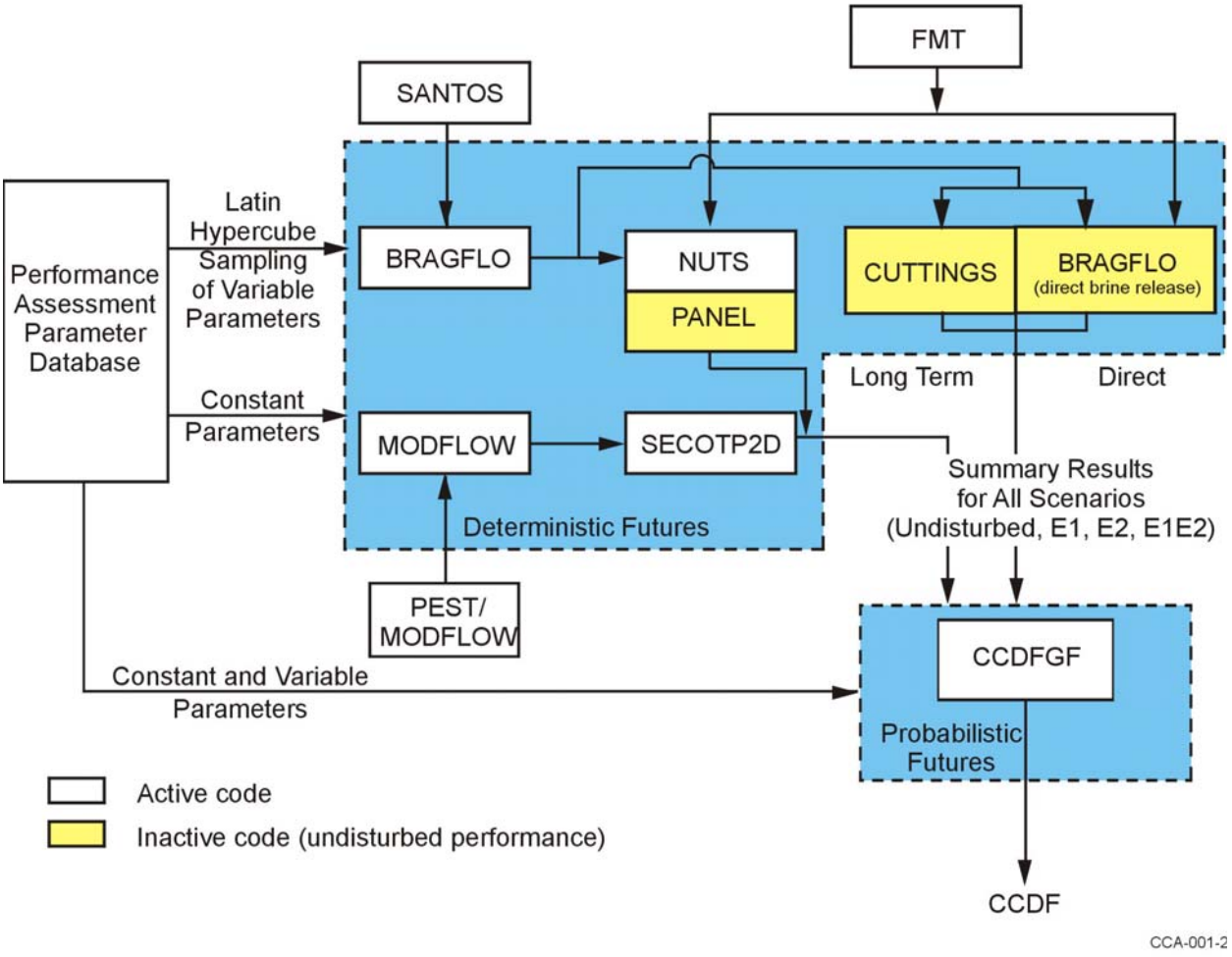

Figure 6-24. Major Codes, Code Linkages, and Flow of Numerical Information in WIPP PA

The PA codes are executed sequentially. Following LHS, BRAGFLO is the first major code executed. Notice that BRAGFLO is listed twice in this sequence. BRAGFLO is used in two applications for PA. In the first application, BRAGFLO calculates the overall movement of gas and brine in the repository and from the Castile to the surface; this movement forms the basis for estimating radionuclide releases to the accessible environment (Appendix PA Sections 4.2 and 6.7). BRAGFLO also contains subsystem models for estimating gas generation in the repository, disposal room closure and consolidation, and interbed fracturing (Appendix PA, Section PA-4.2). BRAGFLO does not calculate the movement of radionuclides. The second application of BRAGFLO is discussed below.

NUTS calculates the overall movement and decay of radionuclides in the repository and disposal system. NUTS uses the same geometry as BRAGFLO, the brine and gas flow fields calculated by BRAGFLO, and the radionuclide source concentrations (solubilities) in the repository defined by the actinide source term models. In simulations of the E1 scenario, NUTS also tracks brine originating in the Castile brine reservoir, including the Castile brine that has flowed out from the borehole and into the waste in the repository. See Appendix PA, Section PA-4.3 for additional

information on the use of NUTS in PA. PANEL calculates actinide source term to the Culebra for the E1E2 scenario, as discussed in Section 6.4.13.5. PANEL is described in detail in Appendix PA, Section PA-4.4.

In all scenarios, the quantity of brine flowing up the shafts or a degraded exploratory borehole to the Culebra is calculated by BRAGFLO, and the concentration of radionuclides in that brine, calculated by NUTS or PANEL, determines the quantity of radionuclides released to the Culebra.

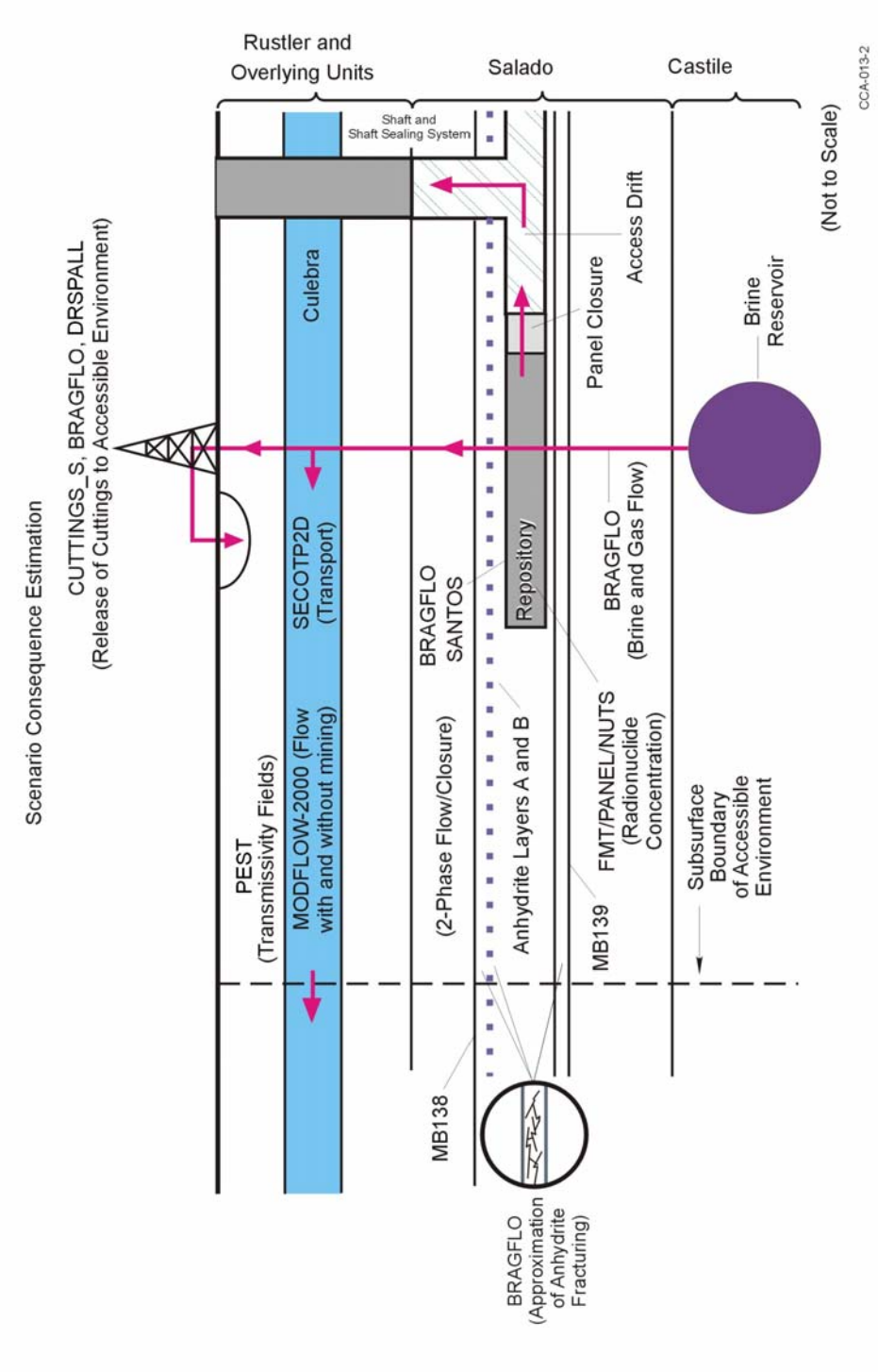

Figure 6-25. Schematic Side View of the Disposal System Associating PA Codes with the Components of the Disposal System Each Code Simulates

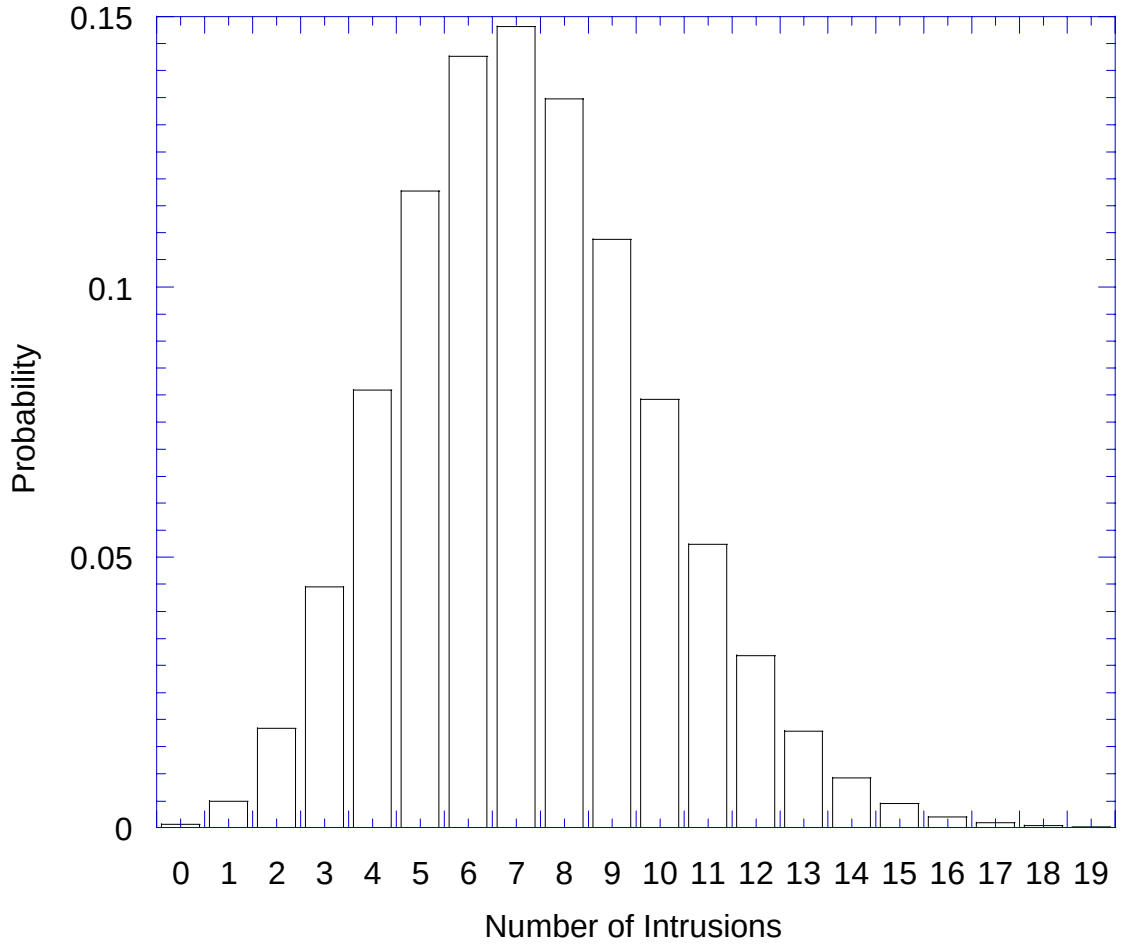

Figure 6-26. Probability of Intrusions in 10,000 Years with Active Institutional Control

CUTTINGS_S and BRAGFLO (direct brine release) evaluate the immediate consequences of inadvertent human intrusion through exploratory drilling. Solid material and brine may be transported to the surface in the drilling fluid. After pressure in the repository is relieved through the first borehole, subsequent boreholes may release less material to the surface. CUTTINGS_S calculates the quantity of solid material transported to the accessible environment at the surface during the drilling activities. This includes material removed directly from the borehole (cuttings), along with cavings and spallings. The code is discussed in Appendix PA, Section PA-4.5. BRAGFLO (direct brine release) calculates the quantity of brine transported up the borehole to the surface.

MODFLOW-2000 and SECOTP2D calculate the detailed movement of radionuclides in the Culebra that occurs if radionuclides flow up the shafts or through a degraded exploratory borehole. MODFLOW-2000 calculates regional Culebra flow fields using an assumption that flow occurs in a single-porosity medium. MODFLOW-2000 uses the transmissivity fields calibrated using PEST (one field in each simulation). SECOTP2D calculates radionuclide transport in a double-porosity medium, accounting for advection in fractures, matrix diffusion, retardation, and decay, as described in Section 6.4.6.2. MODFLOW-2000 and SECOTP2D are

discussed in Appendix PA, Section PA-48 and PA-49, respectively. The NUTS and PANEL codes calculate the actinide source term to the Culebra.

The computer code CCDFGF is used to (1) determine random sequences of future events that may occur over the next 10,000 years at the WIPP site; (2) estimate the radionuclide releases resulting from these random sequences of future events using the results of calculations described thus far; and (3) construct a CCDF for each realization. The manner in which CCDFGF determines random sequences of future events is the subject of Section 6.4.12.

Estimating consequences and constructing a CCDF for these sequences of future events is the subject of Section 6.4.13.

6.4.12 Sequences of Future Events

For this application, sequences of future events that may occur are determined using a random sampling procedure described in Appendix PA, Section PA-3.0. A general description of the technique is presented in this section.

The incorporation of stochastic uncertainty in the PA is based on repeatedly generating independent sequences of events that may occur at the WIPP over the next 10,000 years. Each 10,000-year sequence is generated by randomly sampling six parameters that repeatedly characterize stochastic uncertainty about future events. These parameters include (1) the interval of time between drilling intrusions (which yields both the number and time of intrusions), (2) the location of each drilling intrusion, (3) the activity of the waste penetrated by each drilling intrusion, (4) the plug configuration in the intrusion borehole, (5) the penetration of a Castile brine reservoir, and (6) the occurrence of mining. Probability distribution functions are assigned to each of these six parameters and are discussed in the following sections. Random sampling from these distributions generates 10,000 equally likely, independent futures of the WIPP for each realization executed and CCDF constructed. The computer code CCDFGF (Appendix PA, Sections 3 and PA-6.0) randomly samples sequences of future events, constructs consequences of these sequences, and assembles CCDFs. As described in Section 6.4.13, normalized integrated radionuclide releases to the accessible environment are estimated for each history using the consequence modeling system.

The probability assigned to the occurrence of certain future events at the WIPP site is affected by regulatory guidance and DOE actions taken to deter activities detrimental to WIPP performance. Active and passive institutional controls are discussed extensively in Chapter 7.0. A summary of their use in PA is in this section.

6.4.12.1 Active and Passive Institutional Controls in Performance Assessment

Active institutional controls and passive institutional controls will be implemented at the WIPP site to deter human activity detrimental to repository performance. Active institutional controls and passive institutional controls are described in detail in Chapter 7.0 and in appendices referenced in Chapter 7.0. In this section, the impact of active institutional controls and passive institutional controls on PA is described.

Active institutional controls will be implemented at the WIPP after final facility closure to control site access and ensure that activities detrimental to disposal system performance do not occur within the controlled area. The active institutional controls will preclude human intrusion in the disposal system. A limitation for considering the effectiveness of active institutional controls in PA is established in 40 CFR Part 191. That limitation is 100 years. Because of the nature of the active institutional controls to be implemented and regulatory restrictions, the PA assumes there are no inadvertent human intrusions or mining in the controlled area for 100 years following repository closure.

Passive institutional controls deterr inadvertent human intrusion into the disposal system in PA. Only minimal assumptions were made about future society when designing the passive institutional controls to comply with the assurance requirements. The preamble to 40 CFR Part 194 limits any credit for passive institutional controls in deterring human intrusion to 700 years after disposal (EPA 1996a, 61 FR 5231). Although the DOE originally included credit for passive institutional controls in PA, the CRA-2004 PA does not include such credit. The EPA directed DOE not to take credit for passive institutional controls in the CCA during the certification (EPA 1998, 194.VIII.D.3).

6.4.12.2 Number and Time of Drilling Intrusions

The number of drilling intrusions associated with each 10,000-year history is based on 40 CFR § 194.33(b)(2) and § 194.33(b)(3):

> In performance assessments, drilling shall be assumed to occur in the Delaware Basin at random intervals in time and space during the regulatory time frame. [40 CFR 194.33(b)(2)]
>
> The frequency of deep drilling shall be calculated in the following manner:
>
> (i) Identify deep drilling that has occurred for each resource in the Delaware Basin over the past 100 years prior to the time at which a compliance application is prepared.
>
> (ii) The total rate of deep drilling shall be the sum of the rates of deep drilling for each resource. [40 CFR 194.33(b)(3)]

The DOE's implementation of these criteria is described in this and the following sections.

Mathematically, events that are random in time can be described as following a Poisson process that can be written as

$$P\left[E_n\left(\Delta t\right)\right] = \frac{\left[\lambda\left(\Delta t\right)\right]^n}{n!} e^{-\lambda \Delta t}, \tag{6.18}$$

where $p[E_n(\Delta t)]$ is the probability (p) that some number (n, an integer) of events (E) will occur in a time interval (Δt) given a rate constant λ with units of events per time.

Inadvertent human intrusions may occur at any time between 100 years and 10,000 years after the decommissioning of the facility. Both the number and time of intrusions are determined sequentially by sampling from a CDF derived from the Poisson model that probabilistically describes the time period elapsing between an intrusion at a fixed time and the next intrusion.

The time interval to the next intrusion following an intrusion may vary from 0 years to greater than 9,900 years, with a probability determined by the rate constant λ. The rate constant is derived from the drilling rate established for the Delaware Basin and the area of the waste disposal region, 0.126 km^2 (0.049 mi^2). The drilling rate used in this analysis was 52.5 boreholes per square kilometer per 10,000 years. As discussed in Appendix DATA, Attachment A, this rate is based on a review of past and present drilling activity in the Delaware Basin. The rate constant λ is assigned different values for two time periods. While active institutional controls are effective, it is equal to zero; after active institutional controls cease, λ is assigned to 52.5 boreholes per square kilometer per 10,000 years.

Intrusion times are determined by random sampling. If the sampled time is greater than 9,900 years (100 + 9,900 = 10,000), no intrusions occur between 100 and 10,000 years. If the sampled time is less than 9,900 years, an intrusion occurs at 100 years plus the sampled time. The post-active institutional controls CDF is sampled iteratively to determine whether intrusions occur in the time interval between the last intrusion and 10,000 years until an intrusion is determined to occur after 10,000 years.

The most likely number of intrusions into the waste disposal region during 10,000 years is seven, with a probability of 0.1482. Zero intrusions occur with a probability of 0.0007. The largest number of intrusions that occur with a probability greater than 10^{-3} per 10,000 years (and which can contribute to releases for comparison with the quantitative release limits) is 16, occurring with a probability of 0.0020. Probabilities for other numbers of intrusions within 10,000 years are given in Table 6-30. These probabilities are shown as a histogram in Figure 6-26.

6.4.12.3 Location of Intrusion Boreholes

Drilling events are assumed to be random in time and space, and the location of each intrusion borehole within the waste disposal region is sampled randomly. This is done in the analysis by discretizing a plan view of the area within the passive institutional control berms (see CCA Appendix PIC, Section VIII) into 144 separate regions and requiring each intruding borehole to penetrate a single region (Figure 6-27). The probability of intersecting each location is equal to 1/144 (about 0.00694), and slight variations in the size of regions are disregarded as unimportant.

Each of the 144 regions contains both excavated and unexcavated areas at the repository horizon. A borehole has an approximately 20 percent chance of intruding excavations and an approximately 80 percent chance of passing through unexcavated Salado (see Appendix PA, Section PA-3.4). The berm area and the proportion of excavated to unexcavated regions at the repository horizon are important in the Castile brine reservoir model, as discussed in Section 6.4.12.6.

Boreholes that penetrate excavations may penetrate either CH-TRU waste or RH-TRU waste For long-term releases and direct brine releases, all penetrations into excavations are treated as if CH-TRU waste is penetrated, and the RH-TRU waste inventory is averaged into the CH-TRU waste inventory for source-term determination. For cuttings and cavings direct releases, there is an approximately 12 percent chance that RH-TRU waste canisters are penetrated and an 88 percent chance that CH-TRU waste is penetrated, corresponding to the relative plan-view areas of each waste type (see Appendix PA, Section PA-3.7).

Table 6-30. Probabilities of Different Numbers of Intrusions into the Waste Disposal Region (for 100 years of active institutional control and 9,900 years of uncontrolled activity)

Number of Intrusions	Probability of Occurrence
0	0.0007
1	0.0050
2	0.0183
3	0.0445
4	0.0809
5	0.1177
6	0.1426
7	0.1482
8	0.1348
9	0.1089
10	0.0792
11	0.0524
12	0.0318
13	0.0178
14	0.0092
15	0.0045
16	0.0020
17	0.0009
18	0.0004
19	0.0001

For cuttings and cavings direct releases, the small area of the panel closures is treated as CH-TRU waste and is included in the CH-TRU waste probability. Because of the low permeability of the region surrounding each RH-TRU waste canister, intrusions into RH-TRU waste are not assumed to produce spallings releases or direct brine releases.

6.4.12.4 Activity of the Intersected Waste

Waste shipped to the WIPP will contain quantities of radionuclides that will vary from container to container. Radioactivity may vary by several orders of magnitude from those waste containers with the largest quantities of radionuclides to those with the smallest.

Information about waste radioactivity has been compiled at several different levels (Figure 6-28). The waste-stream level includes information about waste activities from different processes at generator sites that create TRU waste. At this level, a separate waste stream

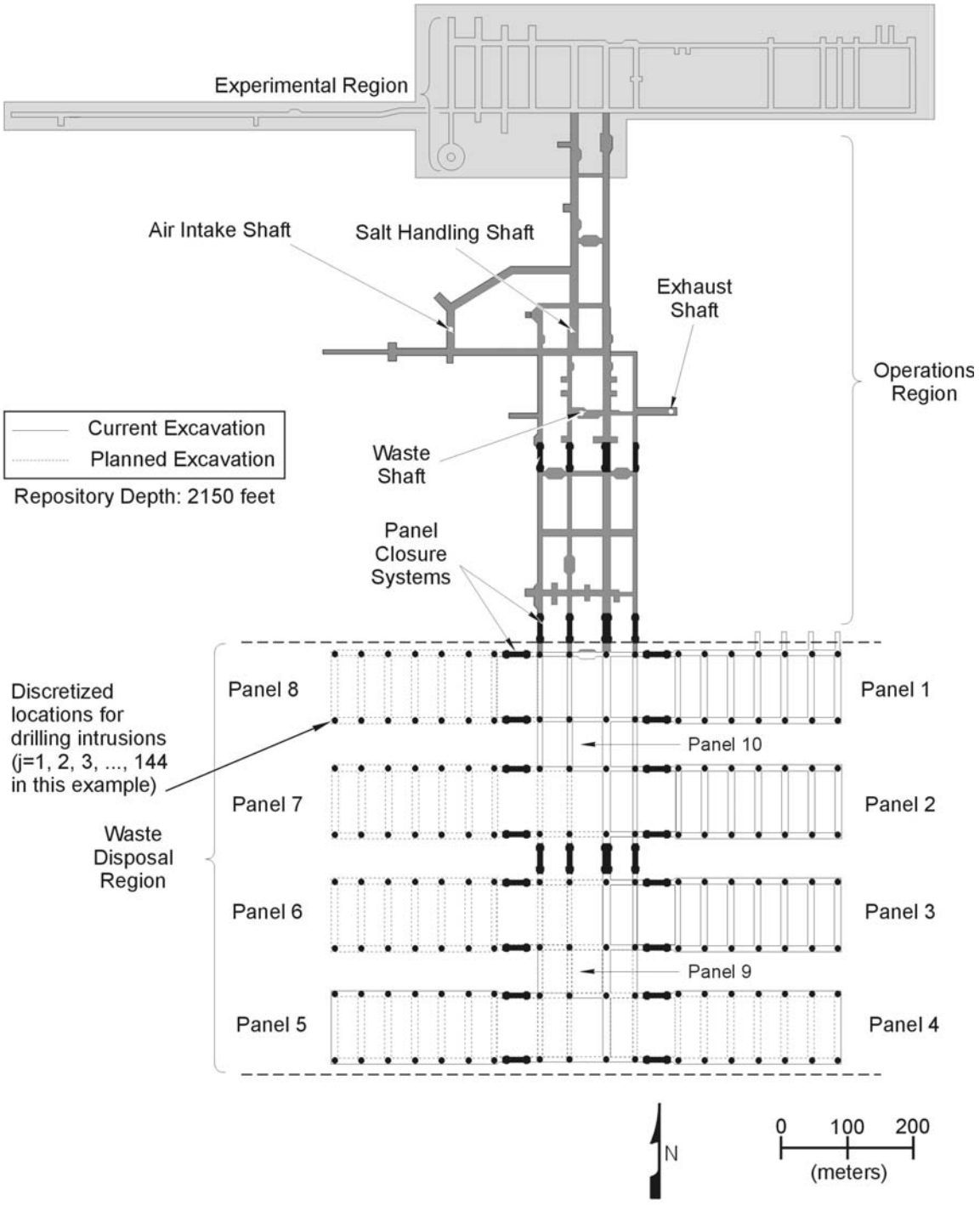

Figure 6-27. Discretized Locations for Random Intrusion by an Exploratory Borehole

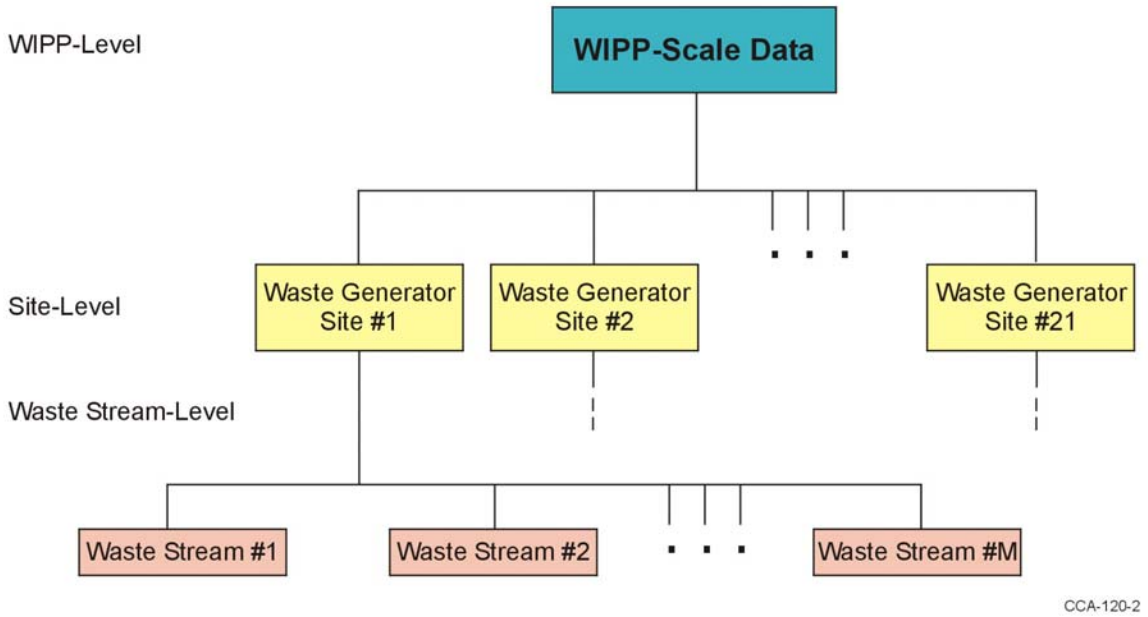

Figure 6-28. Levels of Information Available in the TWBID

characteristic is maintained for RH-TRU. In total, there are approximately 779 CH- and RH-TRU waste streams, of which 693 are CH-TRU. Because the RH-TRU is approximately one percent (actually 1.5 percent) of the total EPA units (not activity) of CH-TRU waste, all the RH-TRU waste was grouped together into one equivalent or average (WIPP-scale) RH-TRU waste stream. Variability in this small fraction is assumed to be negligible. The waste-generator site level includes information integrated over the scale of a generator site. There are 27 generator sites identified for the WIPP (see Section 4.1.2). The WIPP-scale level includes integrated information about all waste destined for the WIPP, including CH- and RH-TRU. Data are present for existing waste and estimates were made for future (to-be-generated) waste. The integration of waste data with the PA is illustrated in Figure 6-29. In the CCA, this information was compiled from the Transuranic Waste Baseline Inventory Database (TWBID), an electronic version of information present in the Transuranic Waste Baseline Inventory Report (TWBIR), Rev. 3, (see CCA Appendix BIR). New information concerning waste inventory has been included in PA for emplaced, stored, and projected waste. The new information is discussed in Chapter 4 and Appendix TRU WASTE (see also Appendix DATA, Section 7.0, Attachment F).

To calculate radionuclide releases from groundwater transport (including direct brine release) and from spallings, spatial variability in the waste activity is assumed to have no significant impact. Concentrations of radionuclides mobilized in repository brine and quantities transported to the ground surface in spallings are assumed to be derived from a sufficiently large volume of waste that container-scale variability can be neglected. Long-term releases and direct brine releases are calculated using WIPP-scale data assuming homogeneous accessibility of RH- and CH-TRU waste activities by liquid in the repository. As discussed previously, spallings releases are not calculated for RH-TRU waste;

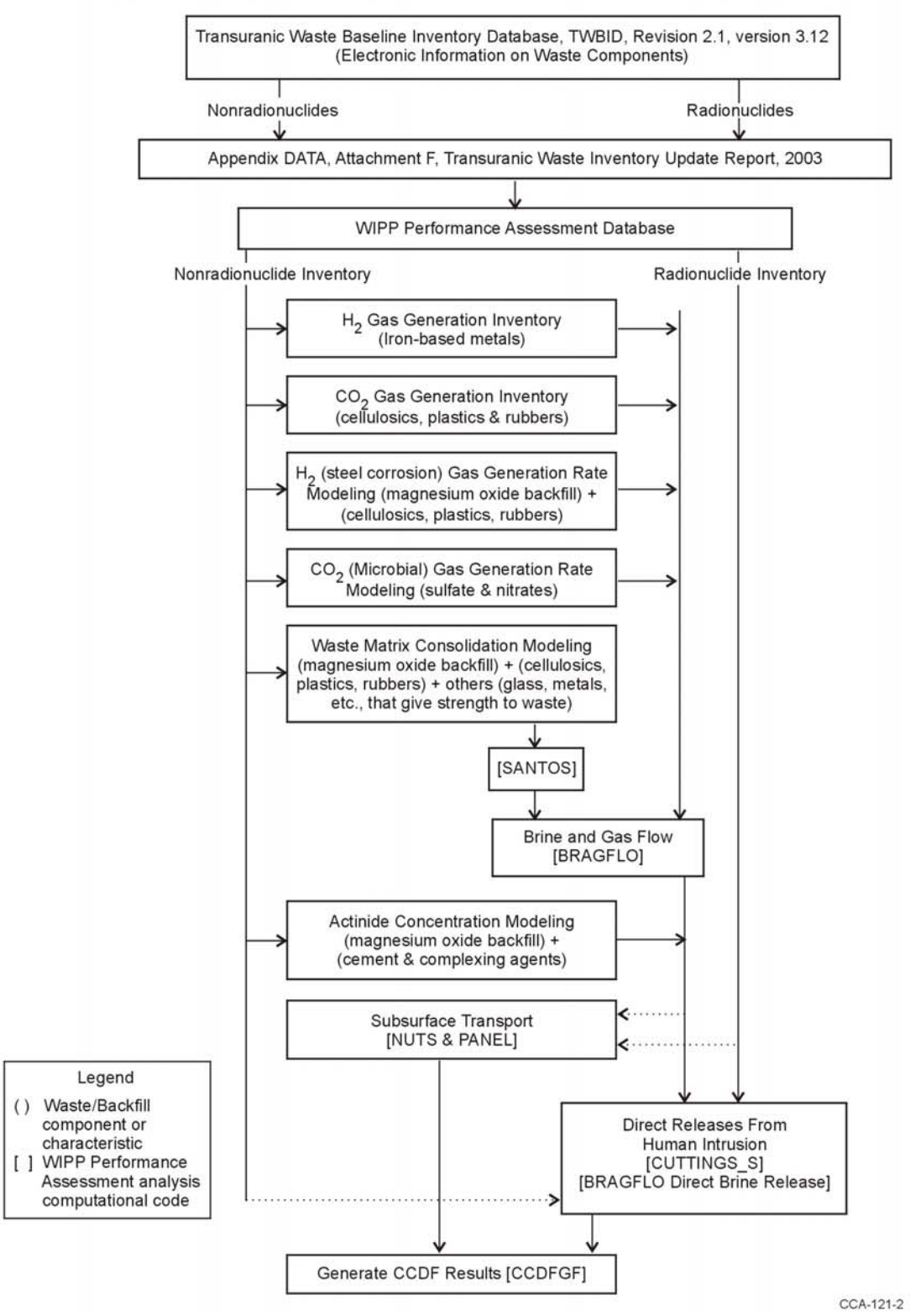

Figure 6-29. Flowchart Showing Integration of TWBID Data in PA Calculations

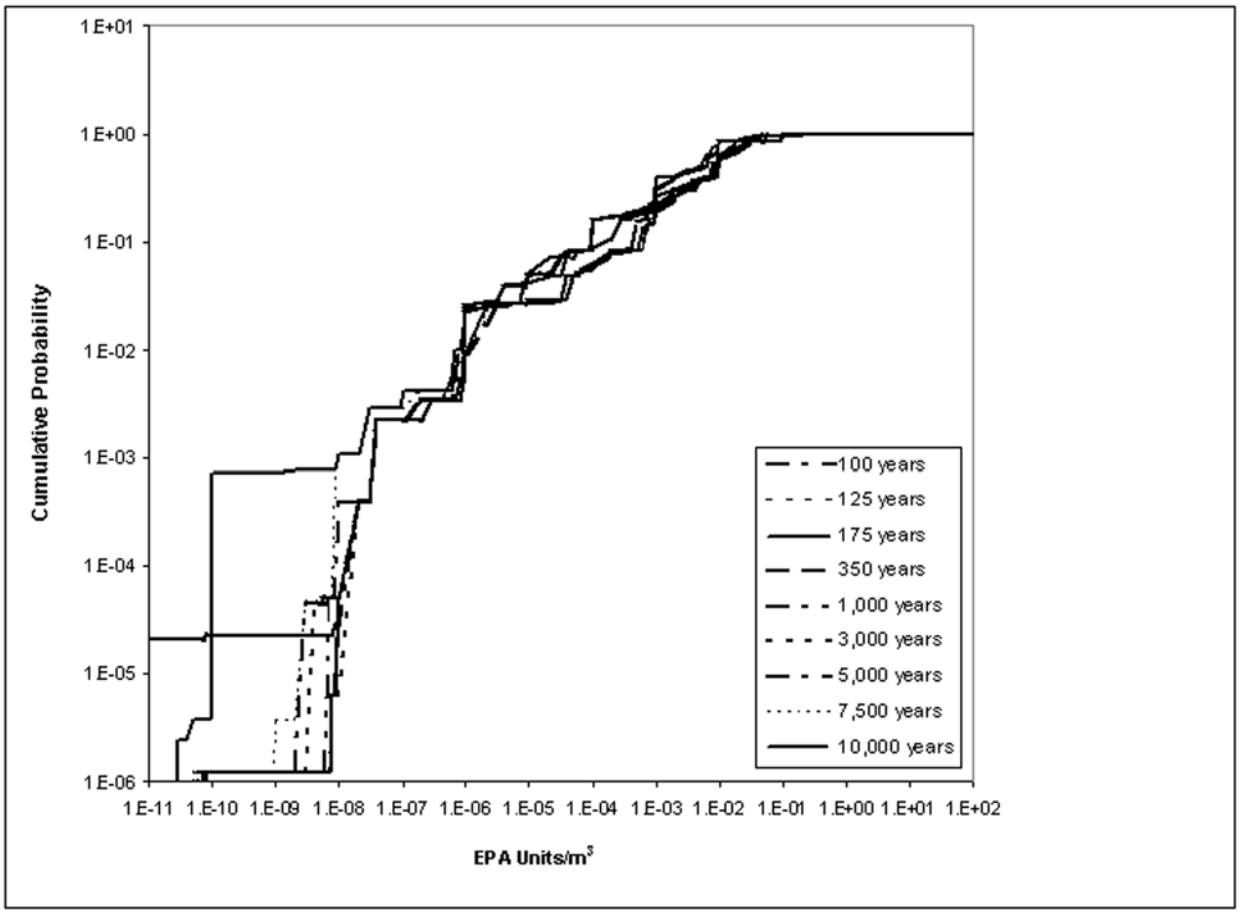

Figure 6-30. Cumulative Distribution Function for Waste Stream EPA Units/Volume

consequently, spallings release activities are determined assuming homogeneous accessibility for only CH-TRU waste.

Direct releases caused by cuttings and cavings access discrete and relatively small portions of the waste, and estimates of the quantity of radioactivity released to the accessible environment may be sensitive to variability in activity loading. The radioactivity of cuttings and cavings releases is calculated using data from the waste-stream level in the following manner.

Containers are assumed to be randomly placed in the WIPP from the various waste streams (see Appendix PA, Attachment MASS, Section 21). Because waste containers are stacked three-high for disposal, a drill bit is assumed to penetrate three containers. The direct-release consequence resulting from a drill bit hitting the edges of containers and generating releases from more than three containers is assumed similar to the consequence of penetrating three containers only (see Appendix PA, Section PA-6.8.3). Each of the three containers penetrated by the drill bit can come from different waste streams and have different associated activities. The waste streams penetrated are randomly sampled according to the relative quantity of waste in each waste stream. Figure 6-30 shows the discretized activities, expressed as the EPA normalized release density, of the 693 CH-TRU waste streams as a CDF and the decay of the waste stream activities through time. Waste stream activities are maintained in PA at 100, 125, 175, 350, 1,000, 3,000,

5,000, 7,500, and 10,000 years. Activities for cuttings and cavings releases at other times are interpolated from these values.

The code CUTTINGS_S calculates the volume of repository material brought to the surface by cuttings and cavings. Of the repository volume removed, approximately 40 percent is waste material; the rest is void space, MgO (backfill), and drum packing material. It is assumed that one-third of the waste material released comes from each of three containers assumed to be intersected. The activity of the release to the surface during drilling by cuttings and cavings is the summed products of one-third the release volume times the three waste stream activities randomly sampled. If random sampling determines that the borehole penetrates RH-TRU waste, 100 percent of the material removed is assumed to be waste and the activity of the release is equal to the volume calculated by CUTTINGS_S times the activity of RH-TRU waste.

6.4.12.5 Diameter of the Intrusion Borehole

Historical Delaware Basin drilling records were reviewed to determine the diameter of a typical intrusion borehole. In PA, the borehole diameter parameter value is held constant for all future drilling and is equal to 0.311 m (12.25 in.). Appendix DATA, Attachment A and CCA Appendix DEL, Attachment 1 discusses current and historical drill stem and drill collar diameters used to drill oil and gas wells in the Delaware Basin. CCA Appendix DEL illustrate a generalized circular cross section of a well plugged according to current practice (see CCA Section DEL.6.1.2.2l and Appendix DATA).

6.4.12.6 Probability of Intersecting a Brine Reservoir

As discussed in Section 6.4.8, there is uncertainty about the existence of brine reservoirs and the probability of intersecting a brine reservoir with a deep borehole. The DOE has examined available data and concluded that there is no reasonable basis to eliminate the possibility of a brine reservoir existing under the site. Therefore, the DOE assumes that a brine reservoir may exist under the waste panels. The DOE determined a reasonable basis for the probability of intersecting a brine reservoir and had pursued three investigations relevant to this issue: geophysical methods, geological structure analysis, and geostatistical correlation (see CCA Section 6.4.8, Appendix MASS Section 18, and MASS Attachments 18-1, 2 and 3 for the investigations that led to the CCA's representation of the brine reservoir). As discussed in Section 6.4.8, the DOE adopted the EPA's representation of the brine reservoir used in the 1997 PAVT (the EPA's basis for this representation is documented in the Technical Support Document for Section 194.23: Parameter Justification Report, A-93-02, V-B-14 and in a technical support document entitled Technical Report Review of TDEM Analysis of WIPP Brine Pockets, A-93-02, V-B-30).

For the CRA-2004 PA, the DOE assumes there is one reservoir under the waste panels and uses probability of a deep borehole hitting the reservoir of between 0.01 to 0.60 (see EPA 1998, VII.B.4.d). The location of boreholes in this area is sampled. They may lie over repository excavations, or over rock in pillar cores, or between panels. The brine reservoir under the waste panels is not assumed to be depleted during the 10,000-year regulatory period by subsequent boreholes drilled anywhere within this area. Boreholes randomly located over rock have the same probability of intersecting the brine reservoir as boreholes located over excavations.

Boreholes located over the excavations are assumed to penetrate waste, and the consequences are modeled as described in Section 6.4.

BRAGFLO calculates the long-term pressure and production of brine from the reservoir for only one two-plug configuration borehole. Subsequent penetrations are assumed to behave identically to the first (see Appendix PA, Section PA-6.8).

6.4.12.7 Plug Configuration in the Abandoned Intrusion Borehole

As stated in Section 6.4.7, three different plug configurations can represent possible future configurations of plugged and abandoned intrusion boreholes. Based on a survey of current practice (see Appendix PA, Attachment MASS, Section 16.0, the two-plug configuration borehole is considered most likely and is assigned a probability of 0.696. The three-plug configuration is considered less likely and is assigned a probability of 0.289. The continuous concrete plug is considered least likely and is assigned a probability of 0.015 (SNL 2003).

6.4.12.8 Probability of Mining Occurring within the Land Withdrawal Area

The EPA has specified the probability of mining in the future. In 40 CFR § 194.32 (b), the EPA states, "Mining shall be assumed to occur with a one in 100 probability in each century of the regulatory time frame."

Also in 40 CFR § 194.32(b), the EPA limits the occurrence of mining to a maximum of once per 10,000 years. The DOE interpreted this probability as a Poisson model with a mining probability of 10^{-4} per year (Appendix PA, Section PA-3.0). The occurrence of mining is sampled from a CDF of the time until mining in a manner similar to the procedure described for the time between drilling intrusions, except that multiple mining events cannot occur.

6.4.13 Construction of a Single CCDF

Construction of a single CCDF requires combining the results of numerical simulations performed using different sets of subjective parameter values (sets selected by LHS) with the probabilistic futures determined by random sampling stochastic parameters (that is, those associated with intermittent drilling) (see Appendix PA, Section PA-3.0). The variety of sequences of events represented in a single CCDF and the impossibility of modeling the details of each future separately requires building a CCDF using methods to construct consequences for any probabilistic future from a limited number of calculations for deterministic, idealized futures. Although this methodology is conceptually straightforward, the details of the process are highly dependent on model and system-specific considerations (see Appendix PA, Section PA-6). Accordingly, insight gained from previous, preliminary PAs as well as analysis of early results for this PA help configure the methodology used for CCDF construction.

Depending on the scenario into which probabilistic futures are classified, different techniques are used for estimating their consequences. The deterministically determined undisturbed performance scenario consequences require no special techniques for application to probabilistic futures. For E1, E2, and E1E2 scenarios, the CCDF construction methodology is primarily based on the principle of scaling, with some simplifying assumptions made for the E2 scenario. Scaling is estimating the consequences of probabilistic futures based on consequence estimates from

deterministic futures. The use of scaling and the building of a CCDF with it is discussed in this section. Note that all of the discussions in Section 6.4.13 are for one vector of parameter values included in the subjective uncertainty analysis. In other words, this section addresses only stochastic variation resulting from uncertainty in the sequence of future events that may occur at the WIPP (see Section 6.1.2).

6.4.13.1 Constructing Consequences of the Undisturbed Performance Scenario

All probabilistic futures in which drilling intrusion and mining within the controlled area do not occur are included in the undisturbed performance scenario. Because there is no stochastic uncertainty for this scenario, all futures within a single LHS vector of undisturbed performance have the same releases to the accessible environment. The following major codes are used to estimate the consequences of undisturbed performance: BRAGFLO, NUTS, and, if actinides reach the Culebra, MODFLOW-2000 and SECOTP2D. To illustrate the flow of information for the undisturbed performance scenario, these codes and the connections between them are highlighted in Figure 6-31. For undisturbed performance, no special techniques are required to modify the results of the deterministic calculation to fit probabilistic futures. Therefore, for a single consequence of undisturbed performance, BRAGFLO is executed once and NUTS is executed once. These calculations determine the release to the accessible environment from transport in the Salado or up the shaft to the surface. If any actinides reach the Culebra following these calculations, MODFLOW-2000 and SECOTP2D determine whether actinides released to the Culebra reach the lateral accessible environment. This information is sufficient to construct consequences for all probabilistic futures that have no intrusion events. This information is also used to evaluate compliance with 40 CFR § 191.15 and 40 CFR § 191.24, described in Chapter 8.0.

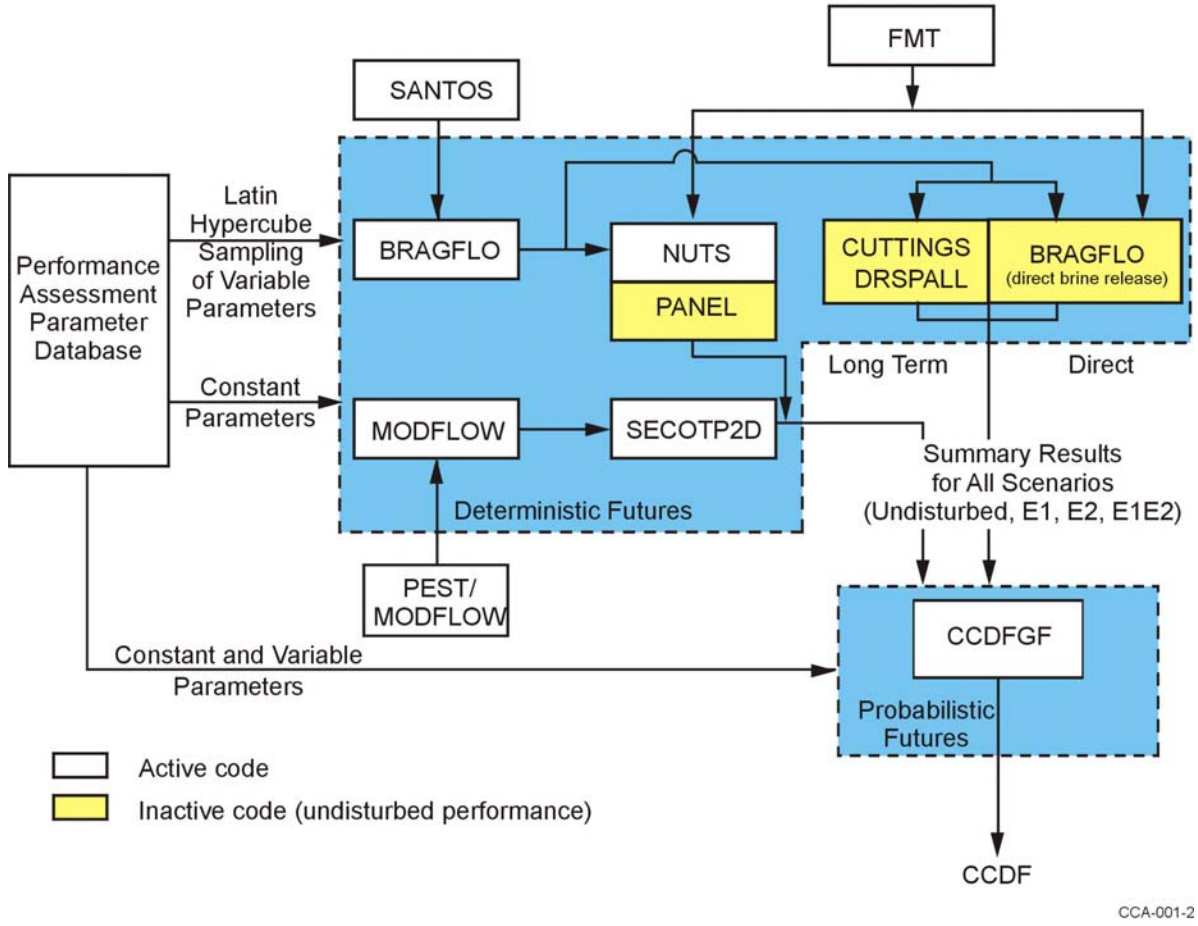

Figure 6-31. Code Configuration for the UP Scenario

6.4.13.2 Scaling Methodology for Disturbed Performance Scenarios

Although 10,000 probabilistic futures are generated to construct a CCDF, the major codes used in PA are executed far fewer times. The results of these calculations are used in part to construct the consequences of all of the probabilistic futures comprising a CCDF in a process called scaling.

The scaling methodology is simple, in concept. First, several simulations are performed with a code to develop a reference behavior for a particular event or process. Each simulation has a defined event occurring at a different time. Then, a large set of futures is developed probabilistically by random sampling. The behavior of the particular event or process in each of the probabilistically sampled futures is estimated by scaling the results of the limited number of deterministic calculations. This scaling is generally simple linear interpolation. For events or processes involving radionuclides, however, scaling becomes more complicated, since it incorporates the effects of radioactive decay and ingrowth. Because scaling is generally less intensive computationally than solving the matrix equations encountered in many PA codes, scaling is an efficient way to develop multiple probabilistic consequence estimates from a

limited number of deterministic calculations. Without scaling, fewer futures would be possible, and resolution in the CCDF would be reduced.

For example, assume that the process of interest is actinides released to the surface during drilling. It is impossible to explicitly model the infinite possibilities present in a probabilistic conceptualization of the future. Thus, scaling is used. To develop a reference behavior for scaling, the CUTTINGS_S code is executed several times with different intrusion times. A probabilistic method is then used to develop a large number of possible, different future intrusion times. To estimate the release to the surface in probabilistic futures, scaling is used in which release at the times in the deterministic calculations closest to the probabilistic time of interest are used as reference points for scaling or interpolation.

Scaling is used for all futures with intrusion boreholes. The times when various codes are executed to develop reference behavior, and how this reference behavior is used by other codes, is the subject of the next two sections. In presenting complete descriptions of the process for each scenario, there will be some duplication of discussion.

6.4.13.3 Estimating Long-Term Releases from the E1 Scenario

The E1 scenario is defined as a single penetration of a panel by a borehole that also intersects a brine reservoir. The code configuration with which the long-term consequences of E1 scenarios are estimated is illustrated in Figure Figure 6-32. For the E1 scenario, BRAGFLO is executed twice more for each CCDF (assuming the undisturbed performance run has already been executed), with the E1-type intrusion occurring at 350 years and 1,000 years. These three BRAGFLO calculations form the foundation for transport modeling that is used for scaling consequences to probabilistic futures.

Consistent with the BRAGFLO intrusion times, NUTS is executed with intrusions occurring at 350 and 1,000 years. These calculations form the basis for (1) estimating releases to the accessible environment via Salado interbeds, or to the surface; and (2) forming the actinide source term to the SECOTP2D code for Culebra transport. For computational efficiency, an intermediate scaling step is conducted prior to calculating the releases associated with probabilistic futures. In this intermediate step, NUTS reference conditions for Culebra releases by an intrusion at 100 years are calculated by using borehole flow from the 350-year intrusion. NUTS reference conditions for intrusions at 3,000, 5,000, 7,000, and 9,000 years are calculated by using borehole flow from the 1,000-year calculation. Thus, to scale consequences of E1 intrusions in probabilistic futures, reference conditions calculated by NUTS are available for 100, 350, 1,000, 3,000, 5,000, 7,000, and 9,000 years postclosure.

Consistent with the BRAGFLO intrusion times, reference behavior for actinide transport in the Culebra is calculated by SECOTP2D for the E1 intrusion occurring at 350 and 1,000 years. Because the equations governing actinide transport and retardation in SECOTP2D are linear, scaling releases to probabilistic E1 penetrations occurring at other times is easily accomplished.

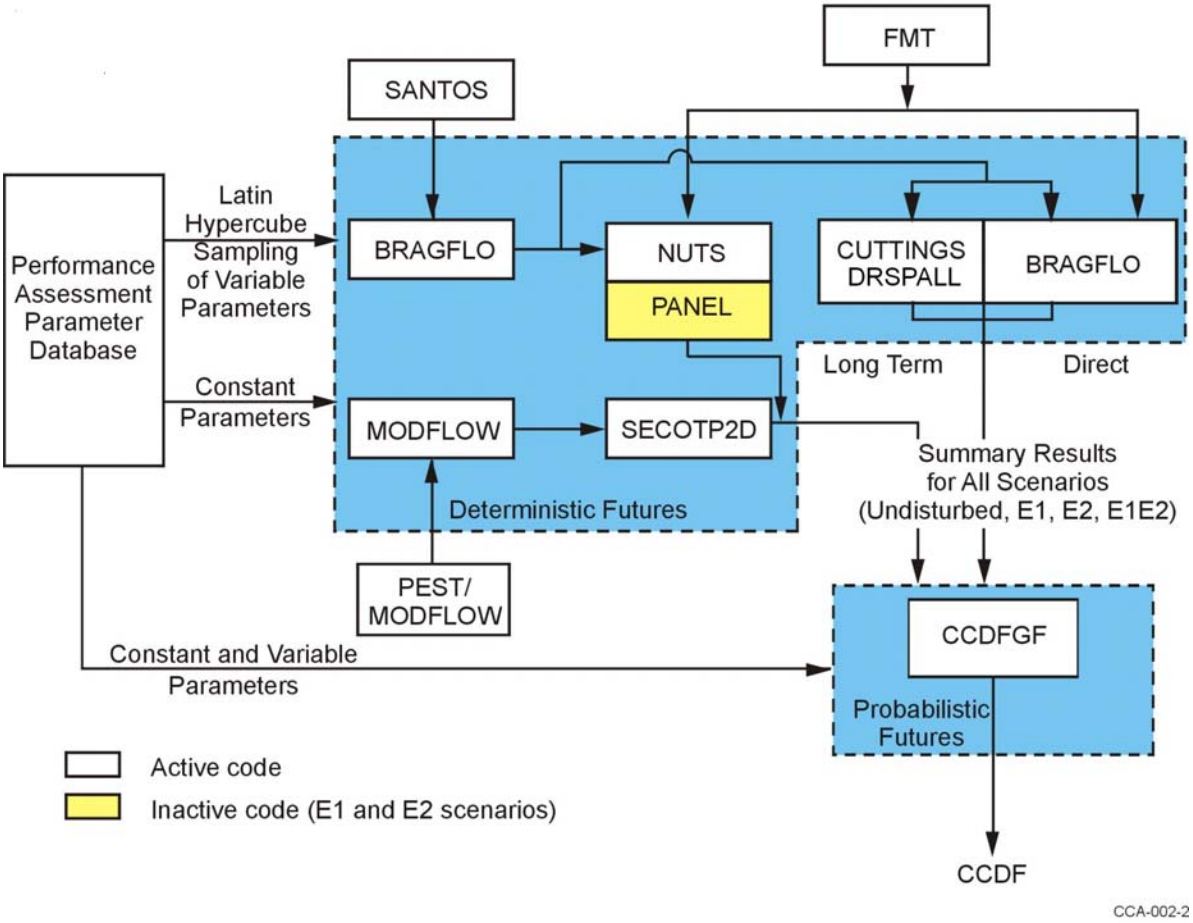

Figure 6-32. Code Configuration for DP Scenarios E1 and E2

6.4.13.4 Estimating Long-Term Releases from the E2 Scenario

The E2 scenario includes all futures with one or more exploratory borehole penetrations of a panel, none of which hits a brine reservoir. Estimating long-term releases from the E2 scenario is slightly more complex than the E1 scenario because the E2 scenario includes the possibility of multiple E2-type intrusions. The same codes used to construct the E1 scenario consequences are used to construct the E2 scenario consequences. These are indicated in Figure 6-33.

As with the E1 scenario, BRAGFLO is executed twice more for each CCDF (assuming the undisturbed performance run has already been executed), with the E2-type intrusion occurring at 350 years and 1,000 years. These three BRAGFLO calculations form the foundation for transport modeling to scale consequences to probabilistic futures.

NUTS is executed with intrusions occurring at 350 and 1,000 years, consistent with the BRAGFLO times of intrusion. These calculations form the basis for (1) estimating releases to the accessible environment via Salado interbeds, or to the surface; and (2) forming the actinide

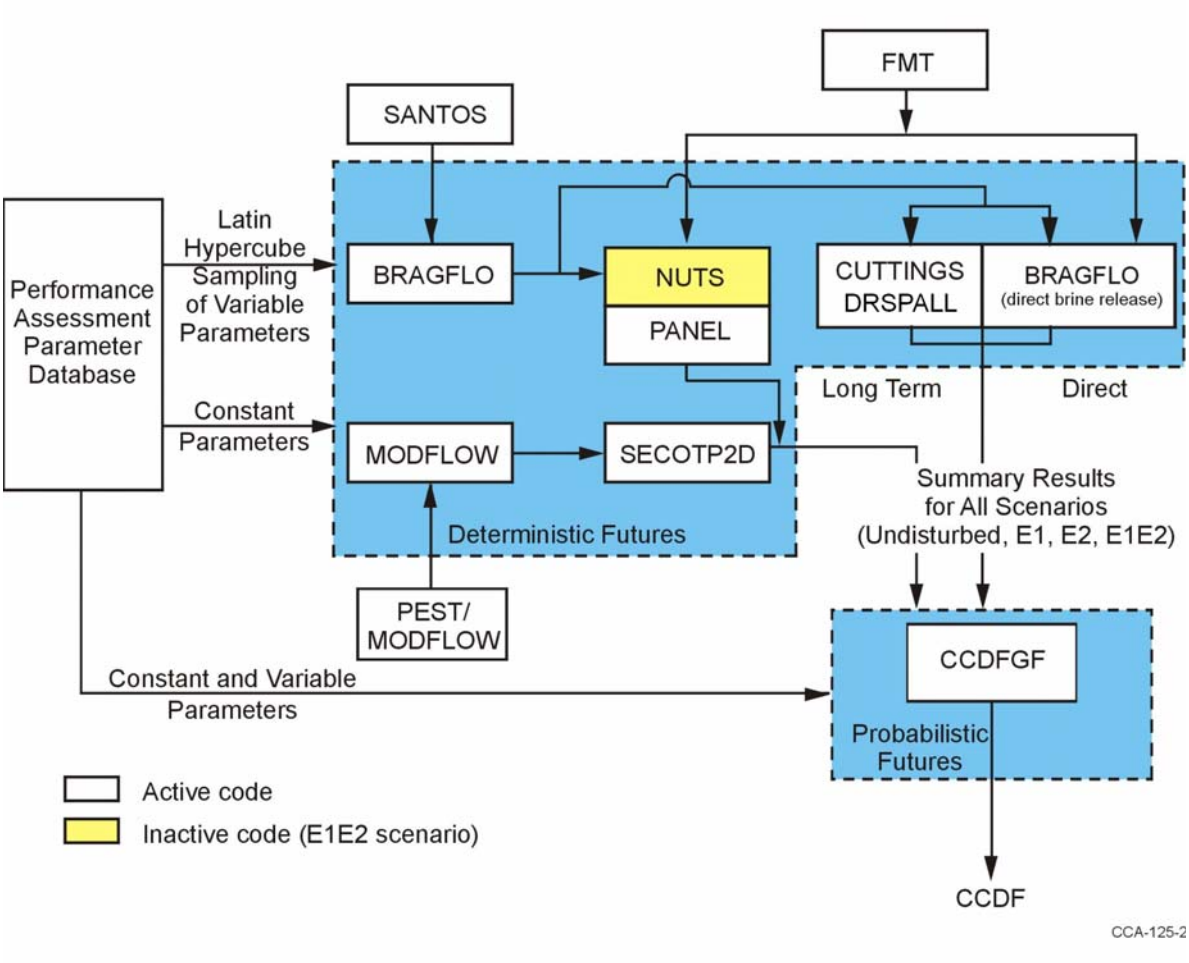

Figure 6-33. Code Configuration for DP Scenario E1E2

source term to the SECOTP2D code for Culebra transport. For computational efficiency, an intermediate scaling step is conducted prior to calculating the releases associated with probabilistic futures. In this intermediate step, NUTS reference conditions for Culebra release by an intrusion at 100 years are estimated by scaling borehole flow from the 350-year intrusion. NUTS reference conditions for intrusions at 3,000, 5,000, 7,000, and 9,000 years are estimated by scaling from the 1,000-year calculation. Thus, to scale consequences of E2 intrusions in probabilistic futures, reference conditions from NUTS calculations are available for 100, 350, 1,000, 3,000, 5,000, 7,000, and 9,000 years.

Consistent with the BRAGFLO intrusion times, reference behavior for actinide transport in the Culebra is calculated by SECOTP2D for the E2 intrusion occurring at 350 and 1,000 years. Because the equations governing actinide transport and retardation in SECOTP2D are linear, scaling releases to probabilistic E2 penetrations occurring at other times is easily accomplished. For futures with two or more E2-type intrusions (and no E1-type intrusions), a simplifying assumption is made. The additional increment to the Culebra's source term for the second and subsequent intrusions is assumed to be zero. This is considered reasonable because in the E2 scenario, the flux of brine to the Culebra is limited by the rate of flow from the Salado to the

waste panels, rather than by borehole properties. For second and subsequent E2 scenarios, only the direct releases to the surface are considered in CCDF construction.

6.4.13.5 Estimating Long-Term Releases from the E1E2 Scenario

The E1E2 scenario is defined as multiple boreholes intersecting a single waste panel, at least one of which is an E1 penetration of a brine reservoir (Section 6.3.2.2.3). The DOE uses both scaling and simplification to develop the consequences of this scenario. Similar to the E1 and E2 scenarios, BRAGFLO and related computer codes are executed with a deterministic sequence of future events to develop reference behavior for the E1E2 consequences (see Figure 6-33). Scaling estimates the consequences for events occurring at different times than those in the BRAGFLO calculations. Simplifying assumptions are used to develop the consequences of E1E2 occurrences in different waste panels, or the consequences of a different sequence of future events leading to the E1E2 scenario, than assumed in the deterministic BRAGFLO calculation.

Reference behavior for brine flow to the Culebra in the E1E2 scenario is predicted by the BRAGFLO disposal system model. This is the same model used to predict brine flow to the Culebra for the E1 and E2 scenarios. The geometry of the grid used is the same as that depicted in Figures 6-14 through 6-16; however, different assumptions are used about the borehole development through time. Even though the E1E2 scenario includes at least two boreholes intersecting the panel, the model used included only one borehole column. As described below, the assumptions used about the way brine mixes in the intruded panel are such that two boreholes are not needed to represent flow through the waste. The assumptions about the development of the borehole are related to the most likely (that is, most probable) sequence of events that gives rise to the E1E2 scenario.

It is most probable that the first borehole into any panel is an E2 borehole (see Section 6.4.12.6). In a BRAGFLO calculation after 1,000 years of undisturbed performance, the properties of the column of elements in BRAGFLO representing the borehole are changed. The changed properties represent the E2 borehole after the Rustler plug has degraded and silty sand fills the borehole. The period during which the plug is effective is not modeled to develop reference behavior for the E1E2 Culebra releases because relatively little happens in the disposal system when the Rustler plug is effective. Reference conditions are developed with the E1 intrusion that follows the initial E2 intrusion occurring after the 200 years it takes Rustler plugs to degrade because it is more probable that a subsequent E1 intrusion occurs after the Rustler plug has degraded. It is assumed that the E1 intrusion occurs 1,000 years after the E2 borehole becomes filled with silty sand, at a simulation time of 2,000 years. At 2,000 years, the properties of the borehole section below the repository horizon are changed to represent an open borehole (the E1 intrusion), allowing flow between the Castile brine reservoir and the repository. After another 200 years, the lower section is assumed to fill with silty sand; after another 1,000 years, the permeability of the lower section is decreased one order of magnitude because of salt creep. These changes are documented in Table 6-31.

Table 6-31. Changes in BRAGFLO Borehole Properties in Developing Reference Behavior for the E1E2 Scenario

Time (years)	Borehole Portion	Properties
0 – 1,000	All	Undisturbed conditions
1,000 – 2,000	Above waste panel Below waste panel	Silty sand Undisturbed conditions
2,000 – 2,200	Above waste panel Below waste panel	Silty sand Open borehole between panel and Castile
2,200 – 3,200	Above waste panel Below waste panel	Silty sand Silty sand
3,200 – 10,000	Above waste panel Below waste panel	Silty sand Silty sand, permeability decreased 1 order of magnitude

Thus, above the waste panel, the E1E2 borehole evolves as an E2 borehole from 1,000 years to 10,000 years. Below the waste panel, the borehole evolves as an E1 borehole from 2,000 to 10,000 years. At 2,200 years, there will be two boreholes above the waste panels with silty-sand properties. The assumption about upper borehole permeability most consistent with that for this scenario of complete mixing in the panel (discussed below) is that the upper portion of the E1 borehole is relatively impermeable and all flow is diverted to the E2 borehole. Therefore, the permeability of the upper borehole remains that of the E2 borehole at 2,200 years.

The concentration of actinides in liquid moving up the borehole assumes homogeneous mixing within the panel and is calculated with the code PANEL. PANEL is a mixing-cell model that sums BRAGFLO fluxes into the waste panel from the boreholes and Salado as inputs to the cell and subtracts the flow up the borehole as a depletion from the model. Brine moving up the borehole is assumed to be at its greatest possible actinide concentration according to the dissolved and colloidal actinide source term models (Sections 6.4.3.5 and 6.4.3.6). In PANEL calculations, all actinides that enter the borehole are conservatively assumed to reach the Culebra.

Random sampling of future events can produce different timing of borehole penetrations. From the time the E2 borehole penetrates until the E1 borehole penetrates, the consequences are determined as they are in the E2 scenario. When the E1 is drilled, completing the E1E2 configuration, the consequences are assumed to be similar to those modeled after the E1 penetration for the reference calculation, accounting for radionuclide decay and ingrowth.

Randomly sampling future events can also produce a different sequence of borehole types. In a randomly sampled future with many E2 intrusions into a waste panel prior to the E1, the consequences are determined as they are for the E2 scenario until the E1 occurs, at which time the E1E2 consequences are used. In a randomly sampled future with the sequence E1 then E2, the consequences are assumed to be similar to an E1 event until the E2 is drilled, whereupon the consequences are assumed to be similar to the E1E2 event following the E1 drilling. In a randomly sampled future with two E1 boreholes, the consequences are assumed to be similar to an E1 borehole until the second E1 is drilled, at which time the consequences are assumed to be similar to the E1E2 behavior.

For computational simplicity, the E1E2 calculations are scaled to E1 intrusions following a prior E2 intrusion occurring at 100, 350, 3,000, 5,000, 7,000, and 9,000 years, similar to the treatment of the E1 and E2 reference conditions.

6.4.13.6 Multiple Scenario Occurrences

For long-term brine flow into the Culebra, scenario occurrences are effectively defined at the panel scale for this PA. It was recognized in preliminary analysis of BRAGFLO results for this analysis that liquid flow between the separate panel and the rest of the repository sections is slow enough that the panel is effectively independent from the rest of the repository. Gas flow does occur, and for this reason, calculations of direct release to the surface are performed at the repository scale. For long-term brine flow to the Culebra, it is considered more reasonable, based on BRAGFLO results, to assume independent panel behavior in developing the CCDF than an interconnected repository.

It is very important to distinguish between model results and model assumptions on this point. For disposal system performance, the DOE is not assuming that panel closures isolate panels from one another. Rather, the DOE has assigned reasonable properties to the panel closures as input to the BRAGFLO calculations and has found that they result in limited liquid flow through the panel closures. Because simplification and scaling must be used to develop CCDFs, the DOE has to assume either that the repository is well interconnected or that the panels behave fairly independently. Based on model results for this analysis, the DOE has established that it is more reasonable in constructing a CCDF to assume that brine does not flow between panels. This simplification of detailed modeling results conducted in BRAGFLO is necessary for CCDF construction. It is not an assumption used in developing conceptual models of disposal system performance. This assumption does affect how scenario consequences are developed.

There are ten panels in the repository and the possibility of many intrusions. If panels behave independently, as they are assumed to in developing consequences of long-term brine flow in the CCDF, it is possible for different configurations of boreholes (scenarios) to occur in different panels. For example, an E1E2 type situation might occur in one panel, an E2 situation in a different panel, and an E1 situation in a third panel. In this example, there are essentially three scenario types occurring. For long-term release, the repository behaves as ten small modules (each comprising one panel), and a different borehole scenario can develop in each of those ten modules. Long-term releases in CCDF construction are based on the premise that releases from each of these modules are independent and that the cumulative release from the repository is equal to the sum of the cumulative releases from the different modules.

6.4.13.7 Estimating Releases During Drilling for All Scenarios

The reference behavior for cuttings and cavings from the first intrusion into a pressurized repository, regardless of whether it is an E1 or E2 intrusion, is established by calculations performed in the CUTTINGS_S code. Cavings releases are also dependent on the effective shear resistance to erosion and the angular velocity of the drill string (Appendix PA, Section PA-4.5). The effects of radioactive decay are captured by calculating reference behavior for cuttings and cavings by the CUTTINGS_S code at 100, 125, 175, 350, 1,000, 3,000, 5,000, 7,500, and 10,000 years.

Spall and direct brine releases during drilling are also dependent on pressure conditions in the repository, and reference releases are calculated by CUTTINGS_S for spall and BRAGFLO (direct brine release) at 100, 350, 1,000, 3000, 5,000, and 10,000 years for intrusions into lower, middle, and upper panels (Appendix PA, Section PA-4.7).

Radionuclide releases from the processes in the CUTTINGS_S code and direct brine release for intrusions occurring at intermediate times are scaled from the closest calculated releases, correcting for radioactive decay (see Section 6.4.12.3 and Figure 6-27). The cuttings and cavings portion of the CUTTINGS_S releases are further adjusted to account for the distribution of CH- and RH-TRU waste streams (see Sections 6.4.12.3 and 6.4.12.4). The processes of spallings and direct brine release are assumed to involve a large enough volume of waste that it is reasonable to use homogeneous waste with average activity to estimate releases.

For multiple-intrusion scenarios, the pressure in the repository at the time of the second and subsequent intrusions may be quite different from that at the time of the first intrusion. This is expected because of the assumptions of relatively permeable boreholes adopted in PA. Therefore, estimates of drilling releases to the accessible environment need to be formed for penetrations of a previously intruded repository. The reference behavior for these subsequent intrusion releases is calculated by the CUTTINGS_S code from BRAGFLO histories with E1- and E2-type intrusions at 350 and 1,000 years. Repository conditions calculated for the effects of a subsequent E1-type penetration are used in consequence analysis for both E1- and E2-type intrusions that follow an E1 intrusion. Conditions from the subsequent E2 calculations are used for intrusions that follow E2 intrusions only. E1 conditions are used for multiple combinations of boreholes that include at least one E1 intrusion, assuming that repository conditions will be dominated by Castile brine if any borehole connects to a brine reservoir. For futures in which more than two E2-type intrusions occur (and no E1-type intrusions occur), third and subsequent spall and direct brine releases are assumed to be the same as for the second release.

For both E1 and E2 conditions following a 350-year intrusion, spall and direct brine release calculations are performed at 550, 750, 2,000, 4,000, and 10,000 years. For the 1,000-year E1 and E2 intrusions, spall and direct brine release calculations are performed at 1,200, 1,400, 3,000, 5,000, and 10,000 years. Because the subsequent intrusion may penetrate either a previously-intruded panel or an unintruded panel, these calculations are done twice, once with initial conditions drawn from the previously-intruded panel in BRAGFLO, and once with conditions drawn from the BRAGFLO subsequent intrusion of the waste-disposal region. As with the first intrusion into a previously undisturbed repository, radionuclide releases from spall and direct brine release for intrusions occurring at intermediate times are scaled from the closest calculated releases, correcting for radioactive decay.

After flow through the repository has occurred for some time, in an E1E2 scenario, portions of the repository may be depleted of actinides. In the estimate of releases during drilling, however, the possibility is not considered that random drilling might penetrate portions of the repository already depleted of actinides from processes initiated by previous drilling. This is conservative because it tends to overestimate releases during drilling.

6.4.13.8 Estimating Releases in the Culebra and the Impact of the Mining Scenario

Ten thousand-year SECOTP2D calculations are performed with Culebra transmissivity fields reflecting undisturbed performance (no future mining within the Land Withdrawal Area) and disturbed performance (see Section 6.4.6.2.3). These calculations are performed with a unit source term of one kilogram of the actinide species of interest at 100 years. Because transport as modeled is a linear process, scaling is used to estimate the consequences of time-variable concentrations and different times of intrusion (see Appendix PA, Section PA-6.8.7). As well, mining may occur at random times in the future. The effect of mining on releases in the Culebra is determined in the following manner.

Boreholes intersecting the repository may provide a source of actinides to the Culebra with concentrations that vary through time. Until mining occurs, the transport behavior of actinides from these borehole sources is estimated by scaling the results of the undisturbed performance Culebra transport calculations. All actinides introduced into the Culebra by the time of mining are transported exclusively in the undisturbed performance flow fields. In other words, actinides in transit in the Culebra when mining occurs are not assumed to be affected and continue to be transported in the undisturbed flow field. Once mining occurs (assumed to be instantaneous), the transport behavior of all actinides subsequently introduced into the Culebra is estimated by scaling the results of the disturbed performance flow fields.

6.4.13.9 Final Construction of a Single CCDF

After consequences for all of the sampled probabilistic futures are estimated by the methodologies presented in the preceding sections, the information necessary to plot the CCDF associated with the probabilistic futures and the particular LHS vector is available.

The sequences of future events used in this PA were generated by random sampling. Thus, each sampled future is assigned an equal weight of occurrence to construct a CCDF. Each sequence of future events is assigned a weight of 1/10,000 of occurrence because 10,000 futures are used for each CCDF. Before plotting, an additional step is performed in which the weights of futures with similar consequences are summed. The first step in the plotting process is to order the grouped futures according to normalized release, as discussed in Section 6.1.1, from lowest normalized release to highest. Following this, the CCDF can be plotted by summing, for a given value of EPA normalized release, the probabilities of all futures whose normalized release exceeds the given value, and where the probabilities are assumed to be equal to the weights. Because the releases cS have been ordered so that $cS_i \le cS_{i+1}$ for i=1 …, nS-1, the probability that cS exceeds a specific consequence value x is determined by the summation routine (duplicated from Section 6.1.1)

$$F(x) = \sum_{j=i}^{nS} pS_j, \tag{6.19}$$

where i is the smallest integer, that $cS_i > x$. This completes an analysis of stochastic uncertainty for a particular vector of variable values from the LHS sampling.

6.4.14 CCDF Family

The process of CCDF construction described in Section 6.4.13 is repeated once for each vector of subjectively uncertain variable values created by LHS. This process yields a family of CCDFs like those presented in Section 6.5. This family of CCDFs provides a complete display of both stochastic and subjective uncertainty as discussed in Section 6.1.2.

6.5 Performance Assessment Results

This section contains results of the recertification PA and demonstrates that the WIPP continues to comply with the quantitative containment requirements in 40 CFR § 191.13(a). See Section 6.1 for a discussion of the containment requirements. Criteria for presenting the results of PAs are provided by the EPA in 40 CFR § 194.34, and are discussed in Section 6.1.3. These criteria are also summarized here for clarity.

This CRA-2004 PA is different than the original certification PA in the CCA because it includes additional information, changes and new data required by 40 CFR§194.15 recertification application requirements. Section 6.0 details the changes and new information included in this PA. The results of this recertification PA conclude that the repository continues to comply with the disposal standards.

Additional detail about the results of the CRA-2004 PA is contained in Appendix PA, Section PA-9.0, which describes sensitivity analyses conducted as the final step in the Monte Carlo analysis. These sensitivity analyses indicate the relative importance of each of the sampled parameters in terms of their contribution to uncertainty in the estimate of disposal system performance. Analyses also examine the sensitivity of intermediate performance measures to the sampled parameters. Examples of such intermediate performance measures include the quantity of radionuclides released to the accessible environment by any one mechanism (for example, cuttings or direct brine releases), and other model results that describe conditions of interest such as disposal region pressure.

6.5.1 Demonstrating Convergence of the Mean CCDF

As discussed in Sections 6.4.13 and 6.4.14, individual CCDFs for the WIPP are constructed by estimating cumulative radionuclide releases to the accessible environment for 10,000 different possible futures. Each CCDF is calculated for a single LHS vector of input parameters and is conditional on the occurrence of that particular combination of parameter values. Multiple realizations of the PA calculations yield a family of CCDFs in which each individual CCDF is generated from a different LHS vector. Families of CCDFs calculated for the WIPP PA are based on 100 LHS vectors drawn from distributions of values for 64 imprecisely known parameters. As discussed in Section 6.1.2, mean and percentile CCDFs are constructed from families and provide summary measures of disposal system performance.

Criteria provided by the EPA in 40 CFR Part 194.34 address the statistical interpretation of CCDFs:

> The number of CCDFs generated shall be large enough such that, at cumulative releases of 1 and 10, the maximum CCDF generated exceeds the 99th percentile of the population of CCDFs with at

> least a 0.95 probability. Values of cumulative release shall be calculated according to Note 6 of Table 1, Appendix A of Part 191 of this chapter. (40 CFR § 194.34(d))
>
> Any compliance application shall provide information which demonstrates that there is at least a 95 percent level of statistical confidence that the mean of the population of CCDFs meets the containment requirements of § 191.13 of this chapter. (40 CFR § 194.34(f))

Information provided by the EPA in the Background Information Document for 40 CFR Part 194 clarifies the intent of these criteria.

In 40 CFR Part 194, EPA decided that the statistical portion of the determination of compliance with 40 CFR Part 191 will be based on the sample mean. The LHS sample sizes should be demonstrated operationally (approximately 300 when 50 variables are considered) to improve (reduce the size of) the confidence interval for the estimated mean. The underlying principle is to show convergence of the mean. (EPA 1996b, 8-41)

The DOE has chosen to demonstrate convergence of the mean and to address the associated criteria of 40 CFR Part 194 using an operational approach of multiple replication as proposed by Iman (1982). The complete set of PA calculations was repeated three times with all aspects of the analysis identical except for the random seed used to initiate the LHS procedure. Thus, PA results are available for three replicates, each based on an independent set of 100 LHS vectors drawn from identical CCDFs for imprecisely known parameters and propagated through an identical modeling system. This technique of multiple replication allows evaluation of the adequacy of the sample size chosen in the Monte Carlo analysis and provides a suitable measure of confidence in the estimate of the mean CCDF used to demonstrate compliance with 40 CFR § 191.13(a).

6.5.2 Complementary Cumulative Distribution Functions for the WIPP

Families of CCDFs for each of the three replicates are shown in Figures 6-36, 6-37, and 6-38. Each figure contains 100 CCDFs. These figures address the criterion stated in 40 CFR § 194.34(e):

> Any compliance application shall display the full range of CCDFs generated.

Figures 6-34 through 6-36 show that all 300 CCDFs lie below and to the left of the limits specified in 40 CFR § 191.13(a). They also show qualitatively that the three replicates yield very similar results. Quantitative verification of the similarity of the three replicates is demonstrated in Figure 6-37, which shows the mean CCDFs calculated for each of the three replicates, together with an overall mean CCDF that is the arithmetic mean of the three individual mean CCDFs. Figure 6-37 demonstrates two key points. First, the

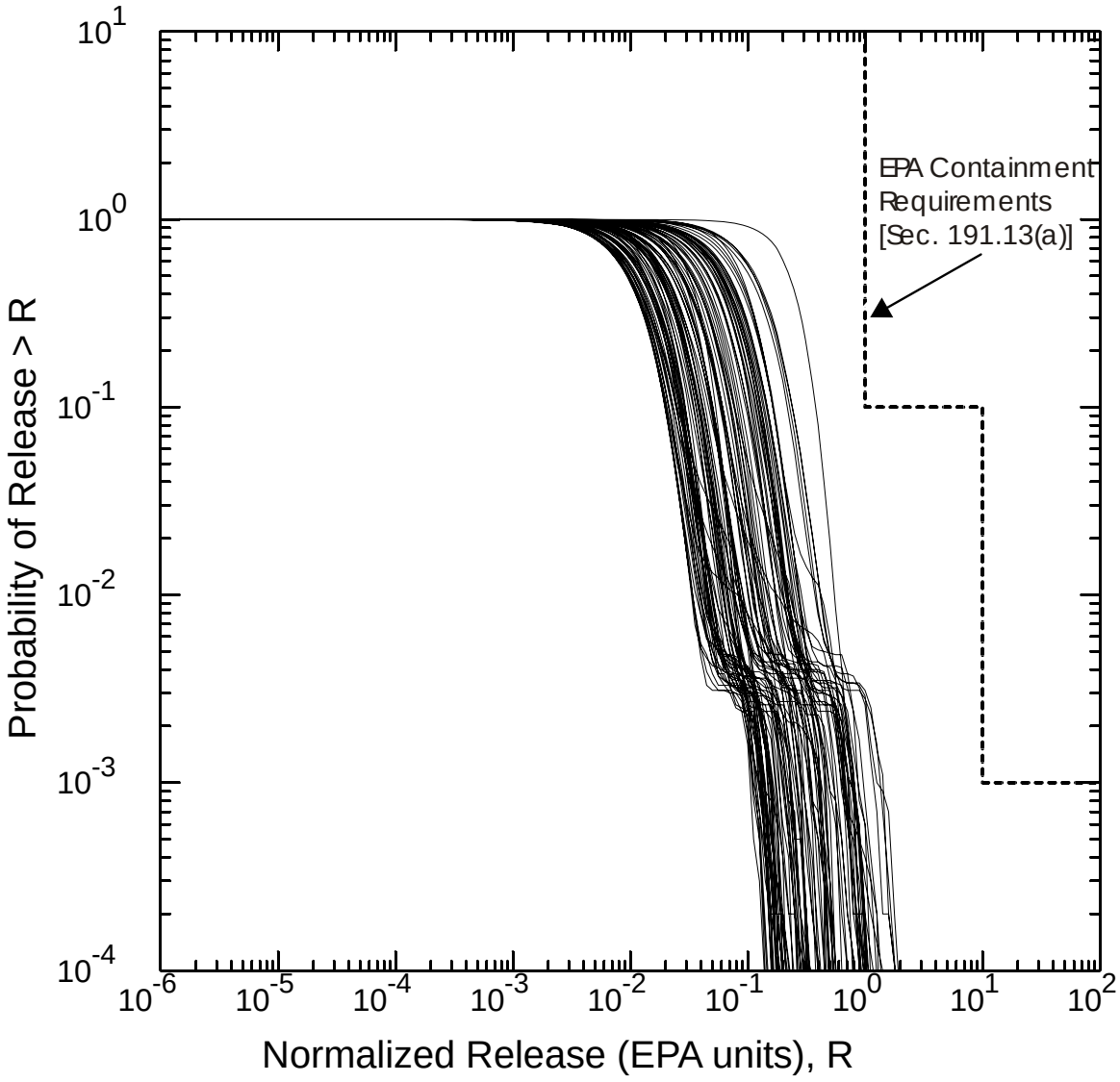

Figure 6-34. Distribution of CCDFs for Normalized Radionuclide Releases to the Accessible Environment from the WIPP, Replicate 1.

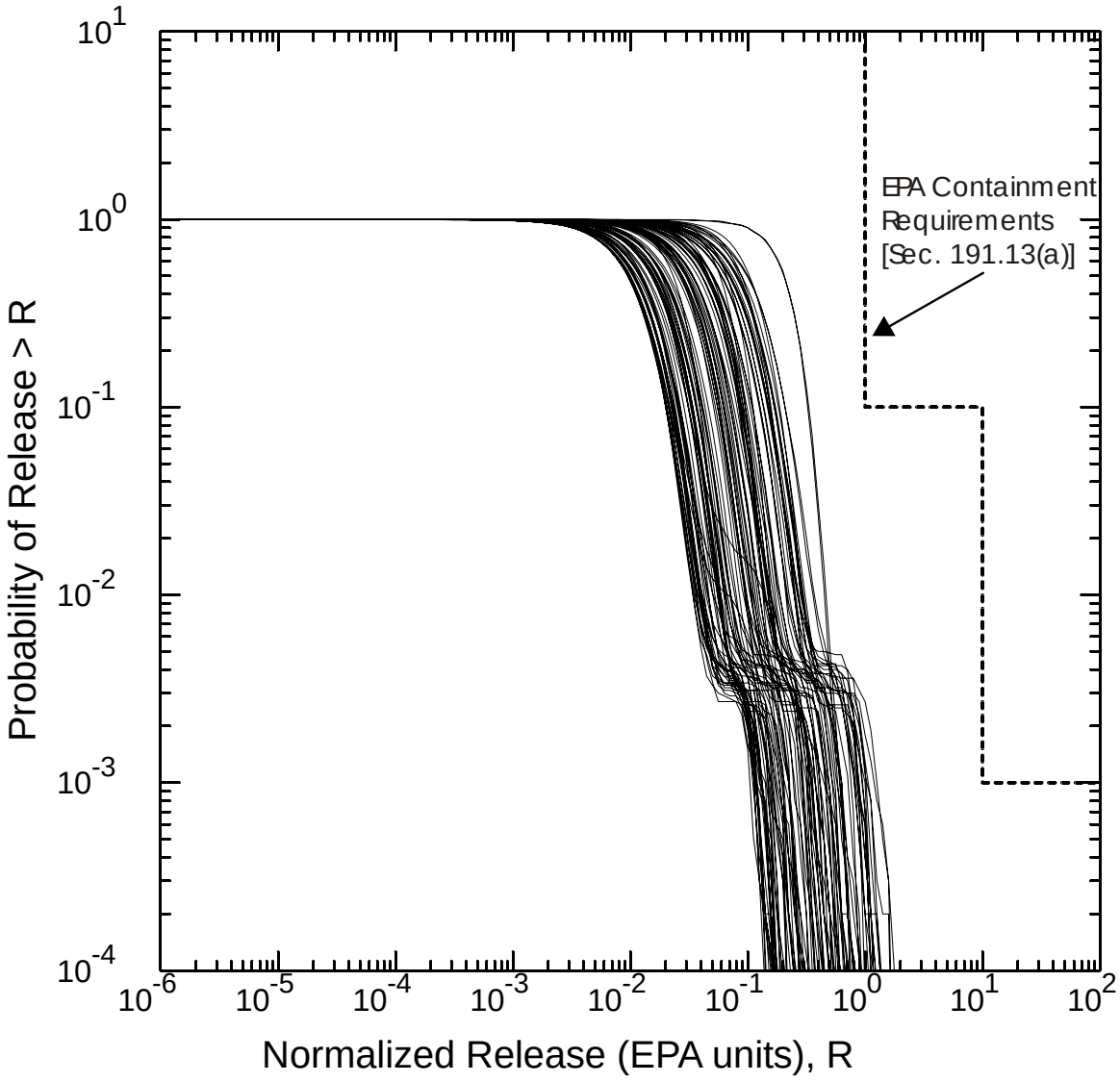

Figure 6-35. Distribution of CCDFs for Normalized Radionuclide Releases to the Accessible Environment from the WIPP, Replicate 2.

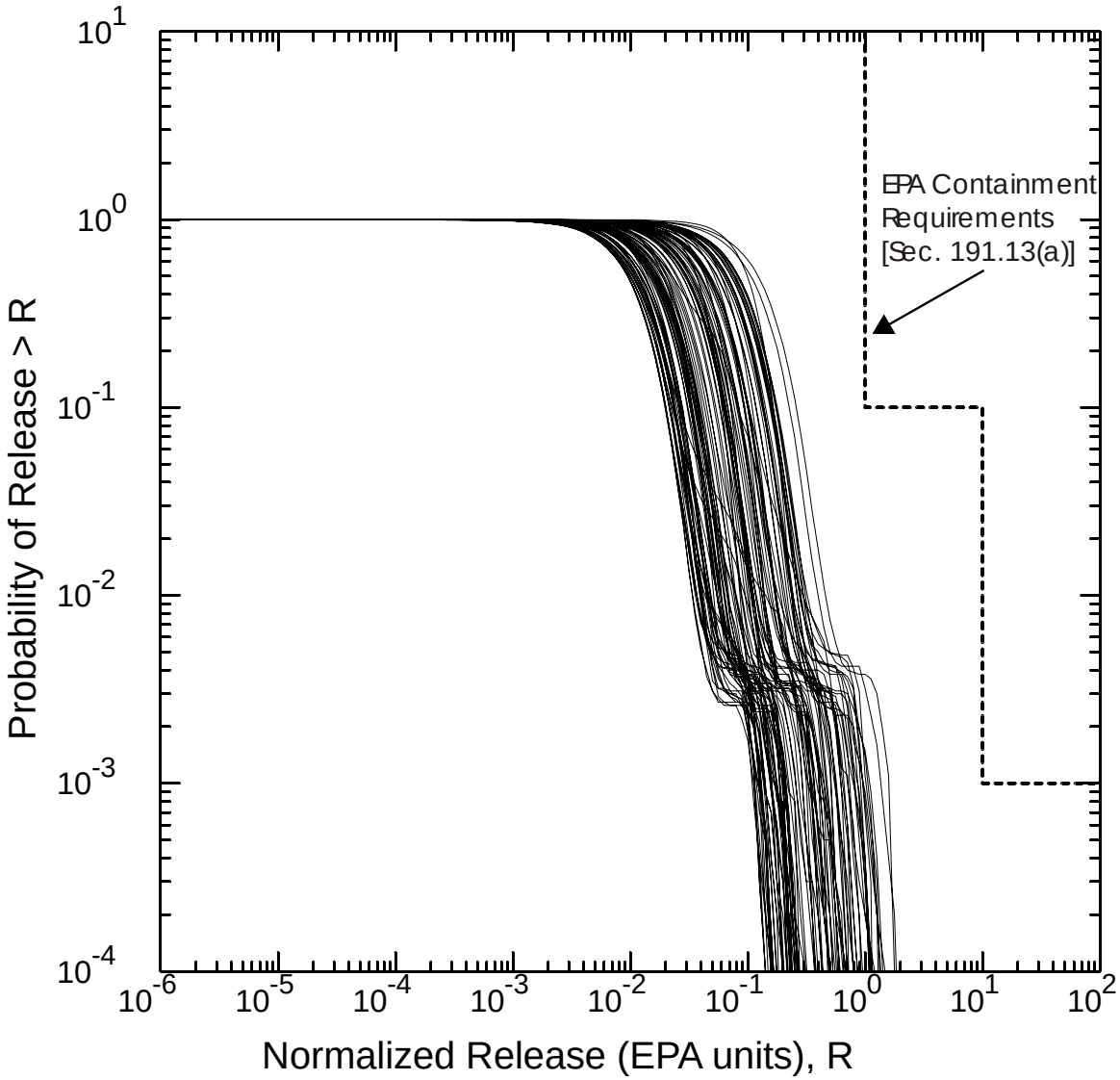

Figure 6-36. Distribution of CCDFs for Normalized Radionuclide Releases to the Accessible Environment from the WIPP, Replicate 3

overall mean CCDF lies entirely below the limits specified in 40 CFR § 191.13(a). Thus, the WIPP is in compliance with the containment requirements of 40 CFR Part 191. Second, the sample size of 100 in each replicate is sufficient to generate a stable distribution of outcomes. Within the region of regulatory interest (that is, at probabilities greater than $10^{-3}/10^{4}$ yr), the mean CCDFs from each replicate are essentially indistinguishable from the overall mean at the resolution of the figure. Figure 6-38 provides quantitative confirmation of the sufficiency of the sample size, by displaying the overall mean together with the 0.95 confidence interval of the Student's t-distribution estimated from the individual means of the three independent replicates (Iman 1982), as shown in Figure 6-37.

Figure 6-1 provides additional summary information about the distributions of CCDFs resulting from the three replicates. This figure shows CCDFs representing the mean,

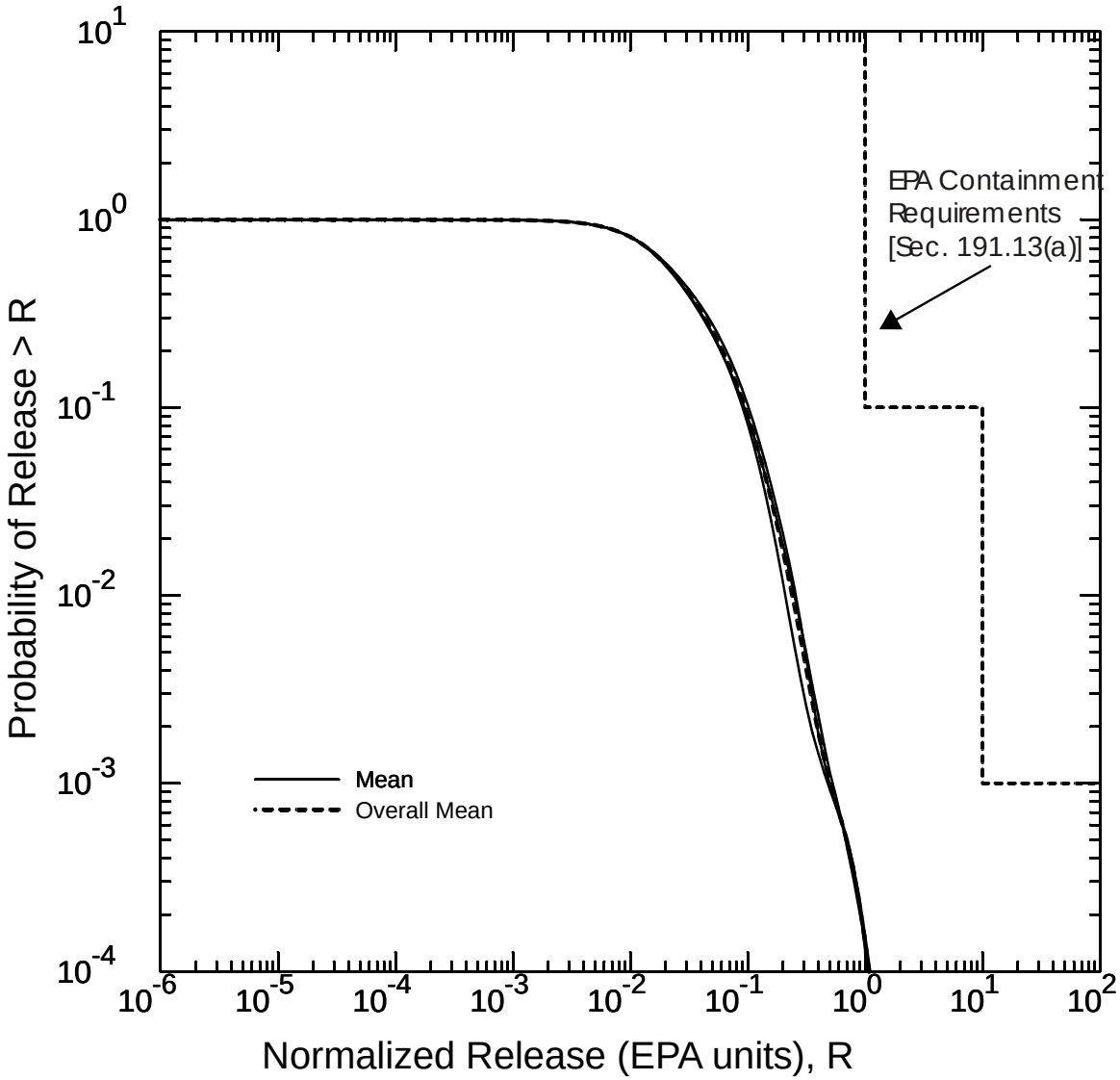

Note: Four CCDFs are shown, including three individual mean CCDFs calculated for each of the three distributions of CCDFs calculated for the three replicates and shown in Figures 6-34, 6-35, 6-36, and an overall mean CCDF that is the arithmetic mean of the three individual mean CCDFs."

Figure 6-37. Mean CCDFs for Normalized Radionuclide Releases to the Accessible Environment

median, and 10th and 90th percentile CCDFs from each replicate, together with the overall mean. Note that for each type of CCDF (for example, the 10th percentile), curves from each replicate overlie closely. This provides quantitative verification of the qualitative observation that distributions from each replicate appear similar.

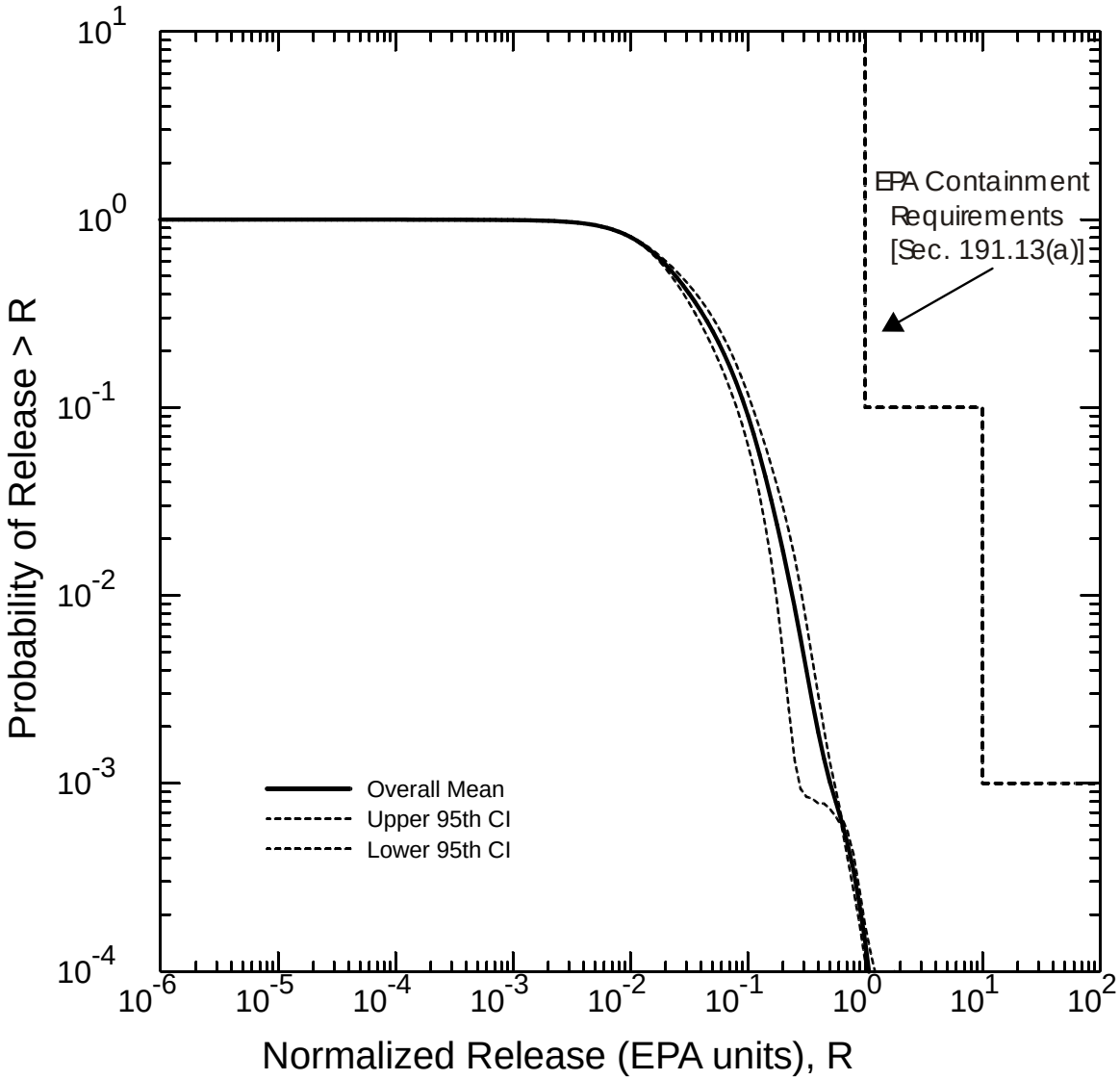

Note: The overall mean CCDF shown in Figure 6-37 is repeated together with the 0.95 confidence interval of the Student-t distribution estimated from the three individual mean CCFDs.

Figure 6-38. Confidence Levels for the Mean CCDF

6.5.3 Release Modes Contributing to the Total Radionuclide Release

Radionuclide releases to the accessible environment can be grouped into four categories according to their mode of release:

(1) cuttings and cavings releases,

(2) spallings releases,

(3) releases resulting from the direct release of brine at the surface during drilling, and

(4) releases in the subsurface following transport in groundwater.

Each of these four modes has the potential to contribute to the total quantity of radionuclides released from the repository, and therefore each has the potential to affect the position of the mean CCDF.

Figure 6-39 provides a display of the relative contribution of each mode to the total release. Releases for each of the three replicates are similar, and results are shown for replicate 1 only for simplicity. Mean CCDFs are shown for the total normalized release (this curve is also shown in Figure 6-1 and is the mean of the family shown in Figure 6-34) and for the normalized releases resulting from cuttings and cavings, spallings, and direct brine release. The mean CCDF for subsurface releases resulting from groundwater transport is not shown because those releases were less than 10^{-6} EPA units and the CCDF cannot be shown at the scale of this figure. Releases from cuttings and cavings are shown to be the most important contributors to the location of mean CCDF, with spallings also making a small contribution. Direct brine releases

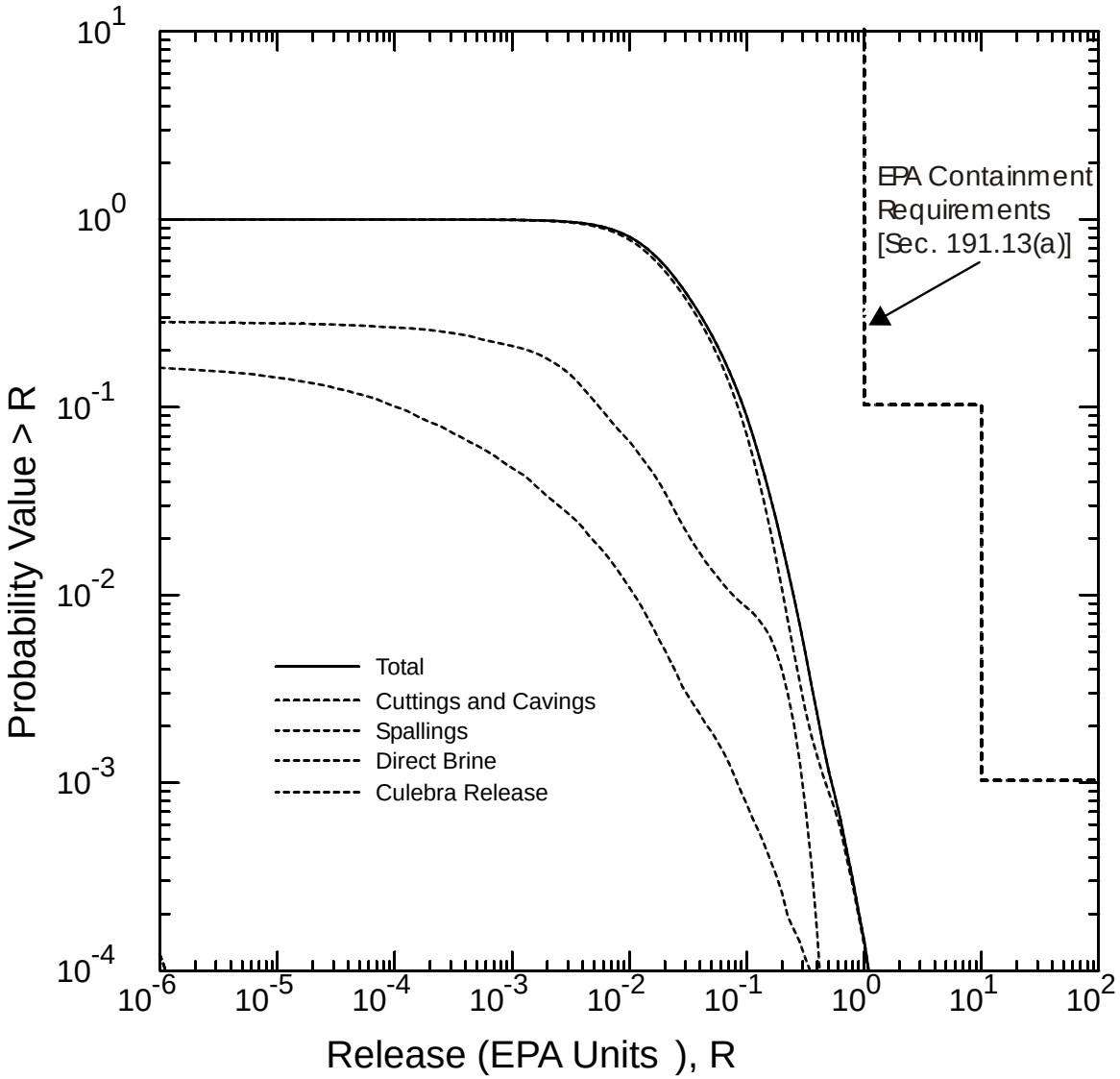

Note: Mean CCDFs are shown for the total normalized release (this curve is also shown in Figure 6-1 and is the mean of the family shown in Figure 6-34) and for the normalized releases resulting from cuttings and cavings, spallings, and direct brine release. The mean CCDF for subsurface releases resulting from groundwater transport is not shown because those releases were less that 10-6 EPA units and the CCDF cannot be shown at the scale of this figure.

Figure 6-39. Mean CCDFs for Specific Release Modes, Replicate 1

are less important, and have very little effect on the location of the mean CCDF. Subsurface groundwater releases are not important, and have essentially no effect on the mean CCDF. See Appendix PA, Section PA-9.0 for additional discussion of the relative importance of the release modes.

6.5.4 Uncertainty and the Role of Conservatism in the Compliance Demonstration

As defined in 40 CFR § 191.12, PAs must "estimate the cumulative releases of radionuclides, considering the associated uncertainties, caused by all significant events and processes."

Site characterization, repository design, and waste characterization activities, as described in Chapters 2.0, 3.0, and 4.0, respectively, have removed much uncertainty from the analysis. Uncertainties remain, however, about how best to characterize some aspects of the disposal system and how best to model the complex interactions between the waste and its surrounding environment. These remaining uncertainties have been incorporated in the performance assessment to the extent practicable through the use of reasonable and realistic assumptions about models and parameter values.

In general, the DOE has not attempted to bias the PA toward a conservative outcome, and the mean CCDF represents a reasonable estimate of the expected and, in the case of future human activities including intrusion, prescribed, performance of the disposal system. However, where realistic approaches to incorporating uncertainty are unavailable or impractical and where the impact of the uncertainty on performance is small, the DOE has chosen to simplify the analysis by implementing reasonable and conservative assumptions. These conservative assumptions are reviewed here, not because they bias the location of the mean CCDF, but rather because an understanding of their effects contributes qualitatively to the "reasonable expectation, on the basis of the record before the implementing agency, that compliance with [§] 191.13(a) will be achieved," as required by Section 191.13(b).

As noted in Section 6.2 and Appendix PA, Attachment SCR, in some cases processes have been omitted from the modeling system for simplicity because the only possible effects of including them would be beneficial to system performance. Examples include the decision to model radionuclide dissolution as an equilibrium process (assuming instantaneous leaching and dissolution), and the decision not to model sorption of radionuclides in the Salado or in the seal system.

In other cases, the DOE has made conservative decisions during the design of the conceptual and computational models, as listed in Table 6-32. Some conservative assumptions listed in this table are mentioned below. For example, within the repository portion of the BRAGFLO model, fluid flow in a single panel is treated as if all rooms were a single void (that is, pillars are omitted). This treatment allows brine flow to and from an intrusion borehole to contact more waste than it would if it followed a more realistic flow path between rooms. The effect is conservative with respect to brine flow up a plugged and abandoned borehole. Similarly, the DOE has chosen to model fluid flow through plugged and abandoned boreholes as if all intrusions occurred into a down-dip (that is, southern) panel. As modeled, downdip panels tend to have more brine in them than up-dip panels (see Appendix PA, Section PA-8.0) and this assumption therefore may result in overestimating the amount of brine present in intruded panels.

Radionuclide dissolution to solubility limits is modeled as instantaneous. For E1E2 scenarios, complete mixing is assumed within the intruded panel, and all brine that flows out of the panel and up the borehole is assumed to have been in contact with waste.

Within the shaft seal system, concrete components are modeled as if they degrade after emplacement, underestimating their potential to limit fluid flow over the long-term. For direct releases and E1E2 releases to the Culebra, processes of actinide transport and retardation are not modeled within the intrusion borehole and all actinides that enter the borehole are assumed to be transported to the surface or into an overlying transmissive unit. Within the Culebra (which

modeling indicates will be the only transmissive unit that will receive long-term flow from the borehole), hydraulically significant fractures are assumed for modeling simplicity to be present everywhere, even though test data indicate that the portions of the Culebra above the waste disposal region behave as an unfractured, single porosity matrix.

These conservative assumptions have not significantly affected the location of the mean CCDF, which, as shown in Section 6.5.3, is dominated by cuttings and cavings releases that are, with one exception, independent of the conservative simplifications described here. As discussed in Appendix PA, the parameter making the largest contribution to uncertainty in the location of the mean CCDF is the effective shear resistance of the waste, which affects the quantity of waste eroded from the borehole wall and transported to the surface as cavings. In the absence of data describing the reasonable and realistic future properties of degraded waste and MgO, effective shear resistance of the waste is a parameter for which the DOE has selected a conservative distribution (see Appendix PAR, Parameter 33).

6.5.5 Summary of the Demonstration of Compliance with the Containment Requirements

The WIPP continues to comply with the containment requirements of 40 CFR § 191.13(a), as shown by Figures 6-34 through 6-38. Figures 6-37 and 6-38 demonstrate that the sample size of 100 chosen for this analysis is sufficient to provide the level of statistical confidence specified in 40 CFR § 194.34.

Additional confidence in the compliance determination comes from examination of Figure 6-39, which shows that the location of the mean CCDF depends almost entirely on the relatively simple processes that contribute to cuttings and cavings releases resulting from inadvertent human intrusion by drilling. Uncertainties related to the characterization of the natural system and the interaction of waste with the disposal system environment have little effect on long-term performance. The natural and engineered barrier systems, as described in Chapters 2.0 and 3.0, will provide robust and effective containment of TRU waste even if the repository is penetrated by multiple borehole intrusions.

Table 6-32. Conservative Model and Parameter Assumptions Used in PA (from Appendix PA, Attachment MASS, Table MASS-1)

Conservative Assumption	Code	Cross-Reference
Long-term flow up plugged and abandoned boreholes is modeled as if all intrusions occur into a down-dip (southern) panel.	BRAGFLO	Section 6.4.3
Pillars, individual drifts and rooms are not modeled for long-term performance, and containers provide no barrier to fluid flow.	BRAGFLO	Section 6.4.3, Appendix PA, Attachment MASS, Section 5.0
Brine in the repository will contain a uniform mixture of dissolved and solid-state species. All actinides have instant access to all repository brine.	NUTS PANEL	Section 6.4.3.4 Appendix PA, Attachment SOTERM, Section 2.2
Radionuclide dissolution to solubility limits is instantaneous.	NUTS PANEL	Sections 6.4.3.5 and 6.4.3.4 (Appendix PA, Attachment SOTERM, Section 3.3,)
Radionuclides are not retarded by shaft seals.	NUTS	Section 6.4.4
Shaft concrete components of the lower shaft are modeled as if they degrade after emplacement.	BRAGFLO	Section 6.4.4 Appendix PA, Attachment PAR
The permeability of the DRZ is sampled with the low value similar to intact halite and the higher value representing a fractured material.	BRAGFLO	Section 6.4.5.3 Appendix PA, Attachment MASS, Section 13.4
The Los Medaños member of the Rustler, Tamarisk, and Forty-niner are assumed to be impermeable.	BRAGFLO SECOFL2D	Sections 6.4.6.1, 6.4.6.3, and 6.4.6.5 Appendix PA, Attachment MASS, Section 14.0
Sorption of actinides in the borehole is not modeled.	NUTS	Section 6.4.5.4 Appendix PA, Attachment MASS, Section 13.5
Sorption occurs on dolomite in the matrix. Sorption on clays present in the Culebra is not modeled.	SECOTP2D	Section 6.4.6.2.1 Appendix PA, Attachment MASS, Section 15.2
Particle waste shear is based on properties of marine clays, considered a worst case.	CUTTINGS_S	Section 6.4.7.1 Appendix PA, Attachment PAR
The concentration of actinides in liquid moving up the borehole in the E1E2 scenario assumes homogeneous mixing within the panel.	CCDFGF PANEL	Section 6.4.13.5

Table 6-32. Conservative Model and Parameter Assumptions Used in PA (from Appendix PA, Attachment MASS, Table MASS-1) — Continued

Conservative Assumption	Code	Cross-Reference
For all direct releases to the surface and the E1E2 source term to the Culebra, any actinides that enter the borehole are assumed to reach the surface or Culebra, respectively.	CUTTINGS_S DRSPALL BRAGFLO PANEL CCDFGF	Section 6.4.7.1 Section 6.4.13.5
A hemispherical geometry with one-dimensional spherical symmetry defines the flow field and cavity in the waste	DRSPALL	Section 6.4.7.1 MASS.16.1
Tensile strength, based on completely degraded waste surrogates, is felt to represent extreme, low-end tensile strengths because it does not account for several strengthening mechanisms	DRSPALL	Section 6.4.7.1 MASS.16.1
Shape factor is 0.1, corresponding to particles that are easier to fluidize and entrain in the flow	DRSPALL	Section 6.4.7.1 MASS.16.1
Retardation is assumed to not occur in the Salado.	NUTS CCDFGF	Section 6.4.5.4.2
Depletion of actinides in parts of the repository that have been penetrated by boreholes is not accounted for in calculating the releases from subsequent intrusions at such locations.	CUTTINGS_S	Section 6.4.13.7
Hydraulically-significant fractures are assumed to be present everywhere in the Culebra.	SECOTP2D	Section 6.4.6.2.1

REFERENCES

Andersson, J., Ed. 1989. *The Joint SKI/SKB Scenario Development Project*. SKB Technical Report 89-35, Authors: J. Andersson, T. Carlsson, T. Eng, F. Kautsky, E. Söderman, and S. Wingefors. Swedish Nuclear Fuel and Waste Management Co., Stockholm, Sweden.

Barr, G.E., Miller, W.B., and Gonzalez, D.D. 1983. *Interim Report on the Modeling of the Regional Hydraulics of the Rustler Formation.* SAND83-0391. Sandia National Laboratories, Albuquerque, NM, pp. 26 – 27. WPO 27557.

Beauheim, R.L. 1987. *Interpretations of Single-Well Hydraulic Tests Conducted At and Near the Waste Isolation Pilot Plant (WIPP) Site, 1983 – 1987*. SAND87-0039. Sandia National Laboratories, Albuquerque, NM, pp. 110 – 118. WPO 27679.

Beauheim, R.L., 1997. "Revision to Castile Brine Reservoir Parameter Packages," Memorandum to Palmer Vaughn, January 16, 1997. Sandia National Laboratories, Albuquerque, NM. WPO# 44699.

Beauheim, R.L. 2000. "Appendix E: Summary of Hydraulic Tests Performed at Tracer-Test Sites." *In Interpretations of Tracer Tests Performed in the Culebra Dolomite at the Waste Isolation Pilot Plant.* L.C. Meigs, R.L. Beauheim, and T.L. Jones, eds. SAND97-3109. Sandia National Laboratories, Albuquerque, NM.

Beauheim, R.L. 2003. "Culebra and Magenta Pressures to Use in CRA BRAGFLO Runs." Memorandum to David Kessel, August 19, 2003. Carlsbad, NM: Sandia National Laboratories. ERMS 530903.

Beauheim, R.L., Wawerisk, W.R., and Roberts, R.M. 1993. "Coupled Permeability and Hydrofracture Tests to Assess the Waste-Containment Properties of Fractured Anhydrite." *International Journal of Rock Mechanics and Mining Sciences & Geomechanical Abstracts*, Vol. 30, No. 7, pp. 1159 – 1163.

Brush, L.H., and Y. Xiong. 2003a. "Calculation of Actinide Solubilities for the WIPP Compliance Recertification Application, Analysis Plan AP-098," Rev 1. Unpublished analysis plan. Carlsbad, NM: Sandia National Laboratories. ERMS 527714.

Brush, L.H., and Y. Xiong. 2003b. "Calculation of Actinide Solubilities for the WIPP Compliance Recertification Application." Unpublished analysis report, May 8, 2003. Carlsbad, NM: Sandia National Laboratories. ERMS 529131.

Butcher, B.M. 1996. Memo to M.S. Tierney, *RE: QAP 9-1 Documentation of the Initial Waste Water Content for the CCA,* January 29, 1996. WPO 30925.

Butcher, B.M., and Mendenhall, F.T., 1992. *A Summary of the Models Used for the Mechanical Response of Disposal Rooms in the Waste Isolation Pilot Plant with Regards to Compliance with 40 CFR 191*, Subpart B, SAND92-0427. Sandia National Laboratories. Albuquerque, NM.

Butcher, B.M., Thompson, T.W., VanBuskirk, R.G., and Patti, N.C. 1991. *Mechanical Compaction of Waste Isolation Pilot Plant Simulated Waste*. SAND90-1206. Sandia National Laboratories, Albuquerque, NM. WPO 23968.

Christian-Frear, G.L., and Webb, S.W. 1996. *The Effect of Explicit Representation of the Stratigraphy on Brine and Gas Flow at the Waste Isolation Pilot Plant*. SAND94-3173. Sandia National Laboratories, Albuquerque, NM.

Corbet, T.F. and Knupp, P.M. 1996. *The Role of Regional Groundwater Flow in the Hydrogeology of the Culebra Member of the Rustler Formation at the Waste Isolation Pilot Plant (WIPP), Southeastern New Mexico.* SAND96-2133. Sandia National Laboratories. Albuquerque, NM.

Cranwell, R.M., Guzowski, R.V., Campbell, J.E., and Ortiz, N.R. 1990. *Risk Methodology for Geologic Disposal of Radioactive Waste: Scenario Selection Procedure.* NUREG/CR-1667, SAND80-1429. Sandia National Laboratories, Albuquerque, NM. WPO 26750.

Davies, P.B. 1991. *Evaluation of the Role of Threshold Pressure in Controlling Flow of Waste-Generated Gas into Bedded Salt at the Waste Isolation Pilot Plant.* SAND90-3246. Sandia National Laboratories, Albuquerque, NM, pp. 17 – 19. WPO 26169.

Downes, P.S. 2003a. "Spreadsheet Calculations of Actinide Solubilities for the WIPP Compliance Recertification Application." Unpublished memorandum to L.H. Brush, April 21, 2003. Carlsbad, NM: Sandia National Laboratories. ERMS 528395.

Downes, P.S. 2003b. "Spreadsheet Calculations of Actinide Solubilities for the WIPP Compliance Recertification Application in Support of AP-098, 'Calculation of Actinide Solubilities for the WIPP Compliance Recertification Application, Analysis Plan AP-098, Rev. 1.'" Unpublished analysis report, July 22, 2003. Carlsbad, NM: Sandia National Laboratories. ERMS 530441.

Freeze, G.A., Larson, K.W., and Davies, P.B. 1995. *A Summary of Methods for Approximating Salt Creep and Disposal Room Closure in Numerical Models of Multiphase Flow*. SAND94-0251. Sandia National Laboratories, Albuquerque, NM. WPO 29557.

Goodwin, B.W., Stephens, M.E., Davison, C.C., Johnson, L.H., and Zach, R. 1994. *Scenario Analysis for the Postclosure Assessment of the Canadian Concept for Nuclear Fuel Waste Disposal*. AECL-10969, COG-94-247. Whiteshell Laboratories, Pinawa, Manitoba, Canada.

Helton, J.C., Bean, J.E., Berglund, J.W., Davies, F.J., Economy, K., Garner, J.W., Johnson, J.D., MacKinnon, R.J., Miller, J., O'Brien, D.G., Ramsey, J.L., Schreiber, J.D., Shinta, A., Smith, L.N., Stoelzel, D.M., Stockman, C., and Vaughn, P. 1998. *"Uncertainty and Sensitivity Analysis Results Obtained in the 1996 Performance Assessment for the Waste Isolation Pilot Plant,"* SAND98-0365. Albuquerque, NM: Sandia National Laboratories. ERMS 252619.

Hobart, D.E., and Moore, R.C., 1996. Analysis of Uranium(VI) *Solubility Data for WIPP Performance Assessment: Implementation of Analysis Plan AP-028,* Revision 0, Aug 12, 1996. Albuquerque, NM: Sandia National Laboratories. ERMS 236488.

Hodgkinson, D.P. and Sumerling, T.J. 1989. "A Review of Approaches to Scenario Analysis for Repository Safety Assessment." In *Proceedings of the IAEA/CEC/NEA (OECD) Symposium on Safety Assessment of Radioactive Waste Repositories* (Paris, 1989). OECD/NEA, Paris, France. pp. 333 – 350.

Holt, R.M. 1997. Conceptual Model for Transport Processes in the Culebra Dolomite Member, Rustler Formation. SAND97-0194. Sandia National Laboratories, Albuquerque, NM.

Holt, R.M., and Powers, D.W. 1984. Geotechnical Activities in the Waste Handling Shaft Waste Isolation Pilot Plant (WIPP) Project Southeastern New Mexico. WTSD-TME-038. U.S. Department of Energy, Carlsbad, NM.

Holt, R.M., and Powers, D.W. 1986. Geotechnical Activities in the Exhaust Shaft. DOE/WIPP-86-008. U.S. Department of Energy, Carlsbad, NM.

Holt, R.M., and Powers, D.W. 1990. Geologic Mapping of the Air Intake Shaft at the Waste Isolation Pilot Plant. DOE/WIPP 90-051. Westinghouse Electric Corporation, Carlsbad, NM.

IAEA (International Atomic Energy Agency). 1981. Safety Assessment for the Underground Disposal of Radioactive Wastes. IAEA Safety Series No. 56, Vienna, Austria.

Iman, R.L., and Conover, W.J. 1982. A Distribution-Free Approach to Inducing Rank Correlation Among Input Variables. Communications in Statistics: Simulation and Computation, Vol. B11, No. 3, pp. 311 – 334.

Kaplan, S., and Garrick, B.J. 1981. On the Quantitative Definition of Risk. Risk Analysis, Vol. 1, No. 1, pp. 11 – 27.

La Venue, A.M., Cauffman, T.L., and Pickens, J.F. 1990. *Ground-Water Flow Modeling of the Culebra Dolomite: Volume 1 - Model Calibration.* SAND89-7068/1, Sandia National Laboratories. Albuquerque, NM.

Lappin, A.R., Hunter, R.L., Garber, D.P., Davies, P.B., Beauheim, R.L., Borns, D.J., Brush, L.H., Butcher, B.M., Cauffman, T., Chu, M.S.Y., Gomez, L.S., Guzowski, R.V., Iuzzolino, H.J., Kelley, V., Lambert, S.J., Marietta, M.G., Mercer, J.W., Nowak, E.J., Pickens, J., Rechard, R.P., Reeves, M., Robinson, K.L., and Siegel, M.D., eds. 1989. Systems Analysis, Long-Term Radionuclide Transport, and Dose Assessments, Waste Isolation Pilot Plant (WIPP), Southeastern New Mexico: March 1989. SAND89-0462. Sandia National Laboratories, Albuquerque, NM. WPO 24125.

Luker, R.S., Thompson, T.W., and Butcher, B.M. 1991. "Compaction and Permeability of Simulated Waste." In Rock Mechanics as a Multidisciplinary Science: Proceedings of the 32nd U.S. Symposium, University of Oklahoma, Norman, OK, July 10-12, 1991, J.C. Roegiers, ed. SAND90-2368C, pp. 694 – 702. A.A. Balkema, Brookfield, VT. WPO 38847.

Marcinowski, F. 2001. Untitled from F. Marcinowski to I.R. Triay, January 11, 2001. Washington, DC: U.S. Enviromental Protection Agency Radiation Protection Division.

Meigs, L.C., Beauheim, R.L., and Jones, T.L., Ed. 2000. *Interpretations of Tracer Tests Performed in the Culebra Dolomite at the Waste Isolation Pilot Plant Site.* SAND97-3109. Sandia National Laboratories, Albuquerque, NM.

Meigs, L.C., and McCord, J.T. 1996. "Appendix A: Physical Transport in the Culebra Dolomite." I*n Analysis Package for the Culebra Flow and Transport Calculations (Task 3) of the Performance Assessment Analyses Supporting the Compliance Certification Application,* Analysis Plan 019, Version 00. J. Ramsey, M. Wallace, and H.-N. Jow. ERMS# 240516. Sandia National Laboratories, Albuquerque, NM.

Mercer, J.W., and Orr, B.R. 1979. *Interim Data Report on Geohydrology of Proposed Waste Isolation Pilot Plant Site, Southeast New Mexico*. Water Resources Investigations 79-98. U.S. Geological Survey, Albuquerque, NM.

Miller, W.M. and Chapman, N.A., Ed. 1992. *Identification of Relevant Processes, System Concept Group Report,* UKDOE/HMIP Report TR-ZI-11, London, England.

NAGRA. 1985. *Nuclear Waste Management in Switzerland: Feasibility Studies and Safety Analyses (Project Gewahr, 1985).* NAGRA Project Report NGB 85-09 (English Summary), Wettingen, Switzerland.

Novak, C.F., R.C. Moore, and R.V. Bynum. 1996. "Prediction of Dissolved Actinide Concentrations in Concentrated Electrolyte Solutions: A Conceptual Model and Model Results for the Waste Isolation Pilot Plant (WIPP)." Unpublished presentation at the 1996 International Conference on Deep Geological Disposal of Radioactive Waste, September 16-19, 1996, Winnipeg, Manitoba, Canada. ERMS 418098, SAND96-2695C

OECD Nuclear Energy Agency. 1992. *Systematic Approaches to Scenario Development.* Organisation for Economic Co-Operation and Development, Paris, France. NWM Library, NNA.920610.0027.

Park, B,Y,. and J.F., Holland. 2003. "*Structual Evaluation of WIPP Disposal Room Raised to Clay G."* SAND2003-3409, Sandia National Laboratories. Carlsbad, NM.

Popielak, R.S., Beauheim, R.L., Black, S.R., Coons, W.E., Ellingson, C.T., and Olsen, R.L. 1983. *Brine Reservoirs in the Castile Formation Waste Isolation Pilot Plant (WIPP) Project Southeastern New Mexico.* TME-3153, Westinghouse Electric Corp, Carlsbad, NM.

Sandia National Laboratories. 1991. *Preliminary Comparison with 40 CFR Part 191, Subpart B for the Waste Isolation Pilot Plant, December 1991. Volume. 1: Methodology and Results.* SAND91-0893/1. Sandia National Laboratories, WIPP Performance Assessment Division, Albuquerque, NM. WPO 26404.

Sandia National Laboratories. 1992-1993. *Preliminary Performance Assessment for the Waste Isolation Pilot Plant, December 1992.* SAND92-0700, Vols. 1 – 5. Sandia National Laboratories, WIPP Performance Assessment Division, Albuquerque, NM. Vol. 1 - WPO 20762, Vol. 2 - WPO 20805, Vol. 3 - WPO 23529, Vol. 4 - WPO 20958, Vol. 5 - WPO 20929.

Sandia National Laboratories. 2003. *Borehole Plugging Probabilities to be used in Compliance Recertification Calculations.* September 3, 2003. Sandia Records Center, Sandia National Laboratories, Carlsbad Programs Group. Carlsbad, NM. ERMS# 531352.

State of New Mexico, Oil Conservation Division, Energy, Minerals, and Natural Resources Department. 1988. "Application of the Oil Conservation Division Upon It's Own Motion to Revise Order R-111, As Amended, Pertaining to the Potash Areas of Eddy and Lea Counties, New Mexico." Case 9316, Revision to Order R-111-P, April 21, 1988. Santa Fe, NM. On file in the NWM Library as KFN2581.

Stenhouse, M.J., Chapman, N.A., and Sumerling, T.J. 1993. *SITE-94 Scenario Development FEP Audit List Preparation: Methodology and Presentation*. SKI Technical Report 93:27. Swedish Nuclear Power Inspectorate, Stockholm. Available from NTIS as DE 94621513.

Thorne, M.C. 1992. *Dry Run 3 - A Trial Assessment of Underground Disposal of Radioactive Wastes Based on Probabilistic Risk Analysis - Volume 8: Uncertainty and Bias Audit.* United Kingdom Department of Environment Report DOE/HMIP/RR/92.040, London, England.

Trovato, E.R. 1997. Untitled letter from E.R. Trovato to G. Dials, April 25, 1997. *Washington, DC: U.S. Environmental Protection Agency Office of Radiation and Indoor Air.*

U.S. Environmental Protection Agency (EPA). 1998a. "40 CFR Part 194: Criteria for the Certification and Re-Certification of the Waste Isolation Pilot Plant's Compliance With the Disposal Regulations "Certification Decision; Final Rule." *Federal Registe*r, Vol. 63, No. 95, pp. 27396, May 18, 1998. Office of Radiation and Indoor Air, Washington D.C.

U.S. Environmental Protection Agency (EPA). 1998b. "Technical Support Document for Section 194.23: Parameter Justification Report." *EPA Air Docket A93-02-V-B-14.* Washington, DC: U.S. Environmental Protection Agency Office of Radiation and Indoor Air.

U.S. Environmental Protection Agency (EPA). 1998c. "Compliance Application Review Documents for the Criteria for the Certification and Recertification of the Waste Isolation Pilot Plant's Compliance with the 40 CFR Part 191 Disposal Regulations: Final Certification Decision. CARD 23: Models and Computer Codes." *EPA Air Docket A93-02-V-B-2.* Washington, DC: U.S. Environmental Protection Agency Office of Radiation and Indoor Air.

U.S. Environmental Protection Agency (EPA). 1998d. "Technical Support Document for Section 194.23 - Models and Computer Codes." *EPA Air Docket A93-02-V-B-6*. Washington, DC: U.S. Environmental Protection Agency Office of Radiation and Indoor Air.

U.S. Environmental Protection Agency (EPA). 1985. "40 CFR Part 191: Environmental Standards for the Management and Disposal of Spent Nuclear Fuel, High-Level and Transuranic Radioactive Wastes; Final Rule." *Federal Register,* Vol. 50, No. 182, pp. 38066 – 38089, September 19, 1985. Office of Radiation and Air, Washington, D.C. WPO 39132.

U.S. Environmental Protection Agency (EPA). 1993. "40 CFR Part 191: Environmental Radiation Protection Standards for the Management and Disposal of Spent Nuclear Fuel, High-Level and Transuranic Radioactive Wastes; Final Rule." *Federal Register,* Vol. 48, No. 242, pp.

66398 – 66416, December 20, 1993. Office of Radiation and Air, Washington, D.C. WPO 39133.

U.S. Environmental Protection Agency (EPA). 1996a. "40 CFR Part 194: Criteria for the Certification and Re-Certification of the Waste Isolation Pilot Plant's Compliance with the 40 CFR Part 191 Disposal Regulations Final Rule." *Federal Register*, Vol. 61, No. 28, pp. 5224 – 5245, February 9, 1996. Office of Radiation and Indoor Air, Washington, D.C. In NWM Library as KF70.A35.C751 1996 (Reference)

U.S. Environmental Protection Agency (EPA). 1996b. *Criteria for the Certification and Re-Certification of the Waste Isolation Pilot Plant's Compliance with the 40 CFR Part 191 Disposal Regulations. Background Information Document for 40 CFR Part 194.* EPA 402-R-96-002. Environmental Protection Agency, Office of Radiation and Indoor Air, Washington, DC.

Vaughn, P., Bean, J., Garner, J., Lord, M., MacKinnon, R., McArthur, D., Schreiber, J., and Shinta, A.. 1995. *FEPs Screening Analysis DR2, DR3, DR6, DR7, and S6*. Record package submitted to SWCF-A:1.1.6.3:PA:QA:TSK:DR2, DR3, DR6, DR7, and S6. Sandia National Laboratories, Albuquerque, NM. WPO 38152.

Vugrin, E. 2004. "Corrected CRA Figures" Memorandum to David Kessel dated December 14, 2004. Sandia National Laboratories. Carlsbad, NM. ERMS #533999

Wallace, M.G., Beauheim, R., Stockman, C., Martell, M.A., Brinster, K., Wilmot, R., and Corbet, T. 1995. *FEPs Screening Analysis, NS-1: Dewey Lake Data Collection and Compilation*. Record package submitted to SWCF-A:1.1.6.3:PA:QA:TSK:NS1. Sandia National Laboratories, Albuquerque, NM. WPO 30650.

INDEX